UNIVERSITA' DEGLI STUDI DI PAVIA

Dipartimento di Biologia e Biotecnologie

"Lazzaro Spallanzani"

Fighting drug-resistant tuberculosis: CTP-synthetase and pantothenate kinase as new targets for multitargeting compounds

Marta Esposito

Dottorato di Ricerca in
Genetica, Biologia Molecolare e Cellulare
XXIX Ciclo – A.A. 2013-2016

UNIVERSITA' DEGLI STUDI DI PAVIA

Dipartimento di Biologia e Biotecnologie

"Lazzaro Spallanzani"

Fighting drug-resistant tuberculosis: CTP-synthetase and pantothenate kinase as new targets for multitargeting compounds

Marta Esposito

Supervised by

Prof. Maria Rosalia Pasca

Dr. Laurent Roberto Chiarelli

Dottorato di Ricerca in
Genetica, Biologia Molecolare e Cellulare
XXIX Ciclo – A.A. 2013-2016

Abstract

Tuberculosis (TB), the infectious disease brought about by *Mycobacterium tuberculosis*, is afflicting human health worldwide. Epidemiological data indicate 3 billion people latently infected globally, and only in 2014, 1.5 million people died due to this infection. Moreover, TB plague does not show signs to stop, particularly in view of the spread of *M. tuberculosis* drug-resistant strains (MDR, XDR and TDR), together with patients co-infected with HIV. Thus, considering all these aspects, the research for new antitubercular drugs and the identification of novel targets that could allow the killing of the pathogen through more efficient tools, are surely indispensable.

Recently, from the screening of the National Institute of Allergy and Infectious Diseases (NIAID) chemical library, two compounds distinguished themselves for their efficacious antitubercular activity. These molecules, the thiophene-carboxamide 7947882 and the carbamothioyl-propanamide 7904688, displayed activity against the pathogen *in vitro*, *ex vivo*, and against a latent model. Genetic and biochemical approaches demonstrated that 7947882 and 7904688 are prodrugs activated by the monooxygenase EthA, already known to be the activator of ethionamide. Moreover, from the sequencing analysis of 7947882 and 7904688 *M. tuberculosis* spontaneous resistant mutants, the CTP-synthetase PyrG and pantothenate kinase PanK emerged as the putative targets of these compounds.

The present work led to the demonstration that PyrG and PanK are the cellular targets of these compounds. Moreover, in view of the importance of finding new drugs targeting more than one cellular function, PyrG and PanK were exploited to perform an *in silico* screening of the Collaborative Drug Discovery (CDD) compound database, and an *in vitro* screening of the GSK TB-set chemical library of compounds against the two enzymes. From these screenings, a number of compounds affecting both enzymes emerged, thus strengthening the usefulness of PyrG and PanK for new multitargeting drugs research.

Finally, all *M. tuberculosis* PyrG inhibitors were tested against human CTP-synthetase-1, identifying one compound that inhibits almost exclusively the mycobacterial enzyme, and not the human one, paving the way for new *M. tuberculosis* PyrG selective inhibitors.

Acknowledgements

First of all I want to thank Prof. Giovanna Riccardi and Prof. Maria Rosalia Pasca for the precious opportunity to spend my Ph.D. period in this laboratory, as well as for the trust in me, the continuous help, support and teaching. This experience was essential for my personal growth.

A special thank is addressed to all the members of the laboratory, particularly to Dr. Laurent Chiarelli, to whom I dedicate a profound gratitude.

Furthermore, I thank all the collaborators that gave a priceless contribution to this project: Dr. Vadim Makarov, (AN Bakh Institute of Biochemistry, Russian Academy of Science, Moscow, Russia), Dr. Marco Bellinzoni and Prof. Pedro Alzari (Institut Pasteur, Paris, France), Dr. Ruben Hartkoorn and Prof. Stewart Cole (Global Health Institute, Ecole Polytechnique Fédérale de Lausanne, Lausanne, Switzerland), Prof. Riccardo Manganelli (Department of Molecular Medicine, University of Padova, Padua, Italy), Dr. Sean Ekins (Collaborative Drug Discovery, USA), Dr. Ana Luisa de Jesus Lopes Ribeiro (Centro de Biologia Molecular ''Severo Ochoa'' Universidad Autònoma de Madrid, Madrid, Spain), Prof. Katarına Mikusova (Department of Biochemistry, Faculty of Natural Sciences, Comenius University in Bratislava, Bratislava, Slovakia), Dr. Luiz Pedro S. de Carvalho (Francis Crick Institute, Mill Hill Laboratory, London, UK), Dr. Lluís Ballell (GlaxoSmithKline, Tres Cantos, Madrid, Spain).

Abbreviations

ADP: adenosine diphosphate
ATP: adenosine triphosphate
BTZs: Benzothiazinones
CoA: Coenzyme A
CTP: cytidine triphosphate
DMSO: Dimethyl Sulfoxide
DPA: Decaprenol-phosphoryl-β-D-arabinose
DPR: decaprenylphosphoryl-β-D ribose
EDTA: Ethylenediaminetetraacetic Acid
EMA: European Medicines Agency
EMB: ethambutol
ETH: Ethionamide
FDA: Food and Drug Administration
HIV: Human immunodeficiency virus
HTS: high throughput screenings
INH: Isoniazid
IPTG: Isopropyl β-D-1-thiogalactopyranoside
LPZ: Lansoprazole
MIC: Minimal Inhibitory Concentration
MDR: MultiDrug-Resistance
MDR-TB: MultiDrug-Resistant Tuberculosis
MM4TB: More Medicines For Tuberculosis
OD: Optical Density
PAS: para-aminosalicylic acid
PZA: pyrazinamide
QRDR: Quinolone Resistance Determining Region
RIF: Rifampicin
RNAP: RNA polymerase
SDS-PAGE: Sodium Dodecyl Sulphate-PolyAcrylamide Gel Electrophoresis
TB: Tuberculosis
TDR: Totally Drug-Resistance
TMM: trehalose monomycolate
UTP: uridine triphosphate
WHO: World Health Organization
X-Gal: 5-bromo-4-chloro-3-indolyl-β-D-galactopyranoside
XDR: Extensively Drug-Resistance
XDR-TB: Extensively Drug-Resistant Tuberculosis

Contents

1. Introduction

1.1 Tuberculosis: a re-emergent worrisome issue

Tuberculosis (TB), one of the deadliest infection afflicting humans, is a contagious disease caused by the *Mycobacterium tuberculosis* complex (Dheda *et al*., 2016). *M. tuberculosis* complex embraces different species of mycobacteria (*M. tuberculosis*, *Mycobacterium bovis*, *Bacille Calmette-Guerín* (BCG) vaccine strain, *Mycobacterium africanum*, *Mycobacterium microti*, *Mycobacterium canettii*, *Mycobacterium caprae*, *Mycobacterium pinnipedii*, *Mycobacterium orygis* and *Mycobacterium mungi*), and its most diffused member, *M. tuberculosis*, is the main causative agent of TB in primates and humans (Broset *et al*., 2015). Although TB generally affects lungs, infection of other organs cannot be excluded: the former kind of infection, the most frequent, is named "pulmonary TB", the latter, more occasional, "extrapulmonary TB" (Riccardi *et al*., 2009).

TB history probably begins 70,000 years ago, thus following human migrations out of Africa (Comas *et al*., 2013). Getting closer to our century, it peaked in Europe in the first half of the 19th century (Dubos and Dubos, 1952), but only in 1882 Robert Koch isolated and identified its etiologic agent, thus named Koch's bacillus (Ducati *et al.*, 2006). Between the 17th and 19th centuries, 20% of deaths have been caused by TB in both Europe and North America, especially because of the complete lack of effective treatments (Wilson and Tsukayama, 2016). Thereafter, even though the introduction of prevention and chemotherapeutic strategies led to a significant fall of TB mortality in developed countries, feeding a new hope for pathogen eradication (Ducati *et al*., 2006), in 1980s novel TB cases appeared. There are several explanations for this "resumption": the most significant ones are the co-infection with HIV and the spread of *M. tuberculosis* drug-resistant strains (Ducati *et al.*, 2006). Recent World Health Organization (WHO) data clearly declared TB as a global plague: in 2014, 1.5 million people were killed by this infection, and 9.6 were affected by TB worldwide (Fig. 1) (WHO, 2015). Among the risk factors that predispose to the disease, there are under nutrition, poverty, smoking, diabetes, HIV infection and all suppressed-immune response conditions (Dheda *et al*., 2016). According to mathematical models, despite their obvious limits, current tools are not sufficient to completely eliminate TB from the world scenario; rather, TB eradication may probably occur in 2050, only if prevention (e.g. vaccines), diagnosis and new drug therapies will combine together to combat and win the fight against TB (Dye *et al.*, 2013).

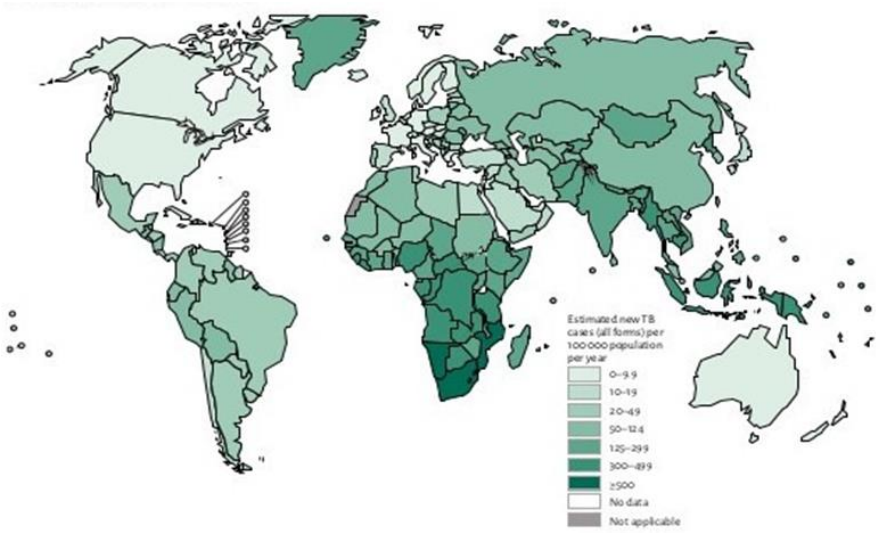

Figure 1. Estimated TB incidence (WHO, 2015).

1.2 *Mycobacterium tuberculosis*: a general overview and the infectious process

M. tuberculosis is an ancient pathogen, highly evolved (Shankar *et al.*, 2014), whose main features are the absence of a flagellum, the impossibility to produce toxins, spores, as well as a surrounding capsule, and a typical road-shape (Ducati *et al.*, 2006). Moreover, the bacillus growth is very slow, having a generation time of around 24 hours, and is able to enter a dormant state, as described below; on solid media it forms opaque and rough colonies (Cole *et al*., 1998). The understanding of the complex biology of the pathogen rests on the deep characterization of *M. tuberculosis* H37Rv strain, being extensively investigated in biomedical research. In 1998, the complete genome sequence of *M. tuberculosis* H37Rv strain was enlightened (Cole *et al*., 1998). The microbe circular genome is 4.4 megabase (Mb) in length and reach in G + C (Cole *et al.*, 1998).

Infectious process follows a series of steps that have been defined utilizing animal models and studying human TB cases (Russel, 2007). Focusing on pulmonary TB, *M. tuberculosis* transmission occurs from one individual to another, inhalating infectious bacilli as exhalated droplets, that can persist in the air for hours (Russel, 2007). This exposure does not mean disease development; on the contrary, symptoms appear very rarely, depending on the immunocompetence of the new host and the strategies developed by *M. tuberculosis* during its evolution to guarantee a successful spread among humans (Dheda *et al*., 2016). Effectively, only 1–5% of

infected people develop the active disease right after the contagion; in all other cases, the bacillus remains in a dormant status without showing any pathological signs (Riccardi *et al.*, 2009). The probability of bacteria reactivation depends on the immune system integrity: in immune-competent patients, the probability of displaying an active disease is 5-10%, whilst in patients co-infected with HIV, this percentage rises every year (Fig. 2) (El-Sadr and Tsiouris, 2008).

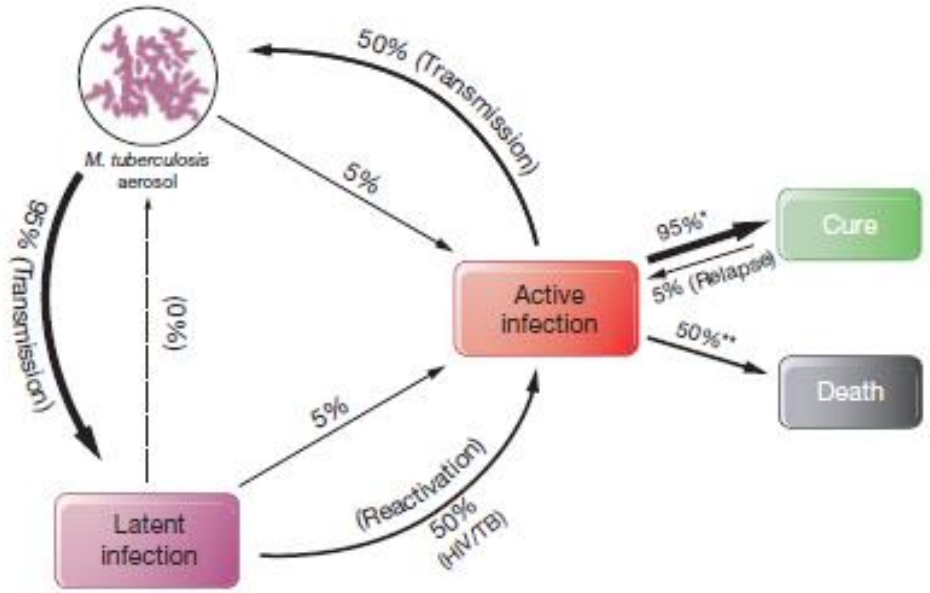

Figure 2. Phases of *M. tuberculosis* infectious process (Koul *et al*., 2011).

Once inside the host, bacteria are internalized by alveolar macrophages, that in turn move to the lung interstitium, thus releasing a series of inflammatory players such as TNF-α, IL-1, IL-6, IL-12 and chemokines, provoking a local pro-inflammatory reaction (Korb *et al*., 2016). This kind of response is followed by the recruitment of different mononuclear cells from blood vessels, hence paving the bases for granuloma formation (Dheda *et al*., 2016) (Fig. 3). Granuloma is defined as the principal pathogenic hallmark of *M. tuberculosis* pulmonary infection (Ulrichs and Kaufmann, 2006). At this point, the majority of infecting bacteria are enclosed within the so called foamy macrophages, that start covering the external part of granuloma (Hoagland *et al*., 2016). Granuloma undergoes a series of changes once has formed (Russel *et al*., 2010); at the beginning, it appears highly vascularized and full of immune response cells,

thus supporting the immune defenses to fight the bacilli, as well as the capability of therapeutic drugs to achieve the infection. Successively, granuloma undergoes further modifications, maturing in a necrotic state. The typical features of a necrotic granuloma are its outer part becoming a harder fibrous capsule, then creating a barrier between immune cells and its internal part, and a caseum core, that eliminates all the residual vascularization (Hoagland *et al*., 2016). In this phase, bacteria are enclosed in the necrotic granuloma, entering their dormant state, and are protected from drug entrance. This status can last for several decades, and in case of a weakening of immune defenses, the granulomas can explode, leaving bacilli free to reach other organs and new hosts (Fig. 3) (Dartois, 2014).

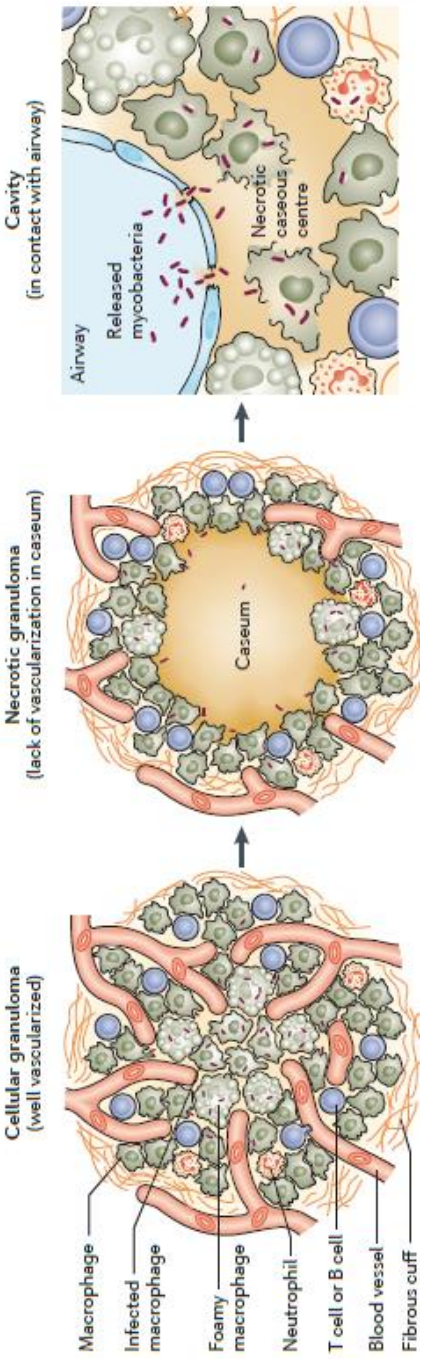

Figure 3. Maturation stages of granuloma during TB infections (Dartois, 2014).

1.3 Standard therapy for drug-sensitive TB

The first drug discovered for TB treatment, streptomycin, was identified in 1940s, but developed resistance soon after its introduction in chemotherapy (Crofton and Mitchison, 1948). Consequently, it was understood very early that single-compound therapy causes fast drug-resistant strains spread, failing in the fight against the pathogen (Crofton and Mitchison, 1948). Streptomycin resistance was counteracted by the administration of a second antitubercular compound, para-aminosalicylic acid (PAS), that was able to reduce cell proliferation (Wilson and Tsukayama, 2016). Being aware of the complexity of the battle against *M. tuberculosis* spread, in 1950s further drugs were developed in order to define a combinational therapy (Zumla *et al.*, 2013a). This strategy was demonstrated to be a valid approach, remaining nowadays the most effective one (Blumberg *et al*., 2003; Shcherbakov *et al.*, 2010). For example, the introduction of isoniazid (INH) in the combination therapy, gave the possibility to get successful results with a complete eradication of the pathogen after 18 to 24 months of treatment (Council, 1962); successively, rifampicin (RIF) was added, permitting to shorten therapy duration to 6 - 9 months (Kurz *et al*., 2016).

Nowadays, WHO classified antitubercular compounds in five groups: first-line drugs are gathered in group 1, whilst second-line compounds are listed in the remaining four groups (Wilson and Tsukayama, 2016). First-line compounds are principally bactericidal, and associate their great efficacy with a modest toxicity, including INH, RIF, ethambutol (EMB) and pyrazinamide (PZA) (Ducati *et al*., 2006). Second-line agents are mainly bacteriostatic, with higher toxicity and less efficacy (Ducati *et al*., 2006). Group 2 is identified by the injectable drugs, including capreomycin and aminoglycosides (streptomycin, kanamycin and amikacin), whilst group 3 contains fluoroquinolones, in particular levofloxacin, ofloxacin, moxifloxacin and gatifloxacin. Ethionamide (ETH), cycloserine and PAS, the remaining second-line drugs, form the group 4, whilst the group 5 presents the most recent antibacterial compounds that are yet to be further investigated from a clinical point of view and concerning the efficacy against *M. tuberculosis* drug-resistant strains, such as linezolid, bedaquiline, delamanid, amoxicillin-clavulanate, clofazimine, meropenem and clarithromycin (Wilson and Tsukayama, 2016).

Current therapy for drug-susceptible TB was set up forty years ago, but is still highly efficacious. During the first 2 months INH, RIF, PZA and EMB are delivered together (Fig. 4) (Hoagland *et al*., 2016). Afterwards, this very intensive phase is followed by a 4-months stage during which RIF

and INH are continually swallowed in order to annihilate remaining bacteria that have entered a latent, slow-growing phase (Kurtz *et al*., 2016).

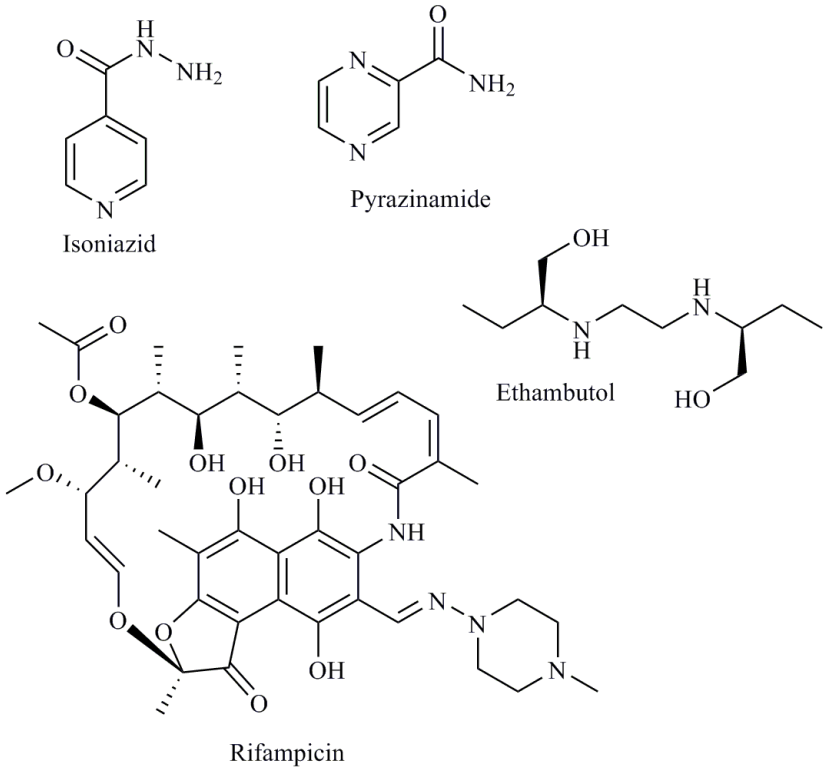

Figure 4. Drugs currently utilized for *M. tuberculosis* drug-susceptible treatment.

INH is a bactericidal drug, very effective, causing a quick bacterial growth inhibition as soon as therapy is initiated (Vilchèze and Jacobs, 2007). In order to be effective, INH requires an activating-step performed by the catalase peroxidase KatG enzyme; once activated, INH forms an adduct with NAD, thus inhibiting the *inhA*-encoded NADH-dependent enoyl-ACP reductase, its cellular target (Vilchèze and Jacobs, 2007). The degree of resistance to INH is correlated to the genetic alterations affecting the bacterial genome: point mutations, missense ones and deletions mapping in the *katG* gene cause high-level resistance, whilst alterations in the *inhA* promoter causing an augmented expression of the correspondent gene, are associated to a low-level of resistance, together with cross-resistance to ETH (Zhang *et al*., 1992; Banerjee *et al*., 1994). Moreover, around 25% clinical isolates showing resistance to INH, are characterized by a point

mutation affecting InhA, either a Ser94Ala or a Ile16Thr, leading to an enzyme having a reduced affinity towards both NADH and the adduct formed by INH-activated form and NAD^+ (Vilchèze and Jacobs, 2014).

RIF is another very effective anti-TB drug, that is able to shorten the duration of the treatment (Kurz *et al.*, 2016). This compound targets the β-subunit of bacterial DNA-dependent RNA polymerase (RNAP), the *rpoB* gene product (Campbell *et al*., 2001). Concerning its mode of action, it has been shown that RIF operates by creating a steric obstacle that blocks RNA synthesis, instead of affecting the enzymatic activity of the target protein (McClure and Cech, 1978). Resistance to RIF is caused by a single mutation affecting a precise region of the gene, increased copy-number of the target gene, efflux pumps activity or modifications of the drug itself (Tupin *et al*., 2010). It is worth to observe that, whilst single resistance to INH is frequent, it is rare to encounter mono-resistance to RIF cases; precisely, RIF resistance tends to develop in strains already resistant to INH (Somoskovi *et al*., 2001).

PZA, a structural analogue of nicotidamide, is a prodrug that requires activation mediated by pyrazinamidase (encoded by *pcnA* gene), thus forming pyrazinoic acid. The active form of PZA targets fatty acid synthetase 1 (Zimhony *et al*., 2000), and resistance to this compound is especially caused by mutations affecting *pcnA* gene (Miotto *et al*., 2015). Its sterilizing activity is widely exploited to defeat persistent bacteria (Zhang and Mitchison, 2003).

EMB is an antitubercular drug that interferes with bacterial cell wall synthesis, targeting the enzyme arabinosyl transferase, coded by *embCAB* cluster, involved in the production of arabinogalactan (Belanger *et al*., 1996).

This 4-drugs therapy, although called "short-course", has as most significant drawback the extent of regimen duration. In fact, the fraction of patients failing to fulfil the complete treatment raises after one month, and varies between 7% and 53.6% (Kruk *et al.*, 2008). Among the several side effects caused by the treatment, hepatotoxicity, gastrointestinal disorders, arthralgias and allergies are the most recurrent (Horsburgh *et al*., 2015). Concerning liver lesions, it has been reported that the frequency of liver injury caused by antitubercular treatment varies between 5% and 33% (Saukkonen *et al.*, 2006), but the majority of recovered data shows a remarkable fraction of patients having an asymptomatic increase in transaminases (Dheda *et al*., 2016). This phenomenon, named "hepatic adaptation", may happen in the first weeks of therapy, but only in case of high risk of hepatotoxicity liver monitoring is recommended; in turn, when clinical hepatitis occurs, the hepatotoxic drugs (RIF, INH or PZA) should be

removed from the therapy, thus adding two second-line compounds to EMB (Dheda *et al.*, 2016).

1.4 Co-infection with human immunodeficiency virus: one of the major obstacles for successful TB treatment

WHO reported that in 2014, at least one-third of individuals infected by HIV, were also affected by TB, and among HIV-positive cases, 1.2 million were also new TB patients. Furthermore, among TB-deaths, 0.4 million people were co-infected with HIV, and among HIV-positive deaths, around one-third died for TB infection (Fig. 5) (WHO, 2015).

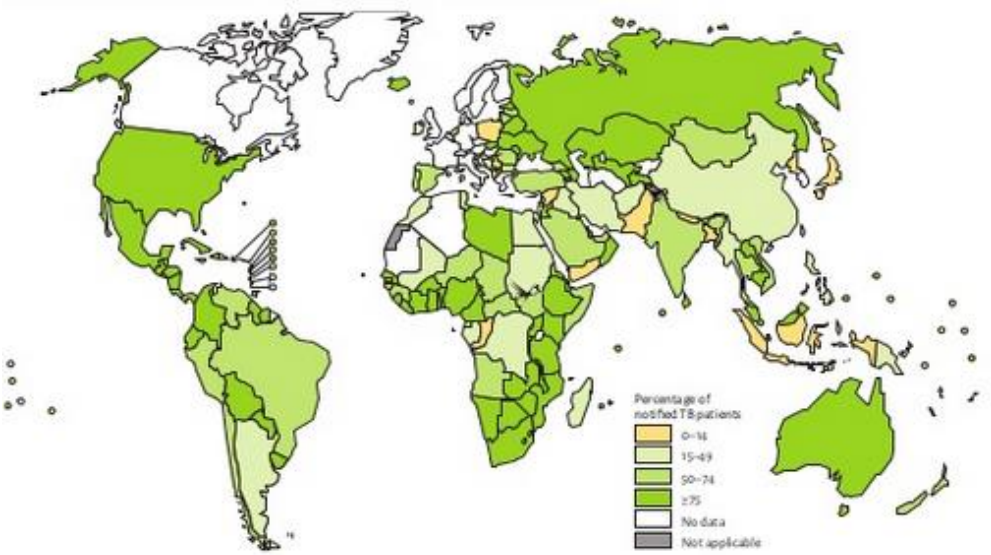

Figure 5. Percentage of notified TB patients with known HIV status by country (WHO, 2015).

The probability of developing active TB importantly increases for patients already living with HIV (WHO, 2015). These data are really worrisome, considering that TB and HIV are two of the greatest public health dangers in the world, taken separately (El-Sadr and Tsiouris, 2008). Although HIV co-infection is a much more diffused in poor countries, especially for living conditions (e.g. neglected sanitation, lacking education, poor socio-economic conditions) that significantly predispose population to this circumstance (WHO, 2013), recently it has been shown that it is gradually diffusing also in developed countries background (Khabbaz *et al*., 2014).

The reasons explaining the earlier active TB development in HIV-positive cases have to be individuated in the immunopathogenesis of the co-infection (Montales *et al.,* 2015). Moreover, it is worth to consider that individual *M. tuberculosis* and HIV pathogens lead to a strong deterioration of immune defences (Pawlowski *et al*., 2012), and in case of co-infection, specific immunological phenomena speed up each disease progression (Shankar *et al.,* 2014). As described before, once *M. tuberculosis* has reached lung alveoli, an inflammatory cascade is initiated with the consequent granuloma formation; here, bacteria remain in a dormant state, and cell-mediated immunity, by activating CD4-T lymphocytes, makes sure that no bacteria re-activation occurs (Cooper, 2009). In turn, HIV, after infection upon genital mucosal exposure and throughout its progression, causes a gradual inactivation of the immune system, an impairment of macrophages activity and a serious CD-4 T lymphocytes reduction, that lead to granuloma disintegration and mycobacteria reactivation (Pawlowski *et al*., 2012; Shankar *et al*., 2014).

It has been demonstrated that macrophages infected with *M. tuberculosis* tend to produce higher amount of IL-1 and IL-6, together with tumor necrotic factor-α (TNF-α), thus favoring HIV replication (Briken *et al.,* 2004), whilst macrophages infected simultaneously with *M. tuberculosis* and HIV, are less prone to apoptotic events than those infected with the microbe alone, due to reduced production of tumor necrotic factor-α (TNF-α) (Patel *et al*., 2009). Concerning the negative effects of HIV infection on the capacity of T-cells to restrict bacterial infection, it has been observed a decreased production of interpheron-γ (IFN-γ) and interleukin-2 (IL-2) by T lymphocytes in co-infected patients compared to those with TB only (Hertoghe *et al*., 2000; Geldmacher *et al.,* 2008). Other evidences demonstrated that a particular peptide-glycolipid localized on *M. tuberculosis* surface, named Wax-D, leads to enhanced CD4 type 1 T-helper cells expansion by stimulating dendritic cells, together with macrophages, to release interleukin-12 (IL-12), thus facilitating viral infection (Briken *et al.,* 2004) (Fig. 6). All these mechanisms, among others, significantly highlight how *M. tuberculosis* and HIV followed a co-evolution, in order to support and facilitate each other during the infection, rendering this phenomenon a new pathogenic scenario worldwide (Shankar *et al*., 2014).

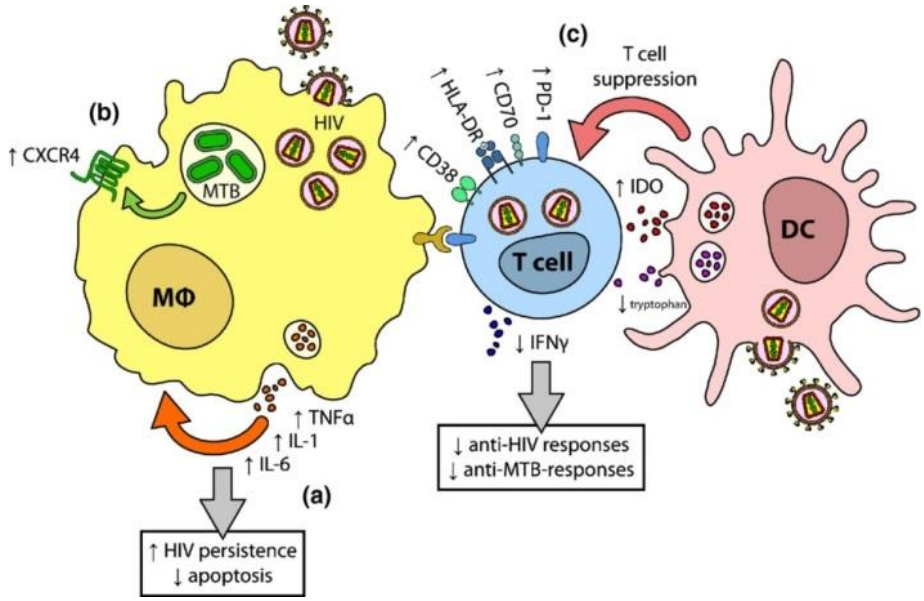

Figure 6. Model for TB-HIV co-infection (Shankar *et al.*, 2014).

1.5 Drug-resistant TB and current therapeutic regimen

The phenomenon of drug resistance is one of the most typical aspect of *M. tuberculosis* spread, inducing several advantages for the survival of mutant strains (Nguyen, 2016). The emergence and spread of drug-resistant strains is accentuated by several risk factors, such as previous treatment for TB, prolonged hospitalization in TB endemic regions, incorrect drug choice and doses for treatment, lack of patients compliance to the treatment and of possibility to supply these expensive drugs at lower prices, delayed diagnosis of the disease, among others. Nevertheless, the lack of patients conformity to TB therapy is still the driving issue (Wilson and Tsukayama, 2016).

Since *M. tuberculosis* possesses several enzymes able to modify many different kinds of molecules, and owing a highly hydrophobic cell membrane rich in mycolic acids, as well as many efflux pumps, it is naturally resistant to several drugs (Ducati *et al*., 2006). Moreover, the majority of *M. tuberculosis* drug-resistant cases originate from spontaneous and independent mutations leading to a decrease in enzymes involved in prodrugs activation, an overexpression of the target gene, or changes in the drug binding site of the target molecule (Cohen *et al.*, 2014).

WHO declared that in 2014, 480.000 TB cases were caused by *M. tuberculosis* strains resistant to both INH and RIF (Fig. 7) (WHO, 2015), thus classified as multidrug-resistant (MDR) (Migliori *et al.*, 2007).

Furthermore, around 9.7% of them exhibited also resistance to at least one of the second-line injectable compounds and one fluoroquinolone, consequently named extensively drug resistant (XDR) (WHO, 2015). Particularly, among the total MDR instances, 3% of them represent new TB infections, whilst 20% are already previously treated cases, and only 50% of patients will survive, successfully concluding the entire treatment path (WHO, 2015). Although the drug-resistant TB scenario is already worrisome considering MDR and XDR cases, the most dangerous infections are represented by the so-called totally-drug resistant (TDR), defined as *M. tuberculosis* strains resistant to all first- and second-line drugs (Parida *et al.*, 2015).

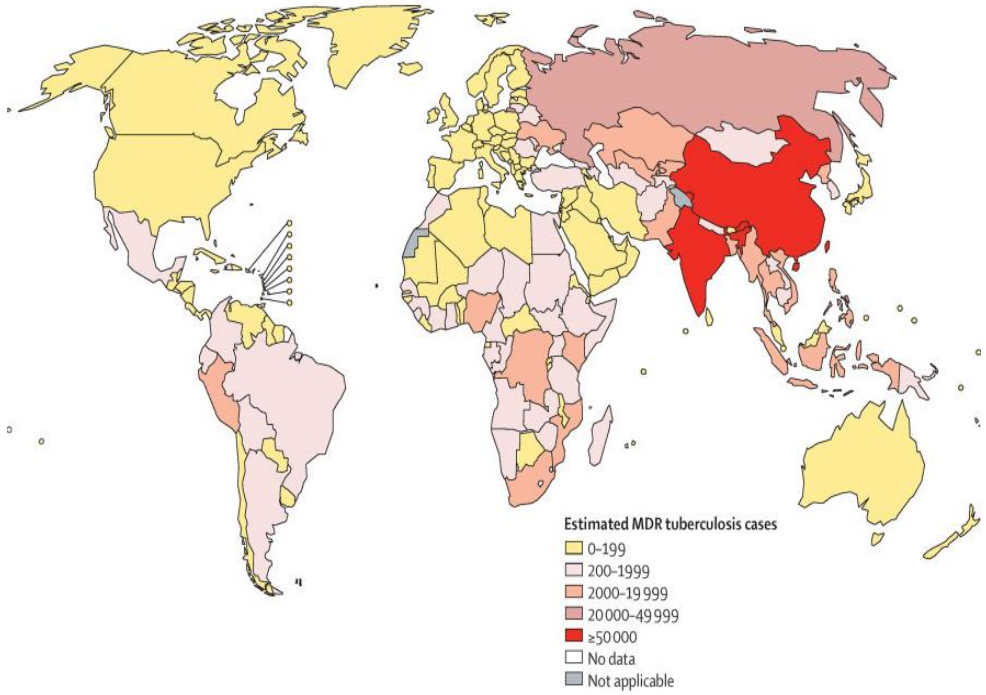

Figure 7. Global distribution of MDR-TB cases in 2014 (WHO, 2015).

Facing *M. tuberculosis* drug-resistant strains is, without any doubts, more complicated compared to drug-susceptible infections, causing the spread of drug-resistant TB all over the world (Kurtz *et al.*, 2016). Therapeutic procedure for drug-resistant TB is poorly tolerated due to the increased toxicity of drugs employed during the treatment, and lengthened up to 2 years, being these compounds less efficacious (Dheda *et al.*, 2016; Kurtz *et al.*, 2016). In case of a mono-resistance to INH, patients have to

follow a 6 months treatment with RIF, PZA and EMB (Mitchison and Nunn, 1986), whilst a mono-resistance to RIF alone, although very uncommon, could be efficaciously defeated in 9 months, employing INH, PZA and streptomycin (Hong Kong Chest Service/British Medical Research Council, 1977). Concerning MDR infections, the best plan of action implicates the use of at least four agents that were shown to be active towards the clinical isolates: among them, one fluoroquinolone (e.g. levofloxacin) additioned to an injectable compound chosen between amikacin, kanamycin and capreomycin (WHO, 2011) are utilized, and any first-line compound with verified efficacy. This treatment has to be followed for 21-24 months, and injectable drugs are usually utilized for 6-8 months (WHO, 2011). In case of XDR infections, the therapeutic strategy becomes even more complicated, requiring the use of linezolid to battle fluoroquinolone resistance, together with a continuous monitoring of treated patients for side effects (Sotgiu *et al*., 2012). In addition, no common agreement about the duration of anti-XDR therapy was achieved so far, highlighting the gravity of this circumstance (Wilson and Tsukayama, 2016). Moreover, the most recent drugs introduced in TB therapy, bedaquiline and delamanid, can be delivered in addition to the other drugs in case the level of resistance and the toxic side effects do not allow a possibly efficacious treatment (WHO, 2013; WHO, 2014).

A further complication of *M. tuberculosis* infections is represented by the co-infection with HIV. One of the most essential reasons that renders this phenomenon highly worrisome, is the fact that RIF, a drug having a central role in TB therapy, is also a strong activator of enzymes involved in drug metabolism, e. g. cytochrome P450 3A4 (Hoagland *et al*., 2016). This acceleration of drug metabolism strongly decreases the plasma concentration of many antiretroviral compounds, thus obligating patients not to perform the two treatments simultaneously (Breen *et al*., 2006). Moreover, considering that co-infected people have a higher probability to interrupt anti-TB therapy ahead of time, they have also a higher frequency of *M. tuberculosis* MDR infections development (Brennan, 1997). Consequently, people affected by both MDR-TB and HIV have few chances to survive, dying in some months (Hoagland *et al*., 2016).

1.6 New antitubercular compounds on the horizon

Among the numerous challenges concerning TB therapy, *M. tuberculosis* drug-resistant spread is one of the most alarming issue. In view of the urgent need of new active agents development, research in TB drug discovery has to never stop, trying to identify new agents that could kill

drug-resistant pathogens, shorten treatment, and limit side effects (Hoagland *et al*., 2016).

After several decades of near inactivity of TB drug development, in the last years a promising pipeline emerged, showing a number of new compounds and repurposed drugs in the different stages of pre-clinical and clinical development (Zumla *et al.*, 2013a) (Tab. 1), as well as the existent gaps in this research, underlying the urgent need for the discovery of new agents (Kana *et al*., 2014).

In this context, two new antituberculars have been recently approved for TB treatment: bedaquiline and delamanid (Fig. 8). Bedaquiline was approved in 2012 by US Food and Drug Administration (FDA) for MDR- and XDR-TB treatment (Cohen, 2013; Wilson and Tsukayama, 2016), and belongs to a new class of antituberculars, diarylquinoline, known to inhibit ATP-synthetase activity (Andries *et al*., 2005). Additionally, it has been shown to be active against murine TB model, as well as against replicating and non-replicating mycobacteria *in vitro* (Matteelli *et al*., 2010). Delamanid, a bactericidal compound active towards both proliferating and non-proliferating bacteria, is a nitroimidazole that has been approved in 2014 in the European Medicines Agency (EMA) (Gler *et al*., 2012; Ryan and Lo, 2014). Delamanid has been shown to be a prodrug, requiring an activating step mediated by the deazaflavin (F420)-dependent nitroreductase (Ddn) (Singh *et al*., 2008). This agent, once activated, inhibits the synthesis of mycolic acids, consequently affecting cell wall formation, the strongest barrier for drugs penetration (Wilson and Tsukayama, 2016). Due to the serious adverse effects observed upon treatment, the approval for bedaquiline and delamanid use was done under certain conditions (Hoagland *et al*., 2016). Specifically, these agents must be inserted in a combination treatment in addition to other three agents shown to be effective, in case no other therapeutic options are available (Wilson and Tsukayama, 2016).

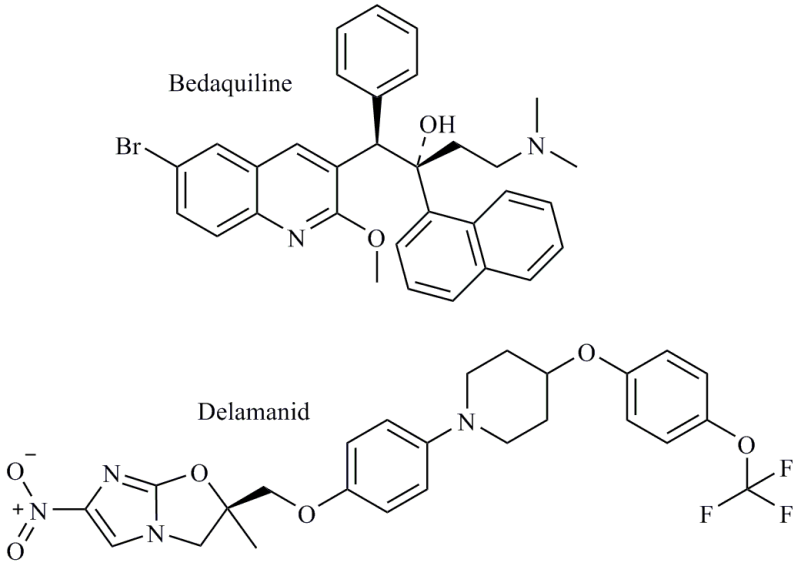

Figure 8. Bedaquiline and delamanid chemical structures.

Another interesting nitroimidazole present in the pipeline, PA824, is nowadays in phase II clinical trials (Tab. 1). This compound, proven to be highly active both *in vitro* and *in vivo*, has been demonstrated to represent a potential drug to abbreviate duration of anti-TB therapy, as well as an active molecule against *M. tuberculosis* drug-resistant strains (Nuermberger *et al.*, 2006; Nuermberger *et al*., 2008). As for delamanid, also PA824 is a prodrug that requires activation mediated by the deazaflavin (F420)-dependent nitroreductase, and once activated, inhibits mycolic acids biosynthesis (Singh *et al*., 2008).

Other compounds present in clinical development, such as SQ109, fluoroquinolones, Q203 and benzothiazinones, with others, will be discussed below.

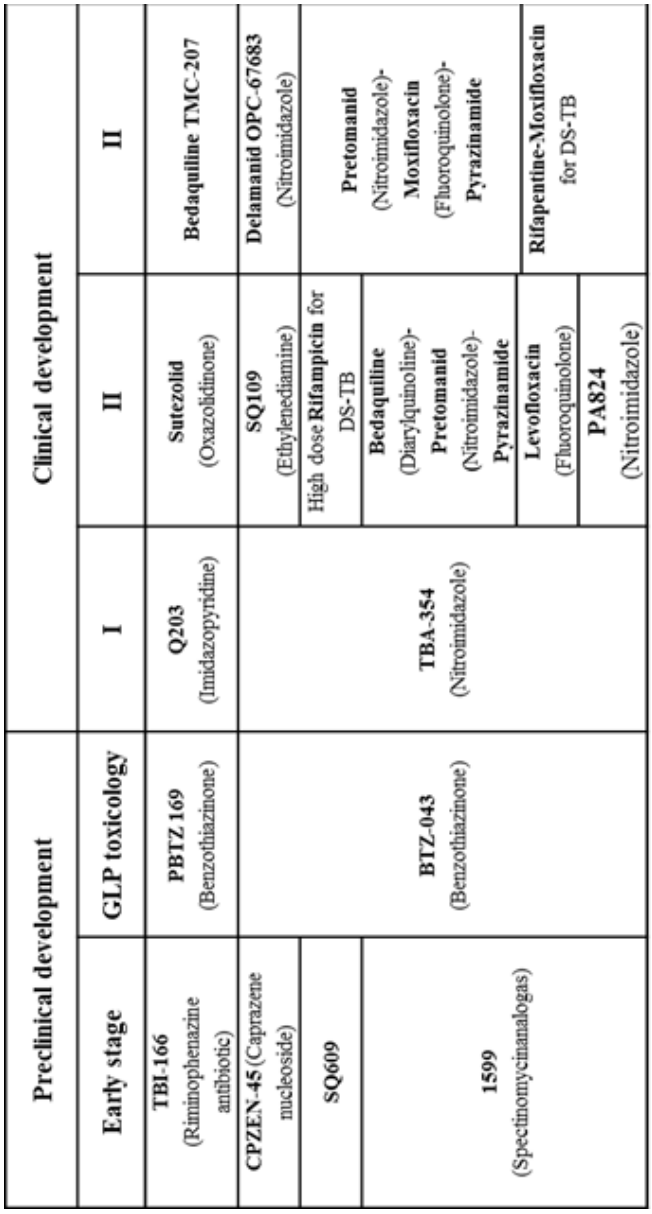

Preclinical development		Clinical development		
Early stage	**GLP toxicology**	**I**	**II**	**II**
TBI-166 (Riminophenazine antibiotic)	**PBTZ 169** (Benzothiazinone)	**Q203** (Imidazopyridine)	**Sutezolid** (Oxazolidinone)	**Bedaquiline TMC-207**
CPZEN-45 (Caprazene nucleoside)	**BTZ-043** (Benzothiazinone)	**TBA-354** (Nitroimidazole)	**SQ109** (Ethylenediamine)	**Delamanid OPC-67683** (Nitroimidazole)
SQ609			High dose **Rifampicin** for DS-TB	**Pretomanid** (Nitroimidazole)-**Moxifloxacin** (Fluoroquinolone)-**Pyrazinamide**
1599 (Spectinomycinanalogas)			**Bedaquiline** (Diarylquinoline)-**Pretomanid** (Nitroimidazole)-**Pyrazinamide**	
			Levofloxacin (Fluoroquinolone)	**Rifapentine-Moxifloxacin** for DS-TB
			PA824 (Nitroimidazole)	

Table 1. Current pipeline of new TB drugs in preclinical and clinical development (From: http://www.newtbdrugs.org/pipeline.php).

1.7 Targets for tuberculosis treatment: past and present

In view of the crucial need of new TB drugs discovery, a significant attention should be focused on the target topic (Fig. 9). In the identification and validation of promising drug targets, it is worth to consider the important properties that a potentially "ideal target" should possess. First of all, it must be essential for *M. tuberculosis* survival, and vulnerable, meaning that a potential drug affecting its activity should kill the pathogen at the lowest concentration as possible (Wei *et al*., 2011; Kana *et al*., 2014). Moreover, a potential target involved in several cellular pathways could supply numerous weapons to rapidly kill the pathogen. Other important features are: a low mutational frequency, a positive aspect that could lead to a reduced drug-resistant strains emergence; and a certain vulnerability in case of TB latent infections (Kana *et al*., 2014). In effect the bacillus develops a latent infection in a high count of infected people, throughout which no pathological symptoms appear. Therefore, since the 2 billion individuals latently infected worldwide represent a convenient storage source for the pathogen, drugs able to eliminate bacteria in latent stage could be extremely precious (Zumla *et al.,* 2013b). Finally, the cellular location of a potential target within the cell is another aspect that could influence the efficacy of a compound: for example, a drug target belonging to enzymatic complexes is more troublesome to be studied in TB drug research, or simply the cell wall could represent a physical unsurmountable barrier to reach an intracellular component (Kana *et al*., 2014). Consequently, an extracellular factor could significantly improve the druggability of an antitubercular compound (Kana *et al*., 2014).

In the research for new TB drugs identification, two main strategies can be followed: the "whole-cell screening" and the "target-based" approaches. The "whole-cell screening" is a phenotypic-based strategy that allowed the identification of several new promising molecules. In particular, all the compounds that are now in clinical development, have derived from this kind of strategy (Lechartier *et al*., 2014). The "whole-cell screening" rational consists in testing definite classes of molecules against *M. tuberculosis*, in order to identify which of them are capable to affect bacterial cell growth or even kill the bacillus (Zuniga *et al*., 2015). The central utility of this kind of screening is providing a direct evidence of tested compounds ability to penetrate bacterial cell wall, thus inhibiting a vulnerable cellular function; on the other side, the negative aspect is that compounds target(s) identification is really tricky, then requiring a lot of additional work, often vain, trying to elucidate the mechanisms of action (Lechartier *et al*., 2014; Zuniga *et al*., 2015).

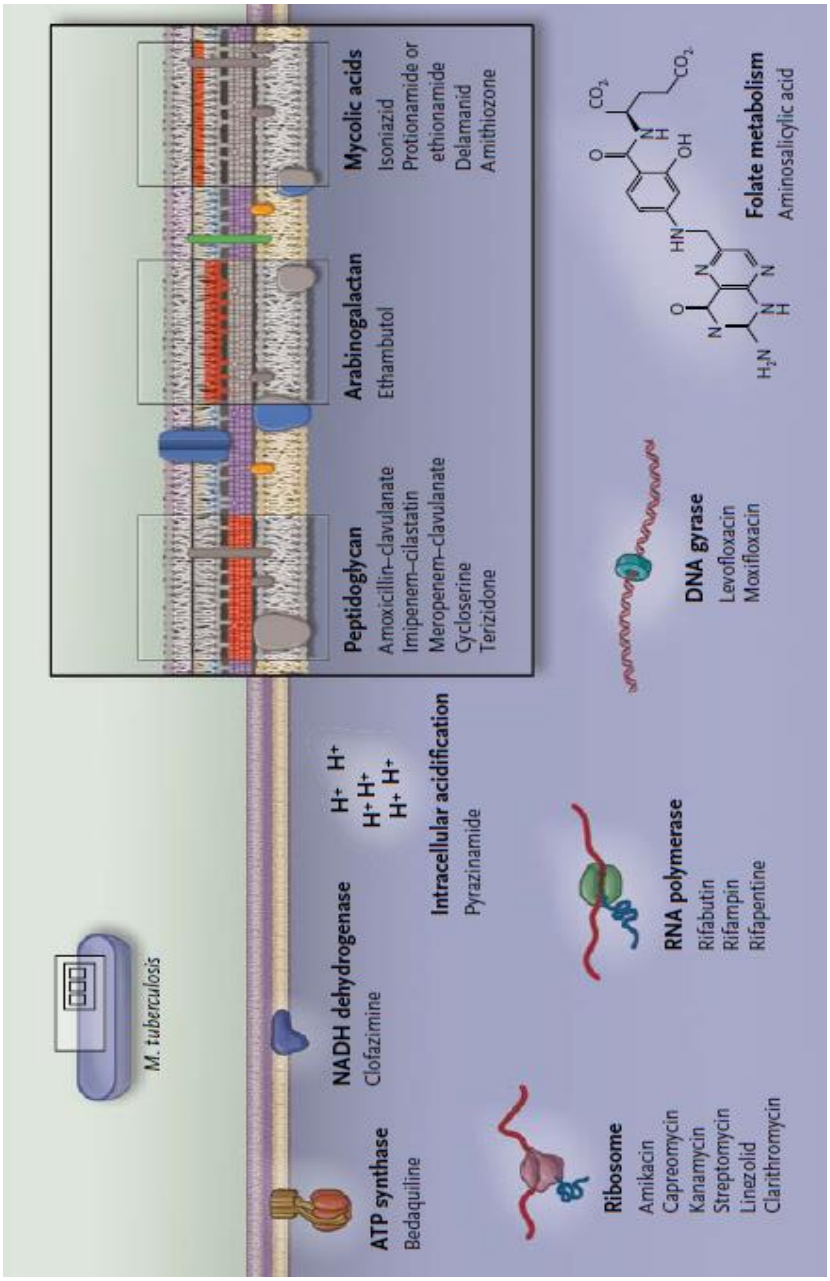

Figure 9. A general overview on the principal *M. tuberculosis* cellular targets and the correspondent drugs that compromise their activity (Horsburgh *et al*., 2015).

The target-based strategy has been employed for a long time, but is quite unsuccessful. In this context, everything starts from a cellular function, usually an enzyme, which is known to be essential for the pathogen life; then, chemical libraries are utilized to perform high throughput screenings (HTS) against this essential enzyme aiming the discovery of active molecules (Cole and Riccardi, 2011). This approach, although selecting compounds that inhibit activity of specific bacterial essential enzymes *in vitro*, usually do not supply the same results at the cellular level (Zuniga *et al*., 2015). There are some possible explanations for that: for example, several of these synthetic compounds are incapable to pass through the mycobacterial cell envelope, or once inside, are immediately brought out *via* efflux pumps, leading to the impossibility to reach the cellular target (Cole and Riccardi, 2011); moreover, the compound could be inactivated by detoxification pathways that occur within the cell, thus losing its activity (Zuniga *et al*., 2015). The consequence is that the tested molecules do not show any bacterial growth inhibition, as well as bactericidal effects (Zuniga *et al*., 2015). A further limitation of the "target-based" approach, is the very limited number of surely validated targets, being the validation process a complex path. There are some criteria that should be satisfied to classify a cellular function as a target of a certain compound: the evidence that the small molecule binds directly to the putative target; the demonstration that the overexpression of the gene encoding for the target enzyme confers a resistant phenotype to the studied compound; and the verification that a decrease in target gene expression increases the sensibility to the compound (Titov and Liu, 2012).

In recent years, in view of the advantages and disadvantages of these two approaches, biochemical and structural studies adopted new strategies to exploit the most beneficial aspects of the two methods. In particular, nowadays tendency of TB drug research, is to combine both "whole-cell screening" and "target-based" approaches, in order to test already known antituberculars against well validated targets, in a sort of "target-based phenotypic screening" (Lechartier *et al*., 2014).

1.7.1 Old targets reintroduction: a cornerstone for new TB drug discovery

A convenient strategy followed to identify new antitubercular compounds, is the proposal of novel derivatives of already known antituberculars inhibiting *M. tuberculosis* targets already characterized to possess essential and extremely vulnerable functions. Among these validated targets, the trans-2enoyl-acyl carrier protein reductase InhA, the β-

subunit of the RNA polymerase and DNA gyrase are the most exploited ones.

InhA is considered a "perfect" target, since once inhibited, mycobacterial cell death immediately occurs (Vilchèze and Jacobs, 2007). Involved in mycolic acids production, it reduces the trans-2enoyl-acyl carrier protein in a NADH-dependent manner, thus allowing fatty acids elongation (Dessen *et al*., 1995). The two best known InhA inhibitors are INH and ETH (Banerjee *et al*., 1994), both prodrugs requiring an activation step to give rise the final active metabolites. As described previously, INH is activated by the peroxidase KatG (Lei *et al*., 2000). Instead, ETH activator is the NADPH-dependent flavin adenine dinucleotide-containing monooxygenase EthA. Once activated, ETH can form, similarly to INH, a covalent adduct with NAD^+, thus bringing about its toxic cellular effects (Vannelli *et al*., 2002). Since high degree of resistance to INH or ETH have been reported to be associated with genetic alterations affecting either *katG* or *ethA* genes, respectively (Vilchèze and Jacobs, 2014), the current effort for new InhA-targeting agents identification consists in searching for molecules that do not require KatG- or EthA-mediated activation.

Considering all the new inhibitors of InhA activity that have been discovered in recent years, one of the most promising for future development is the natural compound pyridomycin (Fig. 10), having an MIC towards *M. tuberculosis* growth of 0.31 μg/ml. What makes this compound even more interesting, is the evidence that pyridomycin and INH/ETH do not share the same mechanism of action; in fact, the mutation causing pyridomycin resistance is a Asp148Gly change. Moreover, *M. tuberculosis* strains resistant to this compound do not show resistance to INH and ETH, and similarly, the most frequent point mutation leading to INH resistance, Ser96Ala, does not confer, instead, resistance to pyridomycin. In view of these knowledges, together with structural analysis, a concrete hope for pyridomycin future studies to combat TB etiologic agent arose (Hartkoorn *et al.*, 2012). In addition, in the last years, to go ahead in this direction, pyridomycin derivatives were chemically synthesized, thus producing even more active compounds (Horlacher *et al*., 2012).

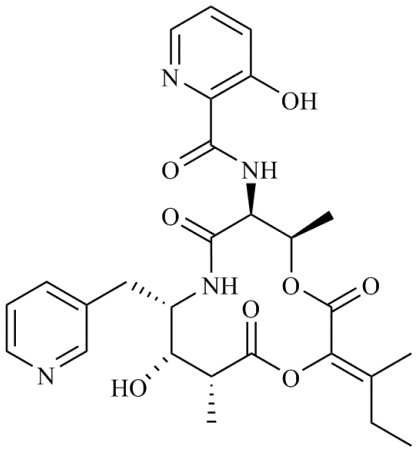

Figure 10. Pyridomycin chemical structure (Hartkoorn *et al.*, 2012).

RNA polymerase (RNAP) is another essential validated *M. tuberculosis* cellular target, largely exploited for TB drug development. The first antitubercular compound identified to affect RNAP is RIF, another key drug for the treatment of drug-susceptible TB infections (Floss and Yu, 2005). Although its efficacy in TB therapy, the RIF-related issues linked to the strong induction of cytochrome P450 and the elevated probability of *M. tuberculosis* resistant mutants emergence represent important limitations. Consequently, researchers felt encouraged to search for new RIF derivatives, trying to overcome these problems.

Two RIF derivatives have been inserted in TB therapy: rifapentine and rifabutin. The former (Fig. 11), even though cross-resistant to RIF, displays important advantages that make this compound useful in TB therapy. First of all, it shows a strong activity against the pathogen both *in vitro* and *in vivo* and, compared to RIF, has a longer half-life, thus giving the possibility to deliver the drug once a week and reduce the treatment span (Benator *et al*., 2002; Sterling *et al*., 2011). The latter (Fig. 11) has been demonstrated to be a less potent cytochrome 450 inducer, thus widely exploited in combination therapy in patients co-infected with TB-HIV. In addition, as rifapentine, it displays a greater efficacy in killing the bacillus compared to RIF (Williamson *et al*., 2013).

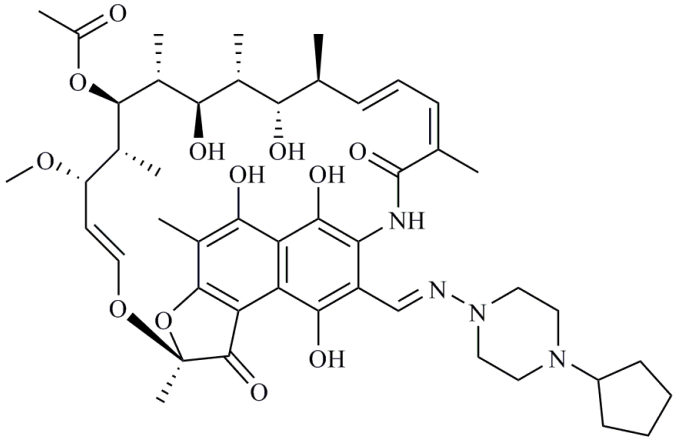

Rifapentine

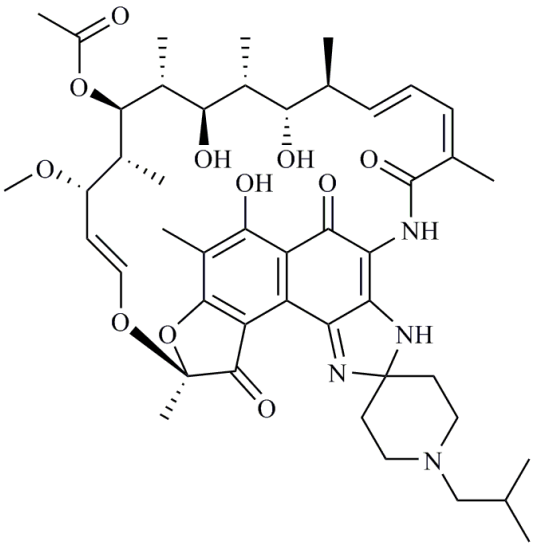

Rifabutin

Figure 11. Rifapentine and rifabutin chemical structures.

DNA gyrase, also known as topoisomerase II, is a *M. tuberculosis* key enzyme involved in monitoring the DNA topology. Precisely, the reaction, which occurs in adenosine triphosphate (ATP) -dependent manner, consists in the formation of a temporary break at DNA level, with a consequent generation of transient covalent bonds between the protein and the broken strands. The final protein structure is composed of four subunits, two encoded by *gyrA* gene, and the remaining two by *gyrB*. These subunits have

distinct functions: the first one is directly involved in the catalytic function of this enzyme, whilst the second contains the site where ATP hydrolysis takes place (Takiff *et al*., 1994; Ehmann and Lahiri, 2014).

The most efficacious class of DNA gyrase inhibitors known so far is represented by fluoroquinolones, and among them, moxifloxacin and gatifloxacin (Fig. 12) emerged as the most active *in vitro*, *in vivo* murine model, (Ji *et al*., 1998; Rodríguez *et al*., 2002) and in humans (Rustomjee *et al*., 2008). Both compounds share a peculiar mechanism of action: the inhibition of DNA gyrase occurs by creating a covalent complex between the enzyme and DNA, thus impeding the generation of the temporary break. Moreover, these two fluoroquinolones, considered potential future first-line compounds, have been already employed to combat MDR-TB infections (Horsburgh *et al*., 2015; Dheda *et al*., 2016; Ruan *et al.,* 2016).

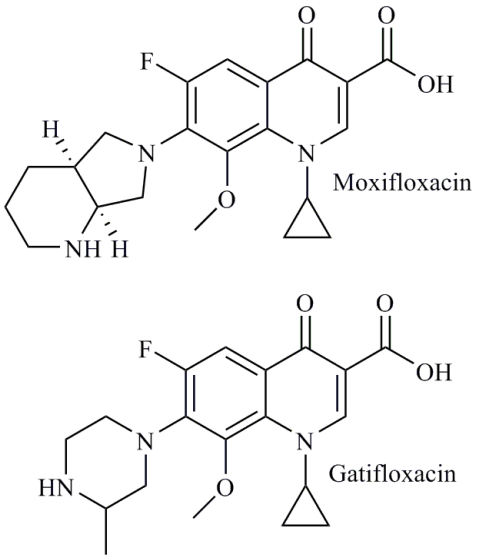

Figure 12. Moxifloxacin and gatifloxacin chemical structures.

Unfortunately, *M. tuberculosis* fluoroquinolone resistant strains already emerged, and genetic studies revealed which are the most frequent mutations responsible for the resistant phenotype. Specifically, these mutations map in a conserved region, named "Quinolone Resistance Determining Region" (QRDR), that overlaps a portion of both *gyrA* and *gyrB* genes (Ginsburg *et al*., 2003).

Trying to overcome fluoroquinolone resistance, TB drug research is attempting to find new DNA gyrase inhibitors. Among the newest

molecules identified, the most promising display inhibitory effects against GyrB ATPase domain, such as aminopyrazinamides (Shirude *et al*., 2013) and the thiazolopyridine urea (Kale *et al*., 2013). In this way, these inhibitors disable the enzyme to utilize the source of energy required to carry out its job (Jeankumar *et al*., 2016). What renders all these new compounds promising topoisomerase II inhibitors, is the fact that mutations responsible for fluoroquinolone resistance mapping in *gyrB*, do not induce, instead, resistance to drugs affecting the DNA gyrase ATPase function, thus justifying the growing interest for them (Jeankumar *et al*., 2016).

1.7.2 New potential targets for the development of new promising antitubercular compounds

In view of the worrisome spread of *M. tuberculosis* drug-resistant strains, with the consequent reduction in therapeutic options to kill the lethal pathogen, the need of novel cellular targets has never been so impelling. Moreover, the achievement of the complete genome sequence of *M. tuberculosis* (Cole *et al.*, 1998), together with the next generation sequencing (NGS) approaches, introduced new tools in drug target discovery panorama. Therefore, in the last years, a number of potential drug targets involved in several essential cellular pathways were identified. The most relevant ones are here described.

Decaprenylphosphoryl-β-D-ribose 2'-oxidase (DprE1), is an enzyme carrying out, together with decaprenylphosphoryl-D-2-keto erytropentose reductase (DprE2), an essential step for the synthesis of mycobacterial arabinan, fundamental component of cell wall arabinogalactan. Precisely, DprE1 and DprE2 convert decaprenylphosphoryl-β-D ribose (DPR) into decaprenylphosphoryl arabinose (DPA), through an epimerization reaction, and specifically, DprE1 is involved in the first part of the reaction, working in a FAD-dependent manner (Mikusová *et al.*, 2005; Kolly *et al*., 2014). Moreover, DprE1 is able to oxidize again its FAD cofactor by reducing several different organic molecules (Neres *et al*., 2012). The wide range of specificity towards different substrates, could explain why so many classes of compounds have been identified so far as DprE1 inhibitors. For this reason, this enzyme has been named "magic drug target" (Manina *et al.*, 2010).

The first class of DprE1 inhibitors identified is represented by the 1,3 benzothiazin-4-ones (BTZs) (Makarov *et al*., 2009). Among them, the 8-nitro benzothiazinone BTZ043 (Fig. 13) emerged as the antitubercular with the highest potency against *M. tuberculosis* growth (Makarov *et al*., 2009).

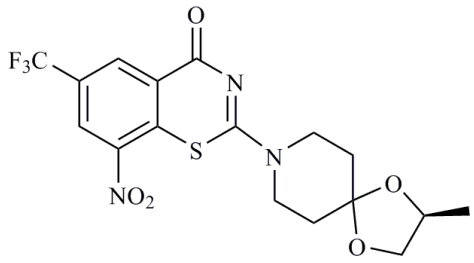

Figure 13. BTZ043 chemical structure.

This compound is a prodrug that requires to be activated in order to fulfill its inhibitory effect. It has been shown that the activating step is performed by DprE1 itself (Neres *et al*., 2012; Trefzer *et al*., 2012), and consists in the reduction of the nitro group to a nitroso one, thus re-oxidizing the FAD cofactor. Then, once activated, it makes up a covalent bond between its nitroso group and a cysteine residue of DprE1 active site, with a consequent irreversible inhibition of the enzymatic activity (Trefzer *et al*., 2012).

Although BTZ043 is the most active antitubercular compound *in vitro*, this efficacy was not reflected in a TB murine model, thus justifying the further investigations that have been performed successively, aiming the improvement of the *in vivo* efficacy of this compounds. From these copious analysis, PBTZ169 came out, derived from the addition of a cyclohexylmethyl-piperazine mojety within the BTZ structure (Makarov *et al.*, 2014) (Fig. 14).

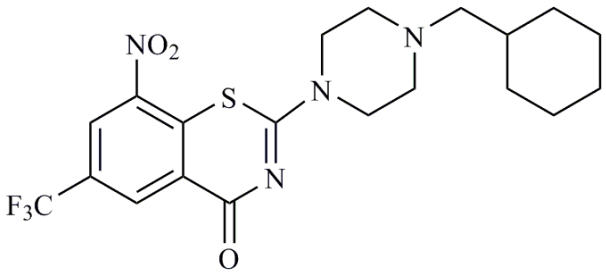

Figure 14. PBTZ169 chemical structure.

PBTZ169 immediately displayed several positive aspects: an increased affinity towards DprE1 cellular target, higher potency in TB mouse model, and a decreased toxicity (Makarov *et al.*, 2014). Consequently, at the beginning of 2016, PBTZ169 entered Phase I clinical trials in Russia (http://www.nearmedic.ru/en/node/690).

Mycobacterial membrane protein large 3 (MmpL3) is an essential transmembrane transporter principally engaged in exporting trehalose monomycolate (TMM) outside the bacterial cell, across the cell membrane *via* a proton antiport system (Varela *et al*., 2012; Tahlan *et al*., 2012; Murakami, 2008). MmpL3 possesses 12 transmembrane domains, and is part of mycobacterial membrane protein large (MmpL) family, which in turn belongs to the group of resistance nodulation division (RND) efflux pumps (Domenech *et al.,* 2005).

Among the compounds identified to affect MmpL3 activity, the first one was the 1,5-diarylpyrrol derivative BM212. This molecule, having displayed activity against a high number of drug-resistant clinical isolates (Deidda *et al*., 1998), was utilized for further investigations in order to find new BM212 derivatives with improved properties, both *in vitro* (Biava *et al*., 2006) and *in vivo* murine models (Poce *et al*., 2013).

Moreover, another compound found to target MmpL3 protein is the 1,2-diamine SQ109 (Fig. 15), nowadays localized in phase II clinical trials (Sacksteder *et al*., 2012). Despite being an EMB analog, SQ109 displayed activity against EMB-resistant *M. tuberculosis* strains, thus highlighting a different mechanism of action (Protopopova *et al*., 2005). Particularly, biochemical analysis revealed that SQ109, by inhibiting MmpL3 activity, causes an intracellular accumulation of TMM, thus blocking cell wall formation (Tahlan *et al*., 2012). In addition, SQ109 is also active against *M. tuberculosis* latent bacilli, phenomenon which was not observed studying other cell wall synthesis inhibitors (Zhang *et al*., 2012). The explanation for this unusual behavior was given by further recent investigations, that uncovered SQ109 to be a compound targeting more than one cellular functions. For instance, it has been demonstrated that this compound and its derivatives, interfere with electron transport and act as uncouplers, thus leading to a failure of pH gradient and membrane potential maintenance, that are at the base of several transporters operations (Li K *et al*., 2014). Then, putting together all these findings, researchers started supposing that the TMM accumulation registered upon SQ109 action, could be mainly induced by the dissipation of the proton gradient, and MmpL3 inhibition may have only a secondary role (Li W *et al.,* 2014). In conclusion, the role of MmpL3 as cellular target of all the inhibitors identified so far, should be re-examined in depth, in order to better clarify their mechanisms of action (Li W *et al*., 2014).

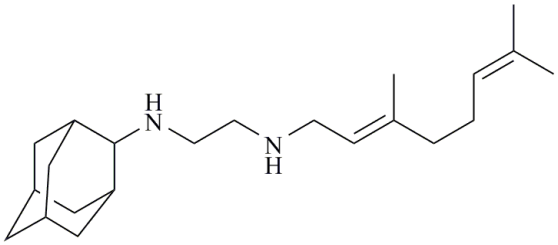

Figure 15. SQ109 chemical structure.

Cytochrome bc_1 complex is an essential enzyme involved in the energy conversion apparatus, linking the passage of electrons from a quinol to a cytochrome-c and the flow of protons throughout the membrane, a fundamental step for ATP production (Kleinschroth *et al*., 2011; Hunte *et al*., 2003). Several observations have confirmed the great relevance of cytochrome bc_1 in bacillus survival and growth, thus encouraging TB drug research to analyze more in depth this promising new target. Furthermore, recent studies highlighted that this complex contains three main catalytic components, cytochrome *b* (QcrB), cytochrome c_1 and the Rieske iron-sulfur protein (Kleinschroth *et al*., 2011). Among the cytochrome bc_1 inhibitors identified so far, Q203 and Lansoprazole emerged, both targeting QcrB component (Pethe *et al*., 2013; Rybniker *et al*., 2015).

The importance of Q203 compound resides in its effectiveness against both *M. tuberculosis* H37Rv reference strain (MIC_{50} equal to 2.7 nM) and drug-resistant clinical isolates, in its pharmacokinetic profile that reveals a bioavailability of 90% and in its capacity of decreasing granuloma development (Pethe *et al*., 2013). Moreover, cytotoxicity studies highlighted a good safety profile, since no cytotoxic sign has been observed up to 10 µM of the compound, and upon a long exposure, Q203 is well tolerated (Pethe *et al*., 2013). All these positive aspects fuel the hope of shortening TB therapy with the possible future use of this compound, being so active at low concentration against the pathogen (Pethe *et al*., 2013).

Lansoprazole (LPZ) is an already known drug widely utilized to treat stomach disorders, in particular those related to an excessive acidic pH (Welage, 2003). This compound is a proton-pump (H+K+- ATPase) inhibitor, and has been demonstrated to be a prodrug that undergoes different kinds of activation. Within the acidic stomach environment, LPZ is converted into the sulfenic acid intermediate that leads to the block of the gastric proton pump. On the other side, once activated within the *M. tuberculosis* intracellular environment through its conversion into lansoprazole sulfide (LPZS), it possesses activity against both *M.*

tuberculosis drug-susceptible and drug-resistant strains (Fig. 16) (Rybniker *et al.*, 2015). LPZS active compound, no more able to inhibit gastric H^+K^+-ATPase, targets both QcrB and ATP synthesis within the bacillus. All these positive aspects make this molecule an extremely interesting lead compound for further development of efficacious antituberculars. It is clear that LPZ is a good example of a new effect identified in a molecule already known for a completely different activity (Rybniker *et al.*, 2015).

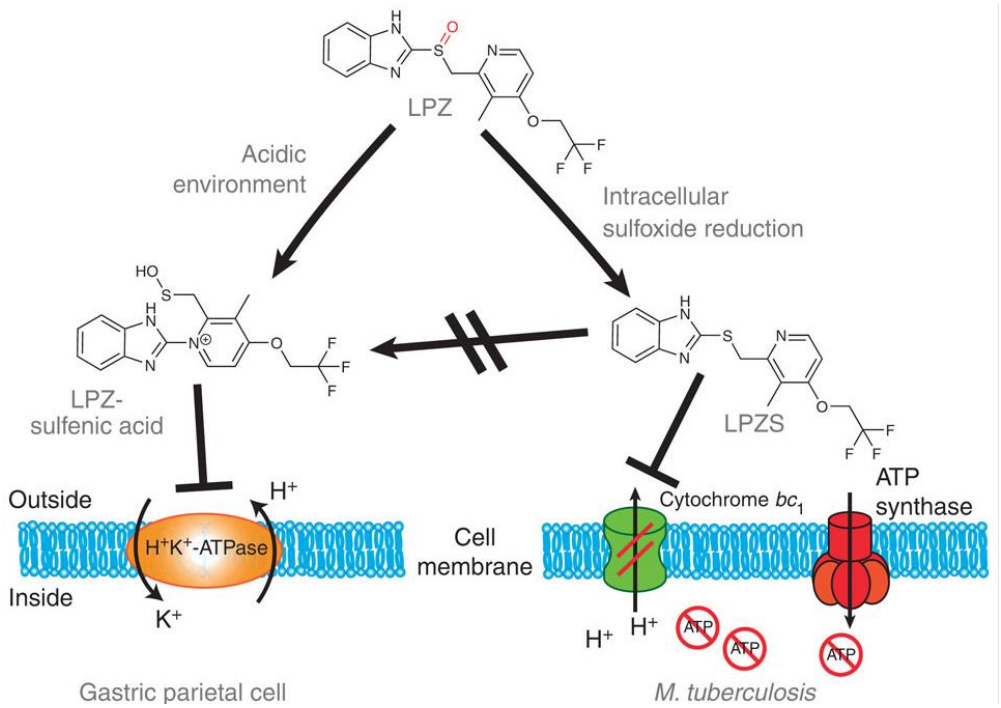

Figure 16. Mechanisms of LPZ activation (Rybniker *et al*., 2015).

ATP synthase is an essential enzyme for *M. tuberculosis* growth involved in the synthesis of ATP through the reaction between adenosine diphosphate (ADP) and inorganic phosphate (P_i). This multi-subunit protein is a membrane-embedded complex made of two domains, named F_1 and F_0, that are structurally connected. The synthase catalytic function, that allows ATP production, resides within the F_1 domain, whilst F_0 contains a rotor ring that produces a rotational energy that is then spread to the F_1 component (Boyer, 1997; Walker, 2013; Preiss *et al*., 2015). It has been shown that *M. tuberculosis* ATP synthase has an important role in favoring pathogen growth even in disadvantageous conditions, like nutrients starvation (Koul *et al*., 2011). Considering the essentiality of this enzyme, it

is understandable the importance of finding inhibitors able to completely block its activity. Among them, the class of diarylquinoline represents the most efficacious one (Andries *et al*., 2005). Bedaquiline, the diarylquinoline described previously, has a mechanism of action consisting in a highly specific direct inhibition of the rotor ring of *M. tuberculosis* ATP synthase (Andries *et al*., 2005; Preiss *et al*., 2015). Being active against both actively replicating and dormant mycobacteria, it captured the attention of TB drug research (Lounis *et al.,* 2006). Particularly, it has been demonstrated that this compound could potentially shorten therapy for people affected by drug-resistant infections, particularly if bedaquiline delivery is coupled with PZA (Lounis *et al*., 2006; Ibrahim *et al*., 2007; Diacon *et al*., 2009). From a chemical point of view, bedaquiline possesses two chiral centers, thus giving rise to four stereoisomers and, among them, the R207910 has been shown to be the best one, with a MIC_{90} of 0.06 µg/ml (Koul *et al*., 2007). Unfortunately, as described before, bedaquiline use has many safety issues that have to be considered. Several adverse effects have been registered, such as altered transaminases, nausea, arthralgia, headache, among others. For these reasons, it is worth to further investigate on new compounds inhibiting ATP synthase activity (Kakkar and Dahiya, 2014).

1.8 Bacterial CTP synthetase and pantothenate kinase: two essential functions as potential targets for antimicrobials development

De novo pyrimidine biosynthesis is an essential pathway that gives rise to important DNA precursors (Djaout *et al.,* 2016). For this reason, inhibitors targeting different steps of this pathway are capturing the attention of TB drug research. In this context, a particular attention was recently focused on the *M. tuberculosis* thymidylate synthase ThyX, an essential enzyme which is not correlated with the correspondent enzyme in humans (Myllykallio *et al*., 2002; Koehn *et al*., 2009). In detail, the reaction catalyzed by this enzyme is a methylation of 2′ -deoxyuridine-5′ -monophosphate (dUMP) thus producing 2′ -deoxythymidine-5′ -monophosphate (dTMP), an essential component for DNA biosynthesis (Djaout *et al.,* 2016). Among the ThyX inhibitors identified so far, naphthoquinone (NQ) was recently uncovered. This drug, already known to possess anti-tumor and anti-malarian effects, unveiled also antibacterial and antimycobacterial activity, successively discovered to inhibit, together with its derivatives, *M. tuberculosis* ThyX (Tran *et al*., 2004; van der Kooy *et al*., 2006; Djaout *et al.,* 2016; Karkare *et al.,* 2013).

Being aware of the importance of pyrimidine biosynthesis for *M. tuberculosis* growth and survival, and in view of the increasing interest

focusing on that, TB research is going ahead in this direction, concentrating also on other parts of this biosynthetic pathway.

Cytidine 5' triphosphate (CTP), a key nucleotide for the biosynthesis of DNA, RNA and phospholipids (Kent and Carman, 1999), is produced by enzymes called CTP-synthetases, that catalyze the conversion of uridine triphosphate (UTP) into CTP in ATP-dependent manner (Fig. 17) (Long and Pardee, 1967; Endrizzi *et al.*, 2004; Barry *et al.*, 2014). CTP levels are highly controlled within the cell, particularly regulated by both CTP and UTP cellular concentration, as well as by GTP (Barry *et al.*, 2014). Moreover, it has been demonstrated that CTP synthase is an essential enzyme for growth of several bacteria, e.g. *Escherichia coli* (Gerdes *et al.*, 2003) and *Haemophilus influenzae* (Akerley *et al.*, 2002). For all these reasons, knowing the desperate need of new drug targets identification, there is a growing interest in investigating this essential pathway to find novel weak points for pathogen killing.

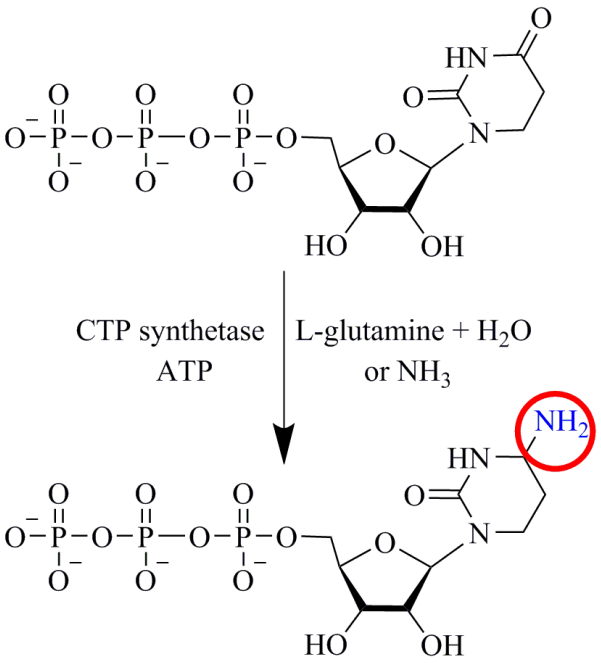

Figure 17. Enzymatic reaction catalyzed by CTP synthetase.

Pantothenate kinase (PanK), instead, is an enzyme that catalyzes the rate-limiting ATP-dependent phosphorylation of pantothenate to 4′-phosphopantothenate (Fig. 18) (Jackowski and Rock, 1981), a fundamental precursor of the cofactor coenzyme A (CoA). It has been demonstrated that PanK is essential for *M. tuberculosis* survival, thus encouraging further investigations on its potential role as new target against TB. However, up to now, no PanK inhibitors with antitubercular activity have been identified (Gerdes *et al*., 2002; Spry *et al*., 2008). Trying to find new *M. tuberculosis* PanK inhibitors, "target-based" approach was widely utilized performing screening of chemical libraries on PanK activity. Among compounds that have been tested, some triazoles and biaryls emerged (Björkelid *et al.*, 2013). Through crystallographic studies, it has been shown that both triazoles and biaryls classes of compounds are able to bind to PanK active site. In particular, all the triazoles tested showed to be competitive inhibitors towards ATP, whilst the biaryl molecules resulted to behave as non-competitive ones (Björkelid *et al.*, 2013). Successively these compounds were tested against *M. tuberculosis* growth, resulting inactive (Björkelid *et al.*, 2013), probably for the "target-based" approach well known limitations.

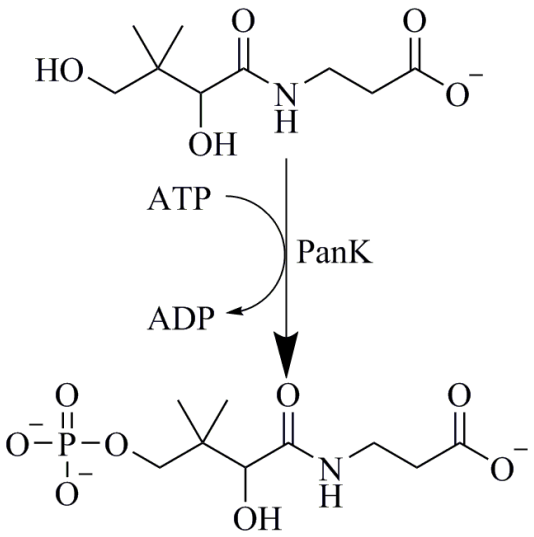

Figure 18. Enzymatic reaction catalyzed by pantothenate kinase.

2. Aims of the work

Tuberculosis (TB), an old disease come back as a serious current issue, is killing an increasingly high number of victims every year worldwide. In fact, World Health Organization declares TB as a major global health problem, and the second leading cause of death provoked by an infectious disease worldwide: new drugs are urgently needed.

This research is inserted in the "More Medicines for Tuberculosis" (MM4TB EC-VII framework program) project, aiming to validate at least five new drug targets and the identification of at least one class of new potential antituberculars. Within this project, two new antitubercular compounds, the 7947882 and 7904688, emerged for their good activity against the pathogen. Genetic and biochemical approaches demonstrated the two agents to be prodrugs activated by the monooxygenase EthA, and sequencing data led us to hypothesize the CTP-synthetase PyrG and the pantothenate kinase PanK being their cellular targets.

Going in this direction, the present research can be divided in three main parts.

Firstly, the aims of the thesis project were the identification of 7947882 and 7904688 active metabolites derived from EthA-mediated activation, together with the definitive validation of PyrG and PanK as targets of the 7947882 and 7904688, by employing biochemical strategies.

Successively, in a context of "multitargeting antituberculars research", the second part focused on the identification of further compounds able to inhibit both PyrG and PanK enzymatic activities bypassing EthA activation, utilizing *in silico* and *in vitro* approaches. In fact, drugs able to inhibit more cellular targets are, without any doubt, more efficacious in killing the pathogen and in overcoming the *M. tuberculosis* drug-resistant strains issue.

Finally, since a certain similarity between *M. tuberculosis* PyrG and human CTP-synthetase-1 (hCTPS-1) has been observed, the third topic of the thesis aimed to express and purify the recombinant human enzyme to test all *M. tuberculosis* PyrG inhibitors. The purpose of this strategy was not only to check the possible cross-reactivity of these agents with the human enzyme, but also the identification of compounds with a selective inhibitory effect against the bacterial enzyme. In fact, agents able to affect only the mycobacterial CTP-synthetase could be employed for further structural optimizations, aiming the achievement of even more effective and less toxic antitubercular derivatives.

3. Materials and methods

3.1 Bacterial and yeast strains

Bacterial and yeast strains utilized in this work are listed in Table 2. *E. coli* XL1 Blue was employed for cloning experiments, whilst *E. coli* BL21(DE3) for recombinant protein expression. *Pichia pastoris* KM71H yeast strain, kindly provided by Prof. Andrea Mattevi, (Pavia University, Pavia, Italy), was utilized for human CTP synthetase-1 (hCTPS-1) expression.

Strains	Features	Source
***E. coli* XL1-Blue**	*endA1 gyrA96*(nal^R) *thi-1 recA1 relA1 lac glnV44* F'[::Tn10 proAB$^+$ lacI^q Δ(lacZ)M15] *hsdR17*(r_K^- m_K^+)	Stratagene
***E. coli* BL21(DE3)**	F- *ompT hsdSB* (*rB- mB-*) *dcm* (DE3)	Laboratory collection
***P. pastoris* KM71H**	*arg4 aox1::ARG4*	Invitrogen

Table 2. Bacterial and yeast strains used in this work.

3.1.1 Growth media and conditions

E. coli XL1-Blue and BL21(DE3) cells were grown in Luria-Bertani (LB) broth/LB LOW SALT or on LB/LB LOW SALT agar (18 g/l) at 37°C. When necessary, media were supplemented with kanamycin (50 μg/ml), ampicillin (100 μg/ml), or zeocin (25 μg/ml), 5-bromo-4-chloro-indolyl-β-D-galactopyranoside (X-Gal) (0.04 μg/ml) and isopropyl β-D-1-thiogalactopyranoside (IPTG) (1.7 μM) (Table 3).

P. pastoris strain was grown in Yeast Extract Peptone Dextrose Medium (YPD) (Table 3) at 30°C for cell competent preparation and transformation, and in Buffered Glycerol-complex Medium (BMGY)/Buffered Methanol-complex Medium (BMM) (Table 3) at 30°C for protein expression.

Medium	Components	
LB broth	Tryptone	10 g/l
	Yeast Extract	5 g/l
	NaCl	10 g/l
	Sterile Water to	1 l
LB broth LOW SALT	Tryptone	10 g/l
	Yeast Extract	5 g/l
	NaCl	5 g/l
	Sterile Water to	1 l
YPD	Yeast Extract	1%
	Peptone	2%
	Dextrose	2%
	Sterile Water	to 1 l
BMGY	Yeast Extract	1%
	Peptone	2%
	Potassium phosphate pH 7.5	100 mM
	YNB	1.34%
	Biotin	4×10^{-50}%
	Glycerol	1%
BMM	Potassium phosphate pH 7.5	100 mM
	YNB	1.34%
	Biotin	4×10^{-50}%
	Methanol	0.5%

Table 3. Components of media used in this work.

3.2 Plasmids and cloning procedures

All DNA manipulation procedures were done according to standard protocols described by Sambrook and Russel (2001).

The genes cloned were purified from agarose gel employing Wizard SV Gel and PCR Clean-Up System (Promega) and ligated into the correspondent vector utilizing T4 ligase (Promega). All the restriction enzymes (Promega) were used following the manufacturer's protocols. Both *E. coli* and *P. pastoris* electrocompetent cells were transformed by electroporation, utilizing Bio-Rad Gene Pulser. After that, *E. coli* cells were plated onto LB plates when transformed with pGEM-T Easy, pET SUMO or

pET-28a vectors (described below), whilst when transformed with pPIZ-B-eGFP vector (described below), were plated on LB LOW SALT. *P. pastoris* cells transformed with pPIZ-B-eGFP vector were plated onto YPD plates. All plates were supplemented with the required antibiotic.

Plasmids purification was done either with an alkaline-lysis extraction (Sambrook and Russell, 2001) or using the Plasmid Mini kit (Qiagen).

pGEM-T Easy plasmid (Promega) is a 3015 bp long vector utilized for cloning and sequencing of PCR products.

Plasmids utilized in this work for expression of *M. tuberculosis* proteins in *E. coli* are shown in Figure 19.

The pET SUMO (Invitrogen) (Fig. 19) expression vector, utilized for *M. tuberculosis* EthA expression, is a plasmid for *E. coli* that allows the expression and purification of recombinant proteins, fused with a small ubiquitin-like modifier (SUMO). Fusion with SUMO increases the solubility of expressed proteins and may increase their expression level. Moreover, the SUMO tertiary structure is recognized and cleaved by an ubiquitin-like protein-processing enzyme, SUMO protease, resulting in the production of a native protein.

The pET-28a (Novagen) (Fig. 19), used for *M. tuberculosis* PyrG and PanK expression, is a 5369 bp vector utilized to express recombinant proteins in *E. coli*. It carries an N-terminal His-Tag/thrombin/T7-Tag configuration in addition to an optional C-terminal His-Tag sequence, together with a kanamycin resistance gene. Moreover, it shows a T7*lac* promoter, thrombin cleavage site and internal T7 epitope tag.

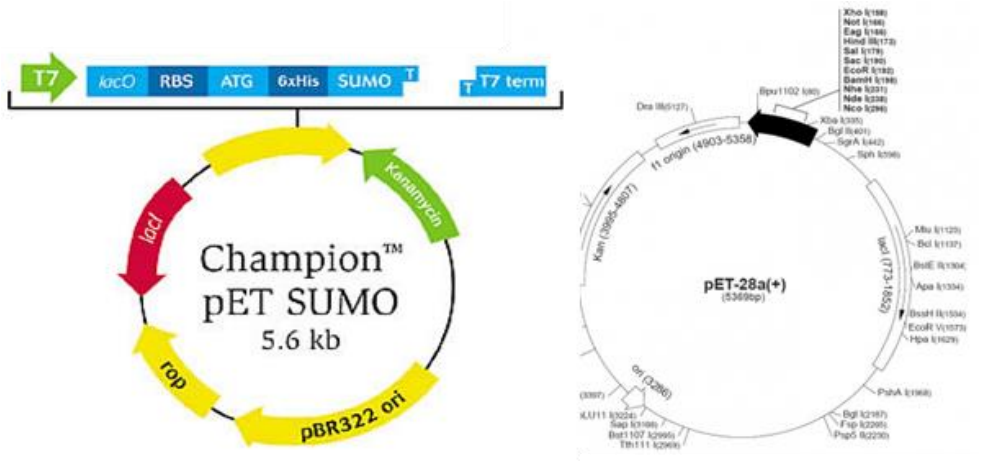

Figure 19. Maps of plasmids used for expression of *M. tuberculosis* proteins.

For cloning and expression of hCTPS-1 in *P. pastoris*, the pPICZ-B-eGFP vector was utilized. The pPICZ-B-eGFP plasmid (Figure 20) is a modified version of the 3.3 kb expression vector pPICZ-B (Invitrogen) in which an enhanced Green Fluorescent Protein (eGFP) was inserted in the cloning site. In this way, the final recombinant protein possesses the eGFP at the C-terminus, in addition to a peptide containing the c-myc epitope and a polyhistidine (6xHis), allowing a direct fluorescent signal detection of the expressed product (Prof. A. Mattevi, personal communication). Moreover, the vector carries a 5' fragment with the AOX1 promoter for methanol-inducible expression of the cloned gene (Ellis *et al.*, 1985; Koutz *et al.*, 1989; Tschopp *et al.*, 1987) and a gene conferring zeocin resistance in both *E. coli* and *P. pastoris* (Drocourt *et al.*, 1990; Baron *et al.*, 1992). The human full length *CTPS-1* cDNA was purchased from Dharmacon, cloned into pOTB7 vector.

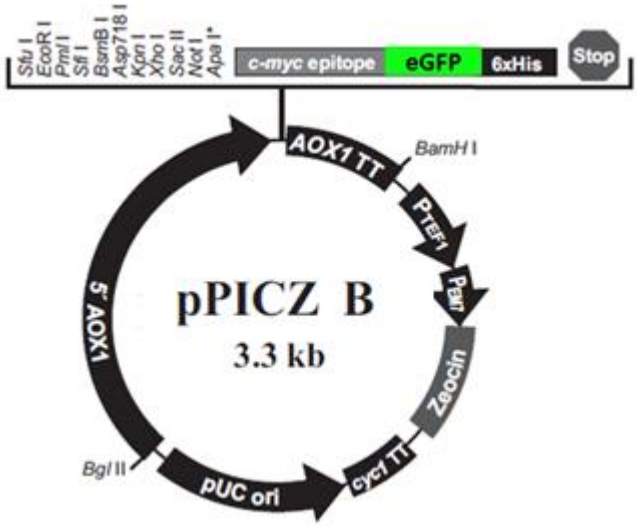

Figure 20. Map of the expression vector pPICZ-B-eGFP.

3.3 Polymerase Chain Reaction (PCR)

PCR procedure is based on the synthesis, performed by DNA polymerase, of a new strand of DNA complementary to a certain template. The reactions are characterized by 20-40 temperature changes, called cycles, that lead to the production of billions of copies of the desired DNA fragment. PCR reactions were performed in a final volume of 40 µl, in which 2 mM of each dNTP, 0.5 pmol/µl of each primer, 2% dimethylsulfoxide (DMSO), 2.5 mM $MgCl_2$, 50 ng of DNA template (plasmid DNA) and 1 U of Pfu DNA Polymerase (Promega) were added.

Cycles conditions were as follow: denaturation step at 95°C for 2 min, then 30/35 cycles of denaturation at 95°C for 1 min, annealing at a temperature depending on melting temperature of the primer utilized, and elongation at 72°C for a time dependent on product sequence length, with a final elongation at 72°C for 5 min. All primers used for PCR are listed in Table 4.

Primers	**Sequence 5'-3'**	**Purpose**
hpyrG28a FOR	TTGGATCCATGAAGTACATTCTG (BamHI)	Cloning of *hCTPS-1* in pET 28a
hpyrG28a REV	TTCTCGAGGTCAGTCATGATTTA (XhoI)	Cloning of *hCTPS-* in pET 28a
hctps1pichia FOR	TTGGATCCAAGTACATTCTGGTT (BamHI)	Cloning of *hCTPS-1* in pPICZ-B
hctps1pichia REV	TTGCGGCCGCGTCATGATTTATTG (NotI)	Cloning of *hCTPS-1* in pPICZ-B
hctps1pichiaseq FOR	AGAACTTTTGTAACATCCACGT	Sequencing of *hCTPS-1* from pPICZ-B
hctps1pichiaseq REV	ACGTGGATGTTACAAAAGTTCT	Sequencing of *hCTPS-1* from pPICZ-B
AOXfor	GACTGGTTCCAATTGACAAGC	Sequencing of *hCTPS-1* from pPICZ-B
AOXrev	GCAAATGGCATTCTGACATCC	Sequencing of *hCTPS-1* from pPICZ-B

Table 4. Primers used in this work.

3.4 *Pichia pastoris* competent cells preparation and transformation

P. pastoris KM71H chemically competent cells (Lin-Cereghino *et al*., 2005) were prepared as follows: 5 ml of *P. pastoris* KM71H cells pre-inoculum was grown overnight in YPD medium at 30°C in shaking conditions (300 rpm); the next day, the pre-inoculum was diluted in a final volume of 50 ml of the same medium, to reach an OD_{600} between 0.15 and 0.2; the yeast colture was grown at 30°C until OD_{600}=0.8-1.0 was reached, and then cells were collected by centrifugation at room temperature; successively, pellet was resuspended in ice-cold BEDS solution (10 mM bicine-NaOH, pH 8.3, 3% (v/v) ethylene glycol, 5% (v/v) dimethyl sulfoxide (DMSO), and 1 M sorbitol) supplemented with 1 M dithiothreitol (DTT), and, after 5 minutes of incubation followed by centrifugation, cells were resuspended in 1 ml of BEDS without adding DTT. Competent cells are stored at -80°C.

For yeast transformation, 50-100 ng of pPICZ-B/*hCTPS-1* recombinant plasmid linearized with *Sac*I restriction enzyme (Promega) were incubated with 40 µl of *P. pastoris* KM71H competent cells, kept on ice for 2 minutes. For cell transformation, electroporator was utilized with a charging voltage of 1500 Volt, a resistance of 200 Ohm and a capacitance of 50 µFaraday. After electroporation, cells were transferred in sterile conditions in 500 µl 1M sorbitol + 500 µl YPD and incubated at 30°C on shaker for 1-3 hours. Then, *P. pastoris* transformed cells were plated on YPD agar plates supplemented with 100 µg/ml zeocin, and plates were incubated at 30°C for 2-3 days until some yeast colonies appeared.

3.5 Protein expression and purification

3.5.1 EthA expression and purification

E. coli BL21(DE3) One Shot® cells transformed with pET-SUMO/*ethA* were grown overnight in a pre-inoculum at 37°C in LB additioned with kanamycin (50 µg/ml). Then, the pre-inoculum was diluted 50 times in 6 l of the same medium and grown at 37°C until cells reached OD_{600nm} = 0.6–0.8. Protein expression was induced by IPTG 0.5 mM, 3 hours at 37°C. Cells were collected by centrifugation and resuspended in lysis buffer (50 mM sodium phosphate pH 8.0, 1% triton-X100, 300 mM NaCl) and broken by sonication. The cellular lysate was then centrifuged and the supernatant applied to a His-trap column (1 ml, GE-Healthcare), equilibrated in lysis buffer. The column was washed with 50 mM imidazole, then EthA was eluted with 250 mM imidazole, dialyzed in 50 mM sodium phosphate pH 8.0, 150 mM NaCl, and incubated with SUMO protease in

order to eliminate the tag, getting a native protein after a second purification step on the His-trap column. The purity was checked with SDS-PAGE analysis, and the protein concentration was calculated by measuring absorbance at 280 nm (ε=97290 M^{-1} cm^{-1}).

3.5.2 PyrG expression and purification

pET-28a/*pyrG* recombinant vector was transformed in *E. coli* BL21(DE3) cells. The transformed cells were grown in a pre-inoculum LB medium additioned with kanamycin (50 µM) up to OD_{600nm} = 0.6–0.8, then diluted 50 times in the same medium. PyrG protein was expressed with the following induction conditions: 0.5 mM IPTG for 12 hours at 25°C. Cells were then harvested by centrifugation, sonicated and resuspended in lysis buffer containing 50 mM sodium phosphate pH 8.0 and 300 mM NaCl. The protein was purified using a HisTrap column, through an elution step with 250 mM imidazole. Therefore, the eluted protein was dialyzed against 50 mM potassium phosphate pH 7.5, 50 mM KCl. The concentration of purified protein was evaluated measuring the absorbance at 280 nm (ε=40715 M^{-1} cm^{-1}) and SDS-PAGE was utilized to check samples purity.

The same procedure was employed to express and purify the PyrG mutant (V186G) enzyme.

3.5.3 PanK expression and purification

E. coli BL21(DE3) cells transformed with pET-28a/*coaA* construct were grown in a pre-inoculum LB liquid medium to which kanamycin was added at the proper concentration, up to OD_{600nm}= 0.6-0.8, diluted 50 times in the same medium and induced with 0.5 mM IPTG for 5 hours at 37°C. After collection, cells were resuspended with lysis buffer containing 50 mM sodium phosphate pH 8, 600 mM NaCl, and 25 mM imidazole, supplemented with protease inhibitor cocktail (Sigma), and then sonicated. Once the cell lysate was centrifuged, the supernatant was applied to a HisTrap column. PanK protein was eluted with 250 mM imidazole and dialyzed against 100 mM TrisHCl pH 8, 150 mM NaCl and 5% glycerol. Protein concentration was determined by absorbance at 280 nm (ε=36900 M^{-1} cm^{-1}), and SDS-PAGE analysis was performed to control the purification steps.

The purification of PanK mutant (Q207R) protein was done with the same protocol.

3.5.4 hCTPS-1 expression and purification

In order to identify *P. pastoris* KM71H cells transformed with pPICZB/*hCTPS-1* expressing hCTPS-1 protein, each colony was inoculated

in 2 ml of BMGY medium utilizing a plate with 24 wells, thus incubated at 30°C shaking at 280 rpm for 60 hours. Successively, for protein expression induction, the medium was exchanged with BMM. In order to establish the best induction time, fluorescence signals were checked after 24, 48 and 72 hours by using a Clariostar plate reader (BMG Labtech; excitation 489 nm, emission 509 nm), thus identifying the clone having the highest fluorescence signal. To scale up, the single positive colony identified was grown in a 15 ml pre-inoculum of BMGY, at 30°C for 30 minutes. Then, the pre-inoculum was diluted 80 times in 1 l of BMGY, divided in 2 flasks of 5 l final volume. The cell cultures were grown at 30°C in a shaking incubator (200 rpm) for 72 hours, after that cells were harvested by centrifugation and resuspended in half-volume of BMM medium for expression induction. 0.5% methanol was added every 24 hours.

After 48 hours of induction, yeast cells were collected and resuspended in lysis buffer containing 50 mM sodium phosphate pH 7.5, 500 mM NaCl, 10% glycerol, 1 mM phenyl-methyl sulfonyl fluoride (PMSF; Sigma-Aldrich), protease inhibitors Complete EDTA-Free (Roche), and 1 mg/ml DNAase. Then, an equal volume of zirconia beads (BioSpech) was added to the suspension, and yeast cells were disrupted in a mechanical way by utilizing a BioSpec Mini Bead-Beater. The mixture was passed through a cloth mesh strainer in order to separate cells from zirconia beads, after that cell lysate was centrifuged at 70,000 rcf for 30 minutes at 4°C. The supernatant was applied on a HisTrap column previously equilibrated with lysis buffer, and the protein was eluted with 500 mM imidazole and dialyzed against 50 mM TrisHCl pH 7.5, 1 mM EDTA, 150 mM NaCl, 10% glycerol, 1 mM DTT. The protein solution was concentrated using Centrifugal Filter Units (Millipore) to 3 mg/ml concentration and fluorescent signal was visualized by ChemiDoc system Bio-Rad (ex. 489 nm, em. 509 nm). Successively, PreScission protease 1:10000 v/v ratio (GE healthcare) was added to the protein solution in order to cleave the tag, together with the eGFP. After a second purification step on HisTrap, a native hCTPS-1 protein was achieved. Protein samples were analyzed by SDS-PAGE.

3.6 Enzymatic assays

All the enzymatic assays were performed employing an Eppendorf BioSpectrometer.

M. tuberculosis EthA activity was checked at 37°C by measuring the NADPH consumed during the course of the reaction at 340 nm (ε= 6.22 mM^{-1} cm^{-1}) (Fraaije *et al.*, 2004). The reaction mixture was composed by 50 mM potassium phosphate pH 8.0, 10 µM serum bovine albumin (BSA), 0.2

mM NADPH. The compounds were tested at a concentration of 50 µM, previously dissolved in dimethylformamide, and the reaction was started by addition of EthA enzyme at concentration of 1µM.

M. tuberculosis PyrG activity was spectrophotometrically assayed at 37°C by measuring the production of CTP starting from UTP (ε= 1.34 mM^{-1} cm^{-1}) at a wavelength of 291 nm (Lunn *et al*., 2008). The reaction mixture contained 50 mM HEPES pH 8.0, 10 mM $MgCl_2$, 1mM UTP, 1 mM ATP and 0.5 µM PyrG enzyme. The reaction was initiated by addition of 100 mM NH_4Cl.

The activity of hCTPS-1 was spectrophotometrically assayed as described for *M. tuberculosis* PyrG, using a final concentration of 1,8 µM of the enzyme.

M. tuberculosis PanK activity was checked by measuring the formation of ADP through a coupled assay that employs pyruvate kinase (PK) and lactate dehydrogenase (LDH) (Yang *et al.,* 2008). The assay was performed at 37°C, in a reaction mixture containing 50 mM potassium phosphate pH 7.0, 25 mM KCl, 10 mM $MgCl_2$, 2 mM DTT, 0.5 mM PEP, 0.24 mM NADH, 10 units PK/LDH, 0.12 mM Mg-ATP, 0.3 mM D-pantothenate and 0.5 µM PanK enzyme. The reaction was started by the addition of PanK to the reaction mix and monitored by observing the change in absorbance at 340 nm.

3.6.1 Steady state kinetics and inhibition assays

Steady-state kinetics parameters for *M. tuberculosis* PyrG and PanK were calculated through enzymatic assays performed at 8 different concentrations of the correspondent enzyme substrates. All the assays were done in triplicates, and the K_m and k_{cat} values were determined fitting the obtained data to the Michaelis-Menten equation using Origin 8 software.

Inhibition assays of *M. tuberculosis* PyrG, PanK and human CTPS-1 were done by dissolving the tested compounds in DMSO, and blank reactions were performed by adding 1 µl DMSO to the reaction mixture. For IC_{50} determinations, the enzyme activities were measured in presence of a serial dilution of each compound and values were estimated by fitting [I] and normalized in response to Equation 1. The K_i values were determined using an adapted equation for competitive inhibition (Equation 2) and an equation for uncompetitive inhibition (Equation 3) (Copeland, 2000).

$$A_{[I]} = A_{[0]} \times \left(1 - \frac{[I]}{[I]+IC_{50}}\right) \qquad \text{Equation 1}$$

$$v = \frac{V_{max}[S]}{[S]+ K_m\left(1+\frac{[I]}{K_i}\right)} \qquad \text{Equation 2}$$

$$v = \frac{V_{max}[S]}{[S]\left(1+\frac{[I]}{\alpha K_i}\right)+K_m\left(1+\frac{[I]}{K_i}\right)} \qquad \text{Equation 3}$$

3.6.2 Compound library screening against PyrG enzyme activity

The GlaxoSmithKline antimycobacterial compound set (GSK TB-set) consists of 204 compounds already known to possess activity against *M. tuberculosis* growth (Ballell *et al*., 2013). This compound library was kindly provided by GlaxoSmithKline. Compounds of this library were employed for a target-based screening against PyrG activity, tested at a final concentration of 100 μM, dissolved in DMSO. Blank reactions were done by adding 1 μl DMSO to the reaction mixture.

Among the 204 compounds checked, three of them were selected, having an inhibitory degree against PyrG higher than 75%. To deeper investigate on them, the three compounds were re-purchased from MolPort (Riga, Latvia): GSK1570606A,(2-(4-fluorophenyl)-N-(4-(pyridin-2-yl)thiazol-2-yl)acetamide, #MolPort-003-158-205; GSK735826A, N-(4-(pyridin-2-yl)thiazol-2-yl)-[1,3]dioxolo[4',5':4,5]benzo[1,2-d]thiazol-6-amine #MolPort-003-038-940; GSK920684A, 2-(3-fluorophenoxy)-N-(4-(pyridin-2-yl)thiazol-2-yl)acetamide, #MolPort-004-106-239.

Consequently, IC_{50} and K_i values were calculated. The three compounds were also tested against hCTPS-1 and IC_{50} values were evaluated.

Successively, the GSK1570606A, GSK735826A and GSK920684A compounds were also tested against PanK, and for those that displayed inhibitory effects, IC_{50} and K_i values were determined.

3.7 EthA activated 7947882 and 7904688 metabolites production and analysis

In order to produce 7947882 active metabolites, 10 mg of EthA recombinant enzyme was incubated in agitation at 37°C with 30 mg of the compound, in 50 mM potassium phosphate pH 8.0, with the addition of 500 µM NADPH and 10 µM BSA. After 5 hours of incubation, the reaction products were extracted with diethyl ether, and the organic component was washed using brine and then dried over Na_2SO_4. After the removal of solvent employing a reduced pressure, the products were partially purified on flash column chromatography (Merck SiO_2 60, 230–400 mesh). The purified products were analyzed in ESI mass spectrometry, both in negative and positive mode, utilizing a Thermo LTQ-XL mass spectrometer.

For the 7904688 active metabolites identification trials, the same procedure was utilized.

3.8 Production of PyrG and PanK complexed with 7947882/7904688 metabolite(s) upon co-incubation with EthA

For obtaining PyrG complexed with the active 7947882 or 7904688 metabolite(s), PyrG recombinant protein (45 µM) was co-incubated with EthA (10 µM) in the presence of either 7947882 or 7904688 at a final concentration of 300 µM. The reaction was performed at 37°C in 50 mM potassium phosphate buffer pH 8.0, adding 300 µM NADPH. In parallel, a blank control was performed in the absence of NADPH, in order to keep EthA enzyme in a no-working state. During the course of the reaction, PyrG activity was monitored as explained in the following paragraph, with ATP at final concentration of 0.2 mM. After 4 hours, PyrG was re-purified on 300 µl of Ni-nitrilotriacetic acid (Ni-NTA) resin (Qiagen) in order to eliminate EthA and all the possible unbound 7947882 or 7904688 metabolites. Thus, the mixture was loaded on the column previously equilibrated with 50 mM potassium phosphate pH 7.5, 50 mM KCl, and PyrG was eluted with 100 mM imidazole, and finally dialyzed for imidazole elimination.

For obtaining PanK-7947882 or PanK-7904688 metabolites complexes, the same protocol was followed.

4. Results

4.1 Background

In view of the alarming TB scenario worldwide, there is an urgent need for new drug targets discovery, together with the identification of new antituberculars with greater potency. In this context, the Molecular Microbiology Laboratory from Pavia University, member of a European project named More Medicines For Tuberculosis (MM4TB, EC-VII framework program), is inserted.

From the screening of the National Institute of Allergy and Infectious Diseases (NIAID) library of 594 chemical compounds (Ananthan *et al*., 2009; Goldman and Laughon, 2009; Maddry *et al*., 2009) performed by Prof. S. T. Cole laboratory (EPFL, Lausanne, Switzerland), the 7947882 and 7904688 molecules (Fig. 21) emerged for their efficacious antitubercular activity (MIC = 0.5 µg/ml for both compounds). Moreover, these two compounds resulted active against *M. tuberculosis* H37Rv *in vitro, ex vivo,* and in TB latent models.

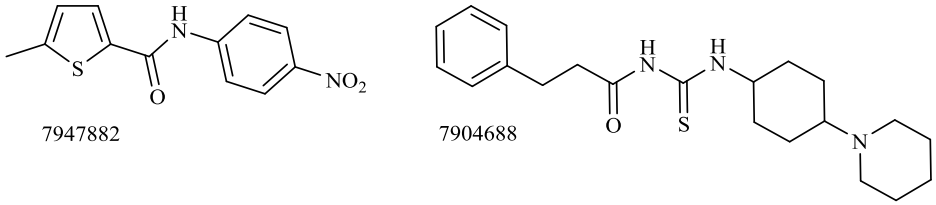

Figure 21. 7947882 and 7904688 chemical structures.

In order to unveil the mechanisms of action and resistance of these two compounds, *M. tuberculosis* resistant mutants to the two compounds were isolated, and Illumina sequencing data highlighted that the resistant mutants were mutated in *ethA*, *pyrG* and *coaA* genes. *ethA* gene product is the non-essential FAD-containing NADPH-dependent monooxygenase EthA, responsible for the activation of ETH (Baulard *et al*., 2000); in turn, *pyrG* is an essential gene encoding the CTP-synthetase PyrG responsible for the conversion of UTP in CTP by using ATP as energy source (Turnbough and Switzer, 2008); and *coaA* codes for the essential pantothenate kinase PanK, that converts pantothenate to 4′-phosphopantothenate in an ATP-dependent manner (Jackowski and Rock, 1981) (Table 5).

Since mutations affecting *ethA* lead to ETH resistance (DeBarber *et al.,* 2000), and *M. tuberculosis* resistant to 7947882 and 7904688 and

mutated in EthA were cross-resistant to ETH, this enzyme was hypothesized to activate both compounds. Moreover, since mutations affecting target gene(s) are often responsible for a drug-resistant phenotype, PyrG and PanK were supposed to be the 7947882 and 7904688 cellular targets.

Through genetic approaches, the role of EthA as an activator of these two compounds has been validated, and biochemical strategies demonstrated the monooxygenase to be able to metabolize both prodrugs.

Consequently, the work of this thesis was focused on the definitive biochemical validation of EthA as the activator of 7947882 and 7904688, the identification of their active metabolite(s) and the validation of the role of PyrG and PanK as cellular targets.

***M. tuberculosis* strains**	**MIC (µg/ml)**			**Mutations**		
	7947**82**	7904**88**	ETH	*ethA*	*pyrG*	*coaA*
H37Rv (wild-type)	0.5	0.5	1	-	-	-
82.14	>40	>40	10	T133C (W45R)	T557G (V186G)	-
82.20	>40	20	2.5	T386C (L129P)	T557G (V186G)	
82.21	>40	>40	10	Δ1283-4 (truncated protein)	-	A620G (Q207R)
88.1, 88.2	2.5	10	0.5	-	-	A620G (Q207R)
88.7, 88.10	5-10	10	0.5	-	T557G (V186G)	-

Table 5. Phenotypic and genotypic profiles of *M. tuberculosis* resistant mutants.

4.2 *M. tuberculosis* PyrG and PanK are affected by 7947882 and 7904688 compounds upon activation by EthA

In order to validate the role of *M. tuberculosis* PyrG and PanK as the cellular targets of the 7947882 and 7904688 compounds, both recombinant wild-type and mutant proteins were expressed in *E. coli*, purified and characterized. PyrG catalytic constants were calculated toward both ATP

and UTP: k_{cat} 21.9 ± 0.5 s^{-1} and K_m 0.18 ± 0.01 mM toward ATP; k_{cat} 22.9 ± 0.9 $s^{-1}$and K_m 0.14 ± 0.01mM toward UTP. These values are very similar to those of the other already characterized bacterial CTP synthetase (Long and Pardee, 1967; Anderson, 1983; Willemoes *et al*., 2005). Conversely, the PyrG V186G mutant enzyme was partially compromised, as observed from the reduced k_{cat} toward both ATP and UTP (1.5 ± 0.11 and 1.6 ± 0.08 s^{-1}, respectively). Additionally, a significantly higher K_m toward ATP (1.46 ± 0.18 mM) was observed, with no differences toward UTP.

Concerning PanK enzyme, the kinetic characterization highlighted a k_{cat} of 6.1 ± 0.2 s^{-1} and a K_m of 0.19 ± 0.02 mM toward ATP, whilst toward pantothenate the catalytic constants were k_{cat} 6.3 ± 0.3 s^{-1} and K_m 0.28 ± 0.03mM. PanK Q207R mutant enzyme, as V186G PyrG, was partially impaired, with a reduction of the k_{cat} values toward both ATP and pantothenate (2.0 ± 0.1 s^{-1} and 1.8± 0.2 s^{-1}, respectively). Moreover, the K_m toward ATP was significantly increased, being equal to 3.56 ± 0,36 mM, indicating a reduced affinity for ATP, whilst no significant differences were observed toward pantothenate.

Due to the resistant phenotype associated with both PyrG V186G and PanK Q207R mutations and in view of the catalytic data, we hypothesized that 7947882 and 7904688 inhibitors could bind to the ATP-binding site of both enzymes. To check this hypothesis, both PyrG and PanK wild-type enzymes were assayed in presence of either 7947882 or 7904688 compounds at a final concentration of 200 µM. However, as expected for compounds requiring activation, they did not affect neither PyrG nor PanK activities.

For this reason, to confirm that the EthA metabolites of the compounds might act on PyrG and PanK, EthA reaction on 7947882 or 7904688 was performed either in the presence of PyrG or PanK, and the activity of the latter enzymes was checked throughout the reaction. The blank control was performed in the absence of NADH, in order to maintain EthA in its inactive state, whilst the full-reaction contained all reaction components. As it is shown in Figure 22, PyrG activity from blank control remained unaffected, whilst PyrG from full reaction completely lost its activity in 4 hours of co-incubation with the 7947882. Similarly, in the presence of the 7904688 compound, PyrG lost the 80% of its activity in the same time (Fig. 22).

Afterwards, PyrG was re-purified from both blank and full reaction, and its activity was tested, showing that the enzyme coming from the control remained active, whilst that from the complete reaction was still inactive. Moreover, the UV-Vis spectra of PyrG from both blank and full reactions in the presence of 7947882 compound were analyzed, highlighting

a peak at 330 nm, characteristic of the 7947882, which was present in the full reaction, and absent in the control one (Fig. 23). Furthermore, UV-Vis spectra of the blank and full reactions with the 7904688 compound displayed a broad peak between 310 and 400 nm, characteristic of this molecule, present in the complete reaction and absent in the blank one (Fig. 23).

Analogous experiments were conducted with PanK. By incubating the pantothenate kinase with a full-active EthA in the presence of the 7947882 compound, 100% of the activity was lost after 24 hours of incubation, whilst the 80% was retained when incubated with EthA in the absence of NADPH (Fig. 24). Similar results were achieved incubating PanK with the 7904688 compound (Fig. 24). The UV-Vis spectra of the blank and full reaction after PanK re-purification, gave analogous results to those of PyrG (Fig. 25).

All these results taken together gave the demonstration that EthA converts the 7947882 and the 7904688 into metabolites that are able to bind both to PyrG and to PanK compromising their enzymatic activity, thus definitively confirming the role of EthA as 7947882 and 7904688 activator.

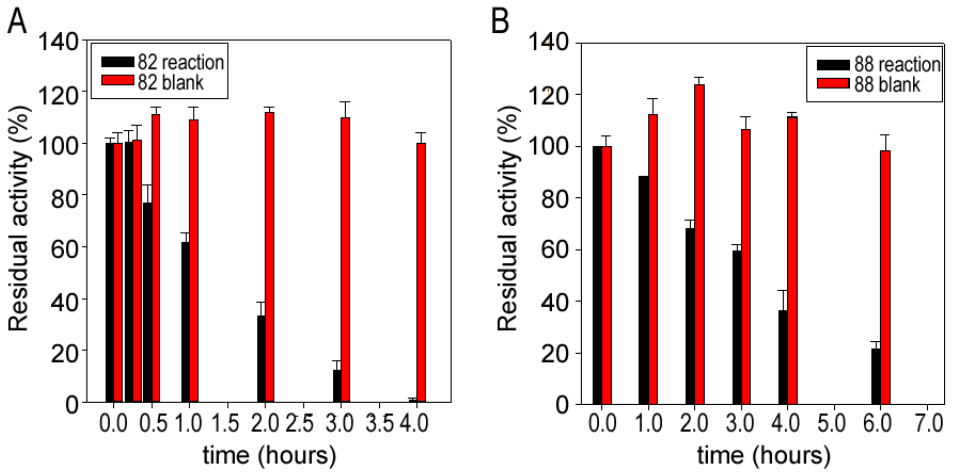

Figure 22. PyrG activity monitored in the presence of the 7947882 (A) or 7904688 (B) compounds. Red bars indicate PyrG activity from the blank reaction, the black bars that from the full reaction.

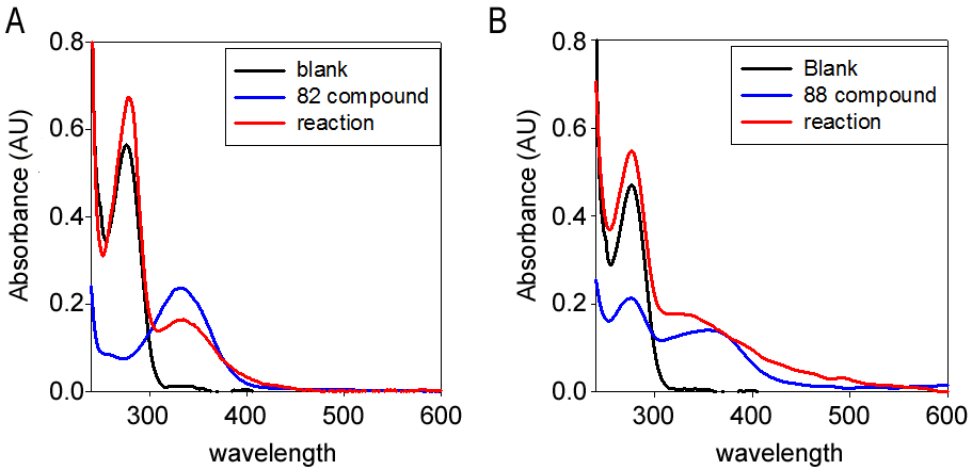

Figure 23. UV-Vis spectra of PyrG incubated with 7947882 (A) and with 7904688 (B) after re-purification. Red line corresponds to PyrG spectrum from full reaction, black line is the spectrum of PyrG from blank reaction, and blue line rapresents the spectrum of the corresponding compound at a concentration equal to 20 μM.

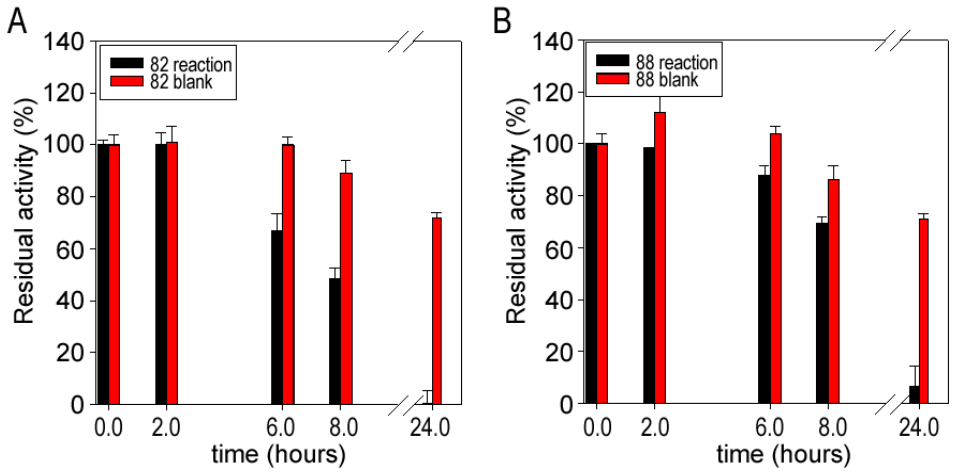

Figure 24. PanK activity monitored in the presence of the 7947882 (A) or 7904688 (B) compounds. Red bars indicate PanK activity from the blank reaction, the black bars that from the full reaction.

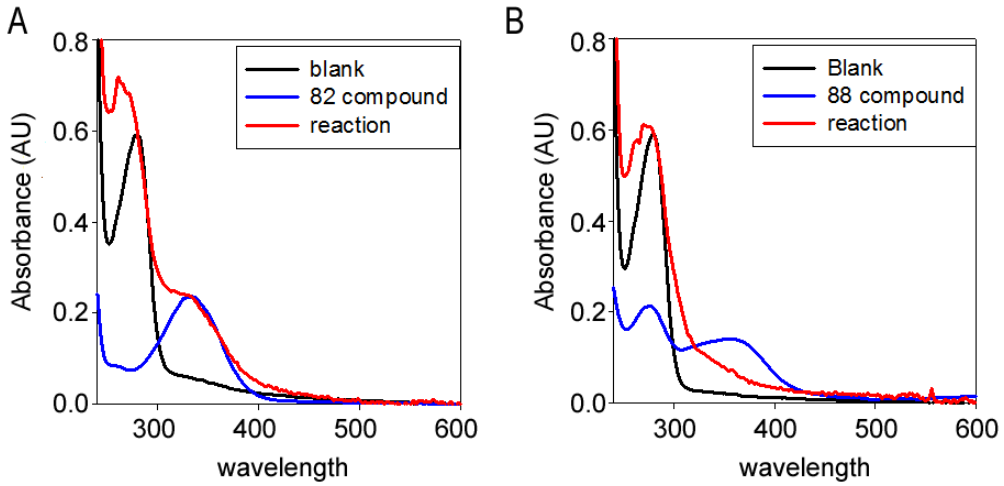

Figure 25. UV-Vis spectrum of PanK incubated with 7947882 (A) and with 7904688 (B) after re-purification. Red line corresponds to PanK spectrum from full reaction, black line is the spectrum of PanK from blank reaction, and blue line rapresents the spectrum of the corresponding compound at a concentration equal to 20 μM.

4.3 Identification of EthA activated 7947882 and 7904688 metabolites

Once the role of EthA as the 7947882 and the 7904688 activator was confirmed, the following step consisted in the identification of the active metabolites, able to affect PyrG and PanK activity.

The monooxygenase EthA has been previously demonstrated to activate ETH by producing the correspondent S-oxide and S-dioxide active cytotoxic metabolites (Fig. 26) (Vannelli *et al.*, 2002; DeBarber *et al.*, 2000).

Thus, we decided to verify whether these kinds of metabolites could arise also upon EthA-mediated 7947882 activation (Fig. 27).

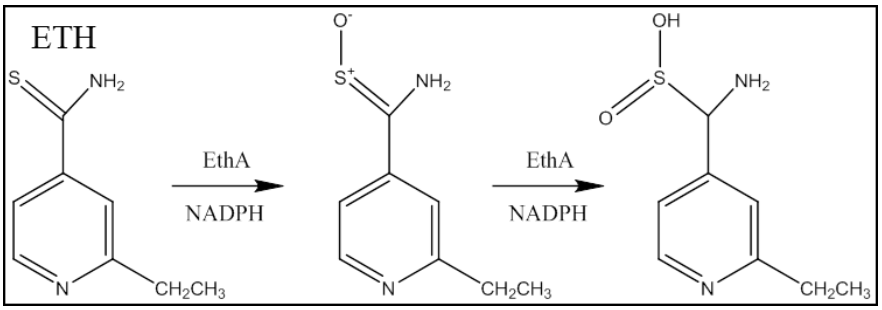

Figure 26. EthA-mediated ETH activation (DeBarber *et al.*, 2000).

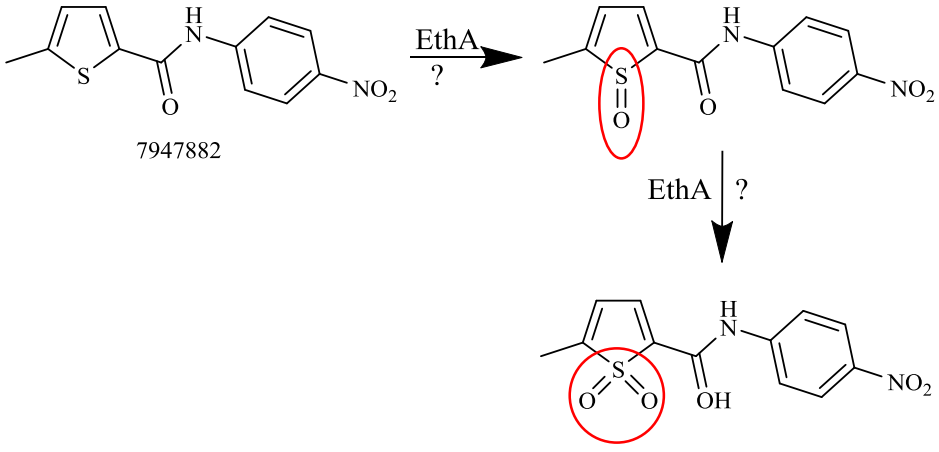

Figure 27. Hypothesized EthA-mediated 7947882 activation.

To confirm this hypothesis, we attempted to identify the active EthA metabolite(s) of the prodrugs.

In order to do that, the products of the EthA and 7947882 co-incubation were purified from the reaction mixture, and analyzed by liquid electron spray ionization-mass spectrometry (ESI-MS). As it is shown in Figure 28, two main products with m/z of 293 and 277, and named M1 and M2, respectively, emerged, being in accordance with S-oxide and S-dioxide 7947882 metabolites. Moreover, fragmentation patterns of these two compounds were comparable to that of the 7947882 compound upon its mono- and di-oxygenation at the thiophene moiety level, confirming our hypothesis (Fig. 29). Then, M1 and M2 purified metabolites were tested against PyrG recombinant protein, showing that its enzyme activity is affected by these derivatives.

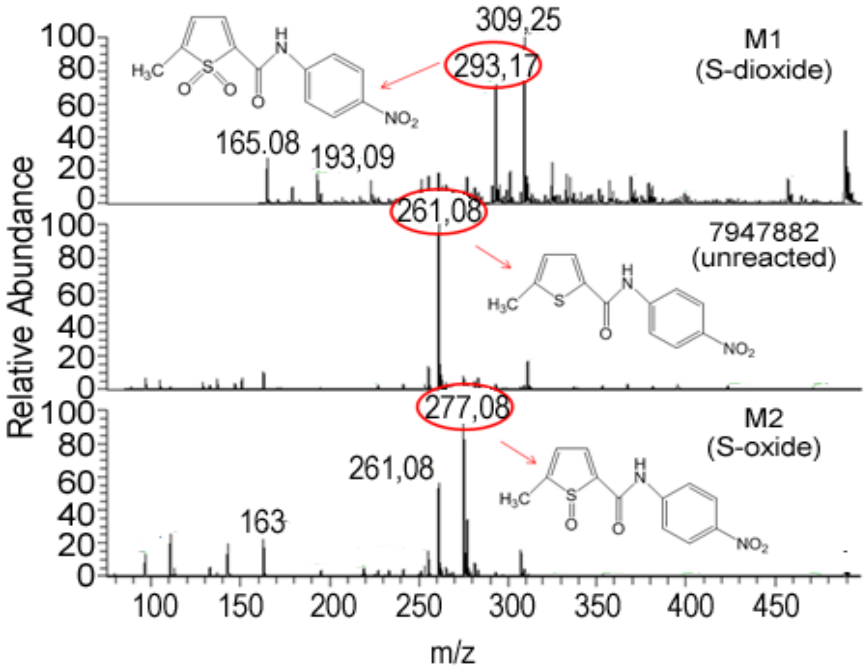

Figure 28. Full ESI-MS of the 7947882 reaction products.

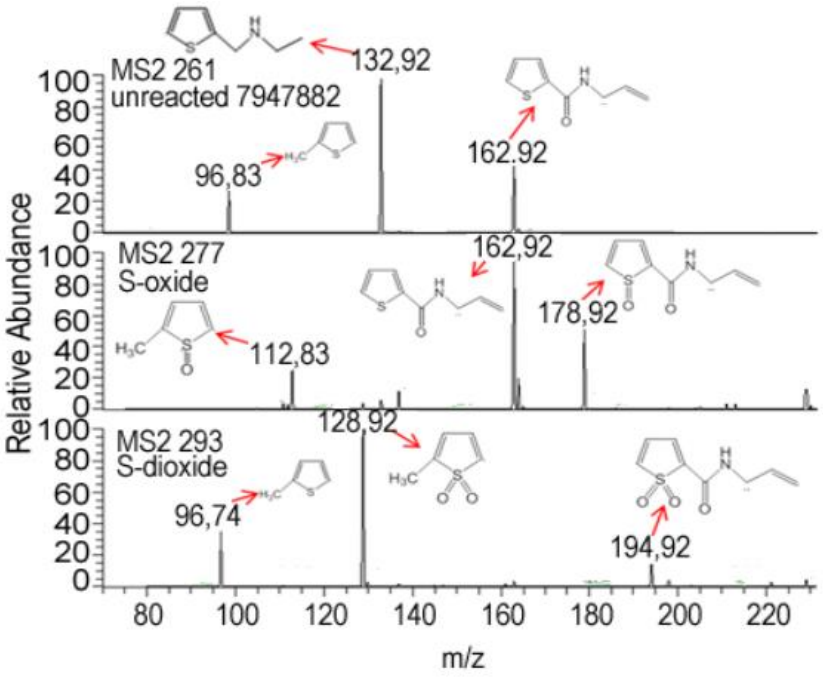

Figure 29. Fragmentation patterns of M1 and M2 putative 7947882 metabolites.

The same approach was employed to identify the EthA-activated 7904688 metabolites. Figure 30 shows ESI-MS analysis of the 7904688 compound, compared with the EthA reaction products, highlighting the presence of m/z 351 compound, very likely corresponding to 3-phenyl-N-[(4-piperidin-1-ylphenyl)carbamoyl]propanamide.

Probably, this metabolite derives from consecutive EthA-mediated reactions on the sulfur atom of the 7904688 compound, as shown in Figure 31 (Chigwada *et al*., 2014).

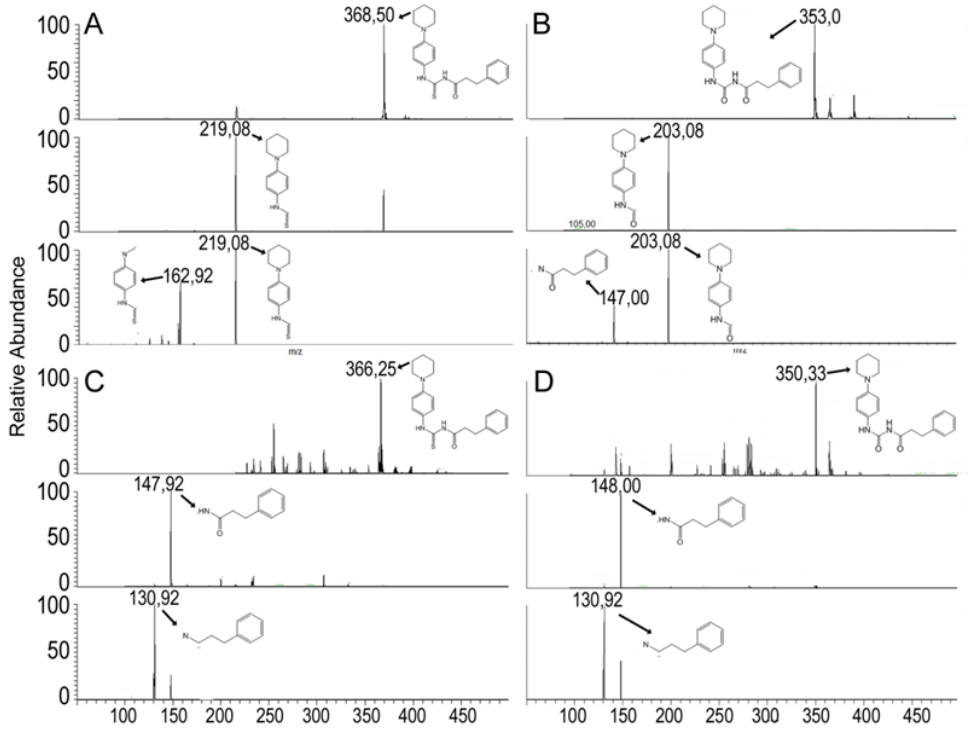

Figure 30. Identification of 7904688 EthA metabolite(s). (A) Mass spectrometry analysis of the 7904688 in positive mode, and MS2 and MS3 fragmentations; (B) mass spectrometry analysis of the EthA metabolite of 7904688 in positive mode, MS2 and MS3 fragmentations; (C) mass spectrometry analysis of 7904688 in negative mode, MS2 and MS3 fragmentations; (D) mass spectrometry analysis of the EthA metabolite of 7904688 compound in negative mode.

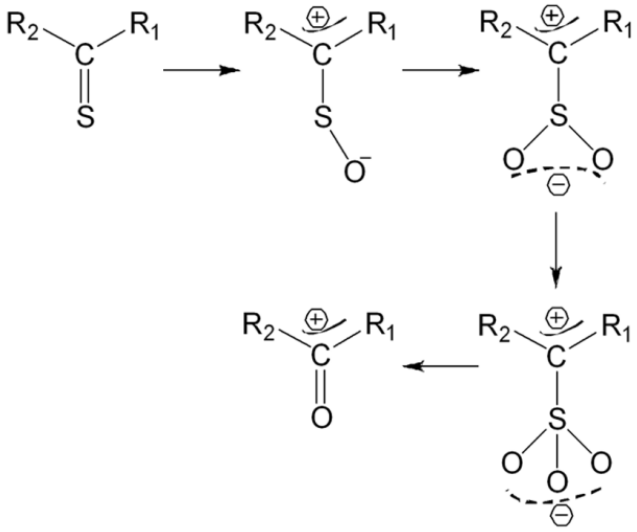

Figure 31. Supposed EthA-mediated oxygenation reactions on the 7904688, leading to the final metabolite.

However, this purified reaction product tested against both PyrG and PanK showed no effects on their activity, indicating that the isolated compound is an inactive end product. Moreover, the mono- and di-oxidation of the 7904688 have been attempted through chemical procedures but without any success; in fact, also with this approach the only one final compound obtained was always the 3-phenyl-N-[(4-piperidin-1-ylphenyl)carbamoyl]propanamide derivative, due to the high reactivity of the intermediates. So, probably the real 7904688 active metabolite is one of these highly reactive intermediate of the EthA-mediated reaction, thus impossible to isolate. For this reason the 7904688 compound was not further investigated.

4.4 Further characterization of the S-dioxide 7947882 derivative: the 11426026 compound

In order to better investigate the 7947882 derivatives, the S-dioxide 7947882 one was chemically synthesized by our collaborator Dr. Vadim Makarov (A. N. Bakh Institute of Biochemistry, Russian Academy of Science, Moscow, Russia) and named 11426026. The mass spectrum of the synthetic compound was compared to that of the M1 EthA metabolite previously isolated, showing a perfect overlapping, thus confirming the M1 identity as the 7947882 S-dioxide derivative.

The MIC to 11426026 compound of *M. tuberculosis* H37Rv strain and *ethA*, *pyrG* and *panK* mutants were evaluated, in order to check the effects of this compound on the mycobacterial growth. As it is shown in Table 6, *M. tuberculosis* H37Rv strain displayed a degree of sensitivity to the 11426026 metabolite that was comparable to that of the 7947882 prodrug. Moreover, the *ethA* mutant strain, resistant to the 7947882, was not resistant, instead, to its S-dioxide derivative, confirming that 11426026 does not require EthA-mediated activation anymore. Concerning *M. tuberculosis pyrG* and *panK* mutant strains, they were still resistant to the metabolite, confirming that PyrG and PanK could be the cellular targets of the 7947882 S-dioxide derivative (Table 6).

		MIC in *M. tuberculosis* (µg/ml)			
Compound	**Structure**	**H37Rv**	***ethA* mutant**	***pyrG* mutant**	***panK* mutant**
11426026	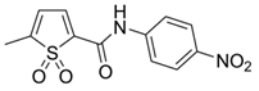	1	1	2.5	2.5
7947882	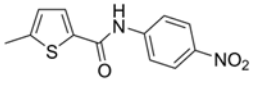	0.5	>40	5-10	2.5

Table 6. MICs to 11426026 and 7947882 compounds of *M. tuberculosis* wild-type and mutant strains.

The 11426026 metabolite was then assayed against PyrG and PanK enzymes, both wild-type and mutant forms. The compound resulted active against PyrG and PanK wild type proteins, whilst it did not show significant effects against the mutant enzymes. In detail, 11426026 inhibits the PyrG wild-type activity with an IC_{50} of 0.035 mM, but is very less active toward the mutant protein with an IC_{50} higher than 1 mM (Fig. 32). In parallel, PanK wild-type activity is moderately affected, with an IC_{50} of 0.105 mM, but not that of the mutant one, showing an IC_{50} of 0.876 mM (Fig. 32). Through further kinetic analysis, 11426026 metabolite resulted to be a competitive inhibitor with respect to ATP for both PyrG and PanK, with a K_i of 0.010± 0.002 mM and 0.023± 0.001 mM, respectively. Moreover, the increased K_m value for ATP of PyrG and PanK mutant enzymes reveals that the identified point mutations could introduce a structural change involving the ATP-binding site, consequently reducing much more the affinity toward 11426026, thus explaining the resistant phenotype.

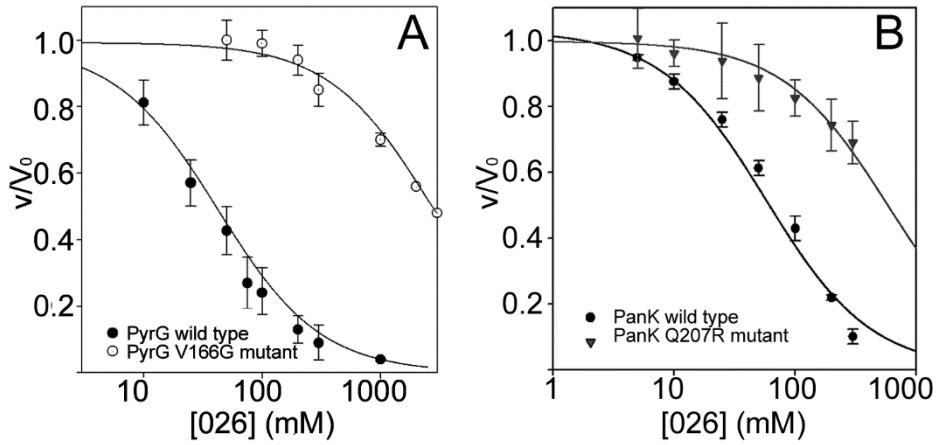

Figure 32. A. PyrG wild-type and PyrG V186G mutant proteins activity at different 11426026 concentrations (μM); B. PanK wild-type and PanK Q207R mutant proteins activity at different 11426026 concentrations (μM).

4.5 Inhibition of PyrG by 7947882 affects *M. tuberculosis* nucleotide metabolism: a metabolomic analysis

Basing on the knowledge concerning the role of PyrG in pyrimidine *de novo* production (Meng *et al*., 2004), metabolomic studies were performed, in collaboration with Prof. Luis Pedro de Carvalho (Francis Crick Institute, London, UK) and Prof. Katarina Mikušová (Comenius University, Bratislava, Slovakia), by analyzing the effects of the 7947882 on the *M. tuberculosis* nucleotide metabolism. Consequently, *M. tuberculosis* cells were grown in the presence of either 7947882 (at a concentration equal to 5X MIC value) compound, or with DMSO as control. Then, metabolites pool was extracted, addressing the attention mainly to nucleotides and bases (de Carvalho *et al*., 2010; Larrouy-Maumus *et al*., 2013). Consistent with PyrG role in pyrimidine biosynthesis, treatment with the 7947882 compound led to a significant increase in purines and pyrimidines intermediates, compared to the control treated with DMSO (Fig. 33A). These metabolomic data markedly draw attention to the effects of a direct PyrG inhibition: CTP nucleotides amount decreases inside the cell, with a consequent fall in nucleotide metabolism.

Moreover, in order to further strengthen the role of PyrG as the cellular target of the 7947882, and in particular of its EthA-activated S-dioxide metabolite 11426026, radiolabeling experiments were done, employing the non-pathogenic *M. tuberculosis* H37Ra strain, whose MIC toward 11426026 compound is 4 μg/ml. Therefore, *M. tuberculosis* was treated with 11426026 (4X MIC) for 1 hour, and then [^{14}C]uracil was added

to the culture for other 3 hours. [^{14}C]uracil is firstly utilized for [^{14}C]uridine monophosphate (UMP) production, and successively is incorporated in all the nucleotides deriving from uracil units. Once *M. tuberculosis* cells treated and not treated with the inhibitor were collected, the nucleotide content was analyzed through autoradiography. In all experiments performed, results highlighted an increase in [^{14}C]UTP and a decrease in [^{14}C]CTP (Fig. 33B), giving a further, unequivocal proof that PyrG is targeted by 11426026 active metabolite of 7947882 prodrug.

Figure 34 shows an outline of PyrG inhibition effects on the cellular metabolism. Being a CTP-synthetase, PyrG inhibition leads to the impairment of DNA and RNA synthesis, together with carbohydrate, fatty acids and amino acids production. Consequently, these data importantly corroborate PyrG as a new, precious tool for TB drug research, since its inhibition interferes with essential pathways for cellular growth and survival (Fig. 34).

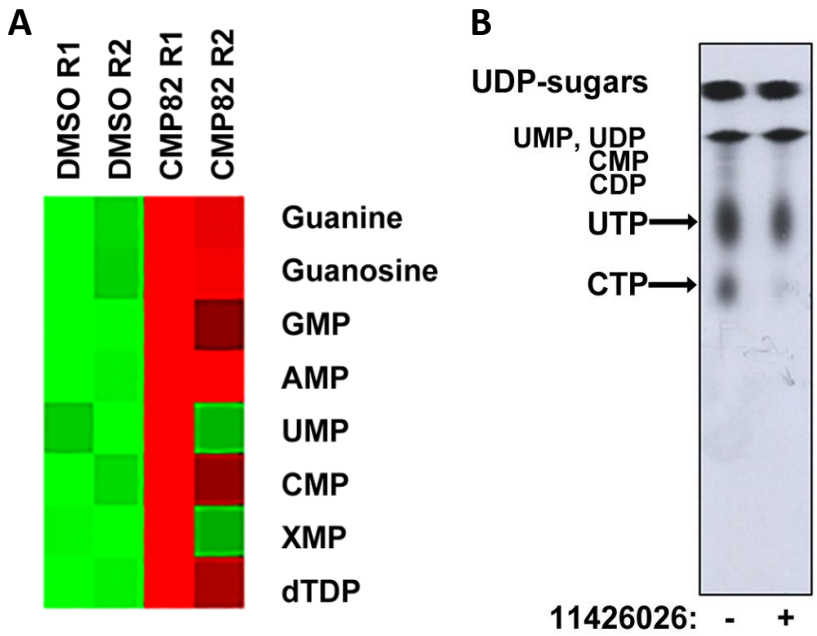

Figure 33. PyrG inhibition affects nucleotide metabolism in *M. tuberculosis*. (A) Heat map illustrating overall changes in nucleotide pool sizes in 7947882-treated *M. tuberculosis* compared to control. Data are derived from two biological replicates. (B) TLC of nucleotide extract from [14C]-uracil-radiolabeled *M. tuberculosis* H37Ra grown on GAS medium. The figure is a representative image from three separate experiments.

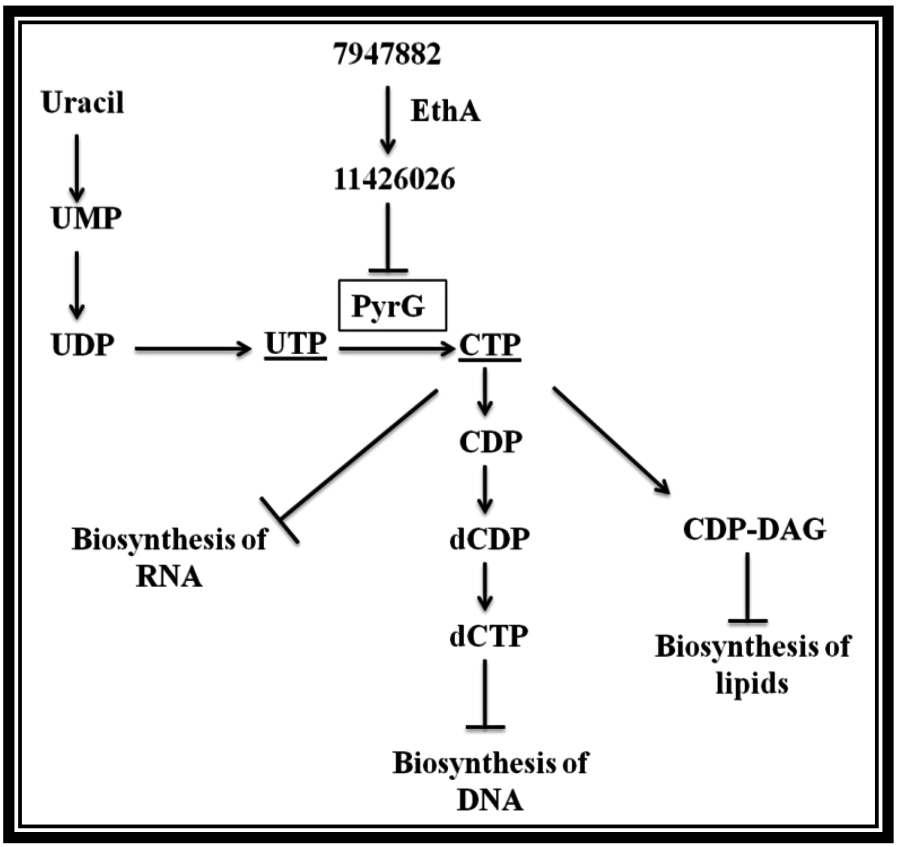

Figure 34. Scheme that summarizes the 7947882 inhibitory effects on PyrG in *M. tuberculosis*.

4.6 Searching for new PyrG and PanK inhibitors that do not require EthA-mediated activation

The 7947882 and 7904688 compounds have been demonstrated to be two multitargeting compounds activated by EthA and affecting both PyrG and PanK enzymatic activities. Since resistant phenotype to prodrugs is frequently caused by mutations in the activator gene, it could be worth to identify new PyrG and PanK inhibitors that do not require the activating step mediated by EthA. In this work, two approaches have been utilized for this purpose: docking experiments, exploiting PyrG and PanK available crystallographic strictures, and a target-based screening of a chemical library.

4.6.1 Docking experiments with the 11426026 compound and PyrG and PanK inhibitors

In collaboration with Prof. P. Alzari and Dr. M. Bellinzoni (Institute Pasteur, Paris, France), the *M. tuberculosis* PyrG crystal structure was solved, highlighting an enzyme formed by two different domains: a synthetase domain, or more precisely the amidoligase domain, located at the N-terminus of the protein, and a glutamine amido-tansferase domain, localized at the C-terminus. These two domains display a Rossmann-like fold, and are connected by a linker component. The functional PyrG protein is a tetramer, in which the synthetase domain represents the central part of the tetramer, whilst the glutamine amido-transferase domain is oriented outward (Fig. 35).

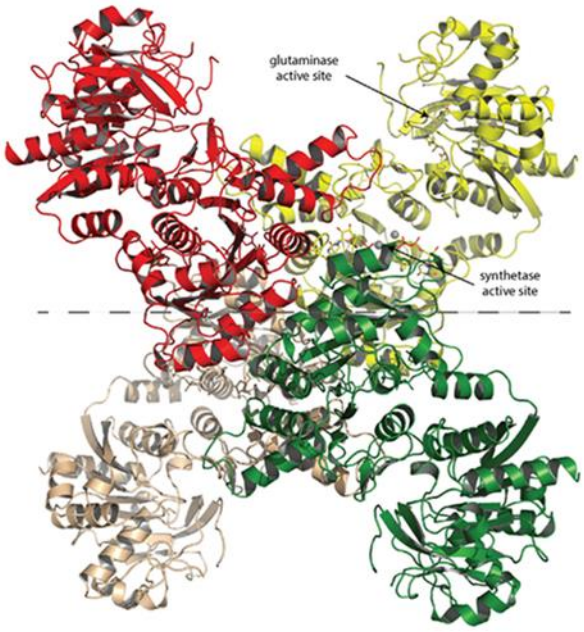

Figure 35. *M. tuberculosis* PyrG crystallographic structure.

M. tuberculosis PanK is a P-loop kinase whose structure was solved for the first time in 2006 (Das *et al*., 2006). This enzyme has a dimeric structure, with each subunit possessing a mononucleotide-binding fold, characterized by seven β-sheets in the central part, and a number of helices on the other side.

The knowledge about PyrG and PanK structures represents a precious resource for the identification of new inhibitors through *in silico* methods. In this context, docking experiments with both PyrG and PanK structures

were performed in collaboration with Dr. Sean Ekins (Collaborative Drug Discovery, Burlingame, CA, USA).

Firstly, in order to examine in depth 11426026 binding to PyrG and PanK, docking analysis was performed, studying all the possible poses of this compound within the crystallographic structures. From this *in silico* analysis, it has been shown that 11426026 compound might exclusively dock in the PyrG or PanK ATP-binding site (Fig. 36).

A

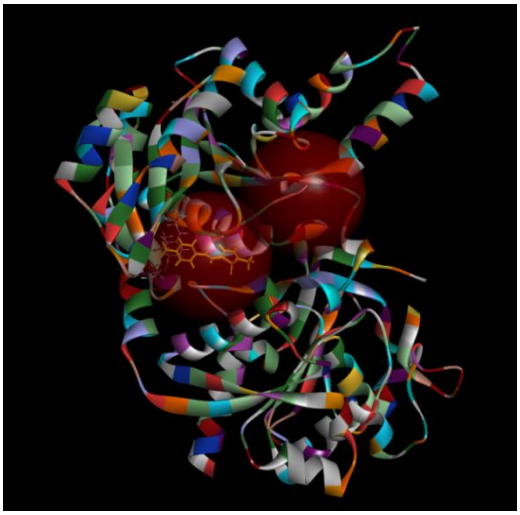

B

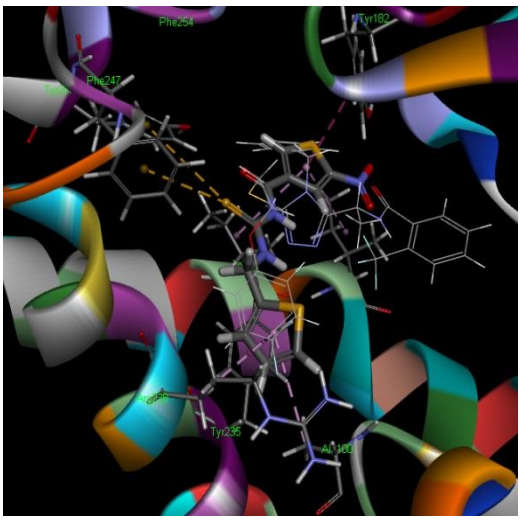

Figure 36. Docking analysis with the 11426026 using PyrG (A) and PanK (B) crystallographic structures (Kindly provided by Dr. S. Ekins).

In view of these results, a virtual screening on PyrG of the Collaborative Drug Discovery (CDD) compounds database (including compounds already known to be active against *M. tuberculosis* growth) was performed (Ananthan *et al*., 2009; Ekins and Bunin, 2013; Ekins *et al*., 2014). Among all the molecules tested, four of them emerged with the best docking score (Fig. 37; Fig. 38; Table 7).

Consequently, the four compounds were tested against PyrG activity, and only the CDD-823953 displayed inhibitory effects against the CTP-synthetase, affecting more than 90% its activity at 200 μM (Table 7), whereas the other ones showed no effects. Moreover, steady-state kinetics proved this compound to be a weak competitive inhibitor toward PyrG ATP binding site, with a K_i of 88.9 μM (Fig. 39).

Successively, docking experiments with the four CDD compounds were performed employing PanK structure. (Fig. 40).

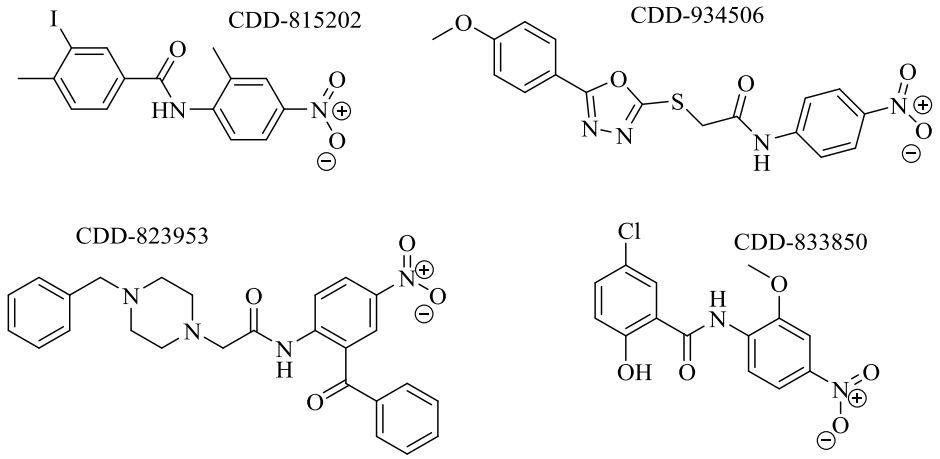

Figure 37. Chemical structures of CDD compounds identified in the virtual screening on PyrG.

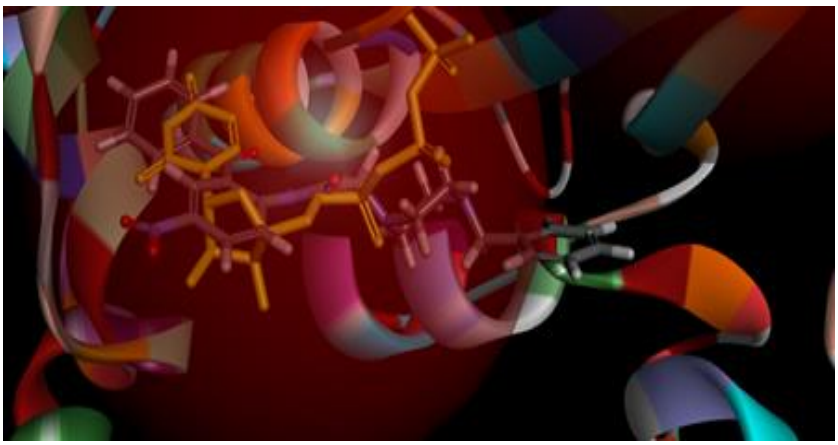

Figure 38. Docking of the CDD-823953 in PyrG crystallographic structure (Kindly provided by Dr. S. Ekins).

Cpd ID	Libdock score	Pose num	MIC (μg/ml)	PyrG inhibition at 200 μM
CDD-815202	71.003	1	< 0.098	n. i.
CDD-833850	64.9544	10	0.159	n. i.
CDD-934506	90.4321	1	0.872	n. i.
CDD-823953	106.701	1	4.392	**> 90%**

Table 7. Docking results of CDD compounds toward PyrG.

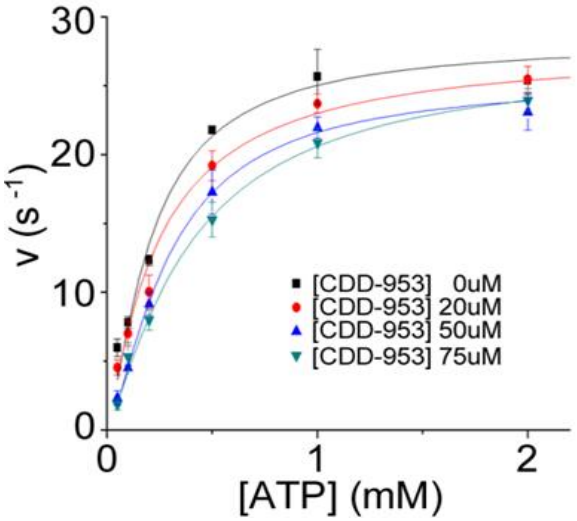

Figure 39. Steady-state kinetics of PyrG towards ATP in the presence of different concentrations of CDD-823953 compound.

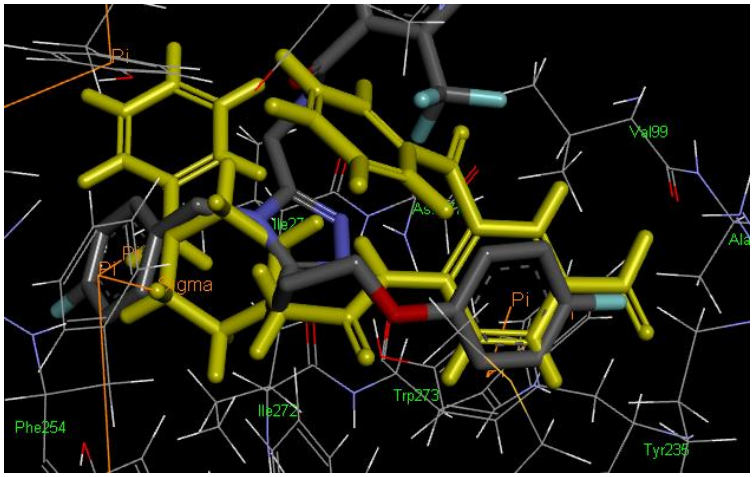

Figure 40. Docking of the CDD-823953 in PanK crystallographic structure (Kindly provided by Dr. S. Ekins).

Since all of them were successfully docked in PanK structure, CDD compounds were tested against PanK enzyme *in vitro*. Two compounds were able to inhibit PanK enzymatic activity at 200 μM: CDD-934506 (80%) and CDD-823953 (50%). The IC_{50} determination demonstrated that CDD-934506 is a moderate PanK inhibitor (40 μM) (Fig. 41).

Concerning the CDD-823953, although having a high IC_{50} value (250 μM), it is worth noting that this inhibitor, like the 11426026 compound, inhibits both PyrG and PanK enzymes (Fig. 41).

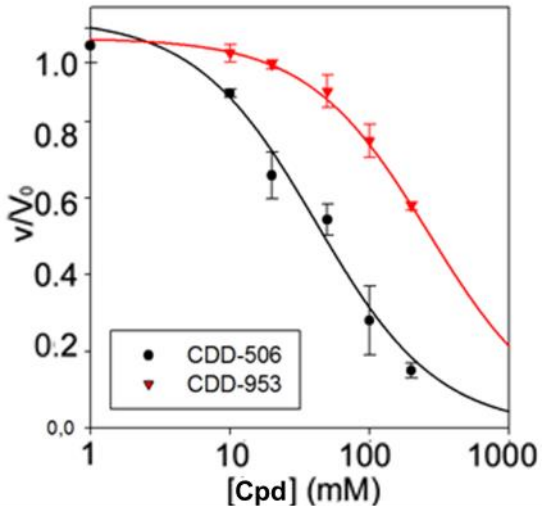

Figure 41. IC_{50} determination of PanK for CDD-934506 and CDD-823953.

4.6.2 *M. tuberculosis* PyrG and PanK: two new validated targets as precious platforms for target-based screening of antitubercular compounds libraries

Once demonstrated the feasibility in the research of new common PyrG and PanK inhibitors, the target-based approach was employed. Considering the compounds affecting both PyrG and PanK activities identified until now, it was observed that the inhibitory degree toward PyrG was always higher compared to that toward PanK. For this reason, a target-based screening of the publically available GlaxoSmithKline antimycobacterial compound set (GSK TB-set) (Ballell *et al*., 2013) kindly provided by GlaxoSmithKline was done first against *M. tuberculosis* PyrG enzyme. All the 204 compounds were tested as described in "Materials and Methods" section (data not shown). Among them, three molecules resulted to inhibit in a significant manner PyrG activity: GSK1570606A, GSK920684A, and GSK735826A, affecting 91%, 75% and 79% of CTP-synthetase activity, respectively (Fig. 42).

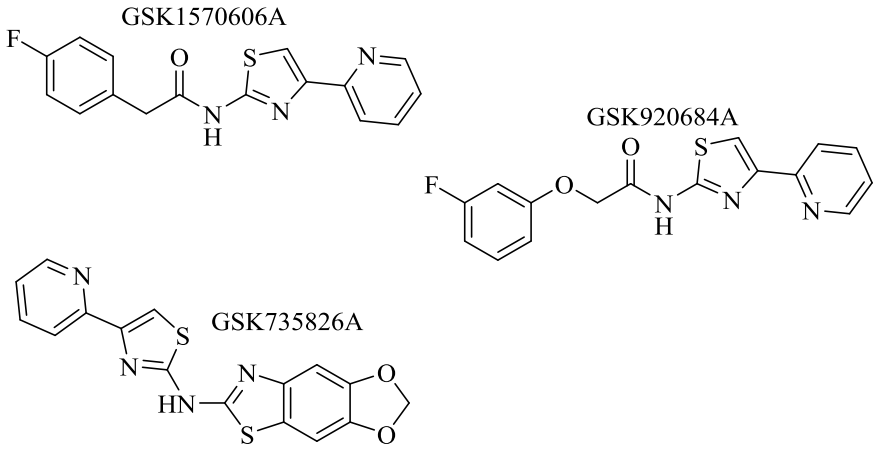

Figure 42. Chemical structures of the GSK compounds that inhibit more than 75% PyrG activity.

To further investigate the three GSK compounds, they were re-purchased and their inhibitory effects against PyrG activity were re-confirmed. Successively, IC_{50} were determined: 2.9 ± 0.61 μM for the GSK1570606A, 23.3 ± 2.15 μM for the GSK920684A, and 19.7 ± 2.16 μM for the GSK735826A (Fig. 43). Moreover, testing PyrG activity by varying the concentration of each compound, steady-state kinetics analysis highlighted that all these molecules are competitive inhibitors towards PyrG ATP-binding site, and K_i were calculated: 3.5 ± 0.4 μM forGSK1570606A, 22.0 ± 0.6 μM for GSK920684A, and 20.3 ± 0.5 μM for GSK735826A (Fig. 44).

On the contrary, the three compounds resulted uncompetitive inhibitors toward UTP (Fig. 45).

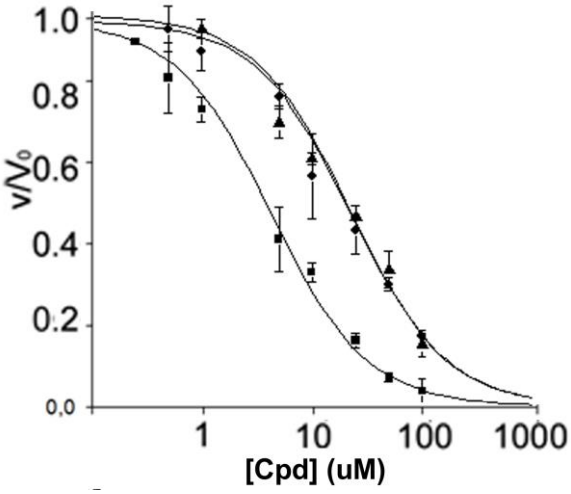

Figura 43. PyrG enzymatic activity in presence of different GSK compounds concentrations (GSK606A: ■; GSK684A: ▲; GSK826A ●).

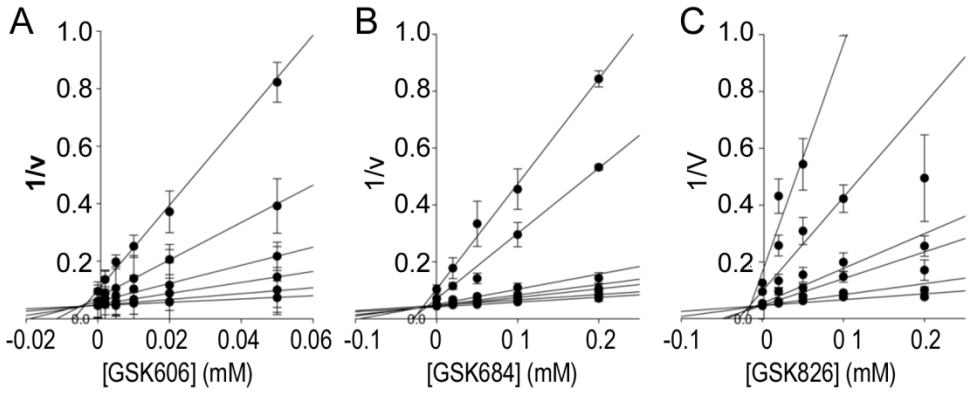

Figure 44. Lineweaver-Burk plots of PyrG towards ATP at different concentrations of GSK1570606A (A), GSK920684A (B) and GSK735826A (C) compounds.

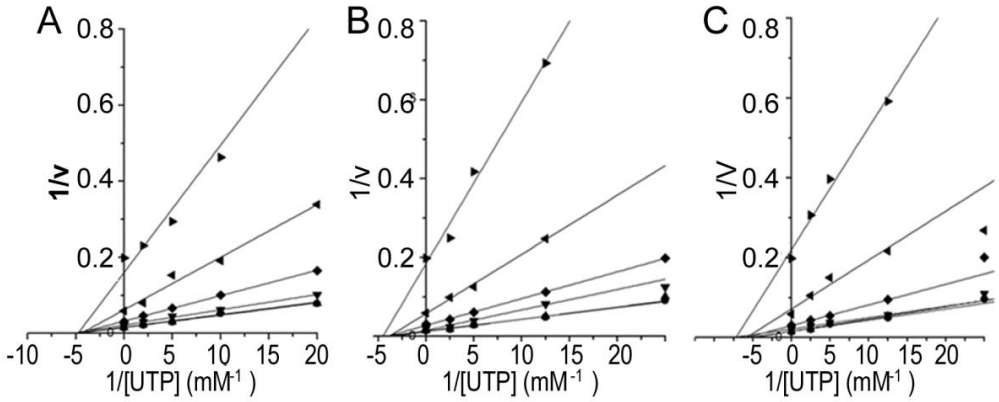

Figure 45. Lineweaver-Burk plot of PyrG towards UTP at different concentrations ofGSK1570606A (A), GSK920684A (B)and GSK735826A (C)compounds.

Docking experiments were performed with these three compounds, showing that they perfectly docked into PyrG active site: GSK1570606A displayed a libdock score of 88.1622, GSK920684A of 92.9566, and GSK735826A of 87.2348 (Fig. 46).

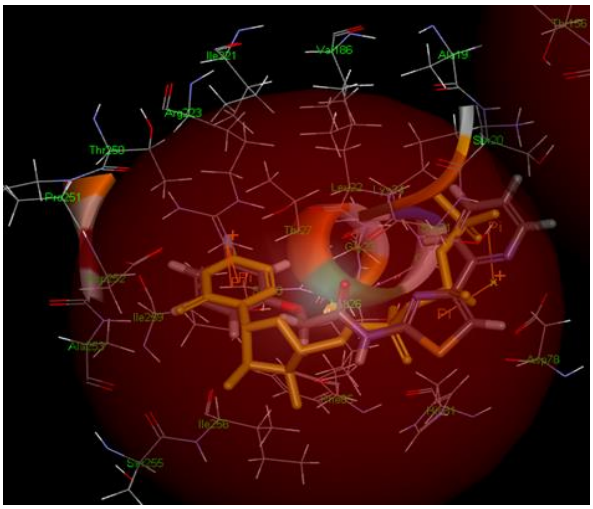

Figure 46. Docking of the GSK735826A into PyrG ATP binding site (Kindly provided by Dr. S. Ekins).

Furthermore, the three GSK compounds were tested against PanK activity, and only the GSK735826A molecule showed to affect the

pantothenate kinase activity, with an IC_{50} of 70 µM. Moreover, the GSK735826A resulted to dock also in PanK structure (Fig. 47).

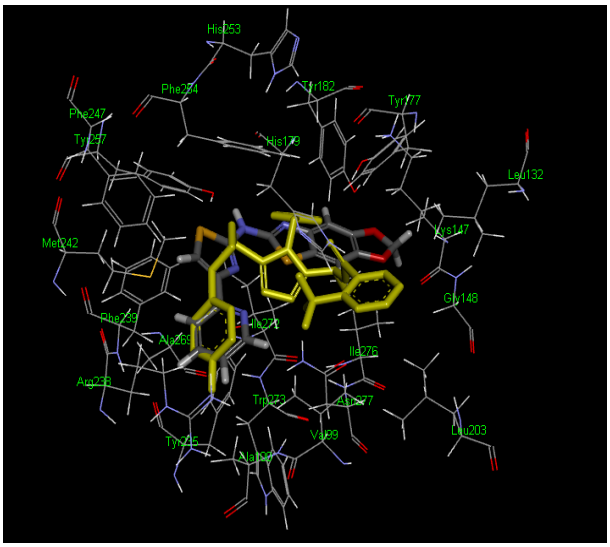

Figure 47. Docking of the GSK735826A into PanK ATP binding site (Kindly provided by Dr. S. Ekins).

Kinetic analysis showed that the GSK735826A compound is also a competitive inhibitor toward PanK ATP-binding site, with a K_i of 65.3 ± 4.33 µM (Fig. 48A). In turn, the compound resulted to exert an uncompetitive inhibition toward pantothenate (Fig. 48B).

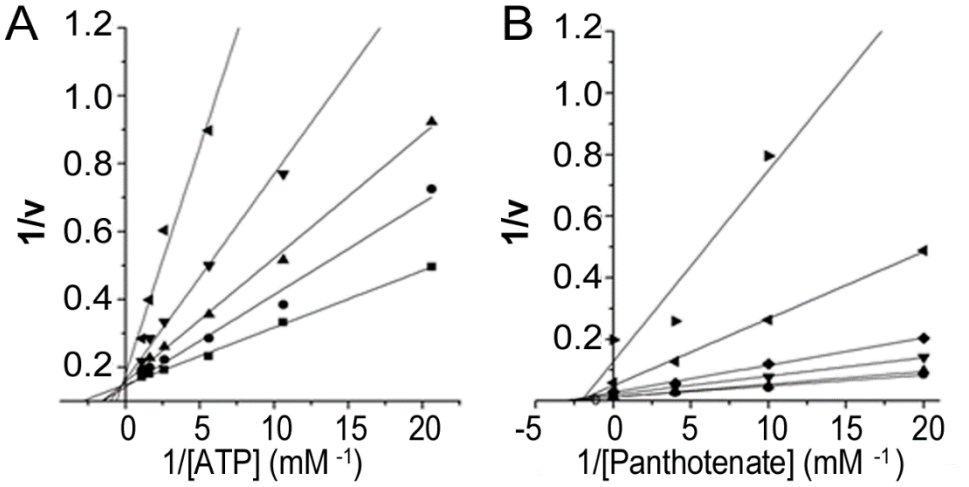

Figure 48. Lineweaver-Burk plots of PanK towards ATP (A) and pantothenate (B) at different concentrations of GSK735826A compound.

4.6.2.1 Validation of *M. tuberculosis* PyrG as cellular target of the GSK1570606A, GSK920684A and GSK735826A compounds

To unveil the mechanism of action of these three GSK compounds, together with the role of PyrG, a *M. tuberculosis* conditional PyrG knock-down (cKD) mutant was built in collaboration with Prof. Riccardo Manganelli (University of Padova, Italy), named TB456. This strain possesses *pyrG* gene under the control of the inducible Pip promoter; consequently, *pyrG* expression is switched on exclusively in the presence of the inducer, Pristinamicine (Pi), and expression levels increase by increasing Pi concentration. The MIC values toward the three GSK compounds were determined in liquid medium by REMA assay, adding different concentrations of the inducer, as shown in Table 8.

Since PyrG is essential for *M. tuberculosis* growth and survival, in the absence of Pi, as expected, the cKD strain is not able to grow. In parallel, the GSK920684A compound does not show any significant change in MIC values at the different Pi concentrations tested. Concerning the remaining two compounds, instead, MIC values display a certain dependence on *pyrG* transcript levels. As shown in Table 8, in the presence of the GSK735826A, the TB456 cKD strain is incapable to grow when Pi concentration is low. Thus, by increasing Pi amount, *pyrG* expression increases, and TB456 strain shows a decrease in MIC values of 4-fold respect to the wild-type. These evidences gave a proof that GSK735826A mechanism of action involves inhibition of the CTP-synthetase. Similar results were obtained with the GSK1570606A compound, but to a lower extent, displaying an MIC two-

fold higher compared to that of the wild-type strain, even at the highest Pi amount in the cell culture.

Compounds	MIC (µg/ml) in *M. tuberculosis*					
	H37Rv	TB456 (Pi, ng/ml)				
		0	5	15	25	50
GSK1570606A	6.2	/	3.12	3.12	3.12	6.25
GSK920684A	12.5	/	12.5	12.5	12.5	12.5
GSK735826A	1.55	/	/	0.39	0.39	0.39

Table 8. MIC values toward GSK1570606A, GSK920684A and GSK735826A compounds of *M. tuberculosis* wild type (H37Rv) and TB456 cDK strain at different Pi concentrations.

These results strongly reinforce the role of PyrG as a cellular target of the GSK735826A and GSK1570606A compounds, whilst concerning the GSK920684A, it may have a secondary role in the mechanism of action of this molecule.

4.7 Expression and purification of human CTP synthetase-1 (hCTPS-1) in *Pichia pastoris*

The results here described are pointing toward PyrG as a good, druggable cellular target for the development of novel antitubercular compounds. Unfortunately, *M. tuberculosis* PyrG has been shown to possess a large similarity with human CTP synthetase-1 and -2 (CTPS-1 and CTPS-2) isoforms. In view of the essential metabolic pathways in which CTP synthetases are involved, deeper investigations on the possible effects of *M. tuberculosis* PyrG inhibitors on the correspondent human enzymes could be fundamental for further development of antimycobacterial agents. For this purpose, it was decided to clone the *hCTPS-1* gene into expression vectors for *E. coli*, in order to express and purify the recombinant enzyme, to be finally tested in the presence of *M. tuberculosis* PyrG inhibitors already identified. Since all our attempts (cloning in different expression vectors and performing expression trials testing several different conditions, co-expression with bacterial molecular chaperones, auto-inducing medium ZYP-5052, etc.) to obtain a soluble and active human enzyme from *E. coli* failed (data not shown), we moved to a eukaryotic expression system in *Pichia pastoris*. Consequently, *hCTPS-1* gene was cloned into pPICZ-B-eGFP vector (described in Material and Methods), allowing expression of the cloned gene, fused with eGFP, under the control of a methanol-inducible

promoter. The linearized recombinant vector was transformed into *P. pastoris* KM71-H cells, and several colonies grew, meaning that the recombinant plasmid has been integrated into yeast genome through homologous recombination within 5' AOX1 region. Among the recombinant clones obtained, 18 were checked for fluorescent signal after 24 hours, 48 hours and 72 hours of induction, and the recombinant clone that gave the highest fluorescent signal (clone 4, Fig. 49) was chosen for further investigations.

P. pastoris clone 4 was checked on a larger scale, to test whether hCTPS-1 is expressed in a soluble and active form.

Starting from 1L of cell culture, the protein was expressed and then purified, as described in "Materials and Methods" section. Purified protein sample was analyzed by SDS-PAGE, and the results were visualized by ChemiDoc system Bio-Rad (Fig. 50).

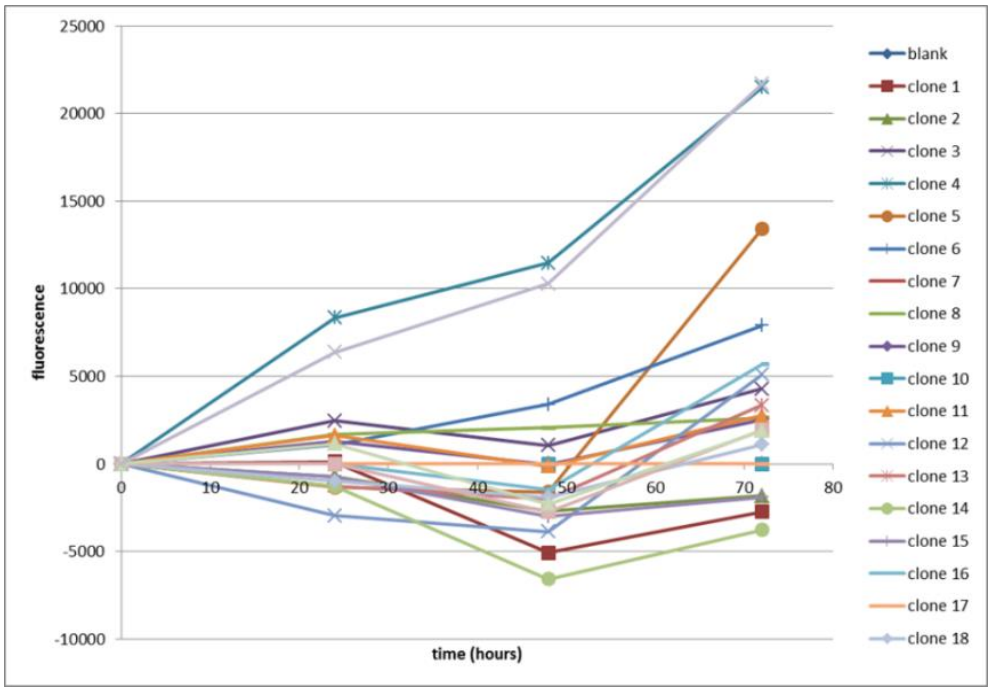

Figure 49. Fluorescence signal of the 18 recombinant clones tested.
Fluorescence was analyzed at time 24 hr, 48 hr and 72 hr.

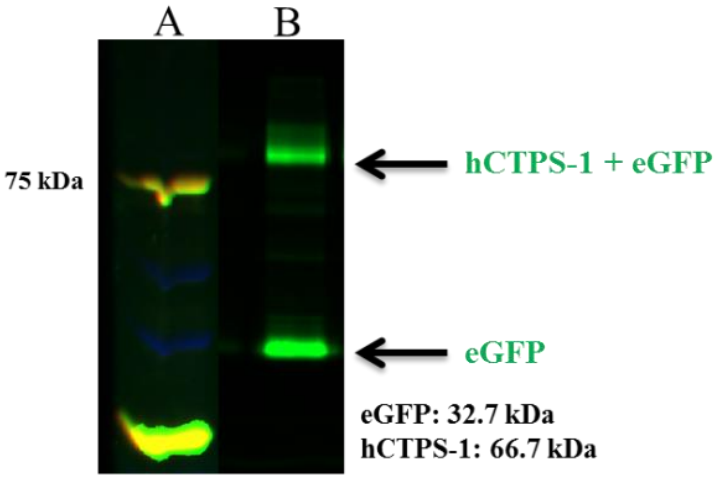

Figure 50. SDS-PAGE detecting eGFP fluorescence of hCTPS-1 protein. A=marker; B=protein sample. The upper band corresponds to the expected molecular weight of eGFP-hCTPS-1 (99.4 kDa); the lower band corresponds to free eGFP (32.7 kDa).

Protein sample was dialyzed and digested with PreScission enzyme and then applied on a Ni-NTA resin (Fig. 51). The digested hCTPS-1 enzyme, recovered from the flow through (FT), was quantified ($\varepsilon_{280\ nm}$= 0.953 mM^{-1} cm^{-1}): from 1L of cell culture, 10 ml of hCTPS-1 were recovered, at concentration of 0.6 mg/ml. Then, the human enzyme was enzymatically tested following the same assay conditions employed for *M. tuberculosis* PyrG, exhibiting full activity.

Successively, hCTPS-1 catalytic constants were calculated toward both ATP and UTP: K_m 0.2 toward ATP; K_m 0.2 mM toward UTP.

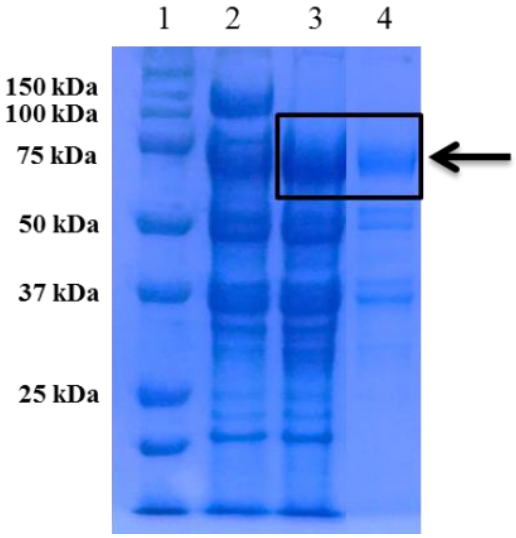

Figure 51. SDS-PAGE of hCTPS-1 protein before and after digestion with PreScission enzyme.
1 = marker; 2 = hCTPS-1 not digested; 3 = hCTPS-1 digested; 4 = hCTPS-1 from FT from Ni-NTA.

4.7.1 hCTPS-1 enzymatic assays in the presence of *M. tuberculosis* PyrG inhibitors

Until now, some new antitubercular compounds targeting *M. tuberculosis* PyrG have been identified: the 11426026 compound, emerged as the S-dioxide active metabolite of the 7947882 prodrug; the CDD-823953, derived from docking experiments; and the GSK compounds GSK1570606A, GSK920684A and GSK735826A, emerged from the target-based screening. All of them have been tested against hCTPS-1 activity, for toxicity studies.

Among them, the most active *M. tuberculosis* PyrG inhibitor, the 11426026, displayed to be nearly ineffective against hCTPS-1, with an IC50 higher than 1000 µM (Table 9; Fig. 52A). This result strongly corroborates the importance of the 11426026 metabolite as potential new platform for antituberculars development.

Concerning the CDD-823953, preliminary results shows that the compound exerts an inhibitory effect against the human enzyme which is approximately five-fold lower compared to that against the mycobacterial PyrG (data not shown).

Instead, the three GSK compounds displayed a certain inhibitory degree against hCTPS-1, that was comparable to that against *M.*

tuberculosis PyrG, as it can be observed from the correspondent IC_{50} values: GSK1570606A displayed an IC50 of 15.1 ± 3.45 μM, GSK920684A of 34.6 ± 5.15 μM, and GSK735826A of 24.2 ± 3.70 μM (Fig. 52B,C,D; Tab. 9).

Consequently, whilst on one hand GSK compounds inhibit both *M. tuberculosis* and human enzymes, the 11426026 compound represents an agent that selectively affects the mycobacterial PyrG activity. Thus, the 11426026 constitutes a starting platform for further optimizations, in order to develop new and more efficacious selective *M. tuberculosis* PyrG inhibitors. In parallel, GSK compounds could be submitted to chemical modifications, aiming to reduce as much as possible the effects against the human enzyme.

Compound	**IC_{50} *M. tuberculosis* PyrG (μM)**	**IC_{50} *h*CTPS-1 (μM)**
11426026	35.0 ± 0.20	> 1000
GSK1570606A	2.9 ± 0.61	15.1 ± 3.45
GSK920684A	23.3 ± 2.15	34.6 ± 5.15
GSK735826A	19.7 ± 2.16	24.2 ± 3.70

Table 9. *M. tuberculosis* PyrG and human CTPS-1 IC50 values toward 11426026, GSK1570606A, GSK920684A and GSK735826A compounds.

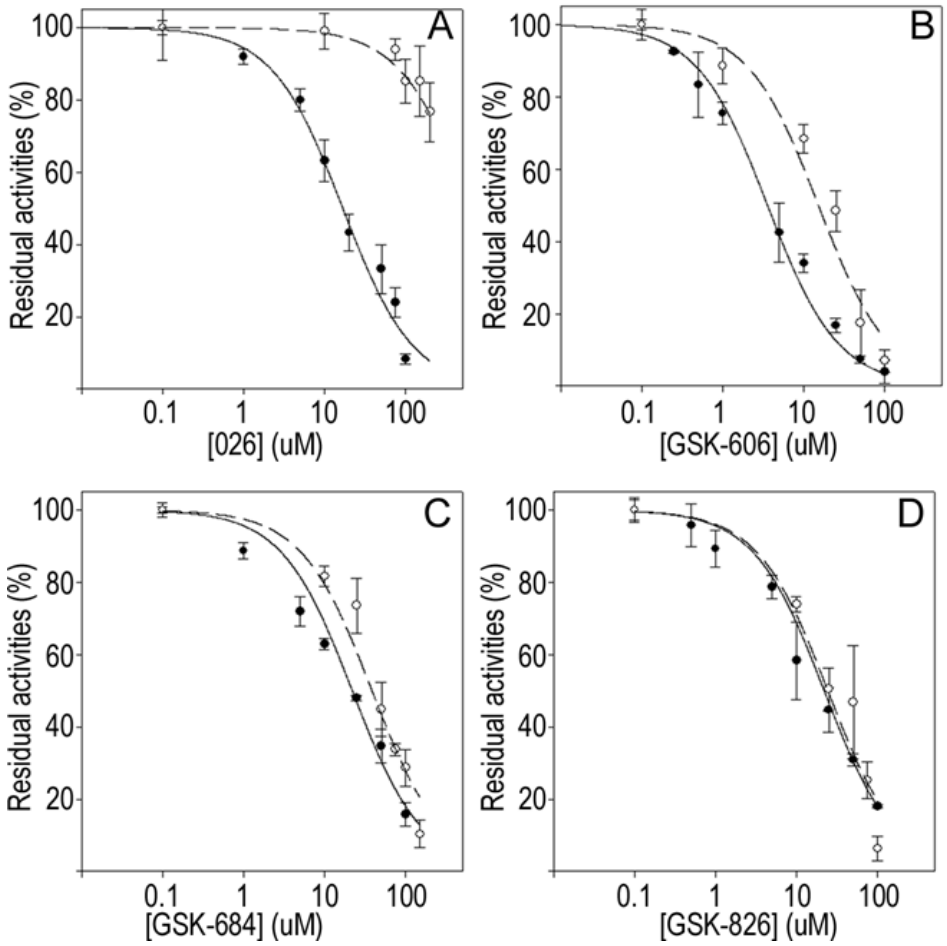

Figure 52. IC50 calculation for 11426026 (A), GSK1570606A (B), GSK920684A (C) and GSK735826A (D) compounds.

5. Discussion and future perspectives

Tuberculosis (TB), despite considered for a long time a completely eradicated infection, started tormenting human health again in 1980s. HIV infections, defects in individuals immune response, poverty, smoking, lack of adequate sanitary conditions and under nutrition, are the main risk factors predisposing to the infectious disease, among others (Dheda *et al*., 2016). Although the short-course therapy is still an efficacious approach (Hoagland *et al*., 2016; Kurtz *et al*., 2016), the spread of *M. tuberculosis* drug-resistant strains (MDR, XDR and TDR) is perpetually augmenting, making all therapeutic strategies more and more ineffective (WHO, 2015). For all these reasons, the research for new, more potent antitubercular drugs, together with the identification of novel cellular druggable targets whose impairment allows killing of *M. tuberculosis* drug-resistant strains, are absolutely required.

Two main routes can be followed for antitubercular compounds identification: "from drug to target" and "from target to drug" (Lechartier *et al*., 2014). The first strategy, employed for the identification of all the compounds nowadays present in clinical development stages, rests on the so called "whole-cell phenotypic screening", namely a screening of libraries of compounds against *M. tuberculosis* growth, to see which of them deserve further investigations. Unfortunately, the principal limitation of this approach is the frequent impossibility to identify the cellular targets, thus limiting the possibility of further development (Lechartier *et al*., 2014). On the other side, the "from target to drug" strategy consists in an *in vitro* screening of chemical libraries against well established and validated cellular targets, permitting the identification of molecules able to affect their enzymatic activity. Regrettably, also this second approach has restrictions, since compounds able to inhibit a certain essential bacterial target, often do not reflect this efficacy when tested against the mycobacterial growth. In view of the limitations characterizing both strategies here described, TB drug research decided to take advantage of a combination of them, by screening compounds having known antitubercular activity, against well validated mycobacterial targets (Lechartier *et al*., 2014). In this work, everything started employing a "whole-cell phenotypic screening"; successively, once interesting compounds have been identified, together with their cellular targets, we decided to combine both strategies, performing a "target-based phenotypic screening".

Getting to the point, this project started from the screening of CB2 library of the National Institute of Allergy and Infectious Diseases (NIAID) (Ananthan *et al*., 2009; Goldman and Laughon, 2009; Maddry *et al*., 2009) through which two molecules, the thiophenecarboxamide 7947882 and thecarbonothioyl-propanamide 7904688 derivatives, emerged for their efficacious activity against *M. tuberculosis* growth. Trying to unveil 7947882 and 7904688 mechanisms of action, isolation of *M. tuberculosis* mutants resistant to these compounds and the sequencing of their genome, allowed the identification of mutations mapping in *ethA*, *pyrG* and *coaA* genes. *ethA* codes for the FAD-containing NADPH-dependent monooxygenase EthA already known to be the activator of ethionamide (ETH). Since mutations in the gene coding for a drug activator are often responsible for a resistant phenotype, we hypothesized EthA being also the activator of the 7947882 and 7904688. Moreover, being *pyrG* and *coaA* two essential genes, the former coding for the CTP-synthetase PyrG, and the latter coding for the pantothenate kinase PanK, both of them were hypothesized to represent the cellular targets of the 7947882 and 7904688.

The CTP synthetase is an enzyme involved in *de novo* pyrimidines biosynthesis, an essential pathway for *M. tuberculosis*, particularly for the production of nucleic acids precursors, already targeted with efficacious antituberculars (Djaout *et al.,* 2016). Among the enzymes involved, thymidylate synthase ThyX inhibition displayed important and interesting results (Djaout *et al*., 2016), being inhibited by the Naphthoquinone (NQ) compounds, that showed to possess also anticancer and antimalarian properties (Tran *et al*., 2004; Djaout *et al*., 2016). Further investigations demonstrated *M. tuberculosis* ThyX being a promising cellular target, with an available crystallographic structure (Sampathkumar *et al*., 2005) and with no correlations with the correspondent human enzyme (Myllykallio *et al*., 2002; Koehn *et al*., 2009). These evidences highlight the vulnerability of this pathway, reinforcing our hypothesis in considering PyrG as a really good potential target for new antitubercular compounds.

On the other side, the pantothenate kinase is involved in another essential pathway for *M. tuberculosis* growth: coenzyme A (CoA) biosynthesis. In detail, PanK catalyzes the rate-limiting phosphorylation of pantothenate, which belongs to a series of reactions that will give rise to CoA production (Reddy *et al*., 2014). Anti-TB drug research is already focusing on this biosynthetic pathway. Particularly, compounds inhibiting one of the enzymes involved in pantothenate production, pantothenate synthetase PanC, have been identified (Spry *et al*., 2008). Among the most recent PanC inhibitors, imidazo[2,1-b]thiazole derivatives displayed moderate activity against *M. tuberculosis*, in both latent and actively

growing stages (Samala *et al*., 2016). Considering, instead, already known PanK inhibitors, some triazoles and biaryls recently emerged through a target-based screening (Björkelid *et al.*, 2013). In view of the importance of the pathway in which PanK is involved, and knowing its essentiality in *M. tuberculosis* (Awasthy *et al*., 2010), it is understandable the growing interest of anti-TB drug research in finding new inhibitors targeting this enzyme.

Moreover, although PyrG and PanK are involved in two different pathways, it is important to note, as it is shown in Figure 53, how they are actually convergent in lipid biosynthesis. Thus, the relevance of the two targets taken individually, together with this important observation, gave us a strong motivation to go ahead in investigating these two enzymes in our research.

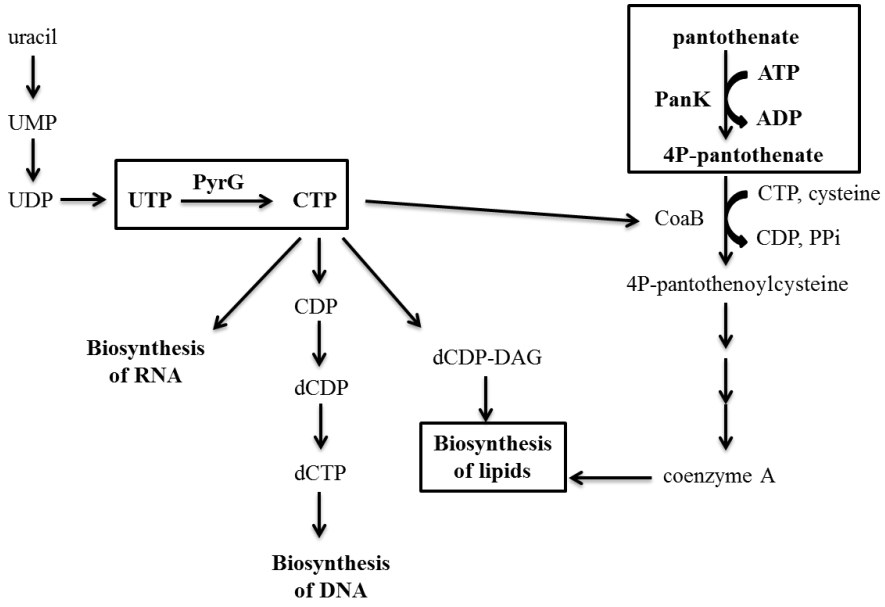

Figure 53. PyrG and PanK biosynthetic pathways.

In view of the drug-resistant TB infections scenario, it is clear that not only new drugs are required, but is of inestimable importance the identification of novel compounds that are able to be "resistance resistant"

(Li K *et al*., 2014). Among the several approaches that can be employed to fight drug-resistant strains spread, one of the most powerful is the research of "multitargeting" compounds, thus affecting more than one target (Silver, 2007; Morphy, 2012). These targets could belong to the same pathway ("series inhibition"), or could work in different pathways, and the inhibitor could be a mimicry of a common substrate or inhibit, for instance, a membrane component ("parallel imitation"). Moreover, in more complex circumstances, a "network inhibition" could be exerted, when several targets in series and/or in parallel are implicated (Li K *et al*., 2014). Moreover, compounds reported to be efficacious in monotherapy, effectively affect more than one cellular function (Silver, 2007), whilst drugs inhibiting only one single target, among which many antituberculars, result more effective when combined with other compounds (Li K *et al*., 2014). Considering these aspects, it is comprehensible the growing interest toward the identification of multitargeting antitubercular compounds, representing a potent tool to kill the pathogen in a more efficient way.

Consequently, this knowledge made the validation of PyrG and PanK as cellular targets of the 7947882 and 7904688 even more important, paving the way for possible future multitargeting antitubercular therapies.

For the genetic validation of the two putative targets, we tried to overexpress either *pyrG* or *coaA* in *M. tuberculosis* wild-type strain, to see whether it could decrease the sensitivity of the bacterium to the 7947882 and 7904688 molecules. Unfortunately, the overexpression of the two genes resulted to be toxic for mycobacterial cells, thus hampering this approach. For this reason, we moved to a biochemical validation, using the recombinant wild-type and mutant PyrG and PanK proteins. However, being the compounds demonstrated to require EthA activation, the monooxygenase was also produced.

This approach demonstrated *in vitro* that the compounds, once activated, are effectively able to inhibit the enzymatic activity of both enzymes. Moreover, the metabolomic experiments reinforced these results, demonstrating that the effects of 7947882 on mycobacterial cells are ascribable to a CTP-synthetase inhibition, causing a reduction in CTP amount and an accumulation of intermediates in pyrimidines and purines biosynthetic pathways.

As reported above, several drug-resistant phenotypes develop as a consequence of mutations affecting drug activators, and in particular, *ethA* mutation frequency has been observed to be significantly high. Being the 7947882 and 7904688 two prodrugs activated by this monooxygenase, they are poorly useful as potential anti-TB drugs, in particular considering that *M. tuberculosis* strains already resistant to ETH, are cross-resistant to the

7947882 and 7904688. Therefore, the development of antituberculars that do not require anymore EthA activation could be of extreme interest for drug research.

Proceeding in this direction, and going on collecting proofs that PyrG and PanK are the targets of these compounds, a 7947882 active metabolite, the S-dioxide derivative, was identified via biochemical approaches, chemically synthetized and named 11426026. Conversely, the 7904688 active metabolites were impossible to identify, probably due to their high reactivity; consequently, we abandoned this series, concentrating our efforts on the 11426026. The compound was tested against PyrG and PanK, showing to be able to directly inhibit both enzymes activity *in vitro*, without further EthA activation. This evidence was further confirmed by the fact that, like the wild type, *M. tuberculosis ethA* mutant strain did not show resistance to the 11426026. Moreover, *pyrG* and *coaA* mutants displayed resistance to the metabolite, thus reinforcing our hypothesis. In conclusion, the 11426026 is a new active antitubercular, affecting two essential targets, subsequently representing an interesting scaffold for the development of further multitargeting compounds (Fig. 54).

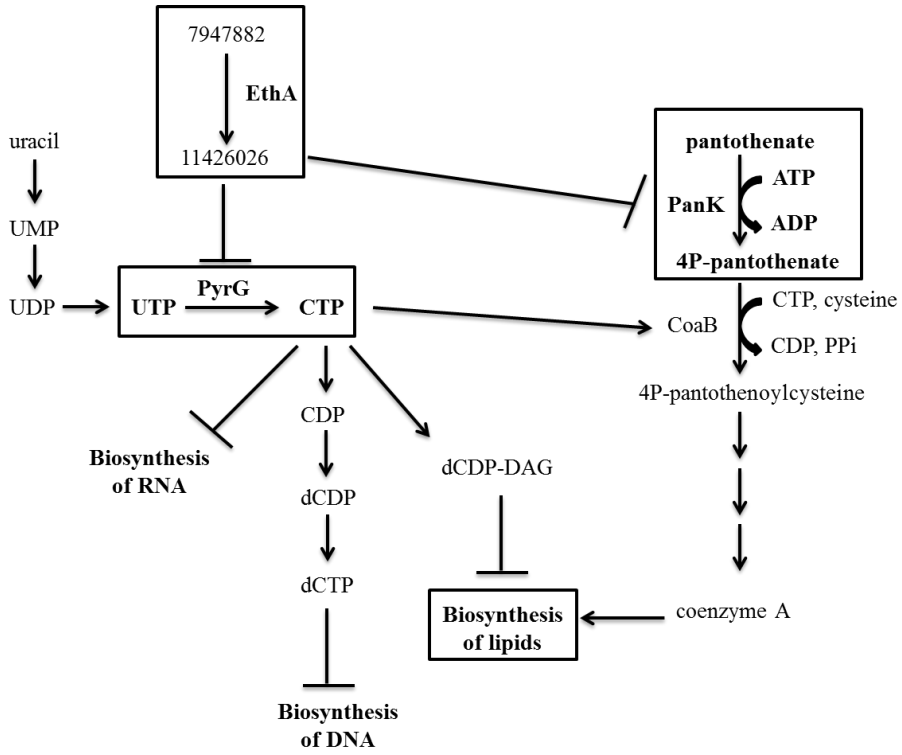

Figure 54. 11426026 effects through both PyrG and PanK inhibition.

In view of the limitations of the "whole-cell phenotypic screening" approach, it is clear why the study of the mechanisms of action and resistance of compounds already proven to possess a good antitubercular activity is very complex, and several strategies should be combined to fulfil this objective. Here, a combination of biochemical, microbiological and metabolomic analysis allowed the demonstration of PyrG and PanK being the cellular essential functions targeted by EthA-activated 7947882 and 7904688. Once these goals have been achieved, the following steps were focused on exploiting the two validated targets to perform "target-based" screenings of chemical libraries of compounds with known antitubercular action. This kind of strategy, becoming an increasingly suitable tool for research, in this specific context represents a convenient path aiming the discovery of new antituberculars that target more than one cellular function.

Thus, in this work, target-based screening approaches were employed in order to identify new multitargeting antitubercular compounds by

exploiting the two validated targets, both with *in silico* and *in vitro* approaches.

The *in silico* method consisted in a virtual screening on PyrG of the Collaborative Drug Discovery (CDD) compounds database. In particular, the 4-Nitroacetanilide substructure of 11426026 was used to search for a set of *M. tuberculosis* active compounds collected in the CDD Database (Ekins and Bunin, 2013). Twelve compounds were retrieved and docked in the PyrG, and subsequently in the PanK ATP binding sites. Successively, the four compounds showing the highest scores were tested against PyrG and PanK activities, providing a moderate inhibitor of both enzymes (CDD 823953), exerting a competitive inhibition toward ATP.

Similarly, the *in vitro* approach consisted in the screening of a chemical library of compounds with known antitubercular activity (GSK TB-set), firstly against PyrG. Among the 204 compounds tested, 15 of them displayed to inhibit more than 50% PyrG activity. In particular, three of them showed to affect more than 75% PyrG activity, and from a structural point of view, the three compounds share a common pyridyl-thiazole moiety. Interestingly, 12 of the 15 compounds identified possess this common moiety, underlining the importance of the pyridyl-thiazole component for PyrG inhibition. Successively, the characterization of PyrG inhibition by the three molecules highlighted again a competitive inhibition toward the ATP-binding site. All of them were tested against PanK activity, and one, the GSK735826A, represents another PyrG inhibitor able to moderately affect also the pantothenate kinase activity, and resulting, as for PyrG, a competitive inhibitor toward ATP.

Whilst PanK enzyme is an already validated antitubercular target (Björkelid *et al*., 2013), PyrG represents an important innovation in the scenario of target validation for anti-TB therapy. However, CTP-synthetases are present also in humans, encoded by *CTPS-1* and *CTPS-2* genes (Martin *et al*., 2014; Kassel *et al*., 2010; van Kuilenburg *et al*, 2000), and show a certain homology with *M. tuberculosis* CTP-synthetase PyrG. Consequently, we decided to produce one of the two human isoforms, hCTPS-1, in order to test *M. tuberculosis* PyrG inhibitors against the human enzyme, for toxicity studies. Since all the attempts to obtain the human enzyme in a prokaryotic system failed, we expressed and purified the CTPS-1 using *Pichia pastoris*, that resulted active. Among the inhibitors tested, the GSK compounds resulted to inhibit the human counterpart, with a potency which is very similar to that observed against the mycobacterial PyrG. On the contrary, the 11426026 compound, the best inhibitor of *M. tuberculosis* PyrG identified so far, does not inhibit the human enzyme, giving a great encouragement to continue working on this compound. Particularly, it could

be worth to submit this molecule to chemical modifications in order to gain even more efficient inhibitors, leaving the human enzyme as more unaffected as possible.

However, concerning the GSK compounds, it is essential to specify that all of them have been reported to exert a low toxicity in humans (Ballell *et al*., 2013). Therefore, the inhibitory effect that has been observed *in vitro* against the human enzyme, does not properly reflect what could be seen at the whole human organism level. Consequently, whilst on one side *M. tuberculosis* PyrG can be coupled with the human CTPS-1 in order to screen chemical libraries against both enzymes, on the other side, every time good but not selective mycobacterial PyrG inhibitors are identified, the inhibitory effects against the human CTP-synthetase should be submitted to further investigations.

Concluding, these results led to the identification and characterization of two new *M. tuberculosis* cellular targets, PyrG and PanK, both inhibited by a certain number of common compounds. Therefore, these two enzymes could be employed in the future as a "double-tool" in performing more efficacious screening of libraries of compounds, in order to proceed in finding new multitargeting antitubercular drugs.

6. References

- Akerley BJ, Rubin EJ, Novick VL, Amaya K, Judson N, Mekalanos JJ (2002) A genome-scale analysis for identification of genes required for growth or survival of *Haemophilus influenzae. Proc Natl Acad Sci USA*. 99:966-71.
- Ananthan S, Faaleolea ER, Goldman RC, Hobrath JV, Kwong CD, Laughon BE, MaddryJA, Mehta A, Rasmussen L, Reynolds RC, Secrist JA 3rd, Shindo N, Showe DN, Sosa MI, Suling WJ, White EL (2009) High-throughput screening for inhibitors of *Mycobacterium tuberculosis* H37Rv. *Tuberculosis* (Edinb). 89:334-53.
- Anderson PM (1983) CTP synthetase from *Escherichia coli*: an improved purification procedure and characterization of hysteretic and enzyme concentration effects on kinetic properties. *Biochemistry*. 22:3285–92.
- Andries K, Verhasselt P, Guillemont J, Göhlmann HW, Neefs JM, Winkler H, Van Gestel J, Timmerman P, Zhu M, Lee E, Williams P, de Chaffoy D, Huitric E, Hoffner S, Cambau E, Truffot-Pernot C, Lounis N, Jarlier V (2005) A diarylquinoline drug active on the ATP synthase of *Mycobacterium tuberculosis*. *Science*. 307:223-7.
- Awasthy D, Ambady A, Bhat J, Sheikh G, Ravishankar S, Subbulakshmi V, Mukherjee K, Sambandamurthy V, Sharma UK (2010) Essentiality and functional analysis of type I and type III pantothenate kinases of *Mycobacterium tuberculosis. Microbiology.* 156:2691–2701.
- Ballell L, Bates RH, Young RJ, Alvarez-Gomez D, Alvarez-Ruiz E, Barroso V, Blanco D, Crespo B, Escribano J, González R, Lozano S, Huss S, Santos-Villarejo A, Martín-Plaza JJ, Mendoza A, Rebollo-Lopez MJ, Remuiñan-Blanco M, Lavandera JL, Pérez-Herran E, Gamo-Benito FJ, García-Bustos JF, Barros D, Castro JP, Cammack N (2013) Fueling open-source drug discovery: 177 small-molecule leads against tuberculosis. *Chem Med Chem*. 8:313-21.
- Banerjee A, Dubnau E, Quemard A, Balasubramanian V, Um KS, Wilson T, Collins D, de Lisle G, Jacobs WR Jr (1994) *inhA*, a gene encoding a target for isoniazid and ethionamide in *Mycobacterium tuberculosis*. *Science*. 263:227-30.
- Baron M, Reynes JP, Stassi D, Tiraby G (1992) A selectable bifunctional beta-galactosidase: phleomycin-resistance fusion protein as a potential marker for eukaryotic cells. *Gene*. 114:239-43.

- Barry RM, Bitbol AF, Lorestani A, Charles EJ, Habrian CH, Hansen JM, Li HJ, Baldwin EP, Wingreen NS, Kollman JM, Gitai Z (2014) Large-scale filament formation inhibits the activity of CTP synthetase. *Elife*. 3:e03638.
- Baulard AR, Betts JC, Engohang-Ndong J, QuanS, McAdam RA, Brennan PJ, Locht C, Besra GS (2000) Activation of the pro-drug ethionamide is regulated in mycobacteria. *J Biol Chem*. 275:28326-31.
- Belanger AE, Besra GS, Ford ME, Mikusová K, Belisle JT, Brennan PJ, Inamine JM (1996) The *embAB* genes of *Mycobacterium avium* encode an arabinosyl transferase involved in cell wall arabinan biosynthesis that is the target for the antimycobacterial drug ethambutol. *Proc Natl Acad Sci USA*. 93:11919-24.
- Benator D, Bhattacharya M, Bozeman L, Burman W, Cantazaro A, Chaisson R, Gordin F, Horsburgh CR, Horton J, Khan A, Lahart C, Metchock B, Pachucki C, Stanton L, Vernon A, Villarino ME, Wang YC, Weiner M, Weis S (2002) Tuberculosis Trials Consortium. Rifapentine and isoniazid once a week versus rifampicin and isoniazid twice a week for treatment of drug-susceptible pulmonary tuberculosis in HIV-negative patients: a randomised clinical trial. *Lancet*. 360:528-34.
- Biava M, Porretta GC, Poce G, Supino S, Deidda D, Pompei R, Molicotti P, Manetti F, Botta M (2006) Antimycobacterial agents. Novel diarylpyrrole derivatives of BM212 endowed with high activity toward *Mycobacterium tuberculosis* and low cytotoxicity. *J Med Chem*. 49:4946-52.
- Björkelid C, Bergfors T, Raichurkar AK, Mukherjee K, Malolanarasimhan K, Bandodkar B, Jones TA (2013) Structural and biochemical characterization of compounds inhibiting *Mycobacterium tuberculosis* pantothenate kinase. *J Biol Chem*. 288:18260-70.
- Blumberg HM, Burman WJ, Chaisson RE, Daley CL, Etkind SC, Friedman LN, Fujiwara P, Grzemska M, Hopewell PC, Iseman MD, Jasmer RM, Koppaka V, Menzies RI, O'Brien RJ, Reves RR, Reichman LB, Simone PM, Starke JR, Vernon AA (2003) American Thoracic Society, Centers for Disease Control and Prevention and the Infectious Diseases Society. American Thoracic Society/Centers for Disease Control and Prevention/Infectious Diseases Society of America: treatment of tuberculosis. *Am J Respir Crit Care Med*. 167:603-62.
- Boyer PD (1997) The ATP synthase--a splendid molecular machine. *Annu Rev Biochem*. 66:717-49.
- Breen RA, Swaden L, Ballinger J, Lipman MC (2006) Tuberculosis and HIV co-infection: a practical therapeutic approach. *Drugs*. 66:2299-308.

- Brennan PJ (1997) Tuberculosis in the context of emerging and reemerging diseases. *FEMS Immunol Med Microbiol*. 18: 263-9.
- Briken V, Porcelli SA, Besra GS, Kremer L (2004) Mycobacterial lipoarabinomannan and related lipoglycans: from biogenesis to modulation of the immune response. *Mol Microbiol*. 53: 391–403.
- Broset E, Martín C, Gonzalo-Asensio J (2015) Evolutionary landscape of the *Mycobacterium tuberculosis* complex from the viewpoint of PhoPR: implications for virulence regulation and application to vaccine development. *MBio*. 6:e01289-15.
- Campbell EA, Korzheva N, Mustaev A, Murakami K, Nair S (2001) Structural mechanism for rifampicin inhibition of bacterial RNA Polymerase. *Cell*. 104:901-12.
- Chigwada T, Mbiya W, Chipiso K, Simoyi, RH (2014) S-oxygenation of thiocarbamides V: oxidation of tetramethylthiourea by chlorite in slightly acidic media. *J Phys Chem A*. 118:5903-14.
- Cohen J (2013) Infectious disease. Approval of novel TB drug celebrated—with restraint. *Science*. 339:130.
- Cohen KA, Bishai WR, Pym AS (2014) Molecular basis of drug resistance in *Mycobacterium tuberculosis*. *Microbiol Spectr*. 2.
- Cole ST, Brosch R, Parkhill J, Garnier T, Churcher C, Harris D, Gordon SV, Eiglmeier K, Gas S, Barry CE 3rd, Tekaia F, Badcock K, Basham D, Brown D, Chillingworth T, Connor R, Davies R, Devlin K, Feltwell T, Gentles S, Hamlin N, Holroyd S, Hornsby T, Jagels K, Krogh A, McLean J, Moule S, Murphy L, Oliver K, Osborne J, Quail MA, Rajandream MA, Rogers J, Rutter S, Seeger K, Skelton J, Squares R, Squares S, Sulston JE, Taylor K, Whitehead S, Barrell BG (1998) Deciphering the biology of *Mycobacterium tuberculosis* from the complete genome sequence. *Nature*. 393:537-44.
- Cole ST, Riccardi G (2011) New tuberculosis drugs on the horizon. *Curr Opin Microbiol*. 14:570-6.
- Comas I, Coscolla M, Luo T, Borrell S, Holt KE, Kato-Maeda M, Parkhill J, Malla B, Berg S, Thwaites G, Yeboah-Manu D, Bothamley G, Mei J, Wei L, Bentley S, Harris SR, Niemann S, Diel R, Aseffa A, Gao Q, Young D, Gagneux S (2013) Out-of-Africa migration and Neolithic coexpansion of *Mycobacterium tuberculosis* with modern humans. *Nat Genet*. 45:1176–82.
- Cooper AM (2009) Cell-mediated immune responses in tuberculosis. *Annu Rev Immunol*. 27:393-422.
- Copeland AR (2000) Enzymes: a practical introduction to structure, mechanism, and data analysis. 2nd Edition. Wiley Online Library.

- Council MR (1962) Long-term chemotherapy in the treatment of chronic pulmonary tuberculosis with cavitation. *Tubercle*. 43:201-67.
- Crofton J, Mitchison DA (1948) Streptomycin resistance in pulmonary tuberculosis. *Br Med J*. 2:1009-15.
- Dartois V (2014) The path of anti-tuberculosis drugs: from blood to lesions to mycobacterial cells. *Nat Rev Microbiol*. 12:159-67.
- Das S, Kumar P, Bhor V, Surolia A, Vijayan M (2006) Invariance and variability in bacterial PanK: a study based on the crystal structure of *Mycobacterium tuberculosis* PanK. *ActaCrystallogr D BiolCrystallogr*. 62:628-38.
- DeBarber AE, Mdluli K, Bosman M, Bekker LG, Barry CE (2000) Ethionamide activation and sensitivity in multidrug-resistant *Mycobacterium tuberculosis*. *Proc Natl Acad Sci USA*. 97:9677–82.
- de Carvalho LP, Zhao H, Dickinson CE, Arango NM, Lima CD, Fischer SM, Ouerfelli O, Nathan C, Rhee, KY (2010) Activity based metabolomic profiling of enzymatic function: identification of Rv1248c as a mycobacterial 2-hydroxy-3-oxoadipate synthase. *Chem Biol*. 17:323–32.
- Deidda D, Lampis G, Fioravanti R, Biava M, Porretta GC, Zanetti S, Pompei R (1998) Bactericidal activities of the pyrrole derivative BM212 against multidrug-resistant and intramacrophagic *Mycobacterium tuberculosis* strains. *Antimicrob Agents Chemother*. 42:3035-7.
- Dessen A, Quémard A, Blanchard JS, Jacobs WR Jr, Sacchettini JC (1995) Crystal structure and function of the isoniazid target of *Mycobacterium tuberculosis*. *Science*. 267:1638-41.
- Dheda K, Barry CE 3rd, Maartens G (2016) Tuberculosis. *Lancet*. 387:1211-26.
- Diacon AH, Pym A, Grobusch M, Patientia R, Rustomjee R, Page-Shipp L, Pistorius C, Krause R, Bogoshi M, Churchyard G, Venter A, Allen J, Palomino JC, De Marez T, van Heeswijk RP, Lounis N, Meyvisch P, Verbeeck J, Parys W, de Beule K, Andries K, Mc Neeley DF (2009) The diarylquinoline TMC207 for multidrug-resistant tuberculosis. *N Engl J Med*. 360:2397-405.
- Djaout K, Singh V, Boum Y, Katawera V, Becker HF, Bush NG, Hearnshaw SJ, Pritchard JE, Bourbon P, Madrid PB, Maxwell A, Mizrahi V, Myllykallio H, Ekins S (2016) Predictive modeling targets thymidylate synthase ThyX in *Mycobacterium tuberculosis*. *Sci Rep*. 6:27792.
- Domenech P, Reed MB, Barry CE 3rd (2005) Contribution of the *Mycobacterium tuberculosis* MmpL protein family to virulence and drug resistance. *Infect Immun*. 73:3492-501.

- Drocourt D, Calmels T, Reynes JP, Baron M, Tiraby G (1990) Cassettes of the *Streptoalloteichus hindustanus ble* gene for transformation of lower and higher eukaryotes to phleomycin resistance. *Nucleic Acids Res*. 18:4009.
- Dubos R, Dubos J (1952) In: The white plague: Tuberculosis, Man, and Society. Rutgers University Press.
- Ducati RG, Ruffino-Netto A, Basso LA, Santos DS (2006) The resumption of consumption: a review on tuberculosis. *Mem Inst Oswaldo Cruz*. 101:697-714.
- Dye C, Glaziou P, Floyd K, Raviglione M (2013) Prospects for tuberculosis elimination. *Annu Rev Public Health*. 34:271-86.
- Ehmann DE, Lahiri SD (2014) Novel compounds targeting bacterial DNA topoisomerase/DNA gyrase. *Curr Opin Pharmacol*. 18:76-83.
- Ekins S, Bunin BA (2013) The Collaborative Drug Discovery (CDD) database. *Methods Mol Biol*. 993:139-54.
- Ekins S, Freundlich JS, Hobrath JV, Lucile White E, Reynolds RC (2014) Combining computational methods for hit to lead optimization in *Mycobacterium tuberculosis* drug discovery. *Pharm Res*. 31:414-35.
- Ellis SB, Brust PF, Koutz PJ, Waters AF, Harpold MM, Gingeras TR (1985) Isolation of alcohol oxidase and two other methanol regulatable genes from the yeast *Pichia pastoris*. *Mol Cell Biol*. 5:1111-21.
- El-Sadr WM, Tsiouris SJ (2008) HIV-associated tuberculosis: diagnostic and treatment challenges. *Semin Respir Crit Care Med*. 29:525-31.
- Endrizzi JA, Kim H, Anderson PM, Baldwin EP (2004) Crystal structure of *Escherichia coli* cytidine triphosphate synthetase, a nucleotide-regulated glutamine amidotransferase/ATP-dependent amidoligase fusion protein and homologue of anticancer and antiparasitic drug targets. *Biochemistry*. 43:6447-63.
- Floss HG, Yu TW (2005) Rifamycin-mode of action, resistance, and biosynthesis. *Chem Rev*. 105:621-32.
- Fraaije MW, Kamerbeek NM, Heidekamp AJ, Fortin R, Janssen DB (2004) The prodrug activator EtaA from *Mycobacterium tuberculosis* is a Baeyer-Villiger monooxygenase. *J Biol Chem*. 279:3354-60.
- Geldmacher C, Schuetz A, Ngwenyama N (2008) Early depletion of *Mycobacterium tuberculosis*-specific T helper 1 cell responses after HIV-1 infection. *J Infect Dis*. 198:1590–8.
- Gerdes SY, Scholle MD, Campbell JW, Balázsi G, Ravasz E, Daugherty MD, Somera AL, Kyrpides NC, Anderson I, Gelfand MS, Bhattacharya A, Kapatral V, D'Souza M, Baev MV, Grechkin Y, Mseeh F, Fonstein MY, Overbeek R, Barabási AL, Oltvai ZN, Osterman AL (2003) Experimental determination

and system level analysis of essential genes in *Escherichia coli* MG1655. *J Bacteriol*. 185:5673-84.

- Gerdes SY, Scholle MD, D'Souza M, Bernal A, Baev MV, Farrell M, Kurnasov OV, Daugherty MD, Mseeh F, Polanuyer BM, Campbell JW, Anantha S, Shatalin KY, Chowdhury SA, Fonstein MY, Osterman AL (2002) From genetic footprinting to antimicrobial drug targets: examples in cofactor biosynthetic pathways. *J Bacteriol*. 184:4555-72.
- Ginsburg AS, Grosset JH, Bishai WR (2003) Fluoroquinolones, tuberculosis, and resistance. *Lancet Infect Dis*. 3:432-42.
- Gler MT, Skripconoka V, Sanchez-Garavito E, Xiao H, Cabrera-Rivero JL, Vargas-Vasquez DE, Gao M, Awad M, Park SK, Shim TS, Suh GY, Danilovits M, Ogata H, Kurve A, Chang J, Suzuki K, Tupasi T, Koh WJ, Seaworth B, Geiter LJ, Wells CD (2012) Delamanid for multidrug-resistant pulmonary tuberculosis. *N Engl J Med.* 366:2151-60.
- Goldman RC, Laughon BE (2009) Discovery and validation of new antitubercular compounds as potential drug leads and probes. *Tuberculosis*. 89:331–333.
- Hartkoorn RC, Sala C, Neres J, Pojer F, Magnet S, Mukherjee R, Uplekar S, Boy-Röttger S, Altmann KH, Cole ST (2012) Towards a new tuberculosis drug: pyridomycin - nature's isoniazid. *EMBO Mol Med*. 4:1032-42.
- Hertoghe T, Wajja A, Ntambi L, Okwera A, Aziz MA, Hirsch C, Johnson J, Toossi Z, Mugerwa R, Mugyenyi P, Colebunders R, Ellner J, Vanham G (2000) T cell activation, apoptosis and cytokine dysregulation in the (co)pathogenesis of HIV and pulmonary tuberculosis (TB). *Clin Exp Immunol.* 122:350–7.
- Hoagland DT, Liu J, Lee RB, Lee RE (2016) New agents for the treatment of drug-resistant *Mycobacterium tuberculosis*. *Adv Drug Deliv Rev*. pii: S0169-409X(16)30136-3.
- Hong Kong Chest Service/British Medical Research Council (1977) Controlled trial of 6-month and 9-month regimens of daily and intermittent streptomycin plus isoniazid plus pyrazinamide for pulmonary tuberculosis in Hong Kong. The results up to 30 months. *Am Rev Respir Dis*. 115:727-35.
- Horlacher OP, Hartkoorn RC, Cole ST, Altmann KH (2012) Synthesis and antimycobacterial activity of 2,1'-dihydropyridomycins. *ACS Med Chem Lett*. 4:264-8.
- Horsburgh CR Jr, Barry CE 3rd, Lange C (2015) Treatment of tuberculosis. *N Engl J Med.* 373:2149-60.
- Hunte C, Palsdottir H, Trumpower BL (2003) Protonmotive pathways and mechanisms in the cytochrome bc1 complex. *FEBS Lett.* 545:39-46.

- Ibrahim M, Andries K, Lounis N, Chauffour A, Truffot-Pernot C, Jarlier V, Veziris N (2007) Synergistic activity of R207910 combined with pyrazinamide against murine tuberculosis. *Antimicrob Agents Chemother*. 51:1011-5.
- Jackowski S, Rock CO (1981) Regulation of coenzyme A biosynthesis. *J Bacteriol.* 148:926–32.
- Jeankumar VU, Saxena S, Vats R, Reshma RS, Janupally R, Kulkarni P, Yogeeswari P, Sriram D (2016) Structure-guided discovery of antitubercular agents that target the gyrase ATPase domain. *Chem Med Chem*. 11:539-48.
- Ji B, Lounis N, Maslo C, Truffot-Pernot C, Bonnafous P, Grosset J (1998) *In vitro* and *in vivo* activities of moxifloxacin and clinafloxacin against *Mycobacterium tuberculosis*. *Antimicrob Agents Chemother.* 42:2066-9.
- Kana BD, Karakousis PC, Parish T, Dick T (2014) Future target-based drug discovery for tuberculosis? *Tuberculosis* (Edinb). 94:551-6.
- Kale MG, Raichurkar A, P SH, Waterson D, McKinney D, Manjunatha MR, Kranthi U, Koushik K, Jena Lk, Shinde V, Rudrapatna S, Barde S, Humnabadkar V, Madhavapeddi P, Basavarajappa H, Ghosh A, Ramya VK, Guptha S, Sharma S, Vachaspati P, Kumar KN, Giridhar J, Reddy J, Panduga V, Ganguly S, Ahuja V, Gaonkar S, Kumar CN, Ogg D, Tucker JA, Boriack-Sjodin PA, de Sousa SM, Sambandamurthy VK, Ghorpade SR (2013) Thiazolopyridine ureas as novel antitubercular agents acting through inhibition of DNA Gyrase B. *J Med Chem*. 56:8834-48.
- Kakkar AK, Dahiya N (2014) Bedaquiline for the treatment of resistant tuberculosis: promises and pitfalls. *Tuberculosis* (Edinb). 94:357-62.
- Karkare S, Chung TT, Collin F, Mitchenall LA, McKay AR, Greive SJ, Meyer JJ, Lall N, Maxwell A (2013) The naphthoquinone diospyrin is an inhibitor of DNA gyrase with a novel mechanism of action. *J Biol Chem*. 288:5149-56.
- Kassel KM, Au da R, Higgins MJ, Hines M, Graves LM (2010) Regulation of human cytidine triphosphate synthetase 2 by phosphorylation. *J Biol Chem*. 285:33727-36.
- Kent C, Carman GM (1999) Interactions among pathways for phosphatidylcholine metabolism, CTP synthesis and secretion through the Golgi apparatus. *Trends Biochem Sci*. 24:146-50.
- Khabbaz RF, Moseley RR, Steiner RJ, Levitt AM, Bell BP (2014) Challenges of infectious diseases in the USA. *Lancet*. 384:53-63.
- Kleinschroth T, Castellani M, Trinh CH, Morgner N, Brutschy B, Ludwig B, Hunte C (2011) X-ray structure of the dimeric cytochrome bc(1) complex from the soil bacterium *Paracoccus denitrificans* at 2.7-Å resolution. *Biochim Biophys Acta*. 1807:1606-15.

- Koehn EM, Fleischmann T, Conrad JA, Palfey BA, Lesley SA, Mathews II, Kohen A (2009) An unusual mechanism of thymidylate biosynthesis in organisms containing the *thyX* gene. *Nature*. 458:919-23.
- Kolly GS, Boldrin F, Sala C, Dhar N, Hartkoorn RC, Ventura M, Serafini A, McKinney JD, Manganelli R, Cole ST (2014) Assessing the essentiality of the decaprenyl-phospho-d-arabinofuranose pathway in *Mycobacterium tuberculosis* using conditional mutants. *Mol Microbiol*. 92:194-211.
- Korb VC, Chuturgoon AA, Moodley D (2016) *Mycobacterium tuberculosis*: manipulator of protective immunity. *Int J Mol Sci*. 17.
- Koul A, Dendouga N, Vergauwen K, Molenberghs B, Vranckx L, Willebrords R, Ristic Z, Lill H, Dorange I, Guillemont J, Bald D, Andries K (2007) Diarylquinolines target subunit c of mycobacterial ATP synthase. *Nat Chem Biol*. 3:323-4.
- Koul A, Arnoult E, Lounis N, Guillemont J, Andries K (2011) The challenge of new drug discovery for tuberculosis. *Nature*. 469:483-90.
- Koutz P, Davis GR, Stillman C, Barringer K, Cregg J, Thill G (1989) Structural comparison of the *Pichia pastoris* alcohol oxidase genes. *Yeast*. 5:167-77.
- Kruk ME, Schwalbe NR, Aguiar CA (2008) Timing of default from tuberculosis treatment: a systematic review. *Trop Med Int Health*. 13:703-12.
- Kurz SG, Furin JJ, Bark CM (2016) Drug-resistant tuberculosis: challenges and progress. *Infect Dis Clin North Am*. 30:509-22.
- Larrouy-Maumus G, Biswas T, Hunt DM, Kelly G, Tsodikov OV, de Carvalho LP (2013) Discovery of a glycerol 3-phosphate phosphatase reveals glycerophospholipid polar head recycling in *Mycobacterium tuberculosis*. *Proc Natl Acad Sci USA*. 110:11320–5.
- Lechartier B, Rybniker J, Zumla A, Cole S (2014) Tuberculosis drug discovery in the post genomic era. *EMBO Mol Med*. 6:158-68.
- Lei B, Wei CJ, Tu SC (2000) Action mechanism of antitubercular isoniazid. Activation by *Mycobacterium tuberculosis* KatG, isolation, and characterization of Inha inhibitor. *J Biol Chem*. 275:2520-6.
- Li K, Schurig-Briccio LA, Feng X, Upadhyay A, Pujari V, Lechartier B, Fontes FL, Yang H, Rao G, Zhu W, Gulati A, No JH, Cintra G, Bogue S, Liu YL, Molohon K, Orlean P, Mitchell DA, Freitas-Junior L, Ren F, Sun H, Jiang T, Li Y, Guo RT, Cole ST, Gennis RB, Crick DC, Oldfield E (2014) Multitarget drug discovery for tuberculosis and other infectious diseases. *J Med Chem*. 57:3126-39.

- Li W, Upadhyay A, Fontes FL, North EJ, Wang Y, Crans DC, Grzegorzewicz AE, Jones V, Franzblau SG, Lee RE, Crick DC, Jackson M (2014) Novel insights into the mechanism of inhibition of MmpL3, a target of multiple pharmacophores in *Mycobacterium tuberculosis*. *Antimicrob Agents Chemother*. 58:6413-23.
- Lin-Cereghino J, Wong WW, Xiong S, Giang W, Luong LT, Vu J, Johnson SD, Lin-Cereghino GP (2005) Condensed protocol for competent cell preparation and transformation of the methylotrophic yeast *Pichia pastoris*. *Biotechniques*. 38:44,46,48.
- Long CW, Pardee AB (1967) Cytidine triphosphate synthetase of *Escherichia coli* B. I. Purification and kinetics. *J Biol Chem*. 242:4715-21.
- Lounis N, Veziris N, Chauffour A, Truffot-Pernot C, Andries K, Jarlier V (2006) Combinations of R207910 with drugs used to treat multidrug-resistant tuberculosis have the potential to shorten treatment duration. *Antimicrob Agents Chemother*. 50:3543-7.
- Lunn FA, MacDonnell JE, Bearne SL (2008) Structural requirements for the activation of Escherichia coli CTP synthase by the allosteric effector GTP are stringent, but requirements for inhibition are lax. *J Biol Chem*. 283:2010-20.
- Maddry JA, Ananthan S, Goldman RC, Hobrath JV, Kwong CD, Maddox C, Rasmussen L, Reynolds RC, Secrist JA 3rd, Sosa MI, White EL, Zhang W (2009) Antituberculosis activity of the molecular libraries screening center network library. *Tuberculosis* (Edinb). 89:354-63.
- Makarov V, Manina G, Mikusova K, Möllmann U, Ryabova O, Saint-Joanis B, Dhar N, Pasca MR, Buroni S, Lucarelli AP, Milano A, De Rossi E, Belanova M, Bobovska A, Dianiskova P, Kordulakova J, Sala C, Fullam E, Schneider P, McKinney JD, Brodin P, Christophe T, Waddell S, Butcher P, Albrethsen J, Rosenkrands I, Brosch R, Nandi V, Bharath S, Gaonkar S, Shandil RK, Balasubramanian V, Balganesh T, Tyagi S, Grosset J, Riccardi G, Cole ST (2009) Benzothiazinones kill *Mycobacterium tuberculosis* by blocking arabinan synthesis. *Science*. 324:801-4.
- Makarov V, Lechartier B, Zhang M, Neres J, van der Sar AM, Raadsen SA, Hartkoorn RC, Ryabova OB, Vocat A, Decosterd LA, Widmer N, Buclin T, Bitter W, Andries K, Pojer F, Dyson PJ, Cole ST (2014) Towards a new combination therapy for tuberculosis with next generation benzothiazinones. *EMBO Mol Med*. 6:372-83.
- Manina G, Pasca MR, Buroni S, De Rossi E, Riccardi G (2010) Decaprenylphosphoryl-β-D-ribose 2'-epimerase from *Mycobacterium tuberculosis* is a magic drug target. *Curr Med Chem*. 17:3099-108.

- Martin E, Palmic N, Sanquer S, Lenoir C, Hauck F, Mongellaz C, Fabrega S, Nitschké P, Esposti MD, Schwartzentruber J, Taylor N, Majewski J, Jabado N, Wynn RF, Picard C, Fischer A, Arkwright PD, LatourS (2014) CTP synthase 1 deficiency in humans reveals its central role in lymphocyte proliferation. *Nature*. 510:288-92.
- Matteelli A, Carvalho AC, Dooley KE, Kritski A (2010) TMC207: the first compound of a new class of potent anti-tuberculosis drugs. *Fut Microbiol*. 5:849-58.
- McClure WR, Cech CL (1978) On the mechanism of rifampicin inhibition of RNA synthesis. *J Biol Chem*. 253:8949-56.
- Meng Q, Turnbough CL, Switzer RL (2004) Attenuation control of *pyrG* expression in *Bacillus subtilis* is mediated by CTP-sensitive reiterative transcription. *Proc Natl Acad Sci* USA. 101:10943–8.
- Migliori GB, Loddenkemper R, Blasi F, Raviglione MC (2007) 125 years after Robert Koch's discovery of the tubercle bacillus: the new XDR-TB threat. Is "science" enough to tackle the epidemic? *Eu Respir J*. 29:423-7.
- Mikusová K, Huang H, Yagi T, Holsters M, Vereecke D, D'Haeze W, Scherman MS, Brennan PJ, McNeil MR, Crick DC (2005) Decaprenylphosphoryl arabinofuranose, the donor of the D-arabinofuranosyl residues of mycobacterial arabinan, is formed *via* a two-step epimerization of decaprenylphosphoryl ribose. *J Bacteriol*. 187:8020-5.
- Miotto P, Cirillo DM, Migliori GB (2015) Drug resistance in *Mycobacterium tuberculosis:* molecular mechanisms challenging fluoroquinolones and pyrazinamide effectiveness. *Chest*. 147:1135-43.
- Mitchison DA, Nunn AJ (1986) Influence of initial drug resistance on the response to short-course chemotherapy of pulmonary tuberculosis. *Am Rev Respir Dis*. 133:423-30.
- Montales MT, Chaudhury A, Beebe A, Patil S, Patil N (2015) HIV-associated TB syndemic: a growing clinical challenge worldwide. *Front Public Health*. 3:281.
- Morphy JR (2012) The challenges of multi-target lead optimization. *Designing Multi-Target Drugs*. Royal Society of Chemistry: London, 141-154.
- Murakami S (2008) Multidrug efflux transporter, AcrB--the pumping mechanism. *Curr Opin Struct Biol*. 18:459-65.
- Myllykallio H, Lipowski G, Leduc D, Filee J, Forterre P, Liebl U (2002) An alternative flavin-dependent mechanism for thymidylate synthesis. *Science*. 297:105-7.

- Neres J, Pojer F, Molteni E, Chiarelli LR, Dhar N, Boy-Röttger S, Buroni S, Fullam E, Degiacomi G, Lucarelli AP, Read RJ, Zanoni G, Edmondson DE, De Rossi E, Pasca MR, McKinney JD, Dyson PJ, Riccardi G, Mattevi A, Cole ST, Binda C (2012) Structural basis for benzothiazinone-mediated killing of *Mycobacterium tuberculosis*. *Sci Transl Med*. 4:150ra121.
- Nguyen L (2016) Antibiotic resistance mechanisms in *M. tuberculosis*: an update. *Arch Toxicol*. [Epub ahead of print].
- Nuermberger E, Rosenthal I, Tyagi S, Williams KN, Almeida D, Peloquin CA, Bishai WR, Grosset JH (2006) Combination chemotherapy with the nitroimidazopyran PA-824 and first-line drugs in a murine model of tuberculosis. *Antimicrob Agents Chemother*. 50:2621-5.
- Nuermberger E, Tyagi S, Tasneen R, Williams KN, Almeida D, Rosenthal I, Grosset JH (2008) Powerful bactericidal and sterilizing activity of a regimen containing PA-824, moxifloxacin, and pyrazinamide in a murine model of tuberculosis. *Antimicrob Agents Chemother*. 52:1522-4.
- Parida SK, Axelsson-Robertson R, Rao MV, Singh N, Master I, Lutckii A, Keshavjee S, Andersson J, Zumla A, Maeurer M (2015) Totally drug-resistant tuberculosis and adjunct therapies. *J Intern Med*. 277:388-405.
- Patel NR, Swan K, Li X, Tachado SD, Koziel H (2009) Impaired *M. tuberculosis*-mediated apoptosis in alveolar macrophages from HIV+ persons: potential role of IL-10 and BCL-3. *J Leukoc Biol*. 86:53-60.
- Pawlowski A, Jansson M, Sköld M, Rottenberg ME, Källenius G (2012) Tuberculosis and HIV co-infection. *PLoS Pathog*. 8:e1002464.
- Pethe K, Bifani P, Jang J, Kang S, Park S, Ahn S, Jiricek J, Jung J, Jeon HK, Cechetto J, Christophe T, Lee H, Kempf M, Jackson M, Lenaerts AJ, Pham H, Jones V, Seo MJ, Kim YM, Seo M, Seo JJ, Park D, Ko Y, Choi I, Kim R, Kim SY, Lim S, Yim SA, Nam J, Kang H, Kwon H, Oh CT, Cho Y, Jang Y, Kim J, Chua A, Tan BH, Nanjundappa MB, Rao SP, Barnes WS, Wintjens R, Walker JR, Alonso S, Lee S, Kim J, Oh S, Oh T, Nehrbass U, Han SJ, No Z, Lee J, Brodin P, Cho SN, Nam K, Kim J (2013) Discovery of Q203, a potent clinical candidate for the treatment of tuberculosis. *Nat Med*. 19:1157-60.
- Poce G, Bates RH, Alfonso S, Cocozza M, Porretta GC, Ballell L, Rullas J, Ortega F, De Logu A, Agus E, La Rosa V, Pasca MR, De Rossi E, Wae B, Franzblau SG, Manetti F, Botta M, Biava M (2013) Improved BM212 MmpL3 inhibitor analogue shows efficacy in acute murine model of tuberculosis infection. *PLoS One*. 8:e56980.
- Preiss L, Langer JD, Yildiz Ö, Eckhardt-Strelau L, Guillemont JE, Koul A, Meier T (2015) Structure of the mycobacterial ATP synthase F_o rotor ring in complex with the anti-TB drug bedaquiline. *Sci Adv*. 1:e1500106.

- Protopopova M, Hanrahan C, Nikonenko B, Samala R, Chen P, Gearhart J, Einck L, Nacy CA (2005) Identification of a new antitubercular drug candidate, SQ109, from a combinatorial library of 1,2-ethylenediamines. *J Antimicrob Chemother*. 56:968-74.
- Reddy BK, Landge S, Ravishankar S, Patil V, Shinde V, Tantry S, Kale M, Raichurkar A, Menasinakai S, Mudugal NV, Ambady A, Ghosh A, Tunduguru R, Kaur P, Singh R, Kumar N, Bharath S, Sundaram A, Bhat J, Sambandamurthy VK, Björkelid C, Jones TA, Das K, Bandodkar B, Malolanarasimhan K, Mukherjee K, Ramachandran V (2014) Assessment of *Mycobacterium tuberculosis* pantothenate kinase vulnerability through target knockdown and mechanistically diverse inhibitors. *Antimicrob Agents Chemother*. 58:3312-26.
- Riccardi G, Pasca MR, Buroni S (2009) *Mycobacterium tuberculosis*: drug resistance and future perspectives. *Fut Microbiol*. 4:597-614.
- Rodríguez JC, Ruiz M, López M, Royo G (2002) *In vitro* activity of moxifloxacin, levofloxacin, gatifloxacin and linezolid against *Mycobacterium tuberculosis. Int J Antimicrob Agent*s. 20:464-7.
- Ruan Q, Liu Q, Sun F, Shao L, Jin J, Yu S, Ai J, Zhang B, Zhang W (2016) Moxifloxacin and gatifloxacin for initial therapy of tuberculosis: a meta-analysis of randomized clinical trials. *Emerg Microbes Infect*. 5:e12.
- Russel DG (2007) Who put the tubercle in tuberculosis? *Nat Rev Microbiol*. 5: 39-47.
- Russell DG, Barry CE 3rd, Flynn JL (2010) Tuberculosis: what we don't know can, and does, hurt us. *Science*. 328: 852-6.
- Rustomjee R, Lienhardt C, Kanyok T, Davies GR, Levin J, Mthiyane T, Reddy C, Sturm AW, Sirgel FA, Allen J, Coleman DJ, Fourie B, Mitchison DA; Gatifloxacin for TB (OFLOTUB) study team (2008) A Phase II study of the sterilising activities of ofloxacin, gatifloxacin and moxifloxacin in pulmonary tuberculosis. *Int J Tuberc Lung Dis*. 12:128-38.
- Ryan NJ, Lo JH (2014) Delamanid: first global approval. *Drugs*. 74: 1041-5.
- Rybniker J, Vocat A, Sala C, Busso P, Pojer F, Benjak A, Cole ST (2015) Lansoprazole is an antituberculous prodrug targeting cytochrome bc1. *Nat Commun*. 6:7659.
- Sacksteder KA, Protopopova M, Barry CE 3rd, Andries K, Nacy CA (2012) Discovery and development of SQ109: a new antitubercular drug with a novel mechanism of action. *Fut Microbiol*. 7:823-37.
- Samala G, Devi PB, Saxena S, Meda N, Yogeeswari P, Sriram D (2016) Design, synthesis and biological evaluation of imidazo[2,1-b]thiazole and

benzo[d]imidazo[2,1-b]thiazole derivatives as *Mycobacterium tuberculosis* pantothenate synthetase inhibitors. *BioorgMedChem*. 24:1298-307.

- Sambrook J, Russell DW (2001) Molecular Cloning: a laboratory manual. Cold Spring Harbor Laboratory Press, Cold Spring Harbor, N.Y, 3rd ed.
- Sampathkumar P, Turley S, Ulmer JE, Rhie HG, Sibley CH, Hol WG. (2005) Structure of the *Mycobacterium tuberculosis* flavin dependent thymidylate synthase (Mtb ThyX) at 2.0A resolution. *J Mol Biol*. 352:1091-104.
- Saukkonen JJ, Cohn DL, Jasmer RM, Schenker S, Jereb JA, Nolan CM, Peloquin CA, Gordin FM, Nunes D, Strader DB, Bernardo J, Venkataramanan R, Sterling TR (2006) ATS (American Thoracic Society) Hepatotoxicity of antituberculosis therapy subcommittee. An official ATS statement: hepatotoxicity of antituberculosis therapy. *Am J Respir Crit Care Med*. 174:935-52.
- Shankar EM, Vignesh R, Ellegård R, Barathan M, Chong YK, Bador MK, Rukumani DV, Sabet NS, Kamarulzaman A, Velu V, Larsson M (2014) HIV-*Mycobacterium tuberculosis* co-infection: a 'danger-couple model' of disease pathogenesis. *Pathog Dis*. 70:110-8.
- Shcherbakov D, Akbergenov R, Matt T, Sander P, Andersson DI, Böttger EC (2010) Directed mutagenesis of *Mycobacterium smegmatis* 16S rRNA to reconstruct the *in vivo* evolution of aminoglycoside resistance *in Mycobacterium tuberculosis*. *Mol Microbiol.* 77:830-40.
- Shirude PS, Madhavapeddi P, Tucker JA, Murugan K, Patil V, Basavarajappa H, Raichurkar AV, Humnabadkar V, Hussein S, Sharma S, Ramya VK, Narayan CB, Balganesh TS, Sambandamurthy VK (2013) Aminopyrazinamides: novel and specific GyrB inhibitors that kill replicating and nonreplicating *Mycobacterium tuberculosis. ACS Chem Biol.* 8:519-23.
- Silver LL (2007) Multi-targeting by monotherapeutic antibacterials. *Nat Rev Drug Discov*. 6:126.
- Singh R, Manjunatha U, Boshoff HI, Ha YH, Niyomrattanakit P, Ledwidge R, Dowd CS, Lee IY, Kim P, Zhang L, Kang S, Keller TH, Jiricek J, Barry CE 3rd (2008) PA-824 kills nonreplicating *Mycobacterium tuberculosis* by intracellular NO release. *Science*. 322:1392-5.
- Somoskovi A, Parsons LM, Salfinger M (2001) The molecular basis of resistance to isoniazid, rifampin, and pyrazinamide in *Mycobacterium tuberculosis*. *Respir Res*. 2:164-8.
- Sotgiu G, Centis R, D'Ambrosio L, Alffenaar JW, Anger HA, Caminero JA, Castiglia P, De Lorenzo S, Ferrara G, Koh WJ, Schecter GF, Shim TS, Singla R, Skrahina A, Spanevello A, Udwadia ZF, Villar M, Zampogna E, Zellweger JP, Zumla A, Migliori GB (2012) Efficacy, safety and tolerability of linezolid

containing regimens in treating MDR-TB and XDR-TB: systematic review and meta-analysis. *Eur Respir J*. 40:1430-42.

- Spry C, Kirk K, Saliba KJ (2008) Coenzyme A biosynthesis: an antimicrobial drug target. *FEMS Microbiol Rev*. 32:56-106.
- Sterling TR, Villarino ME, Borisov AS, Shang N, Gordin F, Bliven-Sizemore E, Hackman J, Hamilton CD, Menzies D, Kerrigan A, Weis SE, Weiner M, Wing D, Conde MB, Bozeman L, Horsburgh CR Jr, Chaisson RE (2011) TB Trials Consortium PREVENT TB Study Team. Three months of rifapentine and isoniazid for latent tuberculosis infection. *N Engl J Med*. 365:2155-66.
- Tahlan K, Wilson R, Kastrinsky DB, Arora K, Nair V, Fischer E, Barnes SW, Walker JR, Alland D, Barry CE 3rd, Boshoff HI (2012) SQ109 targets MmpL3, a membrane transporter of trehalose monomycolate involved in mycolic acid donation to the cell wall core of *Mycobacterium tuberculosis*. *Antimicrob Agents Chemother*. 56:1797-809.
- Takiff HE, Salazar L, Guerrero C, Philipp W, Huang WM, Kreiswirth B, Cole ST, Jacobs WR Jr, Telenti A (1994) Cloning and nucleotide sequence of *Mycobacterium tuberculosis gyrA* and *gyrB* genes and detection of quinolone resistance mutations. *Antimicrob Agents Chemother*. 38:773-80.
- Titov DV, Liu JO (2012) Identification and validation of protein targets of bioactive small molecules. *Bioorg Med Chem*. 20:1902-9.
- Tran T, Saheba E, Arcerio AV, Chavez V, Li QY, Martinez LE, Primm TP (2004) Quinones as antimycobacterial agents. *Bioorg Med Chem*. 12:4809-13.
- Trefzer C, Škovierová H, Buroni S, Bobovská A, Nenci S, Molteni E, Pojer F, Pasca MR, Makarov V, Cole ST, Riccardi G, Mikušová K, Johnsson K (2012) Benzothiazinones are suicide inhibitors of mycobacterial decaprenylphosphoryl-β-D-ribofuranose 2'-oxidase DprE1. *J Am Chem Soc*. 134:912-5.
- Tschopp JF, Brust PF, Cregg JM, Stillman CA, Gingeras TR (1987) Expression of the *lacZ* gene from two methanol-regulated promoters in *Pichia pastoris*. *Nucleic Acids Res*. 15:3859-76.
- Tupin A, Gualtieri M, Roquet-Banères F, Morichaud Z, Brodolin K Leonetti JP (2010) Resistance to rifampicin: at the crossroads between ecological, genomic and medical concerns. *Int J Antimicrob Agents*. 35:519-23.
- Turnbough CL, Switzer RL (2008) Regulation of pyrimidine biosynthetic gene expression in bacteria: repression without repressors. *Microbiol Mol Biol Rev*. 72:266-300.
- Ulrichs T, Kaufmann SH (2006) New insights into the function of granulomas in human tuberculosis. *J Pathol*. 208:261-9.

- van der Kooy F, Meyer JJ, Lall N (2006) Antimycobacterial activity and possible mode of action of newly isolated neodiospyrin and other naphthoquinones from *Euclea natalensis*. *South African Journal of Botany*. 72:349–52.
- van Kuilenburg AB, Meinsma R, Vreken P, Waterham HR, van Gennip AH (2000) Identification of a cDNA encoding an isoform of human CTP synthetase. *BiochimBiophysActa*. 1492:548-52.
- Vannelli TA, Dykman A, Ortiz de Montellano PR (2002) The antituberculosis drug ethionamide is activated by a flavoprotein monooxygenase. *J Biol Chem*. 277:12824-9.
- Varela C, Rittmann D, Singh A, Krumbach K, Bhatt K, Eggeling L, Besra GS, Bhatt A (2012) *MmpL* genes are associated with mycolic acid metabolism in mycobacteria and corynebacteria. *Chem Biol*. 19:498-506.
- Vilchèze C, Jacobs WR Jr (2007) The mechanism of isoniazid killing: clarity through the scope of genetics. *Annu Rev Microbiol*. 61:35-50.
- Vilchèze C, Jacobs WR Jr (2014) Resistance to isoniazid and ethionamide in *Mycobacterium tuberculosis*: genes, mutations, and causalities. *Microbiol Spectr*. 2:MGM2-0014-2013.
- Walker JE (2013) The ATP synthase: the understood, the uncertain and the unknown. *Biochem Soc Trans*. 41:1-16.
- Wei JR, Krishnamoorthy V, Murphy K, Kim JH, Schnappinger D, Alber T, Sassetti CM, Rhee KY, Rubin EJ (2011) Depletion of antibiotic targets has widely varying effects on growth. *Proc Natl Acad Sci USA*. 108:4176-81.
- Welage LS (2003) Pharmacologic properties of proton pump inhibitors. *Pharmacotherapy*. 23:74S-80S.
- World Health Organization (WHO). www.euro.who.int/tuberculosis.
- WHO. WHO update references on management of drug-resistant tuberculosis: guidelines for the programmatic management of drug-resistant tuberculosis – 2011 update. Geneva: World Health Organization (2011).
- WHO. Global Tuberculosis Report 2013. Geneva: World Health Organization (2013).
- WHO. The use of bedaquiline in the treatment of multidrug-resistant tuberculosis: interim policy guidance Geneva: World Health Organization (2013).
- WHO. The use of delamanid in the treatment of multidrug-resistant tuberculosis: interim policy guidance Geneva: World Health Organization (2014).

- WHO. Global tuberculosis report 2015. Geneva: World Health Organization (2015).
- Willemoes M, Mølgaard A, Johansson E, Martinussen J (2005) Lid L11 of the glutamine amidotransferase domain of CTP synthase mediates allosteric GTP activation of glutaminase activity. *FEBS J*. 272:856–64.
- Williamson B, Dooley KE, Zhang Y, Back DJ, Owen A (2013) Induction of influx and efflux transporters and cytochrome P450 3A4 in primary human hepatocytes by rifampin, rifabutin, and rifapentine. *Antimicrob Agents Chemother*. 57:6366-9.
- Wilson JW, Tsukayama DT (2016) Extensively drug-resistant tuberculosis: principles of resistance, diagnosis, and management. *Mayo Clin Proc*. 91:482-95.
- Yang K, Strauss E, Huerta C, Zhang H (2008) Structural basis for substrate binding and the catalytic mechanism of type III pantothenate kinase. *Biochemistry*. 47:1369–80.
- Zhang Y, Heym B, Allen B, Young D, Cole S (1992) The catalase-peroxidase gene and isoniazid resistance of *Mycobacterium tuberculosis*. *Nature*. 358:591-3.
- Zhang Y, Mitchison D (2003) The courious characteristics of pyrazinamide: a review. *Int J Tuberc Lung Dis*. 7:6-21.
- Zhang M, Sala C, Hartkoorn RC, Dhar N, Mendoza-Losana A, Cole ST (2012) Streptomycin-starved *Mycobacterium tuberculosis* 18b, a drug discovery tool for latent tuberculosis. *Antimicrob Agents Chemother*. 56:5782-9.
- Zimhony O, Cox JS, Welch JT, Vilchèze C, Jacobs WR Jr (2000) Pyrazinamide inhibits the eukaryotic-like fatty acid synthetase I (FASI) of *Mycobacterium tuberculosis*. *Nat Med*. 6:1043-7.
- Zumla A, Nahid P, Cole ST (2013a) Advances in the development of new tuberculosis drugs and treatment regimens. *Nature*. 12:388-404.
- Zumla A, Raviglione M, Hafner R, von Reyn CF (2013b) Tuberculosis. *N Engl J Med*. 382:745-55.
- Zuniga ES, Early J, Parish T (2015) The future for early-stage tuberculosis drug discovery. *Fut Microbiol*. 10:217-29.

7. List of original manuscripts

Full paper

- Mori G*, Chiarelli LR*, **Esposito M***, Makarov V*, Bellinzoni M, Hartkoorn RC, Degiacomi G, Boldrin F, Ekins S, de Jesus Lopes Ribeiro AL, Marino LB, Centárová, Svetlíková Z, Blasco J, Kazakova E., Lepioshkin A, Barilone N, Zanoni G, Porta A, Fondi M, Fani R, Baulard AR, Mikušová K, Alzari PM, Manganelli R, de Carvalho LPS, Riccardi G, Cole ST, Pasca MR (2015) Thiophenecarboxamide Derivatives Activated by EthA Kill *Mycobacterium tuberculosis* by Inhibiting the CTP Synthetase PyrG. Chemistry and Biology. 22 (7): 917-27 (*equal contribution).
- Chiarelli LR, Mori G, **Esposito M**, Orena BS, Pasca MR (2016) New and Old Hot Drug Targets in Tuberculosis. Curr Med Chem. *in press.* DOI: 10.2174/1389557516666160831164925 (Review).
- **Esposito M**, Orena BS, Mori G, Degiacomi G, Ballell-Pages L, Bellinzoni M, Ekins S, Manganelli R, Riccardi G, Makarov V, Mikušová K, Pasca MR, Chiarelli LR. (2016) Discovery of new *Mycobacterium tuberculosis* CTP synthetase inhibitors through a combined target based/phenotypic screening. *Manuscript in preparation to be submitted to ACS Chemical Biology.*
- Chiarelli LR, **Esposito M**, Mori G, Orena BS, Hartkoorn RC, Gosetti F, Manfredi M, de Jesus Lopes Ribeiro AL, Makarov V, Mikušová K, Ekins S, Marengo E, Riccardi G, Cole ST, Pasca MR. Pantothenate kinase is a second target of CTP-synthetase inhibitors: a multitargeting approach to fight *Mycobacterium tuberculosis* drug-resistant strains. *Manuscript in preparation.*

Posters

- de Jesus Lopes Ribeiro AL, Mori G, Chiarelli LR, **Esposito M**, Albesa-Jove D, Urresti S, Comino N, Hartkoorn RC, Binda C, Cole ST, Makarov V, Guerin M, Pasca MR, Riccardi G. Rv2466c: a novel drug activator for

new antitubercular compounds. XXX Meeting of "Società Italiana di Microbiologia Generale e Biotecnologie Microbiche (SIMGBM)", Ischia, Italy, 18-21 September 2013.

- Chiarelli LR,* **Esposito M***, Mori G, Orena BS, Makarov V, Bellinzoni M, Degiacomi G, Boldrin F, Manganelli R, Mikušová K, de Carvalho LPS, Cole ST, Riccardi G, Pasca MR. Mechanism of action of the new antitubercular thiophenecarboxamide derivatives: a multidisciplinary approach. XXXI Meeting of "Società Italiana di Microbiologia Generale e Biotecnologie Microbiche (SIMGBM)", Ravenna, Italy, 23-26 September 2015. Abstract selected for oral communication (*equal contribution).
- Mori G, Orena BS, Chiarelli LR, **Esposito M**, Anatriello M, Makarov V, Pasca MR, Riccardi G. Characterization of a new antitubercular compound activated by Rv2466c. XXXI Meeting of "Società Italiana di Microbiologia Generale e Biotecnologie Microbiche (SIMGBM)", Ravenna, Italy, 23-26 September 2015.
- Chiarelli LR, **Esposito M**, Orena BS, Mori G, Buttari N, Degiacomi G, Gosetti F, Manfredi M, Ekins S, Mikušová K, Bellinzoni M, Manganelli R, Marengo E, Ballell-Pages L, Riccardi G, Pasca MR. *Mycobacterium tuberculosis* CTP synthetase and pantothenate kinase: two promising targets for the development of multitargeting drugs. EMBO Conference Tuberculosis 2016, Paris, France, 19-23 September 2016. Abstract selected for oral communication.
- Orena BS, Chiarelli LR, **Esposito M**, Mori G, Buttari N, Degiacomi G, Gosetti F, Manfredi M, Ekins S, Mikušová K, Bellinzoni M, Manganelli R, Marengo E, Ballell-Pages L, Riccardi G, Pasca MR. Multitargeting anti-tubercular compounds: a new precious tool in multidrug resistance age. FISV, Roma, Italy, 20-23 September 2016. Abstract selected for oral communication.

Chemistry & Biology
Article

Thiophenecarboxamide Derivatives Activated by EthA Kill *Mycobacterium tuberculosis* by Inhibiting the CTP Synthetase PyrG

Giorgia Mori,[1,14] Laurent R. Chiarelli,[1,14] Marta Esposito,[1,14] Vadim Makarov,[2,14] Marco Bellinzoni,[3] Ruben C. Hartkoorn,[4] Giulia Degiacomi,[5] Francesca Boldrin,[5] Sean Ekins,[6] Ana Luisa de Jesus Lopes Ribeiro,[1,15] Leonardo B. Marino,[7,8] Ivana Centárová,[9] Zuzana Svetlíková,[9] Jaroslav Blaško,[10] Elena Kazakova,[2] Alexander Lepioshkin,[2] Nathalie Barilone,[3,16] Giuseppe Zanoni,[11] Alessio Porta,[11] Marco Fondi,[12] Renato Fani,[12] Alain R. Baulard,[13] Katarína Mikušová,[9] Pedro M. Alzari,[3] Riccardo Manganelli,[5] Luiz Pedro S. de Carvalho,[7] Giovanna Riccardi,[1] Stewart T. Cole,[4,*] and Maria Rosalia Pasca[1,*]

[1]Department of Biology and Biotechnology "Lazzaro Spallanzani", University of Pavia, 27100 Pavia, Italy
[2]A. N. Bakh Institute of Biochemistry, Russian Academy of Science, 119071 Moscow, Russia
[3]Institut Pasteur, Unité de Microbiologie Structurale, CNRS-UMR3528, Université Paris Diderot, Sorbonne Paris Cité, 25 rue du Dr. Roux, 75724 Paris Cedex 15, France
[4]Global Health Institute, Ecole Polytechnique Fédérale de Lausanne, Station 19, 1015 Lausanne, Switzerland
[5]Department of Molecular Medicine, University of Padova, 35128 Padua, Italy
[6]Collaborative Drug Discovery, 1633 Bayshore Highway, Suite 342, Burlingame, CA 94010, USA
[7]Francis Crick Institute, Mill Hill Laboratory, The Ridgeway, Mill Hill, London NW7 1AA, UK
[8]Faculty of Pharmaceutical Sciences, UNESP - Univ Estadual Paulista, Araraquara, São Paulo 14801-902, Brazil
[9]Department of Biochemistry, Faculty of Natural Sciences, Comenius University in Bratislava, Ilkovičova 6, Mlynská dolina, 84215 Bratislava, Slovakia
[10]Institute of Chemistry, Faculty of Natural Sciences, Comenius University in Bratislava, Ilkovičova 6, Mlynská dolina, 84215 Bratislava, Slovak Republic
[11]Department of Chemistry, University of Pavia, 27100 Pavia, Italy
[12]Department of Biology, University of Florence, Sesto Fiorentino, Florence 50019, Italy
[13]Institut Pasteur de Lille, Center for Infection and Immunity, 59019 Lille, France
[14]Co-first author
[15]Present address: Centro de Biologia Molecular "Severo Ochoa" Universidad Autónoma de Madrid, 28049, Madrid, Spain
[16]Present address: Institut Pasteur, Unité de Neuro-Immunologie Virale, 25 rue du Dr. Roux, 75724 Paris Cedex 15, France
*Correspondence: mariarosalia.pasca@unipv.it (M.R.P.), stewart.cole@epfl.ch (S.T.C.)
http://dx.doi.org/10.1016/j.chembiol.2015.05.016

SUMMARY

To combat the emergence of drug-resistant strains of *Mycobacterium tuberculosis*, new antitubercular agents and novel drug targets are needed. Phenotypic screening of a library of 594 hit compounds uncovered two leads that were active against *M. tuberculosis* in its replicating, non-replicating, and intracellular states: compounds 7947882 (5-methyl-*N*-(4-nitrophenyl)thiophene-2-carboxamide) and 7904688 (3-phenyl-*N*-[(4-piperidin-1-ylphenyl)carbamothioyl]propanamide). Mutants resistant to both compounds harbored mutations in *ethA* (*rv3854c*), the gene encoding the monooxygenase EthA, and/or in *pyrG* (*rv1699*) coding for the CTP synthetase, PyrG. Biochemical investigations demonstrated that EthA is responsible for the activation of the compounds, and by mass spectrometry we identified the active metabolite of 7947882, which directly inhibits PyrG activity. Metabolomic studies revealed that pharmacological inhibition of PyrG strongly perturbs DNA and RNA biosynthesis, and other metabolic processes requiring nucleotides. Finally, the crystal structure of PyrG was solved, paving the way for rational drug design with this newly validated drug target.

INTRODUCTION

Tuberculosis (TB) remains a leading cause of infectious mortality worldwide, killing approximately 1.5 million people each year. Drug-resistant strains of *Mycobacterium tuberculosis* threaten global TB management, with an estimated 450,000 cases being multidrug resistant, defined as resistant to rifampin and isoniazid. A subset of these cases, approximately 10%, is also resistant to the second-line drug classes, fluoroquinolones, and injectable aminoglycosides, and is referred to as extensively drug resistant (WHO, 2014).

Defining the pharmacological target(s) of antitubercular drugs under development and finding new compounds with greater potency are both important aspects in the search for agents that are effective against drug-sensitive and drug-resistant *M. tuberculosis* strains (Lechartier et al., 2014). Several current antimycobacterial agents are prodrugs requiring some form of cellular activation before they can bind to their specific targets

CellPress

Table 1. Activity In Vitro in Latent and Replicating *M. tuberculosis* Growth and Activity Ex Vivo of the Two Selected Compounds

Compound ID	Structure	H37Rv MIC (μg/ml)	ss18b IC_{50}/IC_{90} (μg/ml)	Intracellular IC_{50}/IC_{90} (μg/ml)
7904688	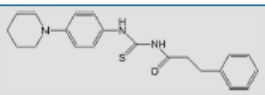	0.5	2.5/20	0.175/0.625
7947882	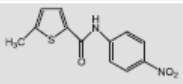	0.5	2.5/10	0.625/1.25

and, in such cases, resistance can be mediated by mutations that prevent the activation step. Therefore, understanding the mode of activation not only helps to decipher the mechanisms of drug resistance, but may also facilitate the development of analogs that do not require activation (Dover et al., 2007).

In this work, by screening a library of compounds with known antitubercular activity, established by the National Institute of Allergy and Infectious Diseases (NIAID) (Ananthan et al., 2009; Goldman and Laughon, 2009; Maddry et al., 2009), a new series of molecules was found, displaying a very low minimum inhibitory concentration (MIC) value (0.5 μg/ml), that includes compounds 7947882 and 7904688. Through the isolation of *M. tuberculosis*-resistant mutants, genetic validation, and biochemical and structural studies, the main mechanisms of activation and resistance of these new antitubercular compounds have been characterized. The combined data indicate that 7947882 and 7904688 are prodrugs activated by the EthA monooxygenase, which then target PyrG, a cytidine triphosphate (CTP) synthetase catalyzing the ATP-dependent amination of uridine triphosphate (UTP) to form the essential pyrimidine nucleotide CTP (Long and Pardee, 1967). CTP synthetase is thus a tractable new TB drug target.

RESULTS AND DISCUSSION

Screening of NIAID Library

A library of 594 compounds, selected by high-throughput screening (HTS) against *M. tuberculosis* H37Rv (Ananthan et al., 2009; Goldman and Laughon, 2009; Maddry et al., 2009), was tested for activity against non-replicating *M. tuberculosis* using the streptomycin-starved 18b (ss18b) model (Sala et al., 2010; Zhang et al., 2012). Two promising compounds were identified: a 5-methyl-*N*-(4-nitrophenyl)thiophene-2-carboxamide (7947882) and a 3-phenyl-*N*-[(4-piperidin-1-ylphenyl) carbamothioyl]propanamide (7904688). Both compounds also showed activity against replicating and intracellular *M. tuberculosis* H37Rv (Table 1). Moreover, the molecules were not cytotoxic to HepG2, A549, Raw, and Huh7 cell lines at concentrations below 40 μg/ml. Compounds were re-purchased from Chembridge Chemical Store (http://www.hit2lead.com/) and the results were confirmed.

Isolation and Characterization of *M. tuberculosis*-Resistant Mutants

To characterize the mechanism of action of 7947882 and 7904688, several spontaneous *M. tuberculosis* mutants resistant to the compounds were isolated. The spontaneous mutants exhibited the same resistance levels to both drugs (10 μg/ml, 20× MIC) (Table 2). Illumina whole-genome sequencing of all mutants revealed mutations either in *ethA* (*rv3854c*), encoding a monooxygenase responsible for ethionamide (ETH) activation (Baulard et al., 2000), and/or *pyrG* (*rv1699*), encoding the CTP synthetase, which performs the ATP-dependent amination of UTP to form CTP as the final step of the pyrimidine nucleotide biosynthetic pathway (Endrizzi et al., 2004) (Table 2). Notably, *M. tuberculosis* mutants resistant to compound 7947882 carried different point mutations in *ethA*, resulting in either an amino acid substitution or a truncated protein. In addition, these mutants all harbored the same mutation in the *pyrG* gene: T557G (Val186Gly). By contrast, no mutations in *ethA* were found in *M. tuberculosis* mutants resistant to compound 7904688, but these all carried the Val186Gly substitution in PyrG (Table 2).

Since *pyrG*, unlike *ethA*, is predicted to be an essential gene in *M. tuberculosis* (Sassetti et al., 2001), it was hypothesized that EthA could be required to activate 7947882 and 7904688 compounds, while the target of the activated metabolites might be PyrG. The finding that all strains harboring a mutation in *ethA* showed cross-resistance to ETH, whereas strains mutated only in *pyrG* remained ETH sensitive, reinforced this hypothesis (Table 2).

EthA Is an Activator of 7947882 and 7904688 Compounds

To verify whether EthA is responsible for the activation of 7947882 and 7904688, the *ethA* gene was cloned in the expression vector pSODIT-2, and *M. tuberculosis* H37Rv cells were transformed with the corresponding recombinant plasmid. A statistically significant shift in the MIC of the transformants was observed with respect to the control; overexpression of *ethA* in *M. tuberculosis* H37Rv increased the sensitivity to 7947882 and 7904688 (Table S1). Moreover, the overexpression of wild-type *ethA* restored the sensitivity to 7947882 in *M. tuberculosis* 82.14 mutant cells, carrying a mutation in *ethA* (Table S1).

To prove that both compounds were activated by EthA, a recombinant form of the *M. tuberculosis* enzyme was expressed in *Escherichia coli* and purified, and its activity toward the two compounds as substrates was assayed. EthA was active toward both 7947882 and 7904688, with k_{cat} values of 2.9 ± 0.08 and 2.4 ± 0.15 min^{-1} and K_m values of 0.037 ± 0.002 and 0.055 ± 0.004 mM for 7947882 and 7904688, respectively. Moreover, both compounds were better substrates for EthA than ETH,

Table 2. Main Features of *M. tuberculosis* Mutants Resistant to 7947882 and 7904688

M. tuberculosis Strains	MIC (μg/ml)			WGS Sequencing Results (Amino Acid Change)	
	7947882	7904688	ETH	*ethA*	*pyrG*
H37Rv	0.5	0.5	1	–	–
82.14	>40	>40	10	T133C (W45R)	T557G (V186G)
82.19	>40	>40	10	T386C (L129P)	T557G (V186G)
82.22	>40	>40	10	ΔT-94	T557G (V186G)
88.7	5–10	10	0.5	–	T557G (V186G)
88.10	5–10	10	0.5	–	T557G (V186G)
81.10[a]	>40	>40	10	Δ1109–1137	–

See Table S1.
[a]Laboratory collection.

showing ~10-fold higher affinity (K_m for ETH 0.34 mM), similar to that for phenylacetone, the best EthA substrate found so far (K_m 0.06 mM and k_{cat} 0.027 s^{-1}) (Fraaije et al., 2004). The body of genetic and biochemical data strongly suggests that these two compounds are prodrugs that need EthA activation.

7947882 and 7904688 Do Not Affect PyrG Enzyme Activity but Require EthA Activation

To check whether compounds 7947882 and 7904688 were able to inhibit PyrG, their effect on the enzyme activity was evaluated. For this purpose, wild-type PyrG and the V186G mutant protein were produced in *E. coli*, purified, and characterized. *M. tuberculosis* PyrG shows catalytic constants (k_{cat} 21.9 ± 0.5 s^{-1} and K_m 0.18 ± 0.01 mM toward ATP; k_{cat} 22.9 ± 0.9 s^{-1} and K_m 0.14 ± 0.01 mM toward UTP) very similar to those of other bacterial CTP synthetases (Anderson, 1983; Long and Pardee, 1967; Willemoës et al., 2005). The PyrG mutant V186G was still active, but partially impaired, displaying reduced k_{cat} values toward both substrates (1.5 ± 0.11 and 1.6 ± 0.08 s^{-1} for ATP and UTP, respectively). Moreover, the mutant enzyme showed a K_m value for ATP that was about 10-fold higher than that of the wild-type protein (1.46 ± 0.18 mM), whereas the affinity for UTP was unchanged.

Since this mutation is associated with resistance to 7947882 and 7904688 (Table 2), it was conceivable that the ATP-binding site was involved in binding the inhibitors. For this reason, the effects of the two compounds were tested on wild-type PyrG at a final concentration of 200 μM. As expected for molecules that need to be activated by EthA, the compounds were ineffective toward PyrG in all the conditions tested.

Thus, to confirm that EthA produces metabolites that might act on PyrG, the EthA enzymatic reaction was performed with either 7947882 or 7904688 in the presence of PyrG, and the activity of the latter enzyme was monitored during the course of the reaction. The blank control was performed omitting reduced nicotinamide adenine dinucleotide phosphate (NADPH) to hinder the EthA-catalyzed reaction, and under these conditions PyrG maintained full activity for up to 6 hr of incubation. By contrast, in the presence of an actively working EthA, PyrG lost full activity within 4 hr when incubated with 7947882, and about 80% of its activity in 6 hr when incubated with 7904688 (Figures 1A and 1C).

At the end of incubation, to remove EthA as well as any unbound compounds, PyrG was re-purified by Ni-NTA (nitrilotriacetic acid) chromatography and dialyzed. Whereas PyrG from the blank reaction preserved its activity, the enzyme incubated in the full reaction remained completely inactive. Moreover, in the UV-Vis spectrum of PyrG incubated with EthA and 7947882, an additional peak appeared at 330 nm (Figure 1B). This peak, which was not present in the PyrG spectrum from blank reactions without NADPH, is characteristic of 7947882, thus demonstrating that, in contrast to its prodrug, the EthA-activated metabolite is able to bind PyrG. Similarly, the spectrum of PyrG incubated with 7904688 showed the broad peak between 310 and 400 nm, typical of the compound; this peak was absent in the blank control (Figure 1D). These results demonstrated that the conversion of 7947882 and 7904688 by EthA leads to active inhibitors of PyrG.

Identification of Active Metabolites of 7947882

EthA is known to catalyze the oxygenation of the thioamide moiety of ETH, leading to the formation of S-oxide and S-dioxide products (Vannelli et al., 2002), as well as the oxygenation of the sulfide group of methyl(*p*-tolyl)sulfide (Fraaije et al., 2004). Thus, it is conceivable that EthA might catalyze a similar reaction on the thiophene moiety of 7947882. To confirm this hypothesis, we attempted to identify the active metabolite(s) of the 7947882 prodrug after purification from the EthA reaction mixture.

Two main products (M1 and M2) were isolated and subjected to mass spectrometry analysis. The two isolated compounds showed *m/z* values of 293 and 277, respectively, which are in agreement with the S-dioxide and the S-monoxide derivatives of the 7947882 compound. Moreover, the fragmentation spectra of the metabolites showed a pattern similar to that of 7947882, in accordance with mono- and di-oxygenation of the thiophene sulfur atom of the substrate (Figures 1E and 1F). The partially purified metabolites were tested against PyrG protein and found to inhibit its enzymatic activity. Notably, the M1 product showed a higher degree of inhibition.

To better characterize the 7947882 metabolites, its S-dioxide derivative was chemically synthesized, giving rise to compound 11426026. The mass spectrum of 11426026 showed the same pattern as the M1 compound, confirming that M1 corresponds to the 7947882 S-dioxide derivative (Figures 1E and 1F). Therefore, the effects of 11426026 toward *M. tuberculosis* growth and toward PyrG activity were assessed. The MIC of 11426026 for *M. tuberculosis* H37Rv, *ethA*, and *pyrG* mutant strains was determined (Table S2). Wild-type *M. tuberculosis* and the *ethA* mutant were similarly sensitive to 11426026 (with MICs close to that of the parent compound 7947882), showing that 11426026 does not require activation by EthA, whereas the *pyrG* mutant strain was resistant, thus demonstrating that PyrG could be the target of this active metabolite.

Indeed, this was confirmed when the inhibitory activity of 11426026 for PyrG was assessed, since the compound was

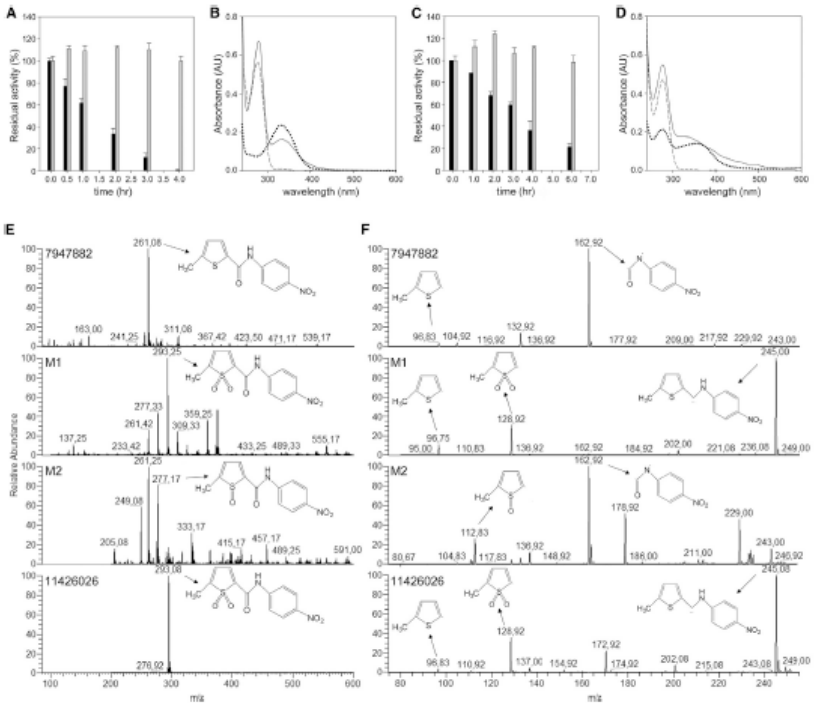

Figure 1. EthA Converts the 7947882 and 7904688 Compounds into Active PyrG Inhibitors

(A) Inhibition of PyrG activity during the co-incubation with EthA and 7947882. Gray bars correspond to the activities of the blank controls in the absence of NADPH, and black bars represent the residual activities after incubation with working EthA.

(B) UV-Vis spectra of the re-purified PyrG after co-incubation with EthA reaction with 7947882 compound. Solid line is the spectrum of PyrG incubated with full EthA reaction; dashed line is the spectrum of PyrG from blank reaction; dotted line is the spectrum of the compound at 20 μM.

(C and D) Co-incubation of PyrG with EthA and 7904688 compound. Conditions are the same as for (A) and (B), respectively.

(E and F) Identification of in vitro EthA metabolites of 7947882 compound. Mass spectrometry analysis (from top to bottom) of the 7947882 compound, the partially purified products of EthA reaction M1 and M2, and the synthetic metabolite 11426026. (E) Full electrospray ionization mass spectrometry of the compounds recorded in negative mode. (F) Fragmentation pattern of the compounds.

See also Figures S1 and S2; Table S2.

effective against the wild-type enzyme. Interestingly, the inhibitory effects were only found at subsaturating concentrations of ATP (IC_{50} 0.035 ± 0.002 mM in the presence of 0.2 mM ATP). Moreover, the compound was not active against the PyrG V186G mutant when tested under the same conditions. In fact, the estimated IC_{50} value was 44-fold higher than against the wild-type enzyme (1.5 ± 0.15 mM), at an ATP concentration of 1.5 mM, which corresponds to the K_m of the mutant for this substrate (Figure S1A).

This evidence confirms the hypothesis that 11426026 affects or binds at the ATP-binding site of PyrG, behaving as a competitive inhibitor with respect to ATP (K_i 0.010 ± 0.002 mM; Figures S1B and S1C). The high K_m value of the PyrG V186G mutant for ATP probably reflects the structural changes resulting from the mutation, which distorts the ATP-binding site and leading to an even lower affinity for the 11426026 derivative, thus explaining the resistance to this compound.

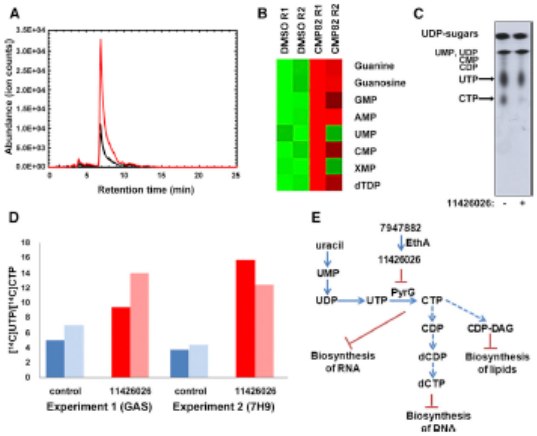

Figure 2. PyrG Inhibition Affects Nucleotide Metabolism in *M. tuberculosis*

(A) Representative EIC for the AMP ion ([M + H]$^+$, m/z = 348.07036) illustrating its increased pool size in 7947882-treated *M. tuberculosis* (red lines) compared with control (black lines).

(B) Heatmap illustrating overall changes in nucleotide pool sizes in 7947882-treated *M. tuberculosis* compared with control. Data are derived from two biological replicates.

(C) Thin-layer chromatography of nucleotide extract from [^{14}C]uracil-labeled *M. tuberculosis* H37Ra grown on glycerol-alanine-salts (GAS) medium. The figure is a representative image from three separate experiments.

(D) Ratio of radioactivity incorporated to [^{14}C]UTP and [^{14}C]CTP. Nucleotides were extracted from [^{14}C]uracil-labeled *M. tuberculosis* H37Ra grown on GAS, or 7H9 media and separated by HPLC. The two columns represent duplicate 2-ml samples removed from the radiolabeled culture, processed separately.

(E) Schematic representation of the major effects of PyrG inhibition in mycobacteria.

See also Figure S3.

The same procedure was used to identify the metabolite(s) derived from 7904688. In this case only one metabolite was found, corresponding to 3-phenyl-*N*-[(4-piperidin-1-ylphenyl) carbamoyl]propanamide (Figure S2). This derivative likely arises from sequential EthA reactions on the sulfur atom of the carbamothioyl moiety (Chigwada et al., 2014). However, this last metabolite showed no effect on PyrG activity. It is conceivable that the active metabolite(s) of 7904688 might be an unstable intermediate, thus precluding its isolation.

7947882 Inhibition of PyrG Alters Nucleotide Metabolism in *M. tuberculosis*

Since PyrG is a key enzyme involved in de novo pyrimidine biosynthesis (Meng et al., 2004), the effect of 7947882 on *M. tuberculosis* nucleotide metabolism was investigated. For this purpose, metabolomic experiments were performed with *M. tuberculosis* exposed for 24 hr to 7947882 (5× MIC) or its solvent, DMSO. Polar metabolites were extracted and analyzed by standard methods (de Carvalho et al., 2010; Larrouy-Maumus et al., 2013) that focused on bases, nucleosides, and nucleotides. *M. tuberculosis* H37Rv cells treated with 7947882 showed a substantial increase in the abundance of all nucleotide intermediates that were detected. Figure 2A illustrates extracted ion chromatograms (EIC) obtained for AMP in *M. tuberculosis* extracts treated with either compound or DMSO alone. Compound-induced changes in abundances of the ions detected are shown in Figure 2B. Taken together, these data demonstrate that direct inhibition of PyrG decreased CTP levels, leading to disruption of the nucleotide metabolic network, characterized by increased levels of several intermediates in the biosynthesis of pyrimidines and purines.

The molecular target of thiophenecarboxamides in mycobacteria was further corroborated through metabolic studies with [^{14}C]uracil and the active metabolite 11426026, using *M. tuberculosis* H37Ra (MIC 4 μg/ml) grown in glycerol-alanine-salts (GAS) medium with or without 11426026 (16 μg/ml) for 1 hr, then [^{14}C]uracil was added and radiolabeling continued for 3 hr. In the cells [^{14}C]uracil is initially incorporated into [^{14}C]uridine monophosphate (UMP) through the action of uracil phosphoribosyltransferase (Upp) from the pyrimidine salvage pathway (Villela et al., 2011). This is then further metabolized to the whole range of nucleotides and sugar nucleotides originating from uracil. After labeling, the cells were harvested and the nucleotide pool was extracted with diluted formic acid (Bochner and Ames, 1982). In the pilot experiment the PyrG substrate [^{14}C]UTP was separated from the PyrG product [^{14}C]CTP by thin-layer chromatography (TLC). An autoradiograph produced from the TLC plate clearly showed a decrease of [^{14}C]CTP relative to [^{14}C]UTP in treated *M. tuberculosis* compared with the control (Figure 2C). To quantify the changes, the labeling experiment was repeated under the same conditions and the nucleotides were analyzed by high-performance liquid chromatography (HPLC). Individual fractions co-eluting with the set of standards comprising UMP, uridine diphosphate (UDP), UTP, cytidine monophosphate, cytidine diphosphate, CTP, UDP-Gal, UDP-GlcNAc, and UDP-MurNAc pentapeptide were collected and quantified by measuring their radiolabel levels. Although incorporation of radioactivity into [^{14}C]UTP and [^{14}C]CTP was rather low in this experiment, the ratio of [^{14}C]UTP/[^{14}C]CTP did increase in the treated culture, as expected for PyrG inhibition (Figure 2D). Higher incorporation of [^{14}C]uracil was achieved by using 7H9/ADC/Tween medium, thereby confirming the trend of increased [^{14}C]UTP/[^{14}C]CTP following 11426026 treatment (Figure 2D; Figure S3).

In conclusion, these experiments highlighted that inhibition of PyrG affects nucleotide metabolism and, thus, very likely several

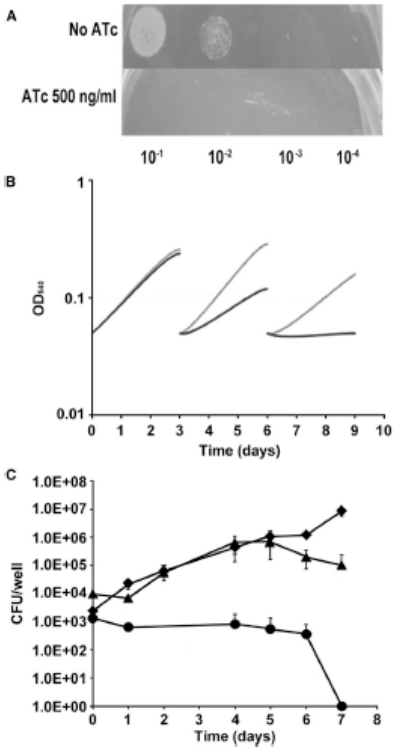

Figure 3. Essentiality of *pyrG* In Vitro and Ex Vivo

(A) Ten microliters of a *pyrG* cKD mutant suspension containing about 10^5 cfu were spotted at the indicated dilutions on Middlebrook 7H10 plates (±500 ng/ml ATc).

(B) Bacteria were grown in 7H9 medium (±500 ng/ml ATc) and diluted 1:10 in fresh media (±500 ng/ml ATc) every 3 days. $OD_{540\ nm}$ was recorded and used to compile the growth curves. Each experiment was repeated at least twice. Gray line, *pyrG* conditional mutant grown without ATc; black line, *pyrG* conditional mutant grown with ATc.

(C) Growth of *pyrG* conditional mutant and its parental strain (control) in THP-1-derived macrophages at an MOI of 1:20 (bacteria/macrophage). The results are expressed as cfu per well. The reported values represent the average and the SE obtained from two parallel independent infections. The experiment was repeated twice using independent bacterial inocula and THP-1 cultures. ATc (200 ng/ml) was added or not to the cell culture medium. Circles, *pyrG* conditional mutant plus ATc; diamonds, control plus ATc; triangles, *pyrG* conditional mutant, no ATc.

aspects of mycobacterial physiology. In particular, the metabolic changes should interfere not only with DNA and RNA biosynthesis, but also with other metabolic processes that require nucleotides, such as fatty acid, carbohydrate and amino acid biosynthesis, cell wall biosynthesis, and cAMP- and c-di-AMP-dependent signaling (Figure 2E).

Validation of PyrG Essentiality In Vivo and Ex Vivo

Since PyrG inhibition by the active metabolite of 7947882 has been unambiguously demonstrated, its validation as a drug target was further investigated. To show the essentiality of *pyrG* in *M. tuberculosis*, a conditional mutant was constructed where the *pyrG* promoter was replaced by the repressible promoter P_{tet} in a strain carrying the TetR-PipOFF repressible system (Boldrin et al., 2010). In this conditional mutant, the expression of *pyrG* was expected to be downregulated by the addition of anhydrotetracycline (ATc) to the culture medium, thus leading to depletion of its protein product. The growth of the *pyrG* conditional mutant was evaluated on solid 7H10 and in liquid 7H9 media (± ATc, 500 ng/ml). In each case, this conditional mutant exhibited inhibition of growth upon ATc exposure, while its parental strain was not affected, thus clearly demonstrating that PyrG is essential for *M. tuberculosis* growth in vitro (Figures 3A and 3B).

PyrG essentiality was also verified during intracellular growth. For this purpose, THP-1-derived macrophages were infected with the *pyrG* conditional mutant or with its parental strain, and the cells were incubated in the presence or absence of ATc (200 ng/ml). While the control was able to divide intracellularly under both conditions, the *pyrG* conditional mutant grew similarly to the control only in the absence of ATc. When *pyrG* expression was downregulated by ATc, the number of viable bacteria dropped rapidly, demonstrating *pyrG* essentiality also during intracellular growth (Figure 3C). Proof that PyrG is essential both in vitro and ex vivo further corroborates the value of this enzyme as a drug target.

PyrG Crystal Structure

The crystal structure of PyrG was solved by molecular replacement on a 2.0-Å resolution data set (Table S3). This structure showed a bidomain enzyme with an N-terminal amidoligase (ALase) domain, also commonly known as the synthetase domain (residues 1–278), connected through an interdomain linker (residues 279–Pro298) to a C-terminal glutamine amidotransferase (GATase) domain (residues 299–552), both domains displaying a Rossmann-like fold (Figure 4A). This bidomain architecture is typical of amidotransferases, already observed in the other available structures of full-length bacterial CTP synthetases (Goto et al., 2004; Endrizzi et al., 2004, 2005; Lauritsen et al., 2011). On the other hand, the 34-residue C-terminal extension of *M. tuberculosis* PyrG, which has no predicted secondary structure or known function, could not be traced due to the lack of supporting electron density, suggesting a high degree of flexibility.

The enzyme, in complex with either UTP, at 2.0-Å resolution, or UTP plus the non-hydrolyzable ATP analog AMP-PCP and the glutamine analog 5-oxo-L-norleucine (3.5 Å; Table S3), is a homotetramer with crystallographic 222 symmetry (Figure 4A), consistent with previous studies reporting positive cooperativity

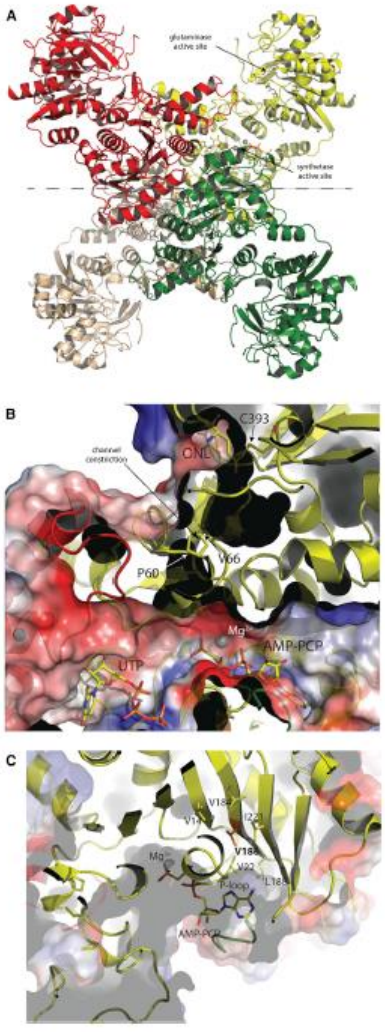

Figure 4. Crystal Structure of *M. tuberculosis* PyrG

(A) Tetrameric structure of *M. tuberculosis* PyrG in complex with nucleotides and analogs, i.e. either UTP or UTP/AMP-PCP/L-DON. As observed in the other available crystal structures of CTP synthetases, the N-terminal synthetase domain is positioned at the center of the tetramer while the C-terminal glutaminase domain is pointing outwards. The gray dashed line indicates the PyrG dimers (yellow/red versus green/brown) as they can be found in the apo structure.

(B) Surface "cut-through" of the synthetase active site, with UTP- and ATP-binding pockets, and "cut section" that shows a possible NH_4^+ channel connecting the glutaminase to the synthetase site. The electrostatic surface potential has been calculated and rendered by PyMol (Schroendinger, http://www.pymol.org).

(C) Surface view of ATP-binding pocket, occupied by AMP-PCP, to show the location of Val186 (orange) mutated in Gly in the *M. tuberculosis*-resistant strains. Side chains of hydrophobic residues surrounding Val186 are depicted as sticks.

See also Table S3; Figures S4 and S5.

for ATP and UTP due to nucleotide-driven tetramerization. Indeed, another structure of the enzyme in the apo form at lower resolution (3.5 Å; Table S3), revealed a homodimeric protein, each homodimer representing half of the functional tetramer and showing a dimerization surface of ~1,350 $Å^2$ per monomer (Figure 4A), all in good agreement with previous structural studies (Endrizzi et al., 2004, 2005; Goto et al., 2004; Lauritsen et al., 2011). Also, consistent with the oligomeric assembly as a dimer of dimers being triggered by ATP/UTP, the nucleotide-binding pockets were delimited by residues from two (ATP) or three (UTP) different subunits (Figures S4A and S4B). Surprisingly, in the highest-resolution structure available (Table S3), UTP was found lying in both pockets, a likely artifact due to the high concentration of the nucleotide (5 mM) in the co-crystallization conditions (Figure S4C). It should be noted that the UTP orientation in the substrate-binding pocket is unproductive for the course of the reaction, as the pyrimidine ring points away from ATP. Moreover, this UTP orientation coincides with the CTP orientation observed in *E. coli* PyrG in complex with CTP and ADP (PDB: 2ad5; Figure S4C), suggesting that this structure likely represents an inhibited enzyme (Endrizzi et al., 2005).

In contrast, in the independent crystal form, grown in the presence of AMP-PCP as well as UTP and the glutamine analog 6-diazo-5-oxo-L-norleucine (L-DON), AMP-PCP lies in the ATP-binding site, as expected, with UTP maintaining the same orientation as above (Figures 4B and S4B). In addition, a covalent adduct was observed between the Cys393 sulfur and oxonorleucine, as expected from the reaction with L-DON (Hart and Powers-Lee, 2008), therefore confirming the role of Cys393 as the catalytic nucleophile within a Gln-hydrolyzing triad that includes His524 and Glu526 (Figures S4D and S4E). In agreement with similar observations made on *E. coli* PyrG (Endrizzi et al., 2004), a putative ammonia diffusion channel was visualized connecting the glutaminase active site in the C-terminal domain to the synthetase site at the N-terminal domain (Figure 4B). However, the tunnel is not continuous, but appears to be blocked by the side chains of residues Pro55, Pro60, and Val66, all located on the long β2 to β3 linker that includes the short α2 (Figures S4D and S4E), forming a constriction in the channel (Figure 4B). The residue Val186 mutated to Gly in the *M. tuberculosis*-resistant mutants lies on the β7 strand behind the conserved P loop (Gly16 to Gly25) that contributes

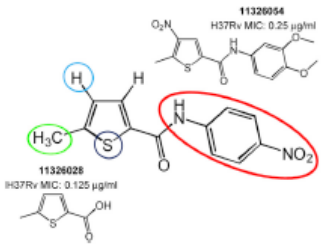

Figure 5. SAR Optimization Strategy of 7947882 Compound
Modifications made on the thiophene ring (positions 4, 5 and the sulfur atom) and the 4-nitroaniline moiety led to two more active compounds (11326028 and 11326054).
See also Tables S4 and S5.

to bind the ATP phosphates, its side chain being at closest ~7 Å from the AMP-PCP β-phosphate (Figure 4C). Despite being located in the proximity of the ATP-binding pocket, the Val186Gly substitution does not provide any obvious explanation for the resistance profile to an ATP competitive inhibitor. Moreover, this mutation should have a destabilizing effect on the P loop and on its proper positioning within the ATP-binding cleft, leading to a decreased affinity for ATP. This hypothesis, suggested by the observation that the Val186 side chain is situated in a hydrophobic pocket delimited by Val14, Leu22 (belonging to the P loop), Leu184, Leu188, and Ile221 (Figure 4C), is further supported by the steady-state kinetics analysis of the V186G mutant enzyme reported above.

The availability of the *M. tuberculosis* PyrG structure is useful for both structure-activity relationship (SAR) studies and in silico docking approaches to find new PyrG inhibitors that do not require EthA activation.

SAR Study of 7947882

To improve the antitubercular activity of 7947882, and to understand the substituent requirements needed to achieve activity against *M. tuberculosis*, SAR studies were performed (Figure 5). 105 derivatives of compound 7947882 were synthesized and tested for their activity against *M. tuberculosis* H37Rv. The substitutions concerned mainly the thiophene ring and the 4-nitroaniline moiety.

Substitution of the thiophene ring (with furan, pyrazole, or methylthiazole) led to inactive compounds (Table S4A). The substitution of the 4-nitroaniline led, in general, to decreased potency of the compounds (Table S4B). The presence of the *p*-nitro group was associated with the best MIC, but was not strictly required, since its substitution with halogen atoms or a methyl group caused only a small increase in MIC. Moreover, the addition of further substituents to the other positions of the phenyl ring did not improve efficacy. For instance, introduction of bulkier substituents, such as S-methyl or sulfonamide, or the substitution of the aniline with formimidamide derivatives, was even detrimental for activity, as these compounds all showed a higher MIC (Table S4B).

Furthermore, no improvement arose from modification of the substituents in the thiophene moiety. Lack of the methyl group in position 5 of the thiophene led to an increase in the MIC (Table S4C), as did introduction of a methyl or nitro group in position 4, with the exception of compound 11326054 which showed a lower MIC value (0.25 µg/ml) (Figure 5; Tables S4D and S4E). Curiously, analogs of this compound lacking the nitro group (11326008) did not show lower MIC (2 µg/ml). Moreover, all compounds with the thiophene moiety substituted with a nitro group showed lower potency than those lacking this group. Such high activity of compound 11326054 is conceivably connected with the antimycobacterial properties of nitrothiophenes (Hartkoorn et al., 2014), and in parallel with the amide moiety discussed in this paper.

Finally, substitution of the aniline with a hydroxy group, to give the 5-methylthiophene-2-carboxylic acid (11326028), led to the most potent compound (MIC of 0.128 µg/ml, Figure 5). The carboxylic group of compound 11326028 was fundamental for its antimycobacterial activity, since the carboxamide derivative was less active and, likewise for compound 7947882, modification of the thiophene substituents led to less active derivatives (Table S4F).

The *M. tuberculosis pyrG* mutant 88.7 showed levels of resistance to both 11326028 and 11326054 derivatives that were significantly higher (MIC values >8 µg/ml) compared with that of the wild-type strain, thus confirming that they still target PyrG. Similarly, the 81.10 mutant (mutated in *ethA* gene) was resistant to both compounds, indicating that they still need to be activated by EthA. This result was confirmed by the fact that the compounds are substrates of the enzyme (k_{cat} values of 1.33 ± 0.02 min^{-1} and 0.98 ± 0.03 min^{-1} for 11326028 and 11326054, respectively).

Finally, five derivatives of the active EthA metabolite 11426026 were synthesized. These compounds were all active toward wild-type PyrG, but not against the V186G mutant. However, none of these compounds showed an improved MIC compared with the active metabolite of 7947882 (Table S5).

Docking of the 11426026 Active Metabolite and PyrG Inhibitors

To acquire insight into the binding between the active metabolite of 11426026 and PyrG, a careful computational analysis of the possible poses of the compound was performed. Docking the 11426026 compound demonstrated that it would only successfully dock in the PyrG ATP site (Figures S5A, S5B and S5C). The superimposition with the UTP molecule shows a partial overlap. The phenyl ring is suggested to pi-stack with Arg223 while the nitro group is proposed to interact with Ala253 and Asp252.

Similarity searching based on the 4-nitroacetanilide portion of the molecule resulted in 12 similar compounds present in the Collaborative Drug Discovery (CDD) database (Ekins and Bunin, 2013; Ananthan et al., 2009; Ekins et al., 2014; Maddry et al., 2009; Reynolds et al., 2012). Four of these compounds were tested in vitro against PyrG enzymatic activity. One compound, CDD-823953 (LibDock score 106.7), was a weak PyrG inhibitor (K_i = 88.9 µM). Figures S5D and S5E show how this compound may bind less optimally in the ATP-binding site with the 4-nitroacetanilide portion in a different position to that seen with 11426026. Docking of compounds may be instructive for SAR

until the co-crystal structure with a ligand is obtained. For example, the 11326054 sulfone was also docked in the PyrG structure and was shown to be in an orientation similar to that of the 11426026 active metabolite (Figures S5F and S5G).

SIGNIFICANCE

New leads and new targets are required for tuberculosis drug development. Using phenotypic screening of a chemical library, two thiophenecarboxamide derivatives were identified that inhibited *M. tuberculosis* under replicating, non-replicating, and intracellular growth conditions. Both compounds were activated by the EthA monooxygenase, and the main metabolite of one of them (7947882), identified by mass spectrometry, was shown to target the CTP synthetase PyrG. The active metabolite was synthesized and shown to behave as a competitive inhibitor toward the ATP-binding site of PyrG, thus validating this enzyme as a new antitubercular drug target. Further validation was obtained genetically using conditional knockdown of *pyrG* to prove its essentiality in all the physiological states. A metabolomic approach demonstrated that the thiophenecarboxamide derivatives caused general deregulation of nucleotide metabolism, consistent with the inhibition of CTP synthetase. The combined evidence strongly indicates that PyrG is potentially a clinically relevant drug target. To overcome the requirement for EthA activation, we obtained high-resolution crystal structures of PyrG to underpin structure-based drug design. This approach has already generated additional lead compounds that inhibit this new drug target under all conditions tested.

EXPERIMENTAL PROCEDURES

NIAID Library Screening

CB2, a library of 594 compounds selected from an HTS screen on *M. tuberculosis* H37Rv (Ananthan et al., 2009; Goldman and Laughon, 2009; Maddry et al., 2009), was kindly provided by NIAID (Prof. R.C. Goldman). These compounds were initially screened at 10 μg/ml in duplicate for activity against H37Rv and ss18b in 96-well format, using the resazurin reduction microtiter assay. Compounds with a percentage of inhibition of H37Rv growth of more than 80% were subsequently analyzed for their MIC, intracellular activity against H37Rv, and cytotoxicity against the human hepatocellular carcinoma cell line HepG2 and Huh7, the human lung epithelial cell line A549, and the murine macrophage cell line RAW 264.7 (see Supplemental Experimental Procedures).

Compounds Used and Synthesis of Their Derivatives

7904688 and 7947882 were purchased from ChemBridge Corp (http://www.chembridge.com/index.php). Synthetic routes of thiophene derivatives, experimental details, and compound characterization data are provided in the Supplemental Experimental Procedures.

Isolation and Characterization of *M. tuberculosis* Mutants Resistant to 7947882 and 7904688

The isolation of *M. tuberculosis* mutants was performed by plating ~10^{10} cells from an exponential growth phase wild-type culture onto 7H11 medium containing different concentrations of 7947882 and 7904688, ranging from 5- to 20-fold the MIC of the wild-type strain.

Genomic DNA of *M. tuberculosis*-resistant mutants and wild-type strain was isolated and sequenced by using Illumina HiSeq2000 technology at IGA Technology Services (Udine, Italy). For the bioinformatic analysis of Illumina data, repetitive PE and PPE gene families were discarded as well as SNPs and indels with less than 50% probability. The mutations found in *ethA* (*Rv3854c*) and *pyrG* (*Rv1699*) (http://tuberculist.epfl.ch/) were confirmed by Sanger sequencing (Eurofins MWG Operon), after PCR amplification using the oligonucleotides presented in the Supplemental Information. PCR products were purified using the Wizard SV Gel and PCR Clean-Up system (Promega).

Overexpression of *ethA* in *M. tuberculosis* H37Rv

M. tuberculosis ethA was cloned into pSODIT-2, a shuttle expression vector containing the hygromycin resistance determinant, after PCR amplification using primers indicated in the Supplemental Information, *Pfu* DNA Polymerase (Promega), and genomic DNA as template. PCR fragments were digested with *Bam*HI and *Hin*dIII and ligated to the pSODIT-2 generating pSODIT/*ethA*. *M. tuberculosis* H37Rv competent cells were transformed with pSODIT-2 or pSODIT/*ethA*, and plated onto complete Middlebrook 7H11 agar plates supplemented with 20 μg/ml hygromycin and different concentrations of 7947882 or 7904688, ranging from 0.125 to 20 μg/mL

Enzyme Production and Characterization

M. tuberculosis PyrG and EthA were obtained in recombinant forms in *E. coli* and purified by standard methods. Enzymatic assays were performed according to the published methods (Fraaije et al., 2004; Lunn et al., 2008). See also Supplemental Experimental Procedures.

Construction of a *M. tuberculosis pyrG* Knockdown Mutant

The first 714 bp of *pyrG* coding sequence was amplified using RP1609 and RP1610 primers and cloned in the suicide plasmid pFRA170 downstream of a P_{pir}-derived promoter. To replace *pyrG* promoter with P_{pir}, 10 μg of this plasmid was used to transform TB38, an H37Rv derivative harboring the TetR-PipOFF system in its genome at the L5 *attB* site (Boldrin et al., 2010). Selection of recombinants was achieved using 7H10 agar plates containing hygromycin (50 μg/ml). Integration of the suicide plasmid was confirmed by PCR. Since *pyrG* might be co-transcribed with its downstream genes (*rv1700-rv1701*), the latter genes were provided in *trans* on a pMV261-derived plasmid. In this way the final *pyrG* conditional knockdown (cKD) strain was obtained. This cKD strain was used for *pyrG* essentiality evaluation in both in vitro and ex vivo experiments (see Supplemental Experimental Procedures).

PyrG Crystallization, Data Collection, and Structure Determination

Crystallization screenings of PyrG in the presence of various ligands were carried out at 18°C by sitting drop in 96-well format (200 + 200 nl drops) with a Mosquito dispensing robot (TTP Labtech). Crystals were identified in several conditions. PyrG in apo form: 10% PEG8000, 200 mM Ca acetate, 100 mM HEPES (pH 7.5); complex with UTP: 17% PEG20000, 100 mM $MgCl_2$, 100 mM Tris-HCl (pH 8.5); complex with AMP-PCP, UTP, and L-DON: 30% PEG2000 MME, 100 mM NaCl, 100 mM bicine (pH 9.0). All data sets were collected on the Proxima-1 beamline at the Soleil synchrotron (Gif-sur-Yvette, France) from single crystals at 100 K, processed with XDS (Kabsch, 2010) and merged with Aimless from the CCP4 suite (Winn et al., 2011). The structure was first solved by molecular replacement with the program MOLREP (Murshudov et al., 1997) on a data set collected from a PyrG-UTP crystal, using the structure of *Thermus thermophilus* CTP synthetase in complex with sulfate (PDB: 1vcn; Goto et al., 2004) as the search model. Refinement was carried out with Refmac5 (Murshudov et al., 2011) or autoBUSTER (Bricogne et al., 2011). The other data sets were solved by molecular replacement with MOLREP and the coordinates of a partially refined *M. tuberculosis* PyrG structure as the search model. Final models were validated through the Molprobity server (Chen et al., 2010). Docking of PyrG inhibitors was performed as described in the Supplemental Experimental Procedures.

In Vitro EthA Metabolite Production and Identification

For in vitro EthA metabolite production, 30 mg of 7947882 was incubated with 10 mg of EthA in 50 mM potassium phosphate (pH 8.0), 500 μM NADPH, 10 μM BSA, at 37°C for 5 hr under agitation. To produce the PyrG-EthA metabolite complex, the EthA reaction was performed in the presence of 45 μM PyrG. Reaction products were purified and analyzed as described in Supplemental Experimental Procedures.

CellPress

Metabolomic Experiments

Experimental Procedures have been described elsewhere (Larrouy-Maumus et al., 2013; Brauer et al., 2006). In brief, *M. tuberculosis* H37Rv was grown initially in 7H9 (with 0.5 g/l BSA, 0.05% tyloxapol, 0.2% glycerol, 0.2% glucose, and 0.085% NaCl) until late logarithmic phase (OD_{600} = 1.0) and 1 ml was layered onto 22-mm nitrocellulose filters (0.22 μm) under vacuum filtration. *M. tuberculosis*-laden filters were placed atop 7H10 (supplemented as 7H9) and incubated at 37°C for 5 days, after which the filters were transferred to 7H10 containing 7947882 (5× MIC = 2.5 μg/ml) or the control. After 24 hr, the bacteria were metabolically quenched by plunging *M. tuberculosis*-laden filters into acetonitrile/methanol/H_2O (2:2:1) pre-cooled to −40°C. The metabolites were extracted by mechanical lysing of the *M. tuberculosis*-containing solution with 0.1-mm zirconia beads. Lysates were clarified by centrifugation, filtered, and metabolites analyzed by liquid chromatography-mass spectrometry as described in Supplemental Experimental Procedures.

For metabolic labeling of *M. tuberculosis* H37Ra with [^{14}C]uracil, 10 ml of the GAS medium (Takayama et al., 1975) was inoculated in the ratio 1:100 with an *M. tuberculosis* H37Ra pre-culture grown in Sauton medium. After 7 days of static growth at 37°C, the culture was split into two aliquots, and 11426026 (final concentration of 16 μg/ml) was added to one and DMSO to the other as a control. After 1 hr, [^{14}C]uracil (American Radiolabeled Chemicals, specific activity 53 mCi/mmol) was added to a final concentration 1 μCi/ml. Radiolabeling was carried out for 3 hr, then two 2-ml batches were removed from each culture. The bacteria were harvested by centrifugation, washed twice with a cold physiologic solution, and immediately extracted with 110 μl of ice-cold 9% (v/v) formic acid for 30 min. The formic acid extract was recovered by centrifugation and its radioactivity was quantified by scintillation spectrometry in 5 ml of EcoLite scintillation liquid (MP Biomedicals). The nucleotide extract was stored at −20°C and was typically analyzed by TLC or HPLC within 24 hr (see Supplemental Experimental Procedures). Alternatively, radiolabeling was performed as above with *M. tuberculosis* H37Ra culture grown to OD_{600} = 0.375 in 7H9 medium at 37°C.

ACCESSION NUMBERS

The PDB accession numbers for coordinates and structure factors of the crystal structures described here are PDB: 4ZDI (PyrG in apo form); PDB: 4ZDJ (PyrG in complex with two molecules of UTP/Mg^{2+}); and PDB: 4ZDK (PyrG in complex with UTP, AMP-PCP, Mg^{2+}, and 5-oxo-L-norleucine).

SUPPLEMENTAL INFORMATION

Supplemental Information includes Supplemental Experimental Procedures, five figures, list of oligonucleotide primers, and five tables and can be found with this article online at http://dx.doi.org/10.1016/j.chembiol.2015.05.016.

AUTHOR CONTRIBUTIONS

R.C.H. performed the screening of NIAID library procured by S.T.C.; G.M., A.L.d.J.L.R., and M.R.P. isolated and characterized the resistant mutants; M.F. performed bioinformatics analysis of Illumina data; G.M., L.R.C., M.E., and N.B. performed cloning, and protein expression and purification; L.R.C. and M.E. performed enzymatic assays; L.R.C., M.E., and A.P. performed metabolite isolation and identification; V.M., E.K., and A.L. performed derivative synthesis; G.D. and F.B. performed studies on *pyrG* essentiality; L.B.M., I.C., Z.S., and J.B. performed metabolomic studies; M.B. performed crystallographic studies; S.E. and M.B. performed docking experiments; R.F., G.Z., V.M., R.M., L.P.S.C., A.R.B., K.M., P.M.A, G.R., S.T.C., and M.R.P. supervised and directed the work; L.R.C., M.B., S.E., R.F., G.Z., V.M., R.M., L.P.S.C., A.R.B., K.M., G.R., S.T.C., and M.R.P. wrote the paper. All authors discussed the results and commented on the manuscript.

ACKNOWLEDGMENTS

We thank R.C. Goldman and the NIAID for providing the CB2 set; J. Bellalou and F. Levi-Acobas (Institut Pasteur, Paris, France) for their help in protein production; Synchrotron Soleil (Gif-sur-Yvette, France) for access to the beamline Proxima-1, as well as the beamline staff for the helpful assistance; Biovia for providing Discovery Study.

The research leading to these results received funding mainly from the European Community's Seventh Framework Program (Grant 260872). Additional funding was from the Slovak Research and Development Agency (Contract No. DO7RP-0015-11), the Francis Crick Institute which receives core funding from Cancer Research UK, the UK Medical Research Council (MC_UP_A253_1111), and the Wellcome Trust. The CDD TB database was funded by the Bill and Melinda Gates Foundation (Grant no. 49852). L.B.M. receives partial support from the FAPESP (2011/21232-1), CNPq (140079/2013-0), and CAPES PDSE (99999.003125/2014-09) programs.

Received: April 24, 2015
Revised: May 25, 2015
Accepted: May 30, 2015
Published: June 18, 2015

REFERENCES

Ananthan, S., Faaleolea, E.R., Goldman, R.C., Hobrath, J.V., Kwong, C.D., Laughon, B.E., Maddry, J.A., Mehta, A., Rasmussen, L., Reynolds, R.C., et al. (2009). High-throughput screening for inhibitors of *Mycobacterium tuberculosis* H37Rv. Tuberculosis (Edinb) *89*, 334–353.

Anderson, P.M. (1983). CTP synthetase from *Escherichia coli*: an improved purification procedure and characterization of hysteretic and enzyme concentration effects on kinetic properties. Biochemistry *22*, 3285–3292.

Baulard, A.R., Betts, J.C., Engohang-Ndong, J., Quan, S., McAdam, R.A., Brennan, P.J., Locht, C., and Besra, G.S. (2000). Activation of the pro-drug ethionamide is regulated in mycobacteria. J. Biol. Chem. *275*, 28326–28331.

Bochner, B.R., and Ames, B.N. (1982). Complete analysis of cellular nucleotides by two-dimensional thin layer chromatography. J. Biol. Chem. *257*, 9759–9769.

Boldrin, F., Casonato, S., Dainese, E., Sala, C., Dhar, N., Palù, G., Riccardi, G., Cole, S.T., and Manganelli, R. (2010). Development of a repressible mycobacterial promoter system based on two transcriptional repressors. Nucleic Acids Res. *38*, e134.

Brauer, M.J., Yuan, J., Bennett, B.D., Lu, W., Kimball, E., Botstein, D., and Rabinowitz, J.D. (2006). Conservation of the metabolomic response to starvation across two divergent microbes. Proc. Natl. Acad. Sci. USA *103*, 19302–19307.

Bricogne, G., Blanc, E., Brandl, M., Flensburg, C., Keller, P., Paciorek, W., Roversi, P., Sharff, A., Smart, O.S., Vonrhein, C., and Womack, T.O. (2011). Buster, Version 2.11.1 (Global Phasing Ltd).

Chen, V.B., Arendall, W.B., Headd, J.J., Keedy, D.A., Immormino, R.M., Kapral, G.J., Murray, L.W., Richardson, J.S., and Richardson, D.C. (2010). MolProbity: all-atom structure validation for macromolecular crystallography. Acta Crystallogr. D Biol. Crystallogr. *66*, 12–21.

Chigwada, T., Mbiya, W., Chipiso, K., and Simoyi, R.H. (2014). S-oxygenation of thiocarbamides V: oxidation of tetramethylthiourea by chlorite in slightly acidic media. J. Phys. Chem. A *118*, 5903–5914.

de Carvalho, L.P., Zhao, H., Dickinson, C.E., Arango, N.M., Lima, C.D., Fischer, S.M., Ouerfelli, O., Nathan, C., and Rhee, K.Y. (2010). Activity-based metabolomic profiling of enzymatic function: identification of Rv1248c as a mycobacterial 2-hydroxy-3-oxoadipate synthase. Chem. Biol. *17*, 323–332.

Dover, L.G., Alahari, A., Gratraud, P., Gomes, J.M., Bhowruth, V., Reynolds, R.C., Besra, G.S., and Kremer, L. (2007). EthA, a common activator of thiocarbamide-containing drugs acting on different mycobacterial targets. Antimicrob. Agents Chemother. *51*, 1055–1063.

Ekins, S., and Bunin, B.A. (2013). The collaborative drug discovery (CDD) database. Methods Mol. Biol. *993*, 139–154.

Ekins, S., Freundlich, J.S., Hobrath, J.V., Lucile White, E., and Reynolds, R.C. (2014). Combining computational methods for hit to lead optimization in *Mycobacterium tuberculosis* drug discovery. Pharm. Res. *31*, 414–435.

Endrizzi, J.A., Kim, H., Anderson, P.M., and Baldwin, E.P. (2004). Crystal structure of *Escherichia coli* cytidine triphosphate synthetase, a nucleotide-regulated glutamine amidotransferase/ATP-dependent amidoligase fusion protein and homologue of anticancer and antiparasitic drug targets. Biochemistry *43*, 6447–6463.

Endrizzi, J.A., Kim, H., Anderson, P.M., and Baldwin, E.P. (2005). Mechanisms of product feedback regulation and drug resistance in cytidine triphosphate synthetases from the structure of a CTP-inhibited complex. Biochemistry *44*, 13491–13499.

Fraaije, M.W., Kamerbeek, N.M., Heidekamp, A.J., Fortin, R., and Janssen, D.B. (2004). The prodrug activator EtaA from *Mycobacterium tuberculosis* is a Baeyer-Villiger monooxygenase. J. Biol. Chem. *279*, 3354–3360.

Goldman, R.C., and Laughon, B.E. (2009). Discovery and validation of new antitubercular compounds as potential drug leads and probes. Tuberculosis *89*, 331–333.

Goto, M., Omi, R., Nakagawa, N., Miyahara, I., and Hirotsu, K. (2004). Crystal structures of CTP synthetase reveal ATP, UTP, and glutamine binding sites. Structure *12*, 1413–1423.

Hart, E.J., and Powers-Lee, S.G. (2008). Mutation analysis of carbamoyl phosphate synthetase: does the structurally conserved glutamine amidotransferase triad act as a functional dyad? Protein Sci. *17*, 1120–1128.

Hartkoorn, R.C., Ryabova, O.B., Chiarelli, L.R., Riccardi, G., Makarov, V., and Cole, S.T. (2014). The mechanism of action of 5-nitrothiophenes against *Mycobacterium tuberculosis*. Antimicrob. Agents Chemother. *58*, 2944–2947.

Kabsch, W. (2010). XDS. Acta Crystallogr. D Biol. Crystallogr. *66*, 125–132.

Larrouy-Maumus, G., Biswas, T., Hunt, D.M., Kelly, G., Tsodikov, O.V., and de Carvalho, L.P. (2013). Discovery of a glycerol 3-phosphate phosphatase reveals glycerophospholipid polar head recycling in *Mycobacterium tuberculosis*. Proc. Natl. Acad. Sci. USA *110*, 11320–11325.

Lauritsen, I., Willemoës, M., Jensen, K.F., Johansson, E., and Harris, P. (2011). Structure of the dimeric form of CTP synthase from *Sulfolobus solfataricus*. Acta Crystallogr. Sect. F Struct. Biol. Cryst. Commun. *67*, 201–208.

Lechartier, B., Rybniker, J., Zumla, A., and Cole, S.T. (2014). Tuberculosis drug discovery in the post-post-genomic era. EMBO Mol. Med. *6*, 158–168.

Long, C.W., and Pardee, A.B. (1967). Cytidine triphosphate synthetase of *Escherichia coli* B. J. Biol. Chem. *242*, 4715–5721.

Lunn, F.A., MacDonnell, J.E., and Bearne, S.L. (2008). Structural requirements for the activation of *Escherichia coli* CTP synthase by the allosteric effector GTP are stringent, but requirements for inhibition are lax. J. Biol. Chem. *283*, 2010–2020.

Maddry, J.A., Ananthan, S., Goldman, R.C., Hobrath, J.V., Kwong, C.D., Maddox, C., Rasmussen, L., Reynolds, R.C., Secrist, J.A., Sosa, M.I., et al. (2009). Antituberculosis activity of the molecular libraries screening center network library. Tuberculosis *89*, 354–363.

Meng, Q., Turnbough, C.L., and Switzer, R.L. (2004). Attenuation control of pyrG expression in *Bacillus subtilis* is mediated by CTP-sensitive reiterative transcription. Proc. Natl. Acad. Sci. USA *101*, 10943–10948.

Murshudov, G.N., Vagin, A.A., and Dodson, E.J. (1997). Refinement of macromolecular structures by the maximum-likelihood method. Acta Crystallogr. D Biol. Crystallogr. *53*, 240–255.

Murshudov, G.N., Skubák, P., Lebedev, A.A., Pannu, N.S., Steiner, R.A., Nicholls, R.A., Winn, M.D., Long, F., and Vagin, A.A. (2011). REFMAC5 for the refinement of macromolecular crystal structures. Acta Crystallogr. D Biol. Crystallogr. *67*, 355–367.

Reynolds, R.C., Ananthan, S., Faaleolea, E., Hobrath, J.V., Kwong, C.D., Maddox, C., Rasmussen, L., Sosa, M.I., Thammasuvimol, E., White, E.L., et al. (2012). High throughput screening of a library based on kinase inhibitor scaffolds against *Mycobacterium tuberculosis* H37Rv. Tuberculosis *92*, 72–83.

Sala, C., Dhar, N., Hartkoorn, R.C., Zhang, M., Ha, Y.H., Schneider, P., and Cole, S.T. (2010). Simple model for testing drugs against nonreplicating *Mycobacterium tuberculosis*. Antimicrob. Agents Chemother. *54*, 4150–4158.

Sassetti, C.M., Boyd, D.H., and Rubin, E.J. (2001). Comprehensive identification of conditionally essential genes in mycobacteria. Proc. Natl. Acad. Sci. USA *98*, 12712–12717.

Takayama, K., Schnoes, H.K., Armstrong, E.L., and Boyle, R.W. (1975). Site of inhibitory action of isoniazid in the synthesis of mycolic acids in *Mycobacterium tuberculosis*. J. Lipid. Res. *16*, 308–317.

Vannelli, T., Dykman, A., and Ortiz de Montellano, P.R. (2002). The antituberculosis drug ethionamide is activated by a flavoprotein monooxygenase. J. Biol. Chem. *277*, 12824–12829.

Villela, A.D., Sanchez-Quitian, Z.A., Ducati, R.G., Santos, D.S., and Basso, L.A. (2011). Pyrimidine salvage pathway in *Mycobacterium tuberculosis*. Curr. Med. Chem. *18*, 1286–1298.

WHO. (2014). Global Tuberculosis Report 2014 (World Health Organization). www.who.int.

Willemoës, M., Molgaard, A., Johansson, E., and Martinussen, J. (2005). Lid L11 of the glutamine amidotransferase domain of CTP synthase mediates allosteric GTP activation of glutaminase activity. FEBS J. *272*, 856–864.

Winn, M.D., Ballard, C.C., Cowtan, K.D., Dodson, E.J., Emsley, P., Evans, P.R., Keegan, R.M., Krissinel, E.B., Leslie, A.G.W., McCoy, A., et al. (2011). Overview of the CCP4 suite and current developments. Acta Crystallogr. D Biol. Crystallogr. *67*, 235–242.

Zhang, M., Sala, C., Hartkoorn, R.C., Dhar, N., Mendoza-Losana, A., and Cole, S.T. (2012). Streptomycin-starved *Mycobacterium tuberculosis* 18b, a drug discovery tool for latent tuberculosis. Antimicrob. Agents Chemother. *56*, 5782–5789.

Send Orders for Reprints to reprints@benthamscience.ae

Current Medicinal Chemistry, 2016, 23, 1-34 1

REVIEW ARTICLE

New and Old Hot Drug Targets in Tuberculosis

Laurent Roberto Chiarelli, Giorgia Mori, Marta Esposito, Beatrice Silvia Orena and Maria Rosalia Pasca*

Department of Biology and Biotechnology Lazzaro Spallanzani, University of Pavia, Pavia, Italy

ARTICLE HISTORY

Received: March 30, 2016
Revised: May 18, 2016
Accepted: June 28, 2016

DOI: 10.2174/1389557516666160831164925

Abstract: Tuberculosis is an infectious disease caused by the bacillus *Mycobacterium tuberculosis*. The World Health Organization publishes global tuberculosis reports annually in order to provide the latest information in the surveillance of drug resistance. Given the alarming rise of resistance to antitubercular drugs worldwide, finding new cellular targets and developing new analogues or new compounds with greater potency against already known targets are both important aspects in fighting drug-sensitive and drug-resistant *M. tuberculosis* strains. In this context, the introduction of the phenotypic screens as an efficient tool for the identification of active compounds for tuberculosis drug discovery has improved the possibility to find new effective targets.

With this review we describe the state of art of the currently well validated antitubercular drug targets as well as the advances in discovery of new ones. The main targets will be discussed starting from the oldest such as the enoyl reductase InhA which is constantly repurposed with new inhibitors, through the well assessed targets like the gyrase, the ATP synthetase or the RNA polymerase, up to the hot promiscuous targets decaprenylphosphoryl-D-ribose oxidase DprE1 and the mycolic acid transporter MmpL3, or the newly validated and promising targets like the CTP synthetase.

Keywords: Tuberculosis, antitubercular drugs, repurposed targets, promiscuous targets, phenotypic screening, drug design.

1. INTRODUCTION

Tuberculosis (TB), the second most damaging among the human infectious diseases, is still a major concern to global public health. In 2014, TB killed 1.5 million people and 9.6 million people were affected by TB worldwide [1, 2]. Moreover, the World Health Organization (WHO) reported that the 3.3% of new tuberculosis cases and the 20% of the previously treated cases had multidrug resistant TB (MDR-TB).

The recommended regimen for drug-sensitive tuberculosis was established four decades ago and is still highly effective; it includes first-line drugs such as isoniazid and rifampicin for 6 months, together with pyrazinamide and ethambutol for the first 2 months. Nevertheless, the major threat is represented by the spread of MDR-TB, resistant at least to rifampicin and isoniazid. These cases are treated with second-line drugs such as new fluoroquinolones (*e.g.* moxifloxacin or levofloxacin), in combination with an injectable drug (amikacin, kanamycin, or capreomycin) [1]. Notwithstanding, 9.7% of MDR-TB has been reported as extensively drug resistant TB (XDR-TB, resistant to first-line drugs and to at least one fluoroquinolone and to one second line injectable drug) in 105 countries [1, 2]. The need of new antitubercular drugs is thus considered a priority and new agents have entered clinical trials after a long period of stagnation (Table **1**).

Among these, many are new inhibitors of old repurposed targets, such as new fluoroquinolones and new rifamycins, targeting DNA gyrase and RNA polymerase, respectively (Table **1**) [2]. However, new drug

*Address correspondence to this author at the Department of Biology and Biotechnology Lazzaro Spallanzani, University of Pavia, via Ferrata 1, Pavia, Italy; Tel.: +39-0382-985576, Fax: +39-0382-528496; E-mail: mariarosalia.pasca@unipv.it

0929-8673/16 $58.00+.00

Table 1. New antitubercular drugs in preclinical and clinical trials.

Preclinical development		Clinical development		
Early stage development	**GLP toxicology**	**Phase I**	**Phase II**	**Phase III**
TBI-166 (Rimino-phenazine)	PBTZ169 (Benzothiazinone)	TBA-354 (Nitroimidazole)	Sutezolid (Oxazolidinone)	Bedaquiline TMC-207 (Diarylquinoline) for MDR-TB
CPZEN-45 (Caprazene nucleoside)			SQ109	
SQ641 (Capuramycin)	BTZ-043 (Benzothiazinone)	Q203 (Imidazopyridine amide)	Rifapentine for DS-TB	Delamanid OPC-67683 (Nitroimidazole) for MDR-TB
			High dose of Rifampicin for Drug Sensitive-TB	
1599 (Spectinamide)			Bedaquiline (Diarylquinoline)-Pretomanid (Nitroimidazole)-Pyrazinamide combination	Pretomanid (Nitroimidazole)-Moxifloxacin (fluoroquinolone)-Pyrazinamide combination
SEQ-9 (Macrolide)			Levofloxacin for MDR-TB	

Modified from www.newtbdrugs.org.

candidates should be characterized by new mechanisms of action in order to prevent cross resistance.

Recently, new drug targets were identified and some of their inhibitors have entered clinical development. Some of these drug candidates comprehend: benzothiazinones (BTZ-043 and PBTZ-169) and SQ109, inhibiting the two promiscuous targets DprE1 and MmpL3, respectively [3-5], and bedaquiline/TMC 207, a diarylquinoline in 2B phase of clinical trials which inhibits ATP synthase [6]. Based on the results of phase 2, bedaquiline received an accelerated approval for MDR-TB by Food and Drug Administration in 2012 [7]. Unfortunately, its use in the treatment of MDR- and XDR-TB is linked to an increased number of unexplained deaths and to an abnormal heartbeat (Long QT syndrome) [2, 8]. Another drug which received conditional approval for MDR-TB by the European Medicines Agency in 2014 is delamanid/OPC 67683, a nitroimidazole inhibiting mycolic acid biosynthesis [9]. However, delamanid has been related to prolonged QT and to potential central nervous system (CNS) toxicity when used in combination with isoniazid or fluoroquinolones during MDR-TB therapy [2, 10]. In addition, mutations in *M. tuberculosis* genome causing resistance to bedaquiline and delamanid have been recently documented [11].

For these reasons and even though new antitubercular drugs are available, TB drug discovery research must continue in order to fight the spread of drug resistance. In this context, particular attention should be given not only to established targets, but also to new targets that have recently emerged.

Herein, we present a review of the main known cellular targets inhibited by antitubercular compounds, going from the first ones characterized (*e.g.* InhA), up to the latest discovered (*e.g.* PyrG), with particular focus on their use in drug design strategies.

2. OLD REPURPOSED TARGET

Among the new compounds under clinical evaluation, some of them were developed as derivatives of already known antitubercular drugs and have now been repurposed for TB treatment because of the essentiality and the vulnerability of their targets: InhA, RNA polymerase and DNA gyrase.

Isoniazid (isonicotinyl hydrazide, INH) is a prodrug whose activation is mediated by the *M. tuberculosis* catalase-peroxidase KatG enzyme, leading to the formation of an INH-NAD adduct. This adduct is able to inhibit the NADH-dependent enoyl-ACP reductase (encoded by *inhA* gene) of the fatty acid synthase type II system, involved in mycolic acid biosynthesis. InhA is considered an ideal drug target, since its inhibition directly results in cellular death [12]. *M. tuberculosis* INH-resistant strains harbour mutations in the *katG* or *inhA* genes. Consequently, putative InhA inhibitors that do not require KatG activation are needed.

Rifampicin (RIF) is another first-line antitubercular compound active against both replicating and non-replicating *M. tuberculosis* strains. It targets the β subunit of the RNA polymerase encoded by *rpoB* gene [13].

Among the second-line drugs, the most used are the fluoroquinolone class of compounds (*e.g.*: moxifloxacin and gatifloxacin): they target the DNA gyrase, a tetramer of two A and two B subunits, encoded by *gyrA* and *gyrB* genes, respectively [14].

InhA, RNA polymerase and DNA gyrase cellular targets are treated in detail in the next paragraphs.

2.1. Trans-2enoyl-Acyl Carrier Protein Reductase (InhA)

InhA is an essential enzyme identified as the cellular target of INH and of the prodrug ethionamide (ETH) (Fig. **1**) [15]. INH and ETH inhibit mycolic acids biosynthesis causing accumulation of long-chain fatty acids, inhibition of C24 and C26 monounsaturated fatty acid biosynthesis and cell death [16]. INH is activated by the KatG peroxidase, thus forming an isonicotinoyl anion or radical [17] that reacts with NAD^+ producing the INH-NAD adduct, which in turns binds InhA [18]. InhA belongs to the fatty acid synthase type II (FASII), which elongates fatty acids up to 56 carbons to form mycolic acids, and catalyzes the NADH-dependent reduction of 2-trans-enoyl-ACP molecules with 16 or more carbons during the last step of fatty acid elongation [19].

The INH-NAD adduct inhibits InhA, blocking mycolic acid biosynthesis then causing cell death. Whereas the majority of the *M. tuberculosis* INH resistant mutants show mutations in the *katG* gene, encoding for the activator, about 25% of the *M. tuberculosis* INH-resistant clinical isolates display Ser94Ala and Ile16Thr mutations in InhA. These mutations cause INH resistance by decreasing the affinity of InhA for the NADH and for the INH-NAD complex [16].

The first InhA crystal structure was solved in complex with NADH (Fig. **2A**) [19]. The InhA enzyme is composed of seven b strands and eight a helices and it has a core structure similar to the dinucleotide-binding fold of many dehydrogenases. The NADH cofactor binding site is in a pocket between the back and the seat of the InhA enzyme and its structure suggests that recognition of NADH is mediated by interactions with an array of polar amino acids and backbone atoms. In the InhA wild-type structure the NADH phosphate forms hydrogen bonds with the main-chain nitrogen atom of the Ile21 and with a well-ordered water molecule. The crystal structure of the Ser94Ala mutant revealed that this water molecule is disordered and forms only a single hydrogen bond with the NADH phosphate, resulting in a fivefold reduced affinity for NADH compared to that of the wild-type strain, thus accounting for INH resistance [19].

ETH (Fig. **1**) is a prodrug activated by the NADPH-specific flavin adenine dinucleotide–containing monooxygenase EthA [20]. ETH active form reacts with NAD^+ yielding an ETH-NAD adduct, which in turns binds InhA, causing the inhibition of mycolic acid biosynthesis [21]. Similarly to INH, mutations in the gene encoding for the EthA activator conferred

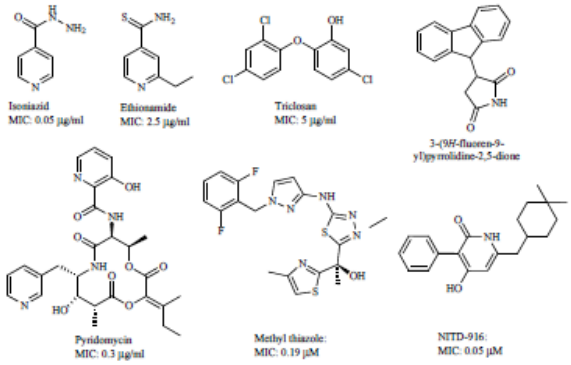

Fig. (1). Main compounds targeting InhA.

high level of resistance to this drug [22]. In order to solve this problem, new drugs targeting InhA and avoiding KatG or EthA activation are required.

Some of the new InhA inhibitors were obtained starting from triclosan (TRC), an uncompetitive InhA inhibitor with a low *in vitro* activity against *M. tuberculosis* (Minimum Inhibitory Concentration, MIC = 5-10 mg/ml) (Fig. **1**) [23]. Among the obtained derivatives, click chemistry allowed the synthesis of 1-dodecyl-4-phenethyl-1H-1,2,3-triazole by replacing the phenolic moiety with 1,4-disubstituted triazole. This derivative displayed MIC values against *M. tuberculosis* H37Rv lower than 2 mg/ml [24]. A new series of triazole derivatives have been synthesized showing analogies with TRC [25]. All of them inhibited *M. tuberculosis* growth and had a good activity against InhA enzyme, even if the best compound (MIC = 0.6 μM) was totally inactive against InhA. Recently, new TRC analogues were obtained with specific modifications in its 5 and 4 positions and seven of the obtained derivatives were highly active against *M. tuberculosis*, compared to TRC. Among them, the most active, the 4-(n-butyl)-1,2,3-triazolyl, had an MIC of 0.6 μg/ml and inhibited InhA activity [26].

Pyridomycin (Fig. **1**) is one of the most interesting and promising among the new InhA inhibitors. It is a natural compound produced by *Dactylosporangium fulvum*, very active against *M. tuberculosis* growth (MIC = 0.31 mg/ml). *M. tuberculosis* pyridomycin resistant mutant harbours the Asp148Gly mutation in InhA, but it is not cross-resistant to INH and ETH. In the same way, the *M. tuberculosis* INH resistant mutant carrying the Ser94Ala mutation is susceptible to pyridomycin. This finding suggested that INH and pyridomycin bind the InhA active site in different ways. In fact, structural studies demonstrated that pyridomycin inhibits InhA binding the core of the enzyme active sites, simultaneously blocking part of the NADH and fatty acyl lipid binding pockets. These findings allowed the discovery of a new druggable pocket in the InhA enzyme [27], thus giving hope in pyridomycin development. In 2013 new pyridomycin derivatives were synthesized, lacking the characteristic enol ester moiety of the hit compound, and leading to a four-fold more active compounds [28].

Through *in silico* screening based on the succinimide core fragment, a new promising pharmacophore moiety was identified in the 3-(9H-fluoren-9-yl)pyrrolidine-2,5-dione (Fig. **1**) [29]. These new derivatives displayed an interesting activity against InhA, with the most active 3,5-dichlorophenylamide-derivative (MIC = 4.7 mM) being also effective against *M. tuberculosis* INH resistant clinical isolates [29].

Another class of direct InhA inhibitors was identified in the methyl thiazole scaffold. The best compounds of this new thiadiazole series showed potent enzyme inhibition (InhA IC_{50} = 0.003 μM) and good MIC against *M. tuberculosis* both *in vitro* (MIC = 0.19 μM) and *in vivo* (MIC = 1 μM), although being less potent than INH (Fig. **1**). The InhA inhibition mechanism was investigated. Most of the InhA inhibitors, like TRC, bind the NAD-InhA complex, whilst this last class of compounds binds tightly (K_d = 13.7 nM) to the NADH-bound enzyme forming a ternary complex [30, 31]. Structural studies of InhA in complex with a methyl thiazole revealed new interactions between the compound and the enzyme active site [30]. Precisely, the compound forms hydrogen bonds between the thiadiazole ring and the Met98, and between the thiazole ring and the ribose moiety of NADH [30]. This information has been exploited to produce improved analogues.

Among the new classes of direct InhA inhibitors, the 4-hydroxy-2-pyridones were recently identified through a phenotypic high-throughput whole-cell screening [32]. These compounds had potent bactericidal activity against several *M. tuberculosis* INH resistant clinical isolates. They do not require KatG activation, and they have an *in vitro* frequency of spontaneous resistant mutants 100 times lower than that of INH resistant mutants. The NITD-916 lead compound (MIC = 0.05 mM) (Fig. **1**) preferably binds the NADH-InhA complex, similarly to methylthiazoles. Since InhA has a higher affinity for NADH rather than for NAD, the inhibitors binding the NADH-InhA complex are likely to be more efficient. NITD-916 shows good efficacy *in vivo*, paving the way for further development of inhibitors of a well assessed old target. [32].

2.2. RNA Polymerase (RNAP)

Rifampicin (RIF) (Fig. **3**), the major frontline antitubercular agent together with INH [33], belongs to the rifamycin class of DNA-dependent RNA synthesis inhibitors. RIF is one of the most potent and broad spectrum antibiotic, it blocks DNA transcription through the inhibition of the RNA-polymerase (RNAP) with a very high affinity for bacterial enzymes (binding constant about 10^{-8} *vs* 10^{-4}-10^{-6} M of eukaryotic RNA-polymerases) [34].

Bacterial RNAP has a $\alpha_2\beta\beta\omega$ subunit composition organized in a shape that is similar to that of a crab claw (Fig **4**), with the two "pincers" formed by the

larger subunits β' and β defining the active site [35]. Structural studies demonstrated that RNAP can adopt several conformations, from a fully open clamp to a fully closed conformation which allows or prevents DNA entry and exit into the active site during the different stages of transcription [36, 37].

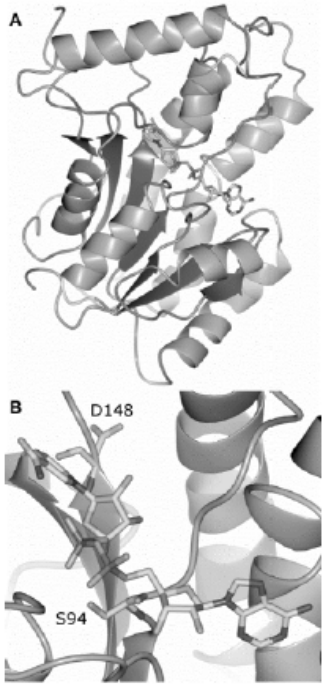

Fig. (2). A) Crystal structure of *M tuberculosis* InhA in complex NADH (PDB: 4DRE). B) Detail of the NADH binding site, showing the residues S94 and D148, involved in resistance to INH and pyridomycin, respectively.

All the mutations conferring resistance to RIF map in *rpoB*, an essential gene encoding the β subunit of the RpoB enzyme. These mutations mainly involve the amino acid residues going from position 420 to 450 [38, 39]. Kinetics analysis demonstrated that RIF does not impair the binding of the promoter to the RNAP, the formation of the open complex, or the formation of the first phosphodiester bond, but it blocks the formation of the second or third phosphodiester bond (depending on whether the transcription initiated with a nucleoside tri-phosphate or with a nucleoside mono-di-phosphate) instead [40]. RIF does not impair the substrate binding or the catalytic activity, but it was suggested that it simply acts as a steric block of the RNA elongation [40], as demonstrated by the crystallographic studies performed on the *Thermus aquaticus* RpoB [13]. Precisely, RIF binds in a pocket of the RNAP β subunit. This pocket is surrounded by those amino acids that confer resistance to the antibiotics when mutated. When RIF binds to the β subunits, it is in contact with almost 11 of the possibly mutated amino acids, mainly through van der waals or hydrogen interactions [13]. It is noteworthy that among the clinical isolates resistant to RIF about 84% of the mutations affect only three residues: Asp516, His526 and Ser531 [39].

RIF is commonly used in therapy, but it shows several disadvantages, such as the high frequency of spontaneous resistant mutants and the serious side effects, such as hepatotoxicity at high dosage. Moreover, this compound is a strong cytochrome P450 inducer, thus leading to several drug-drug interactions, precluding its use in HIV-infected people [41]. Two further rifamycin compounds, rifapentine and rifabutin, have been approved for TB treatment (Fig. 3).

Although rifapentine shows cross-resistance with RIF, it has a better pharmacokinetic profile with a longer half-life, it is more potent *in vivo* and useful for shortening TB therapy [42, 43]. Similarly, rifabutin shows improved potency and better pharmacokinetic compared to RIF. It is a very weak cytochrome P450 inducer, thus reducing drug-drug interactions [44] and being suitable also for HIV-infected patients [45]. The most interesting among the newer RIF derivatives is the benzoxazinorifamycin rifalazil [46], which combines an improved potency with a very reduced cytochrome P450 induction and greatly low toxicity in early rodents studies [47, 48]. However, clinical trials evidenced adverse effects causing the suspension of the development of rifalazil for TB treatment [41, 49].

The antibiotic myxopyronin was the first one identified as inhibitor of the "switch region" of RNAP. This region is a structural element at the base of the RNAP clamp comprising five segments (switch 1 to 5) which can adopt different local conformations, serving as a hinge for their opening or closure (Fig. 4). Different residues of the switch region, particularly switch 1, 2 and 3, interact with the DNA, thus coordinating the clamp closure and DNA binding [35].

Structural studies demonstrated that myxopyronin inhibits transcription by binding a pocket encompass-

ing the switch 1 and switch 2 regions, through interaction with both β' and β subunits, thus locking RNAP in one conformation [35]. The same study demonstrated that two other antibiotics, corallopyronin and ripostatin, shared this same target and mechanism of action. All these compounds do not show cross-reactivity with rifamycins, since their binding sites region do not overlap, thus providing the basis for the development of new different inhibitors of a well assessed target [50].

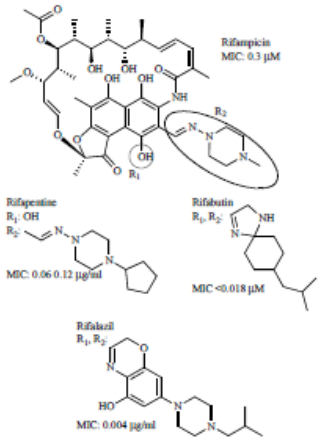

Fig. (3) Most significant rifamycins inhibiting *M tuberculosis* RNAP.

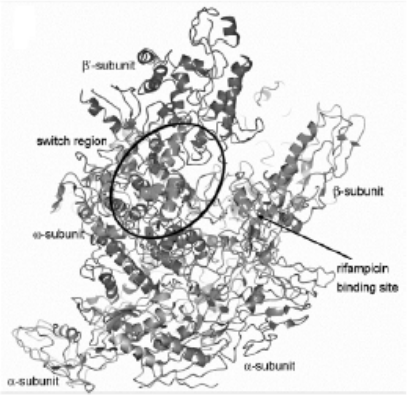

Fig. (4) Crystal structure of *T. aquaticus* RNAP in complex with rifampicin (PDB: I6V).

Soon after, lipiarmycin (also known as tiacumicin B, or fidaxomicin) (Fig. **5**) was identified as a RNAP inhibitor targeting the switch region [51, 52]. It has been demonstrated that lipiarmycin inhibits RNAP by blocking the open conformation of the clamp with a mechanism similar to that of the myxopyronin. However, lipiarmycin interacts with the switch region of RNAP by binding the switch 2 and 3, thus only partially overlapping the myxopyronin binding site [52]. For this reason, lipiarmycin does not show cross-resistance neither with myxopyronin nor with rifamycins [50].

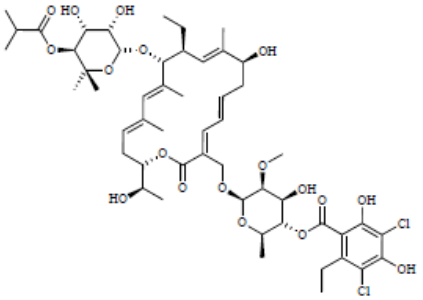

Fig. (5) Structure of lipiarmycin compound targeting the RNAP switch region.

Lipiarmycin has been approved for the treatment of *Clostridium difficile*. It is very active also against *M. tuberculosis* but it actually shows very low oral bioavailability thus limiting its use in the systemic tuberculosis infection [53]. Moreover, despite its isolation in 1975 [54], no SAR studies have been performed and no total synthesis of lipiarmycin have been reported for several years. In spite of that, synthesis of aglycone lipiarmycin has been recently published, finally giving the possibility to develop RNAP switch region inhibitors [55-57].

2.3. DNA Gyrase

Bacterial topoisomerases are still very attractive targets for drug discovery, and fluoroquinolones are one of the most successful classes of antibacterials targeting type II and type IV topoisomerases [58]. Unlike many other bacterial species, *M. tuberculosis* only has topoisomerase II, also known as DNA gyrase. This enzyme is an essential heterotetrameric protein consisting of two A and two B subunits, encoded by the *gyrA* (320 bp) and *gyrB* (375 bp) genes, respectively [59]. These two subunits control the DNA topological state catalys-

ing its negative supercoiling through a transient double strand DNA break, thanks to ATP hydrolysis. Precisely, GyrA contains the tyrosine active-site involved in DNA cleavage and in the formation of the protein-DNA covalent bond, whilst GyrB contains the ATPase active site [59].

Fluoroquinolones inhibit topoisomerases by converting the transient double strand DNA breaks into a covalent enzyme-DNA adduct, forming the so called "cleaved complex". The two most active fluoroquinolones, moxifloxacin and gatifloxacin (Fig 6), are currently under evaluation as promising first-line therapeutics, being already used for MDR-TB treatment [2, 60, 61]. Most of the mutations associated with fluoroquinolones resistance map in the conserved quinolone resistance determining region (QRDR), comprising both *gyrA* and *gyrB* genes. Specifically, the most common mutations identified in *M. tuberculosis* fluoroquinolone-resistant strains involve the substitution of the residues Ala90, Ser91 and Asp94 in GyrA, or Asn499, Thr500 and Glu501 in GyrB (Fig. 7) [14, 59, 62].

The crystallographic structures of the *M. tuberculosis* gyrase cleavage core, complexed with DNA and five fluoroquinolones, has been recently described for the first time [63] (Fig. 7). A biochemical assay demonstrated the importance of the fluoroquinolone/cleaved complex stability in determining the efficacy of the compound. An efficacy ranking among the different fluoroquinolones has been defined with moxifloxacin and its C8 methyl derivative being the most potent among the five analysed. These new fluoroquinolones were followed by the most potent gatifloxacin, and the less efficient ciprofloxacin and levofloxacin [63]. However, the crystal structures did not evidence specific interactions between the different fluoroquinolones and the gyrase, thus explaining the differences in their *in vivo* antibacterial activities.

Recently, new drugs targeting DNA gyrase have been discovered. Among these, the aminopyrazinamides (Fig. 6) were identifed from a high throughput screening against the scantly exploited GyrB ATPase domain of *Mycobacterium smegmatis* protein [64]. These compounds were shown to specifically inhibit mycobacterial GyrB, with a very weak activity against other Gram-positive or Gram-negative bacteria. Structural studies confirmed the unique and specific interaction present between the compound and the GyrB active site. It differs from that of other known GyrB inhibitors, such as novobiocin, thus rendering aminopyrazinamides highly pathogen specific [64]. The aminopyrazinamides class of compunds showed a ro-

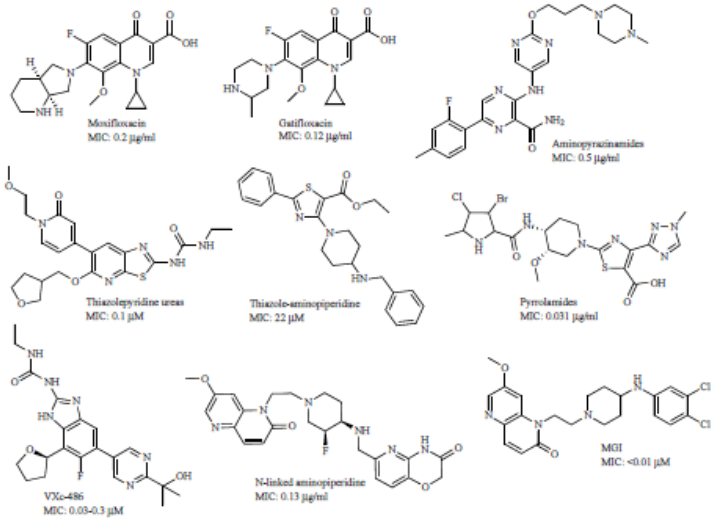

Fig. (6). Compounds targeting DNA gyrase.

bust SAR and they were found to be highly bactericidal against both replicating and non-replicating *M. tuberculosis*. For these reasons, they are considered as a new class with a great potential for further optimization [64].

Another new promising scaffold suitable for ATPase inhibition of GyrB is the thiazolopyridine urea [65] (Fig. 6). Like the other GyrB ATPase inhibitors, these compounds are very active also against *M. tuberculosis* drug-resistant strains, including quinolone-resistant ones, as they target different DNA gyrase activities. The best derivatives, showing antitubercular activities below μM concentration (MIC ≤ 0.1 μM) are efficacious *in vivo* in an acute murine model of tuberculosis [65].

Starting from thiazolopyridine urea scaffold, the thiazolopyridones were designed in order to allow hydrophobic interactions also in the ribose pocket of the GyrB ATP binding region [66]. Resulting compounds showed good activity *in vivo*, but were affected by a low solubility, thus needing further optimization [66].

Since GyrB mutations conferring resistance to fluoroquinolones do not confer resistance to the ATPase inhibitors, the interest in new drugs acting through inhibition of the GyrB ATPase activity increased. New series were then developed using different strategies: the thiazole-aminopiperidine and the quinolone-aminopiperidine, developed by molecular hybridization [67, 68], the pyrrolamides, obtained by drug-design [69, 70] and the aminobenzimidazole, optimized using structure-guided design and structure-activity relationship (SAR) studies of potency against both Gram-positive and some Gram-negative bacterial species [71, 72] (Fig. 6). Pyrrolamides optimization led to compounds showing good bactericidal activity against *M. tuberculosis in vitro* and *ex vivo*, and moderately active *in vivo* [69].

The last optimization of the aminobenzimidazole metabolic profile led to the identification of VXc-486 [72]. VXc-486 was very effective against *M. tuberculosis* drug-sensitive and drug-resistant isolates *in vitro* (MICs of 0.03 to 0.30 μg/ml and 0.08 to 5.48 μg/ml, respectively), *ex vivo* and *in vivo*. Moreover, this compound showed bactericidal activity also against *M. tuberculosis* dormant bacteria. VXc-486 was then improved using a phosphate ester prodrug approach. The obtained prodrug (pVXc-486) was more potent *in vivo* and when used in combination with other antitubercular drugs (rifapentine-pyrazinamide and bedaquiline-pyrazinamide) was effective like moxifloxacin [73]. For all these characteristics pVXc-486 could be considered a promising starting point for future drug development.

Finally, new classes of gyrase inhibitors are emerging. All of them are characterized by different mechanisms of action and they do not show cross resistance with fluoroquinolones. Among these, the N-linked aminopiperidine compounds developed by AstraZeneca exert their inhibition through a single strand cleaved-complex [74]. These compounds have a good *in vitro* and *in vivo* efficacy, a good pharmacokinetic profile and show sufficient structural diversity for further optimization [74].

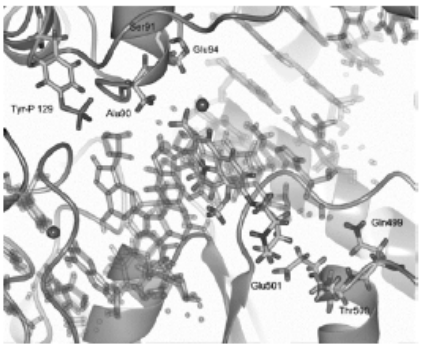

Fig. (7) Detail of the active site of *M. tuberculosis* GyrB in complex with moxifloxacin and DNA, showing the Tyrosine residue involved in protein-DNA covalent linkage, as well as the residues whose mutations are responsible for fluoroquinolones resistance (PDB: 5BS8).

Recently, GSK has identified new topoisomerase inhibitors characterized by new mechanisms of action. These compounds are called MGIs (Fig. 6) and they showed good *in vitro* and *in vivo* antitubercular activity without cross-resistance with fluoroquinolones [75]. The isolated MGIs resistant mutants had mutations in either GyrA or GyrB, suggesting that the binding to the enzyme occurs in proximity of the fluoroquinolone binding site. This hypothesis has been confirmed by DNA gyrase supercoiling and the cleavage complex assay [75]. These recent compounds further confirm the usefulness of the gyrases as well assessed targets for the development of new antitubercular drugs.

3. NOVEL PROMISCUOUS TARGETS

After the first complete sequencing of *M. tuberculosis* genome [76] and the introduction of next generation sequencing platforms, whole genome sequencing

(WGS) was widely and intensively used for identification of the cellular target of novel compounds. The screening of several chemical libraries led to a number of new potential drug targets, some of which inhibited by more than one compound or chemical entity [77, 78]. For this reason, these targets are defined as "promiscuous" [78]. The two more representative *M. tuberculosis* promiscuous targets, the decaprenylphosphoryl-β-D-ribose 2'-oxidase (DprE1) and the transmembrane transporter of trehalose monomycolate MmpL3, are here described.

3.1. Decaprenylphosphoryl-β-D-Ribose 2'-Oxidase (DprE1)

Among the *M. tuberculosis* drug targets, DprE1 is probably the most promiscuous, being defined also as a "magic drug target" [79]. It has been recognized to be inhibited by more than ten different classes of compounds with antitubercular activity [4, 80-91], most of them discovered through independent whole cells screening of different compound libraries.

DprE1 is an essential mycobacterial enzyme which works in concert with DprE2 (decaprenylphosphoryl-D-2-keto erythropentose reductase) to catalyze the epimerization of decaprenylphosphoryl-β-D-ribose (DPR) to decaprenylphosphoryl arabinose (DPA), a precursor for arabinan biosynthesis [92, 93]. Specifically, DprE1 catalyzes the first part of the reaction, the oxidation of DPR into decaprenylphosphoryl-2-keto-β-D-erythro-pentofuranose (DPX), which could then be reduced by DprE2 into DPA [94].

DprE1 is usually reported as an oxidase since it catalyzes a flavin adenine dinucleotide (FAD)-dependent oxidation, but it should be considered a dehydrogenase instead [95]. In fact, although the enzyme can use molecular oxygen to reoxidize the FAD cofactor, it has been observed that it could also use several organic compounds as electron acceptors [95].

Besides its physiological relevance, the ability of DprE1 to reduce organic compounds for the reoxidation of its FAD cofactor explains the peculiar mechanism of action of its covalent inhibitors.

The first DprE1 inhibitors were the 1,3-benzothiazin-4-ones (BTZs), a class of compounds belonging to a series of derivatives of the antibacterial dialkyldithiocarbamates [4]. The lead compound from this series, the 8-nitro benzothiazinone BTZ043, is one of the most active antitubercular agents known to date (MIC = 1 ng/ml). BTZ043 is characterized by the presence of a 8- nitro group that is essential for its activity, since the substitution of this group with an amino (BTZ045) or hydroxylamine (BTZ046) led up to 5000-fold loss in potency [4] (Fig. 8A).

The BTZ043 IC_{50} against DprE1 is only in the micromolar range, but its outstanding antitubercular activity resides in its peculiar mechanism of action. The compound is effectively a pro-drug which, upon the reduction of the nitro to a nitroso group, reacts with a cysteine (Cys387) of DprE1 forming a semimercaptal covalent adduct, irreversibly blocking the enzyme activity [96].

This activation has been demonstrated to be catalyzed by DprE1 itself [95, 96], which uses the nitro group of the BTZ043 to reoxidize its FAD cofactor, thus reducing it to a nitroso. The nitroso group can then readily react with the near cysteine 387 of DprE1 active site, forming the covalent adduct (Fig. 8B).

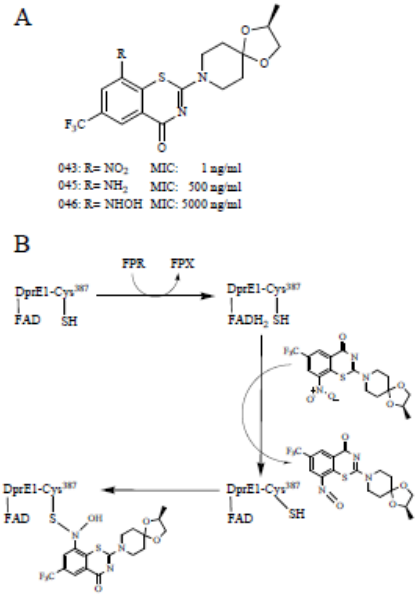

Fig. (8). A) Structure of 1,3-benzothiazin-4-ones. B) Mechanism of activation of BTZ043 by DprE1 itself, with consequent formation of the covalent semicarbamide adduct between Cys384 and BTZ043.

BTZ043 could also be activated by the cysteine itself through a non-enzymatic reduction of the nitro

group induced by the thiolates [97]. However, the fact that the BTZ043-DprE1 covalent adduct does not occur in the absence of the substrate, is in favor of an enzymatic activation [98].

The broad specificity for the different electron acceptors explains the number of the different chemical entities found to inhibit DprE1. In the 3 years following the discovery of DprE1 as the target of the BTZs, three further independent whole cell screenings of different chemical libraries identified new compounds targeting this enzyme (Fig. 9) [80-82]. All these compounds were characterized by a nitro-aromatic group and, although less potent than the BTZ043, behave as covalent inhibitors, thus showing a similar mechanism of action [95, 99].

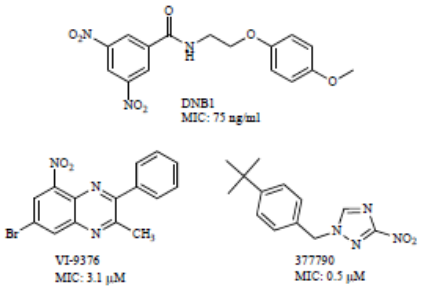

Fig. (9). Covalent inhibitors of DprE1.

Crystallographic studies finally demonstrated that BTZ043 forms a covalent adduct with the cysteine residue of the active site of DprE1. The crystal structures of *M. smegmatis* DprE1, in apo form and in complex with BTZ043 [95], and the crystal structure of the *M. tuberculosis* enzyme in complex with the nitroso analog CT325 [100] have been published at the same time. In both cases, BTZ043 was found to be allocated in front of the FAD cofactor, forming the expected semimercaptal adduct with the Cys387 (Fig. **10**). An additional interaction was found between the side chain of the Lys418, a residue essential for DprE1 enzymatic activity, and the semimercaptal hydroxyl group [95]. Further key interactions are formed between the trifluoromethyl group of BTZ043 and a pocket formed by the His132, Gly133, Lys134, Asn365 and Lys367 residues. In contrast, no particular interactions are present with the spirocyclic piperidine group of BTZ043. Effectively, SAR studies evidenced the essentiality of the nitro group (R_1, Fig. **11**), of the trifluoromethyl group (R_2) and of the sulfur (R_3) and oxygen in the thiazine ring for the antimicrobial activity of BTZ, whereas the spirocyclic piperidine group (R_4) seemed more suitable for derivatization [3, 4].

Despite the outstanding *in vitro* potency of BTZ043, its efficacy in a mouse model of TB was relatively low, mainly due to the poor solubility of the compound. Moreover, BTZ043 was found to be the substrate of nitroreductases, such as the *M. smegmatis* NfnB enzymes, that can transform the compound into its inactive hydroxylamino or amino form [101]. Further SAR studies are therefore needed in order to improve the PK/PD parameters.

As previously mentioned, all strategies designed to modify the nitro group [4, 102, 103] led to a 500- to 5000- fold decrease in potency. Similarly, a loss of potency with a consequent increase in the MIC values results from modifications of the trifluoromethyl group [4], or from modification of the sulfur atoms into sulfoxide or sulfone [104] (Fig. **11**). Because of that, all the major efforts used to improve BTZs properties have been concentrated in the modification of the spirocyclic piperidine moiety (R_4) (Fig. **11**) [3, 105, 106].

PBTZ169, the most attractive DprE1 inhibitor emerged among the numerous studies performed, was obtained upon the introduction of a cyclohexylmethylpiperazine substituent in the BTZ scaffold (Fig. **11**). This compound was more effective than BTZ043 in a TB murine model [3]. The compound improved *in vivo* potency was mainly attributed to the higher affinity for DprE1, reflected in a 10-fold reduced MIC, combined with a lower susceptibility to nitroreductases [3]. PBTZ169 is also less toxic and is a good candidate to enter clinical trials. It was in fact on December 2015 that the Ministry of Health of the Russian Federation gave permission for Phase I clinical trials of PBTZ169 in Russia. In 2016, NEARMEDIC is planning to conduct human clinical trials (http://www.nearmedic.ru/en/node/690).

The high tractability of DprE1 as a drug target is further corroborated by a number of non-covalent reversible antitubercular inhibitors found in recent years. In fact, the enzyme has been found to be the target of several non-nitro compounds (Fig. **12**), some of them deriving from SAR studies of BTZs [89, 102, 103]. However, the majority of these were identified through whole cell screening [84-87], from target based whole cell screening [90], or from structure based approaches [89].

Crystallographic analysis [84, 87] and molecular docking [83, 85, 86, 89, 107] demonstrated these compound to interact with DprE1 in a similar way to that of

the BTZs, despite their structural differences. The crystal structure of DprE1 in complex with Ty38C (Fig. **13 A**) [87] and in complex with TCA1 (Fig. **13 B**) [84] showed how the compounds bind the enzyme in the active site, in front of the FAD cofactor, nearly involving the same residues participating in BTZ binding, such as the backbone of the residues 132-134, and the side chain of Asn365 and Lys418. As expected, since there is not formation of covalent adducts, mutations in the Cys384 residue of DprE1 do not confer resistance to the non-covalent inhibitors. Interestingly, mutations leading to the substitution of the Tyr314 were recurrent among the isolated *M. tuberculosis* mutants resistant to most of the non-covalent DprE1 inhibitors. These compounds showed very high affinity for DprE1, with IC_{50} in the nanomolar range and MIC values higher than that of the BTZs [85-88, 107]. However, most of these DprE1 inhibitors showed no efficacy *in vivo*, with the exception of TCA1 and of the azaindoles [84, 86]. In fact, differently from covalent inhibitors, for non-covalent inhibitors to be efficacious *in vivo* DprE1 inhibition should be characterized by a prolonged occupancy of the active site [103].

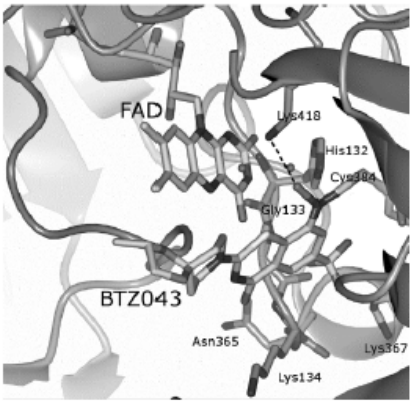

Fig. (10). Detail of the *M. smegmatis* DprE1 crystal structure in complex with BTZ043 (PDB: 4F4Q). For simplicity, the amino acids were numbered according to *M. tuberculosis* sequence.

Although a very high number of different classes of compounds are active against DprE1, this is not sufficient to fully explain the high promiscuity of this enzyme. It has been recently demonstrated that DPA biosynthesis occurs outside the mycobacterial plasma membrane, in the periplasm [108]. Therefore, despite the lack of known export signals, DprE1 is not located in the cytoplasm but in the periplasmic space, thus avoiding the action of efflux pumps or potential cytosolic inactivation mechanisms. DprE1 cellular localization makes the enzyme more accessible to the drugs, thus explaining, together with its particular enzymology, the great potential of this drug target.

3.2. Mycobacterial Membrane Protein Large 3 (MmpL3)

Another "promiscuous" drug target is the trehalose monomycolate transporter MmpL3. This 12 transmembrane domain protein (Fig. **14**) belongs to the mycobacterial membrane protein large (MmpL) family, a class of the resistance-nodulation-division (RND) efflux pump [109] transporters,exporting substrates through a proton antiport mechanism [110]. Among the 13 *mmpL* genes identified in *M. tuberculosis*, *mmpL3* is the only one that is essential, whilst mutations in *mmpL4, mmpL5, mmpL7, mmpL8, mmpL10, mmpL11* lead to growth impairment [111]. MmpL3 is involved in the export of trehalose monomycolate (TMM) [5] and it also has a role in iron uptake, being involved in heme import together with MmpL11 [112].

The first compound described to target MmpL3 is BM212 (Fig. **15**), a 1,5-diarylpyrrole derivative active against several multidrug resistant *M. tuberculosis* clinical isolates [113]. Genomic library screening and WGS of *M. tuberculosis*, *M. bovis* and *M. smegmatis* spontaneous resistant mutants lead to the identification of different mutations in *mmpL3* gene, thus indicating MmpL3 as target of BM212 [114, 115]. Moreover, uptake/efflux experiments excluded that the phenotype was associated to BM212 efflux, thus confirming that the transporter is the target of the compound [114]. From this initial scaffold, several studies were conducted in order to improve the antimycobacterial potency as well as the pharmacokinetic properties [116, 117], leading to improved analogs active in a murine tuberculosis infection model and still targeting MmpL3 [115].

Nearly at the same time, MmpL3 was identified as the target of other two unrelated compounds: the 1,2-diamine SQ109 (Fig. **15**) [5], and the adamantyl urea AU1235 [118, 119]. SQ109 was selected using combinatorial chemistry by screening a chemical library designed around ethambutol (EMB), with the aim to re-

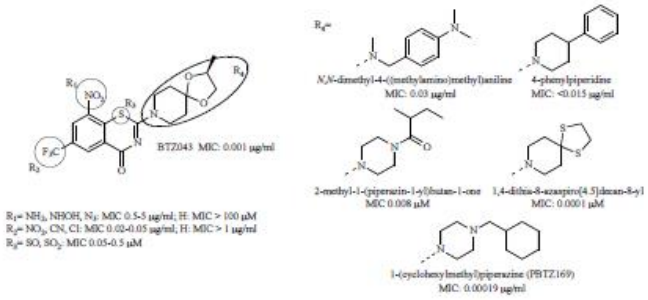

Fig. (11). Most significant DprE1 inhibitors deriving from SAR studies of BTZ043.

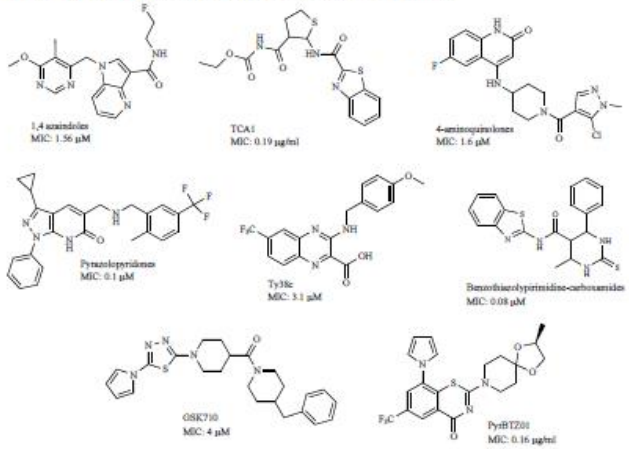

Fig. (12). Most representative non covalent DprE1 inhibitors.

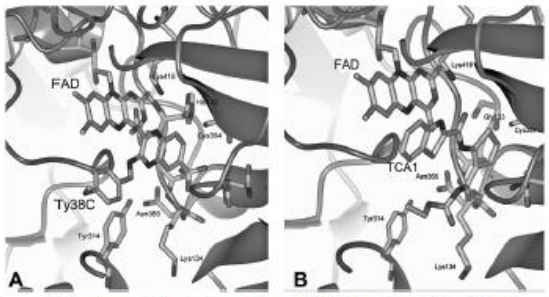

Fig (13). Details of the crystal structure of DprE1 in complex with Ty38C (A) and TCA1 (B) molecules (PDB:4P8K and 4KW5).

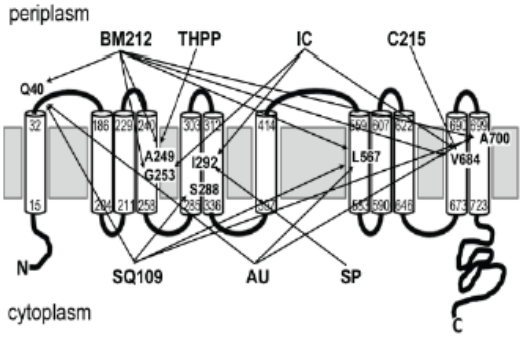

Fig. (14). Predicted topology of the MmpL3 protein and localization of the mutations responsible for the resistance to multiple inhibitors or to their analogs (IC indolecarboxamides, AU adamantyl ureas, SP spiroindenes).

visit this well-established drug [120]. Although designed to be an analog of EMB, SQ109 had a different mechanism of action, being also active against *M. tuberculosis* EMB-resistant strains [121]. SQ109 showed *in vitro* and *in vivo* efficacy, as well as a pharmacokinetic profile, better than EMB [121]. At present, SQ109 is in phase II clinical trial (http://www.newtbdrugs.org/pipeline.php) [122], despite its mechanism of action remained uncharacterized for several years.

The isolation of *M. tuberculosis* spontaneous SQ109 resistant mutants was in all cases unsuccessful. It was only by using less potent analogs of the compound that cross-resistant mutants could be isolated. The WGS of five of these isolated mutants revealed mutations in *mmpL3* gene (leading to Q40R, L567P and A700T mutations, Fig. **14**), indicating MmpL3 as the target. Moreover, concomitant biochemical studies demonstrated that SQ109 disrupts the cell wall assembly, leading to an intracellular accumulation of TMM, thus demonstrating the physiological function of the transporter [5]. Metabolic labelling studies and WGS of *M. tuberculosis* resistant mutants allowed identification of MmpL3 as the target of AU1235 and further confirmed its role in the export of TMM [118].

The high druggability of MmpL3 was demonstrated by a number of further unrelated inhibitors described within the following three years, such as the benzimidazole C215 [82], tetrahydropyrazolo[1,5-a]pyrimidine-3-carboxamides (THPP) [123], spiro compounds [123], indolcarboxamides [124, 125] and spiroindenes [126] (Fig. **15**). Many of them are active in TB mouse model of infection. MmpL3 mutations causing resistance to multiple compounds are numerous and widely distributed along the protein, demonstrating a large cross-resistance among MmpL3 inhibitors. Noteworthy, most of these mutations are present in residues within or near the transmembrane helices 4, 11 and 12, and close to those amino acids probably involved in the proton gradient necessary for the translocation activity of the pump [127].

The resistance levels conferred by these mutations are very different and in several cases quite low, such as 4- to 8-fold increase in MIC for SQ109 [5], up to 16-fold for BM212 [114, 115], 4- to 70 fold for THPP [123] or 8- to 70 fold for indolcarboxamides [124]. Moreover, SQ109, BM212 and THPP also showed activity against different pathogens lacking mycolic acids. However, being a lipophilic amine, SQ109 probably leads to membrane disruption and loss of membrane polarization, possibly causing nonspecific host cell toxicity. Finally, BM212, SQ109 and spiroindenes are active against non-replicant *M. tuberculosis*, differently from the other compounds targeting cell wall biosynthesis [128], suggesting for them a different mechanism of action [127, 129].

Recently, it has been recently shown that SQ109 and its analogs are multitargeting compounds [129]. In addition to Mmpl3, they also inhibit MenA and MenG, two enzymes involved in menaquinone biosynthesis. Moreover, these compounds were shown to act as uncoupler, thus interfering with the pH gradient (ΔpH) and membrane potential ($\Delta\psi$), thus collapsing the proton motive force (PMF) [129].

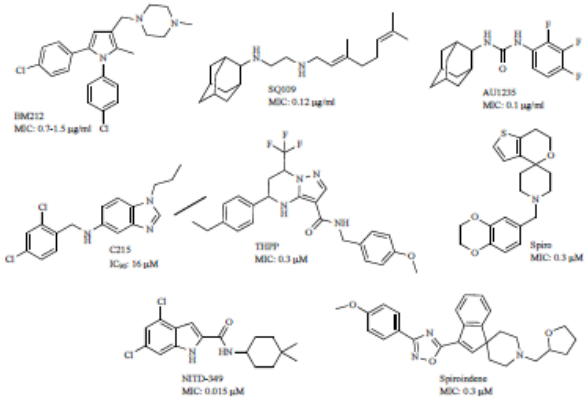

Fig. (15). MmpL3 inhibitor with antimycobacterial activity.

Recently, a series of SQ109 new analogues in which the ethylenediamine linker was replaced by oxa, thia, or heterocyclic species, was tested against different microorganisms including *M. tuberculosis* and *Trypanosoma brucei* [130]. Although none of the analogues showed improved potency against *M. tuberculosis*, they were demonstrated to affect both ΔpH and Δψ, targeting also the mitochondrial membrane potential of *T. brucei* [130]. These additional SQ109 activities explain why this compound is active against non-replicant *M. tuberculosis*, as well as against pathogens lacking mycolic acids. Moreover, the accumulation of TMM should be related to the dissipation of PMF, necessary for the activity of the MmpL pump. These details suggest that MmpL3 is only a secondary target of these compounds, accounting for the low level of resistance conferred by MmpL3 mutation to SQ109.

Further studies demonstrated that BM212, AU1235 and the indolecarboxamides behave as uncouplers, dissipating the PMF and having the same proposed mechanism of action [127]. Nevertheless, this finding seems to be in contradiction with the consistent isolation of spontaneous *M. tuberculosis* resistant mutants carrying mutation in MmpL3. The authors suggested that the MmpL3 mutations represent the first response to the compounds, in order to counteract its early toxic effects [127].

Considering these last results, the notion that these compounds target exclusively MmpL3 should be revisited, although a direct inhibition of MmpL3 cannot be completely excluded [127, 129].

4. NEW PROMISING DRUGGABLE TARGETS

Even though several drugs and targets are already available, the worldwide increase in resistance to the first and second-line TB drugs suggests that further drug targets are needed. Several efforts have now led to new potential antitubercular targets, which encompass different metabolism or processes, such as the biosynthesis of coenzyme A or of nucleotides, cellular division or energetic metabolism. A selection of these promising drug targets is here described.

4.1. Pantothenate Synthetase (PanC)

Pantothenate biosynthetic pathway is essential in prokaryotes, but absent in mammals, and it has been recognized as a promising drug target for the development of antimicrobials [131]. The biosynthesis of the essential precursor of coenzyme A is carried out by four enzymes, PanB and PanE, that realize the D-pantoate synthesis, PanD, that participates in the synthesis of β-alanine, and the pantothenate synthetase PanC [131]. The latter of these enzymes is essential for *M. tuberculosis* growth and has been extensively exploited in drug discovery.

The importance of the pantothenate biosynthetic pathway has been demonstrated in murine models where a pantothenate auxotroph of *M. tuberculosis*, defective in the *de novo* pantothenate synthesis, results in a significantly reduced pathogenicity, protecting mice from the infection [132]. This evidence suggests that pantothenic acid biosynthesis is a valuable drug

target, despite the existence of pantothenate salvage pathways. The growth of this auxotrophic strain was unimpaired *in vitro* when enough exogenous pantothenate was added in high amount, thus highlighting the need of using physiological concentration of metabolites in such screens [131]. Nevertheless, the phosphorylated intermediates of the CoA pathway and CoA itself cannot be utilized by most of the bacteria when supplied exogenously. This pathway is therefore likely to be essential not only for the viability of *M. tuberculosis* but also for that of many more bacteria [131]. Moreover, since this pathway is absent in mammals, PanC has been considered an attractive target for new antitubercular drug development [131].

The product of PanC, pantothenate, besides being a critical precursor of CoA, is also involved in the synthesis of the acyl carrier protein, essential for fatty acids synthesis, as well as for cell signaling, non-ribosomal peptides and polyketides synthesis [131]. PanC catalyzes a double-step reaction to condense D-pantoate with β-alanine in an ATP-dependent manner [133]: firstly, D-pantoate reacts with ATP forming a pantoyl-adenylate intermediate, with a consequent pyrophosphate release, then PanC catalyzes the ligation of β-alanine with the pantoyl-adenylate intermediate, thus forming AMP and panthotenate [133].

The crystal structure of the enzyme from *M. tuberculosis* has been solved, showing that PanC consists of two subunits, each of them made by two well-defined domains. The active site is positioned at the N-terminus of the protein, whilst the C-terminus partially masks the active site cavity [134]. Additionally, crystal structures of PanC in complex with AMPCPP, an ATP analog, with D-pantoate and with the reaction intermediate pantoyl-adenylate have been determined [134], allowing rational drug design approaches.

There are several strategies that could be used to identify PanC inhibitors [135]. Among them there are hit identification by high-throughput screening (HTS) [136], fragment-based approaches [137], energy-based pharmacophore modelling [138], Group Efficiency (GE) analysis [139] and synthesis of pantoyl-adenylate analogues, based on the knowledge of the strong interactions present between this intermediate and the enzyme active site [134].

In this context, the last strategy is the most frequently employed. However, despite the interest in PanC, no effective inhibitors of the *M. tuberculosis* enzyme have been obtained by rational design, and only weak inhibitors have been found by HTS [136, 140, 141]. The first effective PanC inhibitors reported (Ki 0.22 μM) are sulfamoyl adenylate derivatives (Fig. **16**). The crystal structure of PanC in complex with these compounds was solved, allowing elucidation of its binding mode mimicking the pantoyl-adenylate intermediate in the enzyme catalytic site (Fig. **17**) [140].

For this reason the sulfamoyl adenylate scaffold was considered a useful tool for the design of new inhibitors through rational design and fragment-based approaches. However, neither these compounds, nor their further derivatives are effective against *M. tuberculosis* growth [135].

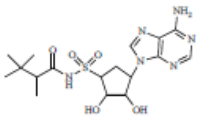

Fig. (16). Sulfamoyl adenylate derivative effective against PanC activity.

Based on the fact that a non-reactive pantoyl-adenylate analog could be an effective inhibitor, several compounds emerged from virtual HTS, molecular hybridization and rational design, such as 2-methylimidazo[1,2-*a*]pyridine-3-carboxamides [142], thiazolidine derivatives [133], tetrahydrothieno[2,3-*c*]pyridine-3-carboxamide [143], 3-biphenyl-4-cyano-pyrrole-2-carboxylic acids [144], 3-phenyl-4,5,6,7-tetrahydro-1*H*-pyrazolo[4,3-*c*]pyridine derivatives [145] (Fig. **18**). The majority of these compounds are not active against *M. tuberculosis* growth, even if some of them are effective against a *M. tuberculosis* strain with downregulated *panC* expression [144].

However, all these PanC inhibitors could serve as scaffolds for new inhibitors identification, in order to increase their potency and hopefully to improve their inhibitory effects against bacterial growth [144].

One explanation of the low or non-existent antimycobacterial activity of most of these compounds could be represented by the presence of several efflux systems in the bacteria that allow survival of the pathogen in the presence of several drugs. Based on this hypothesis, new hits inhibiting PanC have been characterized by firstly exploiting "energy-based pharmacophore modelling" strategy. The best among these derivatives was thiazolidine, with IC_{50} 0.35 μM and moderate activity against *M. tuberculosis* growth (MIC=1.55 μM) (Fig. **18**) [138]. It is noteworthy that the thiazolidines are considered promiscuous compounds, also known as Pan Assay Interference Compounds (PAINs), as they appear as frequent hitters in many biochemical high throughput screens [146, 147].

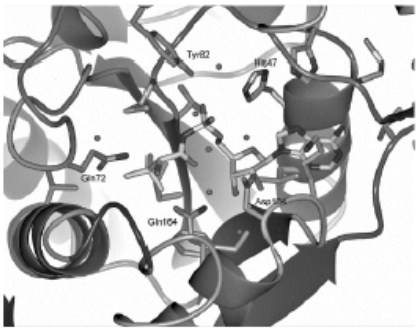

Fig. (17). Detail of the crystal structure of PanC showing the active site occupied by the sulfamoyl adenylate inhibitor (PDB: 3COW).

Afterward, the same compounds were assayed against *M. tuberculosis* growth in combination with known efflux pump inhibitors [138]. Almost all molecules increased the inhibitory power against *M. tuberculosis* growth, with a decrease of MIC values of two- to six-fold. Particularly, the best compounds of this series displayed an MIC of 0.38 μM, demonstrating that inhibition of efflux pumps significantly improves the efficacy of novel antitubercular compounds [138].

Very recently, interesting progress has been made by utilizing the Group Efficiency approach to improve already existing PanC inhibitors [148]. The purpose of this technique is to dissect these compounds to evaluate each single chemical group binding contribution, consequently introducing modifications in the molecules in order to improve binding efficiency. Through this approach, indole sulfonamide derivatives have been obtained (Fig. 18), not only active against *M. tuberculosis* PanC, but also having effects against bacterial growth [148].

Similarly, new imidazo[2,1-b]thiazole derivatives have been recently reported, showing moderate activity against growing and latent *M. tuberculosis*, and also active in a zebrafish model of *Mycobacterium marinum* infection [149].

In conclusion, despite the fact that no PanC inhibitors have been tested *in vivo* in mammalian models, PanC still remains an interesting target.

4.2. DNA Topoisomerase I (TopoI)

DNA topoisomerases are an essential class of enzymes whose role is to maintain topological homeostasis during a variety of DNA transaction processes such as replication, transcription, chromosome segregation and recombination [150, 151]. Topoisomerases are divided into two different groups, type I and type II, based on their structure and mechanism of action [152]. The type I group includes all those enzymes that cleave and rejoin only one strand of DNA. There is a further classification into type IA subfamily, if topoisomerases bind to a 5'-phosphate, and type IB subfamily, if topoisomerases bind to a 3'-phosphate. The type II group includes all those enzymes that cleave and rejoin both strands of DNA. Type II topoisomerases have been divided into type IIA and type IIB subfamilies on the base of the discovery of a novel type II enzyme from hyperthermophilic archeon *Sulfolobus shibatae*, representing the prototype of IIB subfamily [153]. The reaction catalyzed by topoisomerases includes the formation of a phosphotyrosine covalent adduct and a DNA single- or double-strand break during the two transesterification reactions [154].

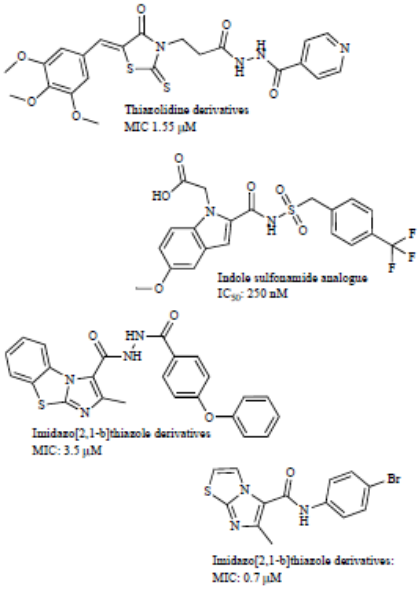

Fig. (18). PanC inhibitors showing good antimycobacterial activity.

Type I topoisomerases, responsible for relaxing negatively supercoiled DNA, are present in all bacteria

and belong to type IA subfamily [155, 156]. *M. tuberculosis*, differently from *E. coli* and other bacteria, possesses only one DNA type I topoisomerase, MttopoI, a protein of 934 amino acids encoded by *topA* gene (*Rv3646c*) [76].

Recently, the crystal structure of MttopoI was solved [157]. The structure of this enzyme is composed of two different parts: a core D1-D4, which contains all conserved motifs (Fig. 19) forming the active site of the protein, and a C-terminal end D5, which is the most variable in size and sequence among species. The D1 N-terminal end includes a TOPRIM (TOpoisomerase-PRIMase) domain, which harbors the metal ion Mg^{2+} coordination motif Asp-X-Asp-X-Glu, essential for the enzyme activity [158, 159], whilst the D5 has several residues though to interact with DNA.

Fig. (19). Crystal structure of Mttopo1 (PDB: 5D5H).

A new expression and purification protocol for *M. tuberculosis* DNA topoisomerase I [156] allowed a better characterization of the enzyme and the DNA cleavage by MttopoI has been characterized for the first time. Based on a careful comparison with *E.coli* DNA topoisomerase I (EctopoI), MttopoI has been shown to possess the same enzymatic efficiency of EctopoI in initial removal of negative supercoils, but the efficiency is lower in removing the remaining negative supercoils. The only specificity for the DNA cleavage sites of MttopoI is a C nucleotide in the -4 position, like most of the bacterial DNA topoisomerases I [156].

Because of its essentiality in many crucial biological pathways, MttopoI represents an ideal target for the discovery of novel antitubercular compounds, causing DNA lesions and cytotoxicity [159, 160]. The main inhibitors of *M. tuberculosis* DNA topoisomerase I are m-AMSA, imipramine, norclomipramine and hydroxycamptothecin (Fig. **20**) [150, 159, 161].

m-AMSA is an isomer of amsacrine (Fig. **20**), an acridine derivative able to act as a eukaryotic topoisomerase II poison, known for its potent anti-neoplastic activity [162]. m-AMSA was identified as a possible *M. tuberculosis* DNA topoisomerase I inhibitor through *in silico* screening which revealed a favorable docking score for this drug. Its inhibitory potential was evaluated against *M. tuberculosis*, *M. smegmatis* and *E. coli* DNA topoisomerase I [161]. The activity of MttopoI and MstopoI was completely inhibited at 10 μM, whilst the inhibition of EctopoI was between 10 and 25 μM. This result clearly indicated that the enzyme activity is inhibited in a concentration dependent manner and that m-AMSA is able to inhibit topoisomerase I of different bacteria, probably binding a region that is shared between the enzymes of different species. Furthermore, two crucial characteristics of the m-AMSA mechanism of action were understood: the first one is that the compound must interact either with the enzyme or the DNA before the formation of the topoI-DNA complex for inhibition of the reaction; otherwise its efficiency could be severely compromised. The second characteristic revealed that the intercalation of the drug to the DNA is required for its activity, like its mechanism of action against eukaryotic topoisomerase II [161]. Unfortunately, considering its powerful activity against eukaryotic topoisomerase II, m-AMSA cannot be introduced in *M. tuberculosis* therapy. However, these data represent a starting point to develop new molecules with a specific activity against mycobacterial topoisomerase I [161].

Imipramine and norclomipramine are two well-known compounds: the first one is clinically used as a tricyclic anti-depressant and the second one is the active metabolite of the tricyclic antidepressant clomipramine (Fig. **20**) [163, 164]. These compounds were identified as mycobacterial topoisomerase I inhibitors by *in silico* screening using a homology model of the enzyme. The inhibitory activities of both compounds were tested against DNA topoisomerase I from *M. tuberculosis*, *M. smegmatis* and *E. coli*. The DNA relaxation assay revealed a complete inhibition of MttopoI and MstopoI at 0.1 μM whilst there was no inhibition of EctopoI, clearly indicating that imipramine and norclomipramine are specific inhibitors of mycobacterial topoisomerase I [159].

To understand their mechanism of action, assays on individual steps of the DNA relaxation cycle of topoisomerase I were performed. Both imipramine and norclomipramine are able to bind the enzyme, the DNA or the enzyme-DNA complex, but their favorite target is the pre-formed enzyme-DNA complex. In particular, they interact with the TOPRIM domain of the enzyme near the Glu112 residue of the metal coordination motif. In addition, it was demonstrated that imipramine and norclomipramine act as cytotoxic agents inducing protein-mediated DNA breaks and affecting cell growth. Finally, it was shown that it is possible to combine the use of imipramine and moxifloxacin, a mycobacterial gyrase inhibitor. This latter discovery is a desirable result considering the alarming spread of *M. tuberculosis* resistant strains [159].

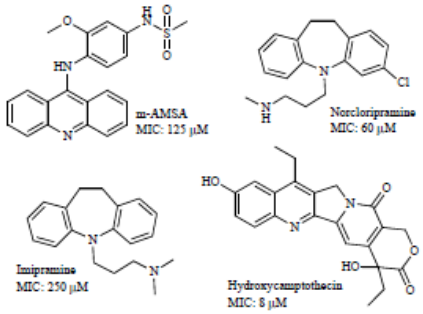

Fig. (20). Principal antitubercular MttopoI inhibitors.

The screening of a chemical library, in which also amsacrine was included, led to the selection of hydroxycamptothecin (Fig. **20**). This compound showed the best inhibitory activity with an IC_{50} of 6.25 μM. Docking study of hydroxycamptothecin suggested some important details about its structure and interaction with MttopoI, where the hydroxyl group of the compound is facing towards the opening of the active site. At this site, the residues Ala41, Pro181, Trp184 and Ala193 are involved in hydrophobic interaction with the compound, whilst the residues Asp113 and Ser495 interact with the compound for the hydrogen bonding [150].

According to these studies and considering its non-cytotoxicity, hydroxycamptothecin was derivatized substituting the terminal hydroxyl group with different hydrophobic moieties, in order to understand the influence of these elements in the compound activity. The best compound, harboring a nitro-benzyl substituent, was very active also against XDR and non-replicating *M. tuberculosis* and, being also active in an *in vivo* zebrafish model of *M. marinum* infection, it represents the most promising MttopoI inhibitor for the development of antitubercular drugs.

4.3. Cytochrome bc_1 Complex – QcrB

Cytochrome bc_1 complex, or ubihydroquinone-cytochrome *c* oxidoreductase, is an energy-transducing enzyme playing an essential role in the energy conversion machinery of respiratory and photosynthetic electron transfer chains [165, 166]. In bacteria, this multisubunit complex is located in the plasma membrane and it oxidizes a membrane-located quinol, reducing a *c*-type cytochrome and promoting the translocation of protons across the membrane [165, 166]. This mechanism is known as Q cycle and it contributes to the proton motive force used for ATP synthase [167]. The catalytic core of the complex is composed by three redox-active subunits: cytochrome *b* (*cyt b*), which has two cofactors heme b_H and b_L and two reactive sites named the ubiquinol oxidation (Q_P) and the ubiquinone reduction (Q_N) sites, cytochrome c_1 (*cyt c1*) which has the cofactor heme c_L and the Rieske iron-sulfur protein (ISP), which contains a [2Fe–2S] cluster [165].

An increasing number of studies have confirmed the importance of cytochrome bc_1 complex for mycobacterial growth, thus providing a novel and excellent opportunity to target *M. tuberculosis* [168, 169]. Among the main inhibitors of cytochrome *b* (QcrB) of bc_1 complex, there are the class of imidazo [1,2-*a*] pyridines (IP), Q203 and Lansoprazole (LPZ) [169-171].

The imidazo [1,2-*a*] pyridines (IP) compounds (Fig. **21**) were identified as a potent class of inhibitors of *M. tuberculosis* subunit *b* of cytochrome bc_1 complex. All of them are active against *M. tuberculosis* growth and are non-cytotoxic antitubercular compounds. Two of them showed metabolic stability both *in vitro* and in murine pharmacokinetic model, one of them revealed a bacteriostatic behavior in *in vivo* models. QcrB was identified as the cellular target of IP compounds by WGS of resistant mutants and by the over-expression of *qcrB* gene [170].

Q203 compound is an imidazopyridine amide (IPA) derivative (Fig. **21**) [171] synthesized in one sequential amide-coupling step with an imidazopyridine acid and as piperidinobenzyl amine. This method allows a large-scale synthesis and low production costs, a feature that is a considerable advantage since *M. tuberculosis* mainly affects people in poor countries [171]. The compound efficacy is enhanced by the introduction of a

long hydrophobic group linked to the carboxamide group [171].

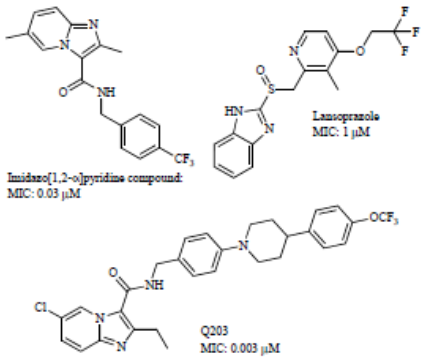

Fig. (21). Cytochrome *bc1* complex inhibitors.

Q203 is very effective against *M. tuberculosis* growth (MIC_{50} = 2.7 nM in culture broth medium and MIC_{50} = 0.28 nM inside macrophages) and is efficient against MDR and XDR clinical isolates. The compound showed also a good safety profile, it was well tolerated at long prolonged exposure level in murine mice and showed a low risk for drug-drug interactions [171]. Pharmacokinetic studies revealed that Q203 has a slow mechanism of action compared to other antitubercular drugs like isoniazid, but it has a bioavailability of 90%, a terminal half-life of 23.4 h and it reduces the formation of granulomatous lesions [171]. QcrB was identified as the cellular target of Q203 by WGS of spontaneous-resistant mutants and, specifically, Q203 hits the ubiquinol Q_P site of the *cyt b* subunit. It has been observed that the compound is able to quickly inhibit ATP synthesis at low concentrations, thus giving further proof that the inhibition of bc_1 complex activity is the main mechanism of action of Q203. All these data suggest that Q203 is a promising antitubercular compound and that, affecting mycobacterial energy metabolism at low doses, it could probably shorten tuberculosis therapy [171].

Recently, an innovative host cell-based high-throughput screen has been developed to select compounds that protect MRC-5 lung fibroblasts from *M. tuberculosis* cytotoxicity. In this way, lansoprazole (LPZ) (Fig. **21**), a gastric proton-pump (H+K+ -ATPase) inhibitor (PPI), has been identified as an antitubercular compound able to protect fibroblasts [169].

In *M. tuberculosis*, Lansoprazole sulfide (LPZS) was identified as the stable and active metabolite of LPZ [169]. LPZS active metabolite was very active against *M. tuberculosis* growth and also against resistant strains but, unfortunately, it showed additive effects when tested in combination with some first- and second-line anti-TB drugs (rifampicin, isoniazid, moxifloxacin, bedaquiline and BTZ043). Finally, as observed for Q203 compound, LPZS inhibits simultaneously QcrB activity, binding at the ubiquinol Q_P site, and the ATP synthesis. LPZ represents a great example of a new activity found for an old drug using an innovative screen [169].

IP, Q203 and LPZ are promising antitubercular compounds and, considering the essentiality of QcrB target, it is possible that they could be active against both replicating and non-replicating *M. tuberculosis*, an important feature for future anti-tubercular drugs.

4.4. ATP Synthase

Bacterial ATP synthase is an ubiquitous enzyme involved in energy metabolism: it utilizes the electrochemical transmembrane ion gradient (H^+ or Na^+) for production of ATP, to satisfy cell demand [172]. It is a macromolecular, membrane-embedded protein complex also known as F_1F_0-ATPase, where F_1 and F_0 represent the hydrophilic and the membrane domain, respectively (Fig. **22**). F_0 domain consists of the subunits $\alpha_1\beta_2\gamma_{10-15}$, whilst the F1 domain is composed in subunits $\alpha_3\beta_3\gamma\delta\varepsilon$, building a structural connection between the two F_0-F_1 domains that is crucial for their functional coupling (Fig. **22**) [173-175].

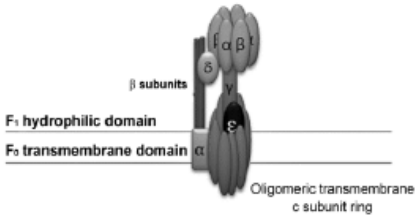

Fig. (22). F_0 and F_1 domains of ATP-synthase and their subunits composition.

Effectively, the oligomeric c-subunit ring of the F_0 domain will rotate when protons flow through this membrane-embedded sector. This is in turn linked to rotation of the c subunit within the $(\alpha\beta)_3$ hexamer of the F_1 domain, leading to the conversion of adenosine diphosphate (ADP) and inorganic phosphate (P_i) into

adenosine triphosphate (ATP) [173-175]. Pathogenic bacteria such as *M. tuberculosis* can reside into the human host for many years, entering a so-called dormant state, which renders this mycobacterium poorly susceptible to most of the currently used antibacterials [176-178]. ATP synthase in bacteria such as *M. tuberculosis* is responsible for facilitating survival under particular conditions found into the human host, *e.g.* low oxygen tensions and/or nutrient limitation [179]. ATP synthase is reported to be essential in *M. tuberculosis* for optimal growth and in the non-pathogenic model strain *M. smegmatis*. ATP synthase activity is completely blocked by the diarylquinoline class of drugs [6, 180-182]. Among the antitubercular compounds belonging to this chemical class, the bedaquiline TMC207 (or R207910) is a promising agent in the fight against TB, directly targeting the rotor ring of the *M. tuberculosis* ATP synthase [6, 183, 184]. Bedaquiline has two chiral centers leading to four stereoisomers, where the R207910 (R,S) stereoisomer (Fig. **23**) is the most active, with minimal concentration required to inhibit 90% of *M. tuberculosis* isolates (MIC_{90}) of 0.06 μg/ml, and with a strong affinity to the c-subunit of the *M. tuberculosis* ATP synthase [181, 185].

Bedaquiline has been proposed to bind in the c-subunit transmembrane region of the *M. tuberculosis* ATP synthase [6, 185]. The c-ring from the nonpathogenic *Mycobacterium phlei* shares 83.7% of sequence identity with its *M. tuberculosis* homolog and displays MIC values very close to that of *M. tuberculosis* (0.05 μg/ml and 0.06 μg/ml, respectively). For these reasons a quite identical mode of interaction between the drug and the rotor ring of these two species has been suggested, and the *M. phlei* c-ring has been thus selected as a model system and co-crystallized with Bedaquiline [6, 184-186]. The ATP synthase c-ring has a membrane-exposed ion-binding site, in which the Bedaquiline molecule can be accommodated upon conformational changes of Phe69, which provides a hydrophobic space for the drug. Several specific molecular interactions will then be formed thanks to changes in the conformation of Bedaquiline itself; one example is an ionic intermolecular H-bond between the dimethyl amino (DMA) moiety group and Glu65 (**Fig. 24**). This Glu65-DMA conformation blocks the c-ring rotation and, consequently, ion exchange in F_0, resulting in halting ATP synthesis and causing subsequent mycobacterial death [184, 187-191]. According to this mechanism, the binding of one single Bedaquiline molecule is enough to completely stop ATP synthesis [184].

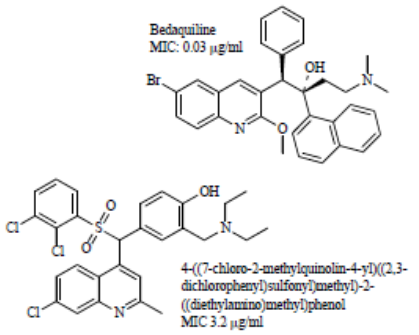

Fig. (23). Most effective *M. tuberculosis* ATP-synthase inhibitors.

Bedaquiline has been approved by the U.S Food and Drug Administration for the treatment of both drug-sensitive and drug-resistant TB, but with a specific attention for the treatment of multidrug-resistant TB (http://www.fda.gov/NewsEvents/Newsroom/PressAnnouncements/ucm333695.htm). Clinical tests confirmed that, in patients receiving the diarylquinoline bedaquiline, sputum cultures turned from positive to negative. Likewise, bacterial clearance occurred earlier in those patients receiving bedaquiline in combination with the first-line antibiotic pyrazinamide, thus shortening the treatment of patients with MDR-TB [192-194]. Diarylquinolines are characterized by a dual bactericidal activity, being able to inhibit both replicating and dormant *M. tuberculosis* bacilli. This unique feature distinguishes this class of drugs from all the presently used antituberculars, such as INH and RIF [192]. Moreover, they display bactericidal activity outreaching the effects of actual first-line antitubercular antibiotics, as demonstrated by *in vivo* experiments in mouse models [192] [6].

Although bedaquiline has remarkable potential for shortening the tuberculosis therapy duration, several side effects such as nausea, chest pain and/or headache have been observed, thus suggesting further chemical exploration of new ATP synthase inhibitors without any possible adverse effect [7].

Taking advantage of the diarylquinolines structure, novel quinoline derivatives with significant *in vitro* bactericidal activity on *M. tuberculosis* have been synthesized [195, 196]. Several efforts led to the development of even more potent, orally bioavailable and ATP synthase inhibitors; the quinolone class of arylsulfonamides compounds [197]. SAR studies identified

low micromolar F_0F_1-inhibitors of the *M. smegmatis* ATP synthase with IC_{50} values ranging from 0.36 to 5.45 μM. Among these, the s di-chlorophenyl sulfonyl compound (Fig. **23**) displayed IC_{50} value of 0.51 μM and led to promising results in mice infected with *M. tuberculosis* H37Rv [197]. The binding mode of the compound at the active site of homology modeled *M. tuberculosis* ATP synthase revealed H-bonds formation similar to that of bedaquiline [197]. The *in vivo* efficacy of this compound doubled that of ethambutol, and its activity against both replicating and dormant *M. tuberculosis* bacilli is comparable to that of bedaquiline [197]. For these reasons, this lead compound is considered a candidate molecule for deeper preclinical investigations.

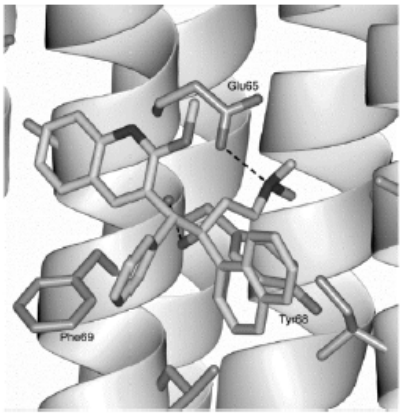

Fig. (24). Bend view of the c-ring ion-binding side showing the interaction of bedaquiline with Phe69 and Glu65 (PDB-Id: 4V1F).

4.5. FtsZ

Filament-forming temperature-sensitive genes "Fts" were identified in 1960 in *E. coli* as genes encoding for proteins involved in septum formation [198]. The bacterial cell division machinery remained unexplored for therapeutic purposes for several years, and it was only in 1991 that the FtsZ protein was discovered to be involved in the initiation of cell division [199, 200]. When GTP is present, FtsZ proteins cooperatively polymerize on the inner membrane at the center of the cell, growing bidirectionally and stacking in a head to tail fashion, with GTP located between two FtsZ subunits, thus forming a highly dynamic helical structure called the "Z-ring". Moreover, a link between GTP hydrolysis and polymerization dynamics was first shown when the formation of FtsZ polymers in solution was found to be coupled with GTP hydrolysis, since polymer loss co-occurred with GTP depletion [201, 202]. FtsZ was shown to form straight filaments when bound to GTP, while FtsZ bound to GDP forms highly curved filaments [203]. This transition from straight filaments to curved conformation suggests that GTP hydrolysis provide the energy for generating the mechanical force for cell division [203]. Other cell division proteins are then recruited, causing Z-ring contraction, septum formation and eventually cell division [204-208].

With FtsZ inactive, septum formation is impaired (Fig. **25**). Accordingly, FtsZ represents a very promising target for new antitubercular drug discovery because of its known biochemical activity and its central role in cell division [199]. Being a novel drug target, new compounds targeting FtsZ would not be affected by already known drug-resistance mechanisms caused by the use of current anti-TB drugs [209].

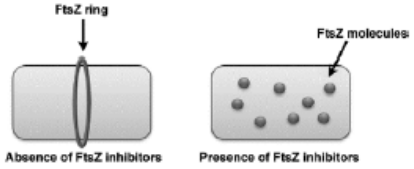

Fig. (25). Z-ring formation is impaired in the presence of FtsZ inhibitors.

The identification of the short amino acid sequence GGGTGTG from the crystal structure of the *Methanococcus jannaschii* FtsZ leads to the identification of FtsZ as a homologue of tubulin, being virtually identical to the motif sequence, (G/A)GGTGSG, found in all α-, β- and γ-tubulins [210].

Although sequence similarity is limited to 10%, FtsZ and tubulin share a common fold made up of two domains linked by a α-helix [211, 212]. Both tubulin and FtsZ polymerize in the presence of GTP into protofilaments while depolymerizing following GTP hydrolysis [206]. GTP hydrolysis represents the major rate-limiting step, and phosphate release rapidly follows. Polymers bound to GDP tend to curve, leading to constriction of the Z ring in cell division. GDP release from the polymer might be partially rate limiting. Depolymerization and GDP release then occurr, followed by nucleotide exchange in the monomers [213, 214].

Structural and functional homology suggests that drugs affecting the assembly of tubulin into microtubules can be used as lead targeting FtsZ assembly. Furthermore, the very low sequence homology at the protein level gives the opportunity to investigate drugs that are FtsZ specific with limited cytotoxicity to eukaryotic cells [208].

FtsZ protein from *M. tuberculosis* (MtbFtsZ) crystallized as a tightly associated dimer in solution, with the A and B subunits associated to form an arc-shaped dimer (Fig. **26**) [215-217]. The GTPase domain is located in the N-terminal domain, which is connected to the C-terminal αβ-domain by a central helix H10. The structures of the two subunits are quite identical, except for an unexpected secondary structural switch at the subunit interface: in subunit A, the H2 helix adopts a α-helical conformation, whilst the H2 helix of subunit B assumes a β-strand conformation instead. This secondary structural switch is located in the GTPase domain, forming most of the dimer interface [206].

FtsZ is pathogen specific, essential and highly conserved in prokaryotes, thus potential FtsZ inhibitors may be developed as broad-spectrum antibacterial agents to which acquiring resistance by mutations in the protein may be demanding for bacteria [218, 219]. Drug development is still at an early stage, nevertheless several classes of compounds have been already found effective against *M. tuberculosis* FtsZ, some of these being classified as promising leads.

Several benzimidazole, pyridopyrazine and pteridine based FtsZ inhibitors have been screened and identified as potential powerful antituberculars [209, 216, 220-224]. Other reported antitubercular agents are benzimidazole derivatives, responsible for a delay in the *M. tuberculosis* cell division process, but very little is known so far (Fig. **27**) [225].

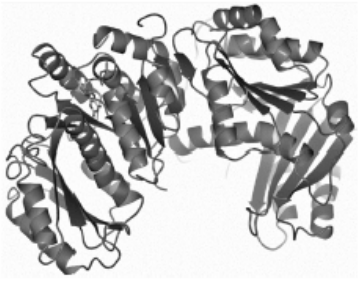

Fig. (26). Crystal structure of *M. tuberculosis* FtsZ in complex with GDP (PDB:1RQ7).

Zantrin Z3 (Fig. **27**) was discovered through a high-throughput screening of inhibitors of the GTPase activity of FtsZ. It was shown to be uniquely active and selective in its inhibition of FtsZ when compared to other molecules. It has no offending electrophilic or phenolic functionality and is the best in terms of overall performance against the protein from multiple species of bacteria under a variety of conditions. Ideally, SAR studies will allow identification of a compound with significantly better inhibition for both cell-based studies and crystallography [226]. Recent SAR studies showed that the introduction of a smaller quinazoline ring, instead of the benzo[*g*]quinozaline, retains the potency of the compound, whilst the incorporation of a small and positively charged side chain improved activity [227].

Taking into account the structural similarity of the pyridopyrazine moiety, pteridine moiety, albendazole, and thiabendazole, it has been hypothesized that the benzimidazole scaffold would be a good starting point for the development of novel FtsZ inhibitors, with good activity against both drug-sensitive and drug-resistant *M. tuberculosis* strains [228]. Specifically, the activity of benzimidazole derivatives (Fig. **27**) against *M. tuberculosis* clinical strains has been reported [225]. Docking, synthesis, structure elucidations, *in vitro* antitubercular activity and cytotoxicity assay against VERO cells of benzimidazole derivatives led to compounds with good *in vitro* antitubercular activity [225]. The potency, selectivity and low cytotoxicity of these compounds make them valid leads for improved antitubercular developments [225].

However, investigations of the benzamide family molecules led to the development of PC190723 (Fig. **27**) [229], which was the first non-nucleotide inhibitor to be co-crystallized with FtsZ [230]. This compound activates the GTPase activity and alters the cooperativity of the FtsZ monomers, as demonstrated by crystallographic studies. Being also active *in vivo*, PC190723 is considered the best inhibitor of FtsZ to date, although actually limited to *Staphylococcus aureus*.

4.6. CTP Synthetase (PyrG)

The biosynthetic and salvage pathways of pyrimidines represent a central point of interest in terms of antitubercular drug development [231]. Among the enzymes involved in this pathway, the CTP synthase is the most intriguing, being recognized as a target of antibacterial [232] and antiprotozoal agents [233, 234] and, recently, of antimycobacterial compounds [235].

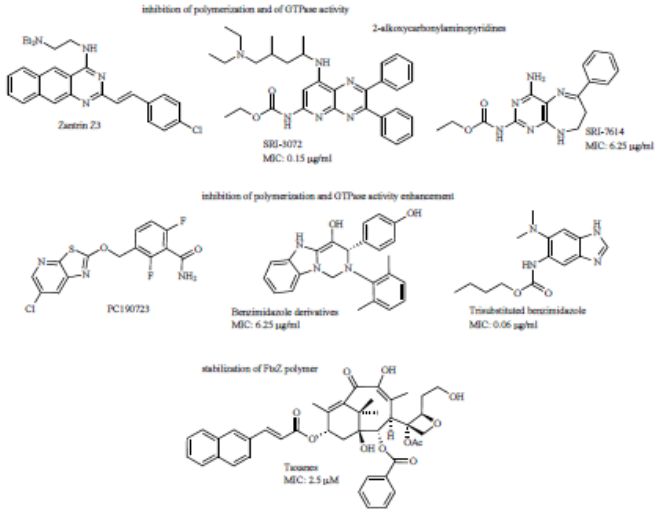

Fig. (27). FtsZ inhibitors divided by their mechanism of action.

The mycobacterial CTP synthetase PyrG is an essential enzyme that catalyzes the production of CTP starting from UTP and glutamine in an ATP-dependent manner. It represents a key player for several biological processes, such as DNA, RNA and phospholipids biosynthesis [236]. The crystal structure of *M. tuberculosis* PyrG has been recently solved on a 2.0-A resolution data set, highlighting the presence of two domains that organize in a tetramer: a synthetase domain located at the N-terminus, and a glutamine amidotransferase domain located at the C-terminus [235].

Through whole cell screening of a 594 compounds chemical library, two *M. tuberculosis* PyrG inhibitors, named 7947882 and 7904688 (Fig. **28**) have been identified. These inhibitors are both prodrugs intracellularly activated by FAD-dependent monooxygenase EthA. The EthA mechanism of activation of these compounds has been defined and was similar to that performed for ETH activation (Fig. **29**). The active S-dioxide metabolite of 7947882 has been synthetized (11426026 compound) and demonstrated to be a competitive inhibitor towards ATP (Ki 10 μM) [235].

This behavior was in accordance with the position of the residues mutated in the resistant mutant, located in the proximity of the ATP-binding site of the enzyme.

Metabolomic studies revealed that, by blocking PyrG, the nucleotide metabolism is significantly damaged, thus confirming its central role in several cellular processes where nucleotides are involved, as well as its strong potentiality as cellular target for new antitubercolars [235].

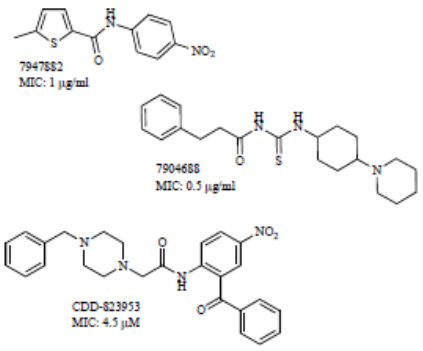

Fig. (28). *M. tuberculosis* PyrG inhibitors.

Afterwards, the virtual screening on PyrG of the Collaborative Drug Discovery (CDD) compounds database identified further compounds, with already

known antitubercular activity, which could likely bind PyrG. Four compounds with high docking score have been identified, and one of them, the CDD-823953, resulted to be active against PyrG activity *in vitro* (Ki of 88.9 μM) [235].

Although the CDD-823953 is a weak PyrG inhibitor, it remains a new antitubercular, not correlated with the previous ones, that inhibits PyrG enzyme activity. All these results suggest that PyrG is a good target for new antitubercular compounds. Identification of inhibitors of CTP-synthetase from other organisms [232-234] makes PyrG a very promising target. Consequently, it could be useful to utilize *M. tuberculosis* PyrG enzyme to screen several other chemical libraries of compound having known antitubercular activity, in order to find new potential compounds for antitubercular treatments.

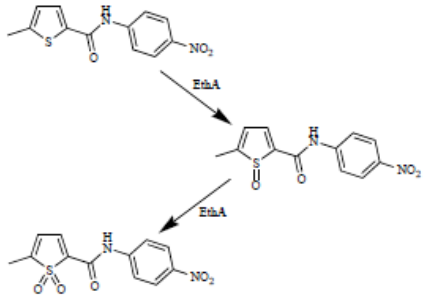

Fig. (29). Mechanism of EthA mediated activation of 7947882 compound.

CONCLUSION

There has been considerable progress in the discovery of new lead compounds for treating tuberculosis.

Among the newly identified antitubercular compounds, several derivatives have been synthetized starting from already known inhibitors of old repurposed targets such as DNA gyrase and RNA polymerase.

A target-based approach can be a faster and more efficient method for drug identification compared to the traditional *de novo* drug-discovery. However, antitubercular compounds often show limited efficacy against *M. tuberculosis*, because of its thick cell wall and its efflux systems, but biochemistry and structural biology are now promoting new drug and target discoveries. For these reasons phenotypic HTS for the identification of scaffolds, followed by target identification and then optimization against the target, remains the best strategy to fight this pathogen.

Clearly, the growing reports of MDR-TB and XDR-TB strains is pointing out the acute need for new cellular targets. Nevertheless, some of the newly identified inhibitors are considered good candidates and have now entered clinical trials. PBTZ169 is one of the most effective inhibitors against the DprE1 promiscuous target and it is planned to enter human clinical trials in 2016. Phenotypic screening has allowed the characterization of new potential drug targets, highlighting the importance and essentiality of some processes, such as coenzyme A biosynthesis, nucleotide biosynthesis, cellular division and energy metabolism. Although the current situation of lead generation against TB has improved in recent years, it is still too slow and extremely wanting in success. Relevant changes are needed in order to shorten TB treatment duration and to produce novel regimens with higher efficacy against drug-resistant TB.

CONFLICT OF INTEREST

The authors confirm that this article content has no conflicts of interest.

ACKNOWLEDGEMENTS

All individuals listed as authors have contributed substantially to the collections and discussions of the reported published work. This work was supported by European Community's Seventh Framework Program (Grant 260872) and "Universitiamo – Tubercolosi: un killer riemergente" (University of Pavia, Italy).

REFERENCES

[1] WHO. W.H.O., Global tuberculosis report. **2015**.
[2] Dheda, K.; Barry, C.E.; Maartens, G. Tuberculosis. *Lancet,* **2015**.
[3] Makarov, V.; Lechartier, B.; Zhang, M.; Neres, J.; van der Sar, A.M.; Raadsen, S.A.; Hartkoorn, R.C.; Ryabova, O.B.; Vocat, A.; Decosterd, L.A.; Widmer, N.; Buclin, T.; Bitter, W.; Andries, K.; Pojer, F.; Dyson, P.J.; Cole, S.T. Towards a new combination therapy for tuberculosis with next generation benzothiazinones. *EMBO Mol. Med.,* **2014**, *6*(3), 372-383.
[4] Makarov, V.; Manina, G.; Mikusova, K.; Möllmann, U.; Ryabova, O.; Saint-Joanis, B.; Dhar, N.; Pasca, M.R.; Buroni, S.; Lucarelli, A.P.; Milano, A.; De Rossi, E.; Belanova, M.; Bobovska, A.; Dianiskova, P.; Kordulakova, J.; Sala, C.; Fullam, E.; Schneider, P.; McKinney, J.D.; Brodin, P.; Christophe, T.; Waddell, S.; Butcher, P.; Albrethsen, J.; Rosenkrands, I.; Brosch, R.; Nandi, V.; Bharath, S.; Gaonkar, S.; Shandil, R.K.; Balasubramanian, V.; Balganesh, T.; Tyagi, S.; Grosset, J.; Riccardi, G.; Cole, S.T. Benzothiazinones kill *Mycobacterium tuberculosis* by blocking arabinan synthesis. *Science,* **2009**, *324*(5928), 801-804.
[5] Tahlan, K.; Wilson, R.; Kastrinsky, D.B.; Arora, K.; Nair, V.; Fischer, E.; Barnes, S.W.; Walker, J.R.; Alland, D.;

Barry, C.E., III; Boshoff, H.I. SQ109 targets MmpL3, a membrane transporter of trehalose monomycolate involved in mycolic acid donation to the cell wall core of *Mycobacterium tuberculosis*. *Antimicrob. Agents Chemother.*, **2012**, *56*(4), 1797-1809.

[6] Andries, K.; Verhasselt, P.; Guillemont, J.; Göhlmann, H.W.; Neefs, J.M.; Winkler, H.; Van Gestel, J.; Timmerman, P.; Zhu, M.; Lee, E.; Williams, P.; de Chaffoy, D.; Huitric, E.; Hoffner, S.; Cambau, E.; Truffot-Pernot, C.; Lounis, N.; Jarlier, V. A diarylquinoline drug active on the ATP synthase of *Mycobacterium tuberculosis*. *Science*, **2005**, *307*(5707), 223-227.

[7] Kakkar, A.K.; Dahiya, N. Bedaquiline for the treatment of resistant tuberculosis: promises and pitfalls. *Tuberculosis (Edinb.)*, **2014**, *94*(4), 357-362.

[8] Worley, M.V.; Estrada, S.J. Bedaquiline: a novel antituberculosis agent for the treatment of multidrug-resistant tuberculosis. *Pharmacotherapy*, **2014**, *34*(11), 1187-1197.

[9] Sotgiu, G.; Pontali, E.; Centis, R.; D'Ambrosio, L.; Migliori, G.B. Delamanid (OPC-67683) for treatment of multi-drug-resistant tuberculosis. *Expert Rev. Anti Infect. Ther.*, **2015**, *13*(3), 305-315.

[10] Harausz, E.; Cox, H.; Rich, M.; Mitnick, C.D.; Zimetbaum, P.; Furin, J. QTc prolongation and treatment of multidrug-resistant tuberculosis. *Int. J. Tuberc. Lung Dis.*, **2015**, *19*(4), 385-391.

[11] Bloemberg, G.V.; Keller, P.M.; Stucki, D.; Trauner, A.; Borrell, S.; Latshang, T.; Coscolla, M.; Rothe, T.; Hömke, R.; Ritter, C.; Feldmann, J.; Schulthess, B.; Gagneux, S.; Böttger, E.C.; Böttger, E.C. Acquired Resistance to Bedaquiline and Delamanid in Therapy for Tuberculosis. *N. Engl. J. Med.*, **2015**, *373*(20), 1986-1988.

[12] Vilchèze, C.; Jacobs, W.R., Jr The mechanism of isoniazid killing: clarity through the scope of genetics. *Annu. Rev. Microbiol.*, **2007**, *61*, 35-50.

[13] Campbell, E.A.; Korzheva, N.; Mustaev, A.; Murakami, K.; Nair, S.; Goldfarb, A.; Darst, S.A. Structural mechanism for rifampicin inhibition of bacterial rna polymerase. *Cell*, **2001**, *104*(6), 901-912.

[14] Ginsburg, A.S.; Grosset, J.H.; Bishai, W.R. Fluoroquinolones, tuberculosis, and resistance. *Lancet Infect. Dis.*, **2003**, *3*(7), 432-442.

[15] Banerjee, A.; Dubnau, E.; Quemard, A.; Balasubramanian, V.; Um, K.S.; Wilson, T.; Collins, D.; de Lisle, G.; Jacobs, W.R., Jr inhA, a gene encoding a target for isoniazid and ethionamide in *Mycobacterium tuberculosis*. *Science*, **1994**, *263*(5144), 227-230.

[16] Vilchèze, C.; Jacobs, W.R. Resistance to Isoniazid and Ethionamide in Mycobacterium tuberculosis: Genes, Mutations, and Causalities *Microbiol. Spectr.*, **2014**, *2*(4) MGM2-0014-2013

[17] Lei, B.; Wei, C.J.; Tu, S.C. Action mechanism of antituberculosis isoniazid. Activation by *Mycobacterium tuberculosis* KatG, isolation, and characterization of inha inhibitor. *J. Biol. Chem.*, **2000**, *275*(4), 2520-2526.

[18] Rozwarski, D.A.; Grant, G.A.; Barton, D.H.; Jacobs, W.R., Jr; Sacchettini, J.C. Modification of the NADH of the isoniazid target (InhA) from *Mycobacterium tuberculosis*. *Science*, **1998**, *279*(5347), 98-102.

[19] Dessen, A.; Quémard, A.; Blanchard, J.S.; Jacobs, W.R., Jr; Sacchettini, J.C. Crystal structure and function of the isoniazid target of *Mycobacterium tuberculosis*. *Science*, **1995**, *267*(5204), 1638-1641.

[20] Baulard, A.R.; Betts, J.C.; Engohang-Ndong, J.; Quan, S.; McAdam, R.A.; Brennan, P.J.; Locht, C.; Besra, G.S. Activation of the pro-drug ethionamide is regulated in mycobacteria. *J. Biol. Chem.*, **2000**, *275*(36), 28326-28331.

[21] Vannelli, T.A.; Dykman, A.; Ortiz de Montellano, P.R. The antituberculosis drug ethionamide is activated by a flavoprotein monooxygenase. *J. Biol. Chem.*, **2002**, *277*(15), 12824-12829.

[22] DeBarber, A.E.; Mdluli, K.; Bosman, M.; Bekker, L.G.; Barry, C.E., III Ethionamide activation and sensitivity in multidrug-resistant *Mycobacterium tuberculosis*. *Proc. Natl. Acad. Sci. USA*, **2000**, *97*(17), 9677-9682.

[23] Parikh, S.L.; Xiao, G.; Tonge, P.J. Inhibition of InhA, the enoyl reductase from Mycobacterium tuberculosis, by triclosan and isoniazid. *Biochemistry*, **2000**, *39*(26), 7645-7650.

[24] Menendez, C.; Gau, S.; Lherbet, C.; Rodriguez, F.; Inard, C.; Pasca, M.R.; Baltas, M. Synthesis and biological activities of triazole derivatives as inhibitors of InhA and antituberculosis agents. *Eur. J. Med. Chem.*, **2011**, *46*(11), 5524-5531.

[25] Menendez, C.; Chollet, A.; Rodriguez, F.; Inard, C.; Pasca, M.R.; Lherbet, C.; Baltas, M. Chemical synthesis and biological evaluation of triazole derivatives as inhibitors of InhA and antituberculosis agents. *Eur. J. Med. Chem.*, **2012**, *52*, 275-283.

[26] Stec, J.; Vilchèze, C.; Lun, S.; Perryman, A.L.; Wang, X.; Freundlich, J.S.; Bishai, W.; Jacobs, W.R., Jr; Kozikowski, A.P. Biological evaluation of potent triclosan-derived inhibitors of the enoyl-acyl carrier protein reductase InhA in drug-sensitive and drug-resistant strains of *Mycobacterium tuberculosis*. *ChemMedChem*, **2014**, *9*(11), 2528-2537.

[27] Hartkoorn, R.C.; Sala, C.; Neres, J.; Pojer, F.; Magnet, S.; Mukherjee, R.; Uplekar, S.; Boy-Röttger, S.; Altmann, K.H.; Cole, S.T. Towards a new tuberculosis drug: pyridomycin - nature's isoniazid. *EMBO Mol. Med.*, **2012**, *4*(10), 1032-1042.

[28] Horlacher, O.P.; Hartkoorn, R.C.; Cole, S.T.; Altmann, K.H. Synthesis and antimycobacterial activity of 2,1'-dihydropyridomycins. *ACS Med. Chem. Lett.*, **2013**, *4*(2), 264-268.

[29] Matviiuk, T.; Rodriguez, F.; Saffon, N.; Mallet-Ladeira, S.; Gorichko, M.; de Jesus Lopes Ribeiro, A.L.; Pasca, M.R.; Lherbet, C.; Voitenko, Z.; Baltas, M. Design, chemical synthesis of 3-(9H-fluoren-9-yl)pyrrolidine-2,5-dione derivatives and biological activity against enoyl-ACP reductase (InhA) and *Mycobacterium tuberculosis*. *Eur. J. Med. Chem.*, **2013**, *70*, 37-48.

[30] Shirude, P.S.; Madhavapeddi, P.; Naik, M.; Murugan, K.; Shinde, V.; Nandishaiah, R.; Bhat, J.; Kumar, A.; Hameed, S.; Holdgate, G.; Davies, G.; McMiken, H.; Hegde, N.; Ambady, A.; Venkatraman, J.; Panda, M.; Bandodkar, B.; Sambandamurthy, V.K.; Read, J.A. Methyl-thiazoles: a novel mode of inhibition with the potential to develop novel inhibitors targeting InhA in *Mycobacterium tuberculosis*. *J. Med. Chem.*, **2013**, *56*(21), 8533-8542.

[31] Šink, R.; Sosič, I.; Zivec, M.; Fernandez-Menendez, R.; Turk, S.; Pajk, S.; Alvarez-Gomez, D.; Lopez-Roman, E.M.; Gonzales-Cortez, C.; Rullas-Triconado, J.; Angulo-Barturen, I.; Barros, D.; Ballell-Pages, L.; Young, R.J.; Encinas, L.; Gobec, S. Design, synthesis, and evaluation of new thiadiazole-based direct inhibitors of enoyl acyl carrier protein reductase (InhA) for the treatment of tuberculosis. *J. Med. Chem.*, **2015**, *58*(2), 613-624.

[32] Manjunatha, U.H.; S Rao, S.P.; Kondreddi, R.R.; Noble, C.G.; Camacho, L.R.; Tan, B.H.; Ng, S.H.; Ng, P.S.; Ma, N.L.; Lakshminarayana, S.B.; Herve, M.; Barnes, S.W.; Yu,

W.; Kuhen, K.; Blasco, F.; Beer, D.; Walker, J.R.; Tonge, P.J.; Glynne, R.; Smith, P.W.; Diagana, T.T. Direct inhibitors of InhA are active against Mycobacterium tuberculosis. *Sci. Transl. Med.*, **2015**, *7*(269), 269ra3.

[33] Floss, H.G.; Yu, T.W. Rifamycin-mode of action, resistance, and biosynthesis. *Chem. Rev.*, **2005**, *105*(2), 621-632.

[34] Hartmann, G.; Behr, W.; Beissner, K.A.; Honikel, K.; Sippel, A. Antibiotics as inhibitors of nucleic acid and protein synthesis. *Angew. Chem. Int. Ed. Engl.*, **1968**, *7*(9), 693-701.

[35] Mukhopadhyay, J.; Das, K.; Ismail, S.; Koppstein, D.; Jang, M.; Hudson, B.; Sarafianos, S.; Tuske, S.; Patel, J.; Jansen, R.; Irschik, H.; Arnold, E.; Ebright, R.H. The RNA polymerase "switch region" is a target for inhibitors. *Cell*, **2008**, *135*(2), 295-307.

[36] Murakami, K.S.; Darst, S.A. Bacterial RNA polymerases: the wholo story. *Curr. Opin. Struct. Biol.*, **2003**, *13*(1), 31-39.

[37] Darst, S.A. Bacterial RNA polymerase. *Curr. Opin. Struct. Biol.*, **2001**, *11*(2), 155-162.

[38] Ramaswamy, S.; Musser, J.M. Molecular genetic basis of antimicrobial agent resistance in *Mycobacterium tuberculosis*: 1998 update. *Tuber. Lung Dis.*, **1998**, *79*(1), 3-29.

[39] Heep, M.; Brandstätter, B.; Rieger, U.; Lehn, N.; Richter, E.; Rüsch-Gerdes, S.; Niemann, S. Frequency of rpoB mutations inside and outside the cluster I region in rifampin-resistant clinical *Mycobacterium tuberculosis* isolates. *J. Clin. Microbiol.*, **2001**, *39*(1), 107-110.

[40] McClure, W.R.; Cech, C.L. On the mechanism of rifampicin inhibition of RNA synthesis. *J. Biol. Chem.*, **1978**, *253*(24), 8949-8956.

[41] Aristoff, P.A.; Garcia, G.A.; Kirchhoff, P.D.; Showalter, H.D. Rifamycins--obstacles and opportunities. *Tuberculosis (Edinb.)*, **2010**, *90*(2), 94-118.

[42] Sterling, T.R.; Villarino, M.E.; Borisov, A.S.; Shang, N.; Gordin, F.; Bliven-Sizemore, E.; Hackman, J.; Hamilton, C.D.; Menzies, D.; Kerrigan, A.; Weis, S.E.; Weiner, M.; Wing, D.; Conde, M.B.; Bozeman, L.; Horsburgh, C.R., Jr; Chaisson, R.E.; Team, T.T. Three months of rifapentine and isoniazid for latent tuberculosis infection. *N. Engl. J. Med.*, **2011**, *365*(23), 2155-2166.

[43] Benator, D.; Bhattacharya, M.; Bozeman, L.; Burman, W.; Cantazaro, A.; Chaisson, R.; Gordin, F.; Horsburgh, C.R.; Horton, J.; Khan, A.; Lahart, C.; Metchock, B.; Pachucki, C.; Stanton, L.; Vernon, A.; Villarino, M.E.; Wang, Y.C.; Weiner, M.; Weis, S.; Consortium, T.T. Rifapentine and isoniazid once a week versus rifampicin and isoniazid twice a week for treatment of drug-susceptible pulmonary tuberculosis in HIV-negative patients: a randomised clinical trial. *Lancet*, **2002**, *360*(9332), 528-534.

[44] Rifabutin. *Tuberculosis (Edinb.)*, **2008**, *88*(2), 145-147.

[45] Williamson, B.; Dooley, K.E.; Zhang, Y.; Back, D.J.; Owen, A. Induction of influx and efflux transporters and cytochrome P450 3A4 in primary human hepatocytes by rifampin, rifabutin, and rifapentine. *Antimicrob. Agents Chemother.*, **2013**, *57*(12), 6366-6369.

[46] Luna-Herrera, J.; Reddy, M.V.; Gangadharam, P.R. In vitro activity of the benzoxazinorifamycin KRM-1648 against drug-susceptible and multidrug-resistant tubercle bacilli. *Antimicrob. Agents Chemother.*, **1995**, *39*(2), 440-444.

[47] Yamamoto, T.; Amitani, R.; Suzuki, K.; Tanaka, E.; Murayama, T.; Kuze, F. In vitro bactericidal and in vivo therapeutic activities of a new rifamycin derivative, KRM-1648, against *Mycobacterium tuberculosis*. *Antimicrob. Agents Chemother.*, **1996**, *40*(2), 426-428.

[48] Mae, T.; Hosoe, K.; Yamamoto, T.; Hidaka, T.; Ohashi, T.; Kleeman, J.M.; Adams, P.E. Effect of a new rifamycin derivative, rifalazil, on liver microsomal enzyme induction in rat and dog. *Xenobiotica*, **1998**, *28*(8), 759-766.

[49] Dietze, R.; Teixeira, L.; Rocha, L.M.; Palaci, M.; Johnson, J.L.; Wells, C.; Rose, L.; Eisenach, K.; Ellner, J.J. Safety and bactericidal activity of rifalazil in patients with pulmonary tuberculosis. *Antimicrob. Agents Chemother.*, **2001**, *45*(7), 1972-1976.

[50] Srivastava, A.; Talaue, M.; Liu, S.; Degen, D.; Ebright, R.Y.; Sineva, E.; Chakraborty, A.; Druzhinin, S.Y.; Chatterjee, S.; Mukhopadhyay, J.; Ebright, Y.W.; Zozula, A.; Shen, J.; Sengupta, S.; Niedfeldt, R.R.; Xin, C.; Kaneko, T.; Irschik, H.; Jansen, R.; Donadio, S.; Connell, N.; Ebright, R.H. New target for inhibition of bacterial RNA polymerase: 'switch region'. *Curr. Opin. Microbiol.*, **2011**, *14*(5), 532-543.

[51] Kurabachew, M.; Lu, S.H.; Krastel, P.; Schmitt, E.K.; Suresh, B.L.; Goh, A.; Knox, J.E.; Ma, N.L.; Jiricek, J.; Beer, D.; Cynamon, M.; Petersen, F.; Dartois, V.; Keller, T.; Dick, T.; Sambandamurthy, V.K. Lipiarmycin targets RNA polymerase and has good activity against multidrug-resistant strains of *Mycobacterium tuberculosis*. *J. Antimicrob. Chemother.*, **2008**, *62*(4), 713-719.

[52] Tupin, A.; Gualtieri, M.; Leonetti, J.P.; Brodolin, K. The transcription inhibitor lipiarmycin blocks DNA fitting into the RNA polymerase catalytic site. *EMBO J.*, **2010**, *29*(15), 2527-2537.

[53] Weiss, K.; Allgren, R.L.; Sellers, S. Safety analysis of fidaxomicin in comparison with oral vancomycin for *Clostridium difficile* infections. *Clin. Infect. Dis.*, **2012**, *55*(Suppl. 2), S110-S115.

[54] Parenti, F.; Pagani, H.; Beretta, G. Lipiarmycin, a new antibiotic from Actinoplanes. I. Description of the producer strain and fermentation studies. *J. Antibiot.*, **1975**, *28*(4), 247-252.

[55] Erb, W.; Grassot, J.M.; Linder, D.; Neuville, L.; Zhu, J. Enantioselective synthesis of putative lipiarmycin aglycon related to fidaxomicin/tiacumicin B. *Angew. Chem. Int. Ed. Engl.*, **2015**, *54*(6), 1929-1932.

[56] Glaus, F.; Altmann, K.H. Total synthesis of the tiacumicin B (lipiarmycin A3/fidaxomicin) aglycone. *Angew. Chem. Int. Ed. Engl.*, **2015**, *54*(6), 1937-1940.

[57] Miyatake-Ondozabal, H.; Kaufmann, E.; Gademann, K. Total synthesis of the protected aglycon of fidaxomicin (tiacumicin B, lipiarmycin A3). *Angew. Chem. Int. Ed. Engl.*, **2015**, *54*(6), 1933-1936.

[58] Ehmann, D.E.; Lahiri, S.D. Novel compounds targeting bacterial DNA topoisomerase/DNA gyrase. *Curr. Opin. Pharmacol.*, **2014**, *18*, 76-83.

[59] Takiff, H.E.; Salazar, L.; Guerrero, C.; Philipp, W.; Huang, W.M.; Kreiswirth, B.; Cole, S.T.; Jacobs, W.R., Jr; Telenti, A. Cloning and nucleotide sequence of *Mycobacterium tuberculosis* gyrA and gyrB genes and detection of quinolone resistance mutations. *Antimicrob. Agents Chemother.*, **1994**, *38*(4), 773-780.

[60] Horsburgh, C.R., Jr; Barry, C.E., III; Lange, C. Treatment of Tuberculosis. *N. Engl. J. Med.*, **2015**, *373*(22), 2149-2160.

[61] Ruan, Q.; Liu, Q.; Sun, F.; Shao, L.; Jin, J.; Yu, S.; Ai, J.; Zhang, B.; Zhang, W. Moxifloxacin and gatifloxacin for initial therapy of tuberculosis: a meta-analysis of randomized clinical trials. *Emerg Microbes Infect*, **2016**, *5*(1), e12.

[62] Xu, C.; Kreiswirth, B.N.; Sreevatsan, S.; Musser, J.M.; Drlica, K. Fluoroquinolone resistance associated with spe-

cific gyrase mutations in clinical isolates of multidrug-resistant *Mycobacterium tuberculosis*. *J. Infect. Dis.*, **1996**, *174*(5), 1127-1130.

[63] Blower, T.R.; Williamson, B.H.; Kerns, R.J.; Berger, J.M. Crystal structure and stability of gyrase-fluoroquinolone cleaved complexes from *Mycobacterium tuberculosis*. *Proc. Natl. Acad. Sci. USA*, **2016**, *113*(7), 1706-1713.

[64] Shirude, P.S.; Madhavapeddi, P.; Tucker, J.A.; Murugan, K.; Patil, V.; Basavarajappa, H.; Raichurkar, A.V.; Hunnabadkar, V.; Hussein, S.; Sharma, S.; Ramya, V.K.; Narayan, C.B.; Balganesh, T.S.; Sambandamurthy, V.K. Aminopyrazinamides: novel and specific GyrB inhibitors that kill replicating and nonreplicating *Mycobacterium tuberculosis*. *ACS Chem. Biol.*, **2013**, *8*(3), 519-523.

[65] Kale, M.G.; Raichurkar, A.; P, S.H.; Waterson, D.; McKinney, D.; Manjunatha, M.R.; Kranthi, U.; Koushik, K.; Jena, Lk.; Shinde, V.; Rudrapatna, S.; Barde, S.; Hunnabadkar, V.; Madhavapeddi, P.; Basavarajappa, H.; Ghosh, A.; Ramya, V.K.; Guptha, S.; Sharma, S.; Vachaspati, P.; Kumar, K.N.; Giridhar, J.; Reddy, J.; Panduga, V.; Ganguly, S.; Ahuja, V.; Gaonkar, S.; Kumar, C.N.; Ogg, D.; Tucker, J.A.; Boriack-Sjodin, P.A.; de Sousa, S.M.; Sambandamurthy, V.K.; Ghorpade, S.R. Thiazolopyridine ureas as novel antitubercular agents acting through inhibition of DNA Gyrase B. *J. Med. Chem.*, **2013**, *56*(21), 8834-8848.

[66] Kale, R.R.; Kale, M.G.; Waterson, D.; Raichurkar, A.; Hameed, S.P.; Manjunatha, M.R.; Kishore Reddy, B.K.; Malolanarasimhan, K.; Shinde, V.; Koushik, K.; Jena, L.K.; Menasinakai, S.; Hunnabadkar, V.; Madhavapeddi, P.; Basavarajappa, H.; Sharma, S.; Nandishaiah, R.; Mahesh Kumar, K.N.; Ganguly, S.; Ahuja, V.; Gaonkar, S.; Naveen Kumar, C.N.; Ogg, D.; Boriack-Sjodin, P.A.; Sambandamurthy, V.K.; de Sousa, S.M.; Ghorpade, S.R. Thiazolopyridone ureas as DNA gyrase B inhibitors: optimization of antitubercular activity and efficacy. *Bioorg. Med. Chem. Lett.*, **2014**, *24*(3), 870-879.

[67] Jeankumar, V.U.; Renuka, J.; Santosh, P.; Soni, V.; Sridevi, J.P.; Suryadevara, P.; Yogeeswari, P.; Sriram, D. Thiazole-aminopiperidine hybrid analogues: design and synthesis of novel *Mycobacterium tuberculosis* GyrB inhibitors. *Eur. J. Med. Chem.*, **2013**, *70*, 143-153.

[68] Medapi, B.; Renuka, J.; Saxena, S.; Sridevi, J.P.; Medishetti, R.; Kulkarni, P.; Yogeeswari, P.; Sriram, D. Design and synthesis of novel quinoline-aminopiperidine hybrid analogues as *Mycobacterium tuberculosis* DNA gyraseB inhibitors. *Bioorg. Med. Chem.*, **2015**, *23*(9), 2062-2078.

[69] P, S.H.; Solapure, S.; Mukherjee, K.; Nandi, V.; Waterson, D.; Shandil, R.; Balganesh, M.; Sambandamurthy, V.K.; Raichurkar, A.K.; Deshpande, A.; Ghosh, A.; Awasthy, D.; Shanbhag, G.; Sheikh, G.; McMiken, H.; Puttur, J.; Reddy, J.; Werngren, J.; Read, J.; Kumar, M.; R, M.; Chinnapattu, M.; Madhavapeddi, P.; Manjrekar, P.; Basu, R.; Gaonkar, S.; Sharma, S.; Hoffner, S.; Hunnabadkar, V.; Subbulakshmi, V.; Panduga, V. Optimization of pyrrolamides as mycobacterial GyrB ATPase inhibitors: structure-activity relationship and in vivo efficacy in a mouse model of tuberculosis. *Antimicrob. Agents Chemother.*, **2014**, *58*(1), 61-70.

[70] Jeankumar, V.U.; Saxena, S.; Vats, R.; Reshma, R.S.; Janupally, R.; Kulkarni, P.; Yogeeswari, P.; Sriram, D. Structure-Guided Discovery of Antitubercular Agents That Target the Gyrase ATPase Domain. *ChemMedChem*, **2016**, *11*(5), 539-548.

[71] Grossman, T.H.; Bartels, D.J.; Mullin, S.; Gross, C.H.; Parsons, J.D.; Liao, Y.; Grillot, A.L.; Stamos, D.; Olson, E.R.; Charifson, P.S.; Mani, N. Dual targeting of GyrB and ParE by a novel aminobenzimidazole class of antibacterial compounds. *Antimicrob. Agents Chemother.*, **2007**, *51*(2), 657-666.

[72] Grillot, A.L.; Le Tiran, A.; Shannon, D.; Krueger, E.; Liao, Y.; O'Dowd, H.; Tang, Q.; Ronkin, S.; Wang, T.; Waal, N.; Li, P.; Lauffer, D.; Sizensky, E.; Tanoury, J.; Perola, E.; Grossman, T.H.; Doyle, T.; Hanzelka, B.; Jones, S.; Dixit, V.; Ewing, N.; Liao, S.; Boucher, B.; Jacobs, M.; Bennani, Y.; Charifson, P.S. Second-generation antibacterial benzimidazole ureas: discovery of a preclinical candidate with reduced metabolic liability. *J. Med. Chem.*, **2014**, *57*(21), 8792-8816.

[73] Locher, C.P.; Jones, S.M.; Hanzelka, B.L.; Perola, E.; Shoen, C.M.; Cynamon, M.H.; Ngwane, A.H.; Wiid, I.J.; van Helden, P.D.; Betoudji, F.; Nuermberger, E.L.; Thomson, J.A. A novel inhibitor of gyrase B is a potent drug candidate for treatment of tuberculosis and nontuberculosis mycobacterial infections. *Antimicrob. Agents Chemother.*, **2015**, *59*(3), 1455-1465.

[74] Hameed P, S.; Patil, V.; Solapure, S.; Sharma, U.; Madhavapeddi, P.; Raichurkar, A.; Chinnapattu, M.; Manjrekar, P.; Shanbhag, G.; Puttur, J.; Shinde, V.; Menasinakai, S.; Rudrapatana, S.; Achar, V.; Awasthy, D.; Nandishaiah, R.; Hunnabadkar, V.; Ghosh, A.; Narayan, C.; Ramya, V.K.; Kaur, P.; Sharma, S.; Werngren, J.; Hoffner, S.; Panduga, V.; Kumar, C.N.; Reddy, J.; Kumar K N, M.; Ganguly, S.; Bharath, S.; Bheemarao, U.; Mukherjee, K.; Arora, U.; Gaonkar, S.; Coulson, M.; Waterson, D.; Sambandamurthy, V.K.; de Sousa, S.M. Novel N-linked aminopiperidine-based gyrase inhibitors with improved hERG and in vivo efficacy against Mycobacterium tuberculosis. *J. Med. Chem.*, **2014**, *57*(11), 4889-4905.

[75] Blanco, D.; Perez-Herran, E.; Cacho, M.; Ballell, L.; Castro, J.; González Del Río, R.; Lavandera, J.L.; Remuiñán, M.J.; Richards, C.; Rullas, J.; Vázquez-Muñiz, M.J.; Woldu, E.; Zapatero-González, M.C.; Angulo-Barturen, I.; Mendoza, A.; Barros, D. *Mycobacterium tuberculosis* gyrase inhibitors as a new class of antitubercular drugs. *Antimicrob. Agents Chemother.*, **2015**, *59*(4), 1868-1875.

[76] Cole, S.T.; Brosch, R.; Parkhill, J.; Garnier, T.; Churcher, C.; Harris, D.; Gordon, S.V.; Eiglmeier, K.; Gas, S.; Barry, C.E., III; Tekaia, F.; Badcock, K.; Basham, D.; Brown, D.; Chillingworth, T.; Connor, R.; Davies, R.; Devlin, K.; Feltwell, T.; Gentles, S.; Hamlin, N.; Holroyd, S.; Hornsby, T.; Jagels, K.; Krogh, A.; McLean, J.; Moule, S.; Murphy, L.; Oliver, K.; Osborne, J.; Quail, M.A.; Rajandream, M.A.; Rogers, J.; Rutter, S.; Seeger, K.; Skelton, J.; Squares, R.; Squares, S.; Sulston, J.E.; Taylor, K.; Whitehead, S.; Barrell, B.G. Deciphering the biology of *Mycobacterium tuberculosis* from the complete genome sequence. *Nature*, **1998**, *393*(6685), 537-544.

[77] Takiff, H.E.; Feo, O. Clinical value of whole-genome sequencing of *Mycobacterium tuberculosis*. *Lancet Infect. Dis.*, **2015**, *15*(9), 1077-1090.

[78] Lechartier, B.; Rybniker, J.; Zumla, A.; Cole, S.T. Tuberculosis drug discovery in the post-post-genomic era. *EMBO Mol. Med.*, **2014**, *6*(2), 158-168.

[79] Manina, G.; Pasca, M.R.; Buroni, S.; De Rossi, E.; Riccardi, G. Decaprenylphosphoryl-β-D-ribose 2'-epimerase from *Mycobacterium tuberculosis* is a magic drug target. *Curr. Med. Chem.*, **2010**, *17*(27), 3099-3108.

[80] Christophe, T.; Jackson, M.; Jeon, H.K.; Fenistein, D.; Contreras-Dominguez, M.; Kim, J.; Genovesio, A.; Carralot, J.P.; Ewann, F.; Kim, E.H.; Lee, S.Y.; Kang, S.; Seo, M.J.;

Park, E.J.; Skovierová, H.; Pham, H.; Riccardi, G.; Nam, J.Y.; Marsollier, L.; Kempf, M.; Joly-Guillou, M.L.; Oh, T.; Shin, W.K.; No, Z.; Nehrbass, U.; Brosch, R.; Cole, S.T.; Brodin, P. High content screening identifies decaprenyl-phosphoribose 2′ epimerase as a target for intracellular antimycobacterial inhibitors. *PLoS Pathog.*, **2009**, *5*(10), e1000645.

[81] Magnet, S.; Hartkoorn, R.C.; Székely, R.; Pató, J.; Triccas, J.A.; Schneider, P.; Szántai-Kis, C.; Orfi, L.; Chambon, M.; Banfi, D.; Bueno, M.; Turcatti, G.; Kéri, G.; Cole, S.T. Leads for antitubercular compounds from kinase inhibitor library screens. *Tuberculosis (Edinb.)*, **2010**, *90*(6), 354-360.

[82] Stanley, S.A.; Grant, S.S.; Kawate, T.; Iwase, N.; Shimizu, M.; Wivagg, C.; Silvis, M.; Kazyanskaya, E.; Aquadro, J.; Golas, A.; Fitzgerald, M.; Dai, H.; Zhang, L.; Hung, D.T. Identification of novel inhibitors of *M. tuberculosis* growth using whole cell based high-throughput screening. *ACS Chem. Biol.*, **2012**, *7*(8), 1377-1384.

[83] Shirude, P.S.; Shandil, R.; Sadler, C.; Naik, M.; Hosagrahara, V.; Hameed, S.; Shinde, V.; Bathula, C.; Humnabadkar, V.; Kumar, N.; Reddy, J.; Panduga, V.; Sharma, S.; Ambady, A.; Hegde, N.; Whiteaker, J.; McLaughlin, R.E.; Gardner, H.; Madhavapeddi, P.; Ramachandran, V.; Kaur, P.; Narayan, A.; Guptha, S.; Awasthy, D.; Narayan, C.; Mahadevaswamy, J.; Vishwas, K.G.; Ahuja, V.; Srivastava, A.; Prabhakar, K.R.; Bharath, S.; Kale, R.; Ramaiah, M.; Choudhury, N.R.; Sambandamurthy, V.K.; Solapure, S.; Iyer, P.S.; Narayanan, S.; Chatterji, M. Azaindoles: noncovalent DprE1 inhibitors from scaffold morphing efforts, kill *Mycobacterium tuberculosis* and are efficacious in vivo. *J. Med. Chem.*, **2013**, *56*(23), 9701-9708.

[84] Wang, F.; Sambandan, D.; Halder, R.; Wang, J.; Batt, S.M.; Weinrick, B.; Ahmad, I.; Yang, P.; Zhang, Y.; Kim, J.; Hassani, M.; Huszar, S.; Trefzer, C.; Ma, Z.; Kaneko, T.; Mdluli, K.E.; Franzblau, S.; Chatterjee, A.K.; Johnsson, K.; Mikusova, K.; Besra, G.S.; Fütterer, K.; Robbins, S.H.; Barnes, S.W.; Walker, J.R.; Jacobs, W.R., Jr; Schultz, P.G.; Schultz, P.G. Identification of a small molecule with activity against drug-resistant and persistent tuberculosis. *Proc. Natl. Acad. Sci. USA*, **2013**, *110*(27), E2510-E2517.

[85] Naik, M.; Humnabadkar, V.; Tantry, S.J.; Panda, M.; Narayan, A.; Guptha, S.; Panduga, V.; Manjrekar, P.; Jena, L.K.; Koushik, K.; Shanbhag, G.; Jatheendranath, S.; Manjunatha, M.R.; Gorai, G.; Bathula, C.; Rudrapatna, S.; Achar, V.; Sharma, S.; Ambady, A.; Hegde, N.; Mahadevaswamy, J.; Kaur, P.; Sambandamurthy, V.K.; Awasthy, D.; Narayan, C.; Ravishankar, S.; Madhavapeddi, P.; Reddy, J.; Prabhakar, K.; Saralaya, R.; Chatterji, M.; Whiteaker, J.; McLaughlin, B.; Chiarelli, L.R.; Riccardi, G.; Pasca, M.R.; Binda, C.; Neres, J.; Dhar, N.; Signorino-Gelo, F.; McKinney, J.D.; Ramachandran, V.; Shandil, R.; Tommasi, R.; Iyer, P.S.; Narayanan, S.; Hosagrahara, V.; Kavanagh, S.; Dinesh, N.; Ghorpade, S.R. 4-aminoquinolone piperidine amides: noncovalent inhibitors of DprE1 with long residence time and potent antimycobacterial activity. *J. Med. Chem.*, **2014**, *57*(12), 5419-5434.

[86] Panda, M.; Ramachandran, S.; Ramachandran, V.; Shirude, P.S.; Humnabadkar, V.; Nagalapur, K.; Sharma, S.; Kaur, P.; Guptha, S.; Narayan, A.; Mahadevaswamy, J.; Ambady, A.; Hegde, N.; Rudrapatna, S.S.; Hosagrahara, V.P.; Sambandamurthy, V.K.; Raichurkar, A. Discovery of pyrazolopyridones as a novel class of noncovalent DprE1 inhibitor with potent anti-mycobacterial activity. *J. Med. Chem.*, **2014**, *57*(11), 4761-4771.

[87] Neres, J.; Hartkoorn, R.C.; Chiarelli, L.R.; Gadupudi, R.; Pasca, M.R.; Mori, G.; Venturelli, A.; Savina, S.; Makarov, V.; Kolly, G.S.; Molteni, E.; Binda, C.; Dhar, N.; Ferrari, S.; Brodin, P.; Delorme, V.; Landry, V.; de Jesus Lopes Ribeiro, A.L.; Farina, D.; Saxena, P.; Pojer, F.; Carta, A.; Luciani, R.; Porta, A.; Zanoni, G.; De Rossi, E.; Costi, M.P.; Riccardi, G.; Cole, S.T. 2-Carboxyquinoxalines kill *mycobacterium tuberculosis* through noncovalent inhibition of DprE1. *ACS Chem. Biol.*, **2015**, *10*(3), 705-714.

[88] Landge, S.; Mullick, A.B.; Nagalapur, K.; Neres, J.; Subbulakshmi, V.; Murugan, K.; Ghosh, A.; Sadler, C.; Fellows, M.D.; Humnabadkar, V.; Mahadevaswamy, J.; Vachaspati, P.; Sharma, S.; Kaur, P.; Mallya, M.; Rudrapatna, S.; Awasthy, D.; Sambandamurthy, V.K.; Pojer, F.; Cole, S.T.; Balganesh, T.S.; Ugarkar, B.G.; Balasubramanian, V.; Bandodkar, B.S.; Panda, M.; Ramachandran, V. Discovery of benzothiazoles as antimycobacterial agents: Synthesis, structure-activity relationships and binding studies with *Mycobacterium tuberculosis* decaprenylphosphoryl-β-D-ribose 2′-oxidase. *Bioorg. Med. Chem.*, **2015**, *23*(24), 7694-7710.

[89] Chikhale, R.; Menghani, S.; Babu, R.; Bansode, R.; Bhargavi, G.; Karodia, N.; Rajasekharan, M.V.; Paradkar, A.; Khedekar, P. Development of selective DprE1 inhibitors: Design, synthesis, crystal structure and antitubercular activity of benzothiazolylpyrimidine-5-carboxamides. *Eur. J. Med. Chem.*, **2015**, *96*, 30-46.

[90] Batt, S.M.; Izquierdo, M.C.; Pichel, J.C.; Stubbs, C.J.; Del Peral, L.V.; Pérez-Herrán, E.; Dhar, N.; Mouzon, B.; Rees, M.; Hutchinson, J.P.; Young, R.J.; McKinney, J.D.; Aguirre, D.B.; Ballell, L.; Besra, G.S.; Argyrou, A. Whole Cell Target Engagement Identifies Novel Inhibitors of *Mycobacterium tuberculosis* Decaprenylphosphoryl-β-d-ribose Oxidase. *ACS Infect Dis*, **2015**, *1*(12), 615-626.

[91] Landge, S.; Ramachandran, V.; Kumar, A.; Neres, J.; Murugan, K.; Sadler, C.; Fellows, M.D.; Humnabadkar, V.; Vachaspati, P.; Raichurkar, A.; Sharma, S.; Ravishankar, S.; Guptha, S.; Sambandamurthy, V.K.; Balganesh, T.S.; Ugarkar, B.G.; Balasubramanian, V.; Bandodkar, B.S.; Panda, M. Nitroarenes as Antitubercular Agents: Stereoelectronic Modulation to Mitigate Mutagenicity. *ChemMedChem*, **2016**, *11*(3), 331-339.

[92] Mikusová, K.; Huang, H.; Yagi, T.; Holsters, M.; Vereecke, D.; D'Haeze, W.; Scherman, M.S.; Brennan, P.J.; McNeil, M.R.; Crick, D.C. Decaprenylphosphoryl arabinofuranose, the donor of the D-arabinofuranosyl residues of mycobacterial arabinan, is formed via a two-step epimerization of decaprenylphosphoryl ribose. *J. Bacteriol.*, **2005**, *187*(23), 8020-8025.

[93] Kolly, G.S.; Boldrin, F.; Sala, C.; Dhar, N.; Hartkoorn, R.C.; Ventura, M.; Serafini, A.; McKinney, J.D.; Manganelli, R.; Cole, S.T. Assessing the essentiality of the decaprenyl-phospho-d-arabinofuranose pathway in *Mycobacterium tuberculosis* using conditional mutants. *Mol. Microbiol.*, **2014**, *92*(1), 194-211.

[94] Wolucka, B.A. Biosynthesis of D-arabinose in mycobacteria - a novel bacterial pathway with implications for antimycobacterial therapy. *FEBS J.*, **2008**, *275*(11), 2691-2711.

[95] Neres, J.; Pojer, F.; Molteni, E.; Chiarelli, L.R.; Dhar, N.; Boy-Röttger, S.; Buroni, S.; Fullam, E.; Degiacomi, G.; Lucarelli, A.P.; Read, R.J.; Zanoni, G.; Edmondson, D.E.; De Rossi, E.; Pasca, M.R.; McKinney, J.D.; Dyson, P.J.; Riccardi, G.; Mattevi, A.; Cole, S.T.; Binda, C. Structural basis

for benzothiazinone-mediated killing of *Mycobacterium tuberculosis*. *Sci. Transl. Med.*, **2012**, *4*(150), 150ra121.

[96] Trefzer, C.; Škovierová, H.; Buroni, S.; Bobovská, A.; Nenci, S.; Molteni, E.; Pojer, F.; Pasca, M.R.; Makarov, V.; Cole, S.T.; Riccardi, G.; Mikušová, K.; Johnsson, K. Benzothiazinones are suicide inhibitors of mycobacterial decaprenylphosphoryl-β-D-ribofuranose 2′-oxidase DprE1. *J. Am. Chem. Soc.*, **2012**, *134*(2), 912-915.

[97] Tiwari, R.; Moraski, G.C.; Krchňák, V.; Miller, P.A.; Colon-Martinez, M.; Herrero, E.; Oliver, A.G.; Miller, M.J. Thiolates chemically induce redox activation of BTZ043 and related potent nitroaromatic anti-tuberculosis agents. *J. Am. Chem. Soc.*, **2013**, *135*(9), 3539-3549.

[98] Riccardi, G.; Pasca, M.R.; Chiarelli, L.R.; Manina, G.; Mattevi, A.; Binda, C. The DprE1 enzyme, one of the most vulnerable targets of *Mycobacterium tuberculosis*. *Appl. Microbiol. Biotechnol.*, **2013**, *97*(20), 8841-8848.

[99] Ribeiro, A.L.; Degiacomi, G.; Ewann, F.; Buroni, S.; Incandela, M.L.; Chiarelli, L.R.; Mori, G.; Kim, J.; Contreras-Dominguez, M.; Park, Y.S.; Han, S.J.; Brodin, P.; Valentini, G.; Rizzi, M.; Riccardi, G.; Pasca, M.R. Analogous mechanisms of resistance to benzothiazinones and dinitrobenzamides in *Mycobacterium smegmatis*. *PLoS One*, **2011**, *6*(11), e26675.

[100] Batt, S.M.; Jabeen, T.; Bhowruth, V.; Quill, L.; Lund, P.A.; Eggeling, L.; Alderwick, L.J.; Fütterer, K.; Besra, G.S. Structural basis of inhibition of *Mycobacterium tuberculosis* DprE1 by benzothiazinone inhibitors. *Proc. Natl. Acad. Sci. USA*, **2012**, *109*(28), 11354-11359.

[101] Manina, G.; Bellinzoni, M.; Pasca, M.R.; Neres, J.; Milano, A.; Ribeiro, A.L.; Buroni, S.; Skovierová, H.; Dianišková, P.; Mikušová, K.; Marák, J.; Makarov, V.; Giganti, D.; Haouz, A.; Lucarelli, A.P.; Degiacomi, G.; Piazza, A.; Chiarelli, L.R.; De Rossi, E.; Salina, E.; Cole, S.T.; Alzari, P.M.; Riccardi, G. Biological and structural characterization of the *Mycobacterium smegmatis* nitroreductase NfnB, and its role in benzothiazinone resistance. *Mol. Microbiol.*, **2010**, *77*(5), 1172-1185.

[102] Tiwari, R.; Miller, P.A.; Chiarelli, L.R.; Mori, G.; Šarkan, M.; Centárová, I.; Cho, S.; Mikušová, K.; Franzblau, S.G.; Oliver, A.G.; Miller, M.J. Design, Syntheses, and Anti-TB Activity of 1,3-Benzothiazinone Azide and Click Chemistry Products Inspired by BTZ043. *ACS Med. Chem. Lett.*, **2016**, *7*(3), 266-270.

[103] Makarov, V.; Neres, J.; Hartkoorn, R.C.; Ryabova, O.B.; Kazakova, E.; Šarkan, M.; Huszár, S.; Piton, J.; Kolly, G.S.; Vocat, A.; Conroy, T.M.; Mikušová, K.; Cole, S.T. The 8-Pyrrole-Benzothiazinones Are Noncovalent Inhibitors of DprE1 from *Mycobacterium tuberculosis*. *Antimicrob. Agents Chemother.*, **2015**, *59*(8), 4446-4452.

[104] Tiwari, R.; Miller, P.A.; Cho, S.; Franzblau, S.G.; Miller, M.J. Syntheses and Antituberculosis Activity of 1,3-Benzothiazinone Sulfoxide and Sulfone Derived from BTZ043. *ACS Med. Chem. Lett.*, **2015**, *6*(2), 128-133.

[105] Karoli, T.; Becker, B.; Zuegg, J.; Möllmann, U.; Ramu, S.; Huang, J.X.; Cooper, M.A. Identification of antitubercular benzothiazinone compounds by ligand-based design. *J. Med. Chem.*, **2012**, *55*(17), 7940-7944.

[106] Peng, C.T.; Gao, C.; Wang, N.Y.; You, X.Y.; Zhang, L.D.; Zhu, Y.X.; Xv, Y.; Zuo, W.Q.; Ran, K.; Deng, H.X.; Lei, Q.; Xiao, K.J.; Yu, L.T. Synthesis and antitubercular evaluation of 4-carbonyl piperazine substituted 1,3-benzothiazin-4-one derivatives. *Bioorg. Med. Chem. Lett.*, **2015**, *25*(7), 1373-1376.

[107] Shirude, P.S.; Shandil, R.K.; Manjunatha, M.R.; Sadler, C.; Panda, M.; Panduga, V.; Reddy, J.; Saralaya, R.; Nanduri, R.; Ambady, A.; Ravishankar, S.; Sambandamurthy, V.K.; Hunnabadkar, V.; Jena, L.K.; Suresh, R.S.; Srivastava, A.; Prabhakar, K.R.; Whiteaker, J.; McLaughlin, R.E.; Sharma, S.; Cooper, C.B.; Mdluli, K.; Butler, S.; Iyer, P.S.; Narayanan, S.; Chatterji, M. Lead optimization of 1,4-azaindoles as antimycobacterial agents. *J. Med. Chem.*, **2014**, *57*(13), 5728-5737.

[108] Brecik, M.; Centárová, I.; Mukherjee, R.; Kolly, G.S.; Huszár, S.; Bobovská, A.; Kilacsková, E.; Mokošová, V.; Svetlíková, Z.; Šarkan, M.; Neres, J.; Korduláková, J.; Cole, S.T.; Mikušová, K. DprE1 Is a Vulnerable Tuberculosis Drug Target Due to Its Cell Wall Localization. *ACS Chem. Biol.*, **2015**, *10*(7), 1631-1636.

[109] Domenech, P.; Reed, M.B.; Barry, C.E., III Contribution of the *Mycobacterium tuberculosis* MmpL protein family to virulence and drug resistance. *Infect. Immun.*, **2005**, *73*(6), 3492-3501.

[110] Murakami, S. Multidrug efflux transporter, AcrB--the pumping mechanism. *Curr. Opin. Struct. Biol.*, **2008**, *18*(4), 459-465.

[111] Varela, C.; Rittmann, D.; Singh, A.; Krumbach, K.; Bhatt, K.; Eggeling, L.; Besra, G.S.; Bhatt, A. MmpL genes are associated with mycolic acid metabolism in mycobacteria and corynebacteria. *Chem. Biol.*, **2012**, *19*(4), 498-506.

[112] Owens, C.P.; Chim, N.; Graves, A.B.; Harmston, C.A.; Iniguez, A.; Contreras, H.; Liptak, M.D.; Goulding, C.W. The *Mycobacterium tuberculosis* secreted protein Rv0203 transfers heme to membrane proteins MmpL3 and MmpL11. *J. Biol. Chem.*, **2013**, *288*(30), 21714-21728.

[113] Deidda, D.; Lampis, G.; Fioravanti, R.; Biava, M.; Porretta, G.C.; Zanetti, S.; Pompei, R. Bactericidal activities of the pyrrole derivative BM212 against multidrug-resistant and intramacrophagic *Mycobacterium tuberculosis* strains. *Antimicrob. Agents Chemother.*, **1998**, *42*(11), 3035-3037.

[114] La Rosa, V.; Poce, G.; Canseco, J.O.; Buroni, S.; Pasca, M.R.; Biava, M.; Raju, R.M.; Porretta, G.C.; Alfonso, S.; Battilocchio, C.; Javid, B.; Sorrentino, F.; Ioerger, T.R.; Sacchettini, J.C.; Manetti, F.; Botta, M.; De Logu, A.; Rubin, E.J.; De Rossi, E. MmpL3 is the cellular target of the antitubercular pyrrole derivative BM212. *Antimicrob. Agents Chemother.*, **2012**, *56*(1), 324-331.

[115] Poce, G.; Bates, R.H.; Alfonso, S.; Cocozza, M.; Porretta, G.C.; Ballell, L.; Rullas, J.; Ortega, F.; De Logu, A.; Agus, E.; La Rosa, V.; Pasca, M.R.; De Rossi, E.; Wae, B.; Franzblau, S.G.; Manetti, F.; Botta, M.; Biava, M. Improved BM212 MmpL3 inhibitor analogue shows efficacy in acute murine model of tuberculosis infection. *PLoS One*, **2013**, *8*(2), e56980.

[116] Biava, M.; Porretta, G.C.; Poce, G.; Supino, S.; Deidda, D.; Pompei, R.; Molicotti, P.; Manetti, F.; Botta, M. Antimycobacterial agents. Novel diarylpyrrole derivatives of BM212 endowed with high activity toward *Mycobacterium tuberculosis* and low cytotoxicity. *J. Med. Chem.*, **2006**, *49*(16), 4946-4952.

[117] Biava, M.; Porretta, G.C.; Poce, G.; Battilocchio, C.; Alfonso, S.; de Logu, A.; Manetti, F.; Botta, M. Developing pyrrole-derived antinycobacterial agents: a rational lead optimization approach. *ChemMedChem*, **2011**, *6*(4), 593-599.

[118] Grzegorzewicz, A.E.; Pham, H.; Gundi, V.A.; Scherman, M.S.; North, E.J.; Hess, T.; Jones, V.; Gruppo, V.; Born, S.E.; Korduláková, J.; Chavadi, S.S.; Morisseau, C.; Lenaerts, A.J.; Lee, R.E.; McNeil, M.R.; Jackson, M. Inhibi-

tion of mycolic acid transport across the *Mycobacterium tuberculosis* plasma membrane. *Nat. Chem. Biol.*, **2012**, *8*(4), 334-341.

[119] North, E.J.; Scherman, M.S.; Bruhn, D.F.; Scarborough, J.S.; Maddox, M.M.; Jones, V.; Grzegorzewicz, A.; Yang, L.; Hess, T.; Morisseau, C.; Jackson, M.; McNeil, M.R.; Lee, R.E. Design, synthesis and anti-tuberculosis activity of 1-adamantyl-3-heteroaryl ureas with improved in vitro pharmacokinetic properties. *Bioorg. Med. Chem.*, **2013**, *21*(9), 2587-2599.

[120] Lee, R.E.; Protopopova, M.; Crooks, E.; Slayden, R.A.; Terrot, M.; Barry, C.E., III Combinatorial lead optimization of [1,2]-diamines based on ethambutol as potential antituberculosis preclinical candidates. *J. Comb. Chem.*, **2003**, *5*(2), 172-187.

[121] Protopopova, M.; Hanrahan, C.; Nikonenko, B.; Samala, R.; Chen, P.; Gearhart, J.; Einck, L.; Nacy, C.A. Identification of a new antitubercular drug candidate, SQ109, from a combinatorial library of 1,2-ethylenediamines. *J. Antimicrob. Chemother.*, **2005**, *56*(5), 968-974.

[122] Sacksteder, K.A.; Protopopova, M.; Barry, C.E., III; Andries, K.; Nacy, C.A. Discovery and development of SQ109: a new antitubercular drug with a novel mechanism of action. *Future Microbiol.*, **2012**, *7*(7), 823-837.

[123] Remuiñán, M.J.; Pérez-Herrán, E.; Rullás, J.; Alemparte, C.; Martínez-Hoyos, M.; Dow, D.J.; Afari, J.; Mehta, N.; Esquivias, J.; Jiménez, E.; Ortega-Muro, F.; Fraile-Gabaldón, M.T.; Spivey, V.L.; Loman, N.J.; Pallen, M.J.; Constantinidou, C.; Minick, D.J.; Cacho, M.; Rebollo-López, M.J.; González, C.; Sousa, V.; Angulo-Barturen, I.; Mendoza-Losana, A.; Barros, D.; Besra, G.S.; Ballell, L.; Cammack, N. Tetrahydropyrazolo[1,5-a]pyrimidine-3-carboxamide and N-benzyl-6',7'-dihydrospiro[piperidine-4,4'-thieno[3,2-c]pyran] analogues with bactericidal efficacy against *Mycobacterium tuberculosis* targeting MmpL3. *PLoS One*, **2013**, *8*(4), e60933.

[124] Rao, S.P.; Lakshminarayana, S.B.; Kondreddi, R.R.; Herve, M.; Camacho, L.R.; Bifani, P.; Kalapala, S.K.; Jiricek, J.; Ma, N.L.; Tan, B.H.; Ng, S.H.; Nanjundappa, M.; Ravindran, S.; Seah, P.G.; Thayalan, P.; Lim, S.H.; Lee, B.H.; Goh, A.; Barnes, W.S.; Chen, Z.; Gagaring, K.; Chatterjee, A.K.; Pethe, K.; Kuhen, K.; Walker, J.; Feng, G.; Babu, S.; Zhang, L.; Blasco, F.; Beer, D.; Weaver, M.; Dartois, V.; Glynne, R.; Dick, T.; Smith, P.W.; Diagana, T.T.; Manjunatha, U.H. Indolcarboxamide is a preclinical candidate for treating multidrug-resistant tuberculosis. *Sci. Transl. Med.*, **2013**, *5*(214), 214ra168.

[125] Lun, S.; Guo, H.; Onajole, O.K.; Pieroni, M.; Gunosewoyo, H.; Chen, G.; Tipparaju, S.K.; Ammerman, N.C.; Kozikowski, A.P.; Bishai, W.R. Indoleamides are active against drug-resistant *Mycobacterium tuberculosis*. *Nat. Commun.*, **2013**, *4*, 2907.

[126] Tantry, S.J.; Degiacomi, G.; Sharma, S.; Jena, L.K.; Narayan, A.; Guptha, S.; Shanbhag, G.; Menasinakai, S.; Mallya, M.; Awasthy, D.; Balakrishnan, G.; Kaur, P.; Bhattacharjee, D.; Narayan, C.; Reddy, J.; Naveen Kumar, C.N.; Shandil, R.; Boldrin, F.; Ventura, M.; Manganelli, R.; Hartkoorn, R.C.; Cole, S.T.; Panda, M.; Markad, S.D.; Ramachandran, V.; Ghorpade, S.R.; Dinesh, N. Whole cell screen based identification of spiropiperidines with potent antitubercular properties. *Bioorg. Med. Chem. Lett.*, **2015**, *25*(16), 3234-3245.

[127] Li, W.; Upadhyay, A.; Fontes, F.L.; North, E.J.; Wang, Y.; Crans, D.C.; Grzegorzewicz, A.E.; Jones, V.; Franzblau, S.G.; Lee, R.E.; Crick, D.C.; Jackson, M. Novel insights into the mechanism of inhibition of MmpL3, a target of multiple pharmacophores in *Mycobacterium tuberculosis*. *Antimicrob. Agents Chemother.*, **2014**, *58*(11), 6413-6423.

[128] Zhang, M.; Sala, C.; Hartkoorn, R.C.; Dhar, N.; Mendoza-Losana, A.; Cole, S.T. Streptomycin-starved Mycobacterium tuberculosis 18b, a drug discovery tool for latent tuberculosis. *Antimicrob. Agents Chemother.*, **2012**, *56*(11), 5782-5789.

[129] Li, K.; Schurig-Briccio, L.A.; Feng, X.; Upadhyay, A.; Pujari, V.; Lechartier, B.; Fontes, F.L.; Yang, H.; Rao, G.; Zhu, W.; Gulati, A.; No, J.H.; Cintra, G.; Bogue, S.; Liu, Y.L.; Molohon, K.; Orlean, P.; Mitchell, D.A.; Freitas-Junior, L.; Ren, F.; Sun, H.; Jiang, T.; Li, Y.; Guo, R.T.; Cole, S.T.; Gennis, R.B.; Crick, D.C.; Oldfield, E. Multitarget drug discovery for tuberculosis and other infectious diseases. *J. Med. Chem.*, **2014**, *57*(7), 3126-3139.

[130] Li, K.; Wang, Y.; Yang, G.; Byun, S.; Rao, G.; Shoen, C.; Yang, H.; Gulati, A.; Crick, D.C.; Cynamon, M.; Huang, G.; Docampo, R.; No, J.H.; Oldfield, E. Oxa, Thia, Heterocycle, and Carborane Analogues of SQ109: Bacterial and Protozoal Cell Growth Inhibitors. *ACS Infect Dis*, **2015**, *1*(5), 215-221.

[131] Spry, C.; Kirk, K.; Saliba, K.J. Coenzyme A biosynthesis: an antimicrobial drug target. *FEMS Microbiol. Rev.*, **2008**, *32*(1), 56-106.

[132] Sambandamurthy, V.K.; Wang, X.; Chen, B.; Russell, R.G.; Derrick, S.; Collins, F.M.; Morris, S.L.; Jacobs, W.R., Jr A pantothenate auxotroph of *Mycobacterium tuberculosis* is highly attenuated and protects mice against tuberculosis. *Nat. Med.*, **2002**, *8*(10), 1171-1174.

[133] Zheng, R.; Blanchard, J.S. Steady-state and pre-steady-state kinetic analysis of *Mycobacterium tuberculosis* pantothenate synthetase. *Biochemistry*, **2001**, *40*(43), 12904-12912.

[134] Wang, S.; Eisenberg, D. Crystal structures of a pantothenate synthetase from *M. tuberculosis* and its complexes with substrates and a reaction intermediate. *Protein Sci.*, **2003**, *12*(5), 1097-1108.

[135] Xu, Z.; Yin, W.; Martinelli, L.K.; Evans, J.; Chen, J.; Yu, Y.; Wilson, D.J.; Mizrahi, V.; Qiao, C.; Aldrich, C.C. Reaction intermediate analogues as bisubstrate inhibitors of pantothenate synthetase. *Bioorg. Med. Chem.*, **2014**, *22*(5), 1726-1735.

[136] White, E.L.; Southworth, K.; Ross, L.; Cooley, S.; Gill, R.B.; Sosa, M.I.; Manouvakhova, A.; Rasmussen, L.; Goulding, C.; Eisenberg, D.; Fletcher, T.M., III A novel inhibitor of *Mycobacterium tuberculosis* pantothenate synthetase. *J. Biomol. Screen.*, **2007**, *12*(1), 100-105.

[137] Silvestre, H.L.; Blundell, T.L.; Abell, C.; Ciulli, A. Integrated biophysical approach to fragment screening and validation for fragment-based lead discovery. *Proc. Natl. Acad. Sci. USA*, **2013**, *110*(32), 12984-12989.

[138] Devi, P.B.; Samala, G.; Sridevi, J.P.; Saxena, S.; Alvala, M.; Salina, E.G.; Sriram, D.; Yogeeswari, P. Structure-guided design of thiazolidine derivatives as *Mycobacterium tuberculosis* pantothenate synthetase inhibitors. *ChemMedChem*, **2014**, *9*(11), 2538-2547.

[139] Verdonk, M.L.; Rees, D.C. Group efficiency: a guideline for hits-to-leads chemistry. *ChemMedChem*, **2008**, *3*(8), 1179-1180.

[140] Ciulli, A.; Scott, D.E.; Ando, M.; Reyes, F.; Saldanha, S.A.; Tuck, K.L.; Chirgadze, D.Y.; Blundell, T.L.; Abell, C. Inhibition of *Mycobacterium tuberculosis* pantothenate synthetase by analogues of the reaction intermediate. *ChemBioChem*, **2008**, *9*(16), 2606-2611.

[141] Velaparthi, S.; Brunsteiner, M.; Uddin, R.; Wan, B.; Franzblau, S.G.; Petukhov, P.A. 5-tert-butyl-N-pyrazol-4-yl-4,5,6,7-tetrahydrobenzo[d]isoxazole-3-carboxamide derivatives as novel potent inhibitors of *Mycobacterium tuberculosis* pantothenate synthetase: initiating a quest for new antitubercular drugs. *J. Med. Chem.,* **2008**, *51*(7), 1999-2002.

[142] Samala, G.; Nallangi, R.; Devi, P.B.; Saxena, S.; Yadav, R.; Sridevi, J.P.; Yogeeswari, P.; Sriram, D. Identification and development of 2-methylimidazo[1,2-a]pyridine-3-carboxamides as *Mycobacterium tuberculosis* pantothenate synthetase inhibitors. *Bioorg. Med. Chem.,* **2014**, *22*(15), 4223-4232.

[143] Samala, G.; Devi, P.B.; Nallangi, R.; Sridevi, J.P.; Saxena, S.; Yogeeswari, P.; Sriram, D. Development of novel tetrahydrothieno[2,3-c]pyridine-3-carboxamide based *Mycobacterium tuberculosis* pantothenate synthetase inhibitors: molecular hybridization from known antimycobacterial leads. *Bioorg. Med. Chem.,* **2014**, *22*(6), 1938-1947.

[144] Kumar, A.; Casey, A.; Odingo, J.; Kesicki, E.A.; Abrahams, G.; Vieth, M.; Masquelin, T.; Mizrahi, V.; Hipskind, P.A.; Sherman, D.R.; Parish, T. A high-throughput screen against pantothenate synthetase (PanC) identifies 3-biphenyl-4-cyanopyrrole-2-carboxylic acids as a new class of inhibitor with activity against *Mycobacterium tuberculosis*. *PLoS One,* **2013**, *8*(11), e72786.

[145] Samala, G.; Devi, P.B.; Nallangi, R.; Yogeeswari, P.; Sriram, D. Development of 3-phenyl-4,5,6,7-tetrahydro-1H-pyrazolo[4,3-c]pyridine derivatives as novel *Mycobacterium tuberculosis* pantothenate synthetase inhibitors. *Eur. J. Med. Chem.,* **2013**, *69*, 356-364.

[146] Baell, J.B.; Holloway, G.A. New substructure filters for removal of pan assay interference compounds (PAINS) from screening libraries and for their exclusion in bioassays. *J. Med. Chem.,* **2010**, *53*(7), 2719-2740.

[147] Baell, J.B. Feeling Nature's PAINS: Natural Products, Natural Product Drugs, and Pan Assay Interference Compounds (PAINS). *J. Nat. Prod.,* **2016**, *79*(3), 616-628.

[148] Hung, A.W.; Silvestre, H.L.; Wen, S.; George, G.P.; Boland, J.; Blundell, T.L.; Ciulli, A.; Abell, C. Optimization of Inhibitors of *Mycobacterium tuberculosis* Pantothenate Synthetase Based on Group Efficiency Analysis. *ChemMedChem,* **2016**, *11*(1), 38-42.

[149] Samala, G.; Devi, P.B.; Saxena, S.; Meda, N.; Yogeeswari, P.; Sriram, D. Design, synthesis and biological evaluation of imidazo[2,1-b]thiazole and benzo[d]imidazo[2,1-b]thiazole derivatives as *Mycobacterium tuberculosis* pantothenate synthetase inhibitors. *Bioorg. Med. Chem.,* **2016**, *24*(6), 1298-1307.

[150] Sridevi, J.P.; Suryadevara, P.; Janupally, R.; Sridhar, J.; Soni, V.; Anantaraju, H.S.; Yogeeswari, P.; Sriram, D. Identification of potential *Mycobacterium tuberculosis* topoisomerase I inhibitors: a study against active, dormant and resistant tuberculosis. *Eur. J. Pharm. Sci.,* **2015**, *72*, 81-92.

[151] Vos, S.M.; Tretter, E.M.; Schmidt, B.H.; Berger, J.M. All tangled up: how cells direct, manage and exploit topoisomerase function. *Nat. Rev. Mol. Cell Biol.,* **2011**, *12*(12), 827-841.

[152] Forterre, P.; Gribaldo, S.; Gadelle, D.; Serre, M.C. Origin and evolution of DNA topoisomerases. *Biochimie,* **2007**, *89*(4), 427-446.

[153] Champoux, J.J. DNA topoisomerases: structure, function, and mechanism. *Annu. Rev. Biochem.,* **2001**, *70*, 369-413.

[154] Schoeffler, A.J.; Berger, J.M. Recent advances in understanding structure-function relationships in the type II topoisomerase mechanism. *Biochem. Soc. Trans.,* **2005**, *33*(Pt 6), 1465-1470.

[155] Godbole, A.A.; Leelaram, M.N.; Bhat, A.G.; Jain, P.; Nagaraja, V. Characterization of DNA topoisomerase I from *Mycobacterium tuberculosis*: DNA cleavage and religation properties and inhibition of its activity. *Arch. Biochem. Biophys.,* **2012**, *528*(2), 197-203.

[156] Annamalai, T.; Dani, N.; Cheng, B.; Tse-Dinh, Y.C. Analysis of DNA relaxation and cleavage activities of recombinant *Mycobacterium tuberculosis* DNA topoisomerase I from a new expression and purification protocol. *BMC Biochem.,* **2009**, *10*, 18.

[157] Tan, K.; Cao, N.; Cheng, B.; Joachimiak, A.; Tse-Dinh, Y.C. Insights from the Structure of *Mycobacterium tuberculosis* Topoisomerase I with a Novel Protein Fold. *J. Mol. Biol.,* **2016**, *428*(1), 182-193.

[158] Berger, J.M. Structure of DNA topoisomerases. *Biochim. Biophys. Acta,* **1998**, *1400*(1-3), 3-18.

[159] Godbole, A.A.; Ahmed, W.; Bhat, R.S.; Bradley, E.K.; Ekins, S.; Nagaraja, V. Targeting *Mycobacterium tuberculosis* topoisomerase I by small-molecule inhibitors. *Antimicrob. Agents Chemother.,* **2015**, *59*(3), 1549-1557.

[160] Tse-Dinh, Y.C. Bacterial topoisomerase I as a target for discovery of antibacterial compounds. *Nucleic Acids Res.,* **2009**, *37*(3), 731-737.

[161] Godbole, A.A.; Ahmed, W.; Bhat, R.S.; Bradley, E.K.; Ekins, S.; Nagaraja, V. Inhibition of *Mycobacterium tuberculosis* topoisomerase I by m-AMSA, a eukaryotic type II topoisomerase poison. *Biochem. Biophys. Res. Commun.,* **2014**, *446*(4), 916-920.

[162] Pommier, Y.; Leo, E.; Zhang, H.; Marchand, C. DNA topoisomerases and their poisoning by anticancer and antibacterial drugs. *Chem. Biol.,* **2010**, *17*(5), 421-433.

[163] Glowinski, J.; Axelrod, J. Inhibition of uptake of tritiated-noradrenaline in the intact rat brain by imipramine and structurally related compounds. *Nature,* **1964**, *204*, 1318-1319.

[164] Kelly, M.W.; Myers, C.W. Clomipramine: a tricyclic antidepressant effective in obsessive compulsive disorder. *DICP,* **1990**, *24*(7-8), 739-744.

[165] Kleinschroth, T.; Castellani, M.; Trinh, C.H.; Morgner, N.; Brutschy, B.; Ludwig, B.; Hunte, C. X-ray structure of the dimeric cytochrome bc(1) complex from the soil bacterium *Paracoccus denitrificans* at 2.7-Å resolution. *Biochim. Biophys. Acta,* **2011**, *1807*(12), 1606-1615.

[166] Hunte, C.; Palsdottir, H.; Trumpower, B.L. Protonmotive pathways and mechanisms in the cytochrome bc1 complex. *FEBS Lett.,* **2003**, *545*(1), 39-46.

[167] Hunte, C.; Solmaz, S.; Palsdóttir, H.; Wenz, T. A structural perspective on mechanism and function of the cytochrome bc (1) complex. *Results Probl. Cell Differ.,* **2008**, *45*, 253-278.

[168] Matsoso, L.G.; Kana, B.D.; Crellin, P.K.; Lea-Smith, D.J.; Pelosi, A.; Powell, D.; Dawes, S.S.; Rubin, H.; Coppel, R.L.; Mizrahi, V. Function of the cytochrome bc1-aa3 branch of the respiratory network in mycobacteria and network adaptation occurring in response to its disruption. *J. Bacteriol.,* **2005**, *187*(18), 6300-6308.

[169] Rybniker, J.; Vocat, A.; Sala, C.; Busso, P.; Pojer, F.; Benjak, A.; Cole, S.T. Lansoprazole is an antituberculous prodrug targeting cytochrome bc1. *Nat. Commun.,* **2015**, *6*, 7659.

[170] Abrahams, K.A.; Cox, J.A.; Spivey, V.L.; Loman, N.J.; Pallen, M.J.; Constantinidou, C.; Fernández, R.; Alemparte, C.; Remuiñán, M.J.; Barros, D.; Ballell, L.; Besra, G.S. Identification of novel imidazo[1,2-a]pyridine inhibitors targeting *M. tuberculosis* QcrB. *PLoS One,* **2012**, *7*(12), e52951.

[171] Pethe, K.; Bifani, P.; Jang, J.; Kang, S.; Park, S.; Ahn, S.; Jiricek, J.; Jung, J.; Jeon, H.K.; Cechetto, J.; Christophe, T.; Lee, H.; Kempf, M.; Jackson, M.; Lenaerts, A.J.; Pham, H.; Jones, V.; Seo, M.J.; Kim, Y.M.; Seo, M.; Seo, J.J.; Park, D.; Ko, Y.; Choi, I.; Kim, R.; Kim, S.Y.; Lim, S.; Yim, S.A.; Nam, J.; Kang, H.; Kwon, H.; Oh, C.T.; Cho, Y.; Jang, Y.; Kim, J.; Chua, A.; Tan, B.H.; Nanjundappa, M.B.; Rao, S.P.; Barnes, W.S.; Wintjens, R.; Walker, J.R.; Alonso, S.; Lee, S.; Kim, J.; Oh, S.; Oh, T.; Nehrbass, U.; Han, S.J.; No, Z.; Lee, J.; Brodin, P.; Cho, S.N.; Nam, K.; Kim, J. Discovery of Q203, a potent clinical candidate for the treatment of tuberculosis. *Nat. Med.,* **2013**, *19*(9), 1157-1160.

[172] Walker, J.E. The ATP synthase: the understood, the uncertain and the unknown. *Biochem. Soc. Trans.,* **2013**, *41*(1), 1-16.

[173] Boyer, P.D. The ATP synthase--a splendid molecular machine. *Annu. Rev. Biochem.,* **1997**, *66*, 717-749.

[174] Noji, H.; Yasuda, R.; Yoshida, M.; Kinosita, K., Jr Direct observation of the rotation of F1-ATPase. *Nature,* **1997**, *386*(6622), 299-302.

[175] Diez, M.; Zimmermann, B.; Börsch, M.; König, M.; Schweinberger, E.; Steigmiller, S.; Reuter, R.; Felekyan, S.; Kudryavtsev, V.; Seidel, C.A.; Gräber, P. Proton-powered subunit rotation in single membrane-bound F0F1-ATP synthase. *Nat. Struct. Mol. Biol.,* **2004**, *11*(2), 135-141.

[176] Rao, S.P.; Alonso, S.; Rand, L.; Dick, T.; Pethe, K. The protonmotive force is required for maintaining ATP homeostasis and viability of hypoxic, nonreplicating *Mycobacterium tuberculosis*. *Proc. Natl. Acad. Sci. USA,* **2008**, *105*(33), 11945-11950.

[177] Bald, D.; Koul, A. Advances and strategies in discovery of new antibacterials for combating metabolically resting bacteria. *Drug Discov. Today,* **2013**, *18*(5-6), 250-255.

[178] Bald, D.; Koul, A. Respiratory ATP synthesis: the new generation of mycobacterial drug targets? *FEMS Microbiol. Lett.,* **2010**, *308*(1), 1-7.

[179] Koul, A.; Arnoult, E.; Lounis, N.; Guillemont, J.; Andries, K. The challenge of new drug discovery for tuberculosis. *Nature,* **2011**, *469*(7331), 483-490.

[180] Haagsma, A.C.; Abdillahi-Ibrahim, R.; Wagner, M.J.; Krab, K.; Vergauwen, K.; Guillemont, J.; Andries, K.; Lill, H.; Koul, A.; Bald, D. Selectivity of TMC207 towards mycobacterial ATP synthase compared with that towards the eukaryotic homologue. *Antimicrob. Agents Chemother.,* **2009**, *53*(3), 1290-1292.

[181] Koul, A.; Dendouga, N.; Vergauwen, K.; Molenberghs, B.; Vranckx, L.; Willebrords, R.; Ristic, Z.; Lill, H.; Dorange, I.; Guillemont, J.; Bald, D.; Andries, K. Diarylquinolines target subunit c of mycobacterial ATP synthase. *Nat. Chem. Biol.,* **2007**, *3*(6), 323-324.

[182] Tran, S.L.; Cook, G.M. The F1Fo-ATP synthase of *Mycobacterium smegmatis* is essential for growth. *J. Bacteriol.,* **2005**, *187*(14), 5023-5028.

[183] Nesci, S.; Ventrella, V.; Trombetti, F.; Pirini, M.; Pagliarani, A. Thiol oxidation of mitochondrial F0-c subunits: a way to switch off antimicrobial drug targets of the mitochondrial ATP synthase. *Med. Hypotheses,* **2014**, *83*(2), 160-165.

[184] Preiss, L.; Langer, J.D.; Yildiz, Ö.; Eckhardt-Strelau, L.; Guillemont, J.E.; Koul, A.; Meier, T. Structure of the mycobacterial ATP synthase Fo rotor ring in complex with the anti-TB drug bedaquiline. *Sci Adv,* **2015**, *1*(4), e1500106.

[185] de Jonge, M.R.; Koymans, L.H.; Guillemont, J.E.; Koul, A.; Andries, K. A computational model of the inhibition of *Mycobacterium tuberculosis* ATPase by a new drug candidate R207910. *Proteins,* **2007**, *67*(4), 971-980.

[186] Huitric, E.; Verhasselt, P.; Koul, A.; Andries, K.; Hoffner, S.; Andersson, D.I. Rates and mechanisms of resistance development in *Mycobacterium tuberculosis* to a novel diarylquinoline ATP synthase inhibitor. *Antimicrob. Agents Chemother.,* **2010**, *54*(3), 1022-1028.

[187] Koul, A.; Vranckx, L.; Dhar, N.; Göhlmann, H.W.; Özdemir, E.; Neefs, J.M.; Schulz, M.; Lu, P.; Mørtz, E.; McKinney, J.D.; Andries, K.; Bald, D. Delayed bactericidal response of *Mycobacterium tuberculosis* to bedaquiline involves remodelling of bacterial metabolism. *Nat. Commun.,* **2014**, *5*, 3369.

[188] Pogoryelov, D.; Krah, A.; Langer, J.D.; Yildiz, Ö.; Faraldo-Gómez, J.D.; Meier, T. Microscopic rotary mechanism of ion translocation in the F(o) complex of ATP synthases. *Nat. Chem. Biol.,* **2010**, *6*(12), 891-899.

[189] Matthies, D.; Zhou, W.; Klyszejko, A.L.; Anselmi, C.; Yildiz, Ö.; Brandt, K.; Müller, V.; Faraldo-Gómez, J.D.; Meier, T. High-resolution structure and mechanism of an F/V-hybrid rotor ring in a Na^+-coupled ATP synthase. *Nat. Commun.,* **2014**, *5*, 5286.

[190] Hakulinen, J.K.; Klyszejko, A.L.; Hoffmann, J.; Eckhardt-Strelau, L.; Brutschy, B.; Vonck, J.; Meier, T. Structural study on the architecture of the bacterial ATP synthase Fo motor. *Proc. Natl. Acad. Sci. USA,* **2012**, *109*(30), E2050-E2056.

[191] Allegretti, M.; Klusch, N.; Mills, D.J.; Vonck, J.; Kühlbrandt, W.; Davies, K.M. Horizontal membrane-intrinsic α-helices in the stator a-subunit of an F-type ATP synthase. *Nature,* **2015**, *521*(7551), 237-240.

[192] Lounis, N.; Veziris, N.; Chauffour, A.; Truffot-Pernot, C.; Andries, K.; Jarlier, V. Combinations of R207910 with drugs used to treat multidrug-resistant tuberculosis have the potential to shorten treatment duration. *Antimicrob. Agents Chemother.,* **2006**, *50*(11), 3543-3547.

[193] Diacon, A.H.; Pym, A.; Grobusch, M.; Patientia, R.; Rustomjee, R.; Page-Shipp, L.; Pistorius, C.; Krause, R.; Bogoshi, M.; Churchyard, G.; Venter, A.; Allen, J.; Palomino, J.C.; De Marez, T.; van Heeswijk, R.P.; Lounis, N.; Meyvisch, P.; Verbeeck, J.; Parys, W.; de Beule, K.; Andries, K.; Mc Neeley, D.F. The diarylquinoline TMC207 for multidrug-resistant tuberculosis. *N. Engl. J. Med.,* **2009**, *360*(23), 2397-2405.

[194] Ibrahim, M.; Andries, K.; Lounis, N.; Chauffour, A.; Truffot-Pernot, C.; Jarlier, V.; Veziris, N. Synergistic activity of R207910 combined with pyrazinamide against murine tuberculosis. *Antimicrob. Agents Chemother.,* **2007**, *51*(3), 1011-1015.

[195] Lilienkampf, A.; Mao, J.; Wan, B.; Wang, Y.; Franzblau, S.G.; Kozikowski, A.P. Structure-activity relationships for a series of quinoline-based compounds active against replicating and nonreplicating *Mycobacterium tuberculosis*. *J. Med. Chem.,* **2009**, *52*(7), 2109-2118.

[196] Upadhayaya, R.S.; Vandavasi, J.K.; Vasireddy, N.R.; Sharma, V.; Dixit, S.S.; Chattopadhyaya, J. Design, synthesis, biological evaluation and molecular modelling studies of novel quinoline derivatives against *Mycobacterium tuberculosis*. *Bioorg. Med. Chem.,* **2009**, *17*(7), 2830-2841.

[197] Singh, S.; Roy, K.K.; Khan, S.R.; Kashyap, V.K.; Sharma, A.; Jaiswal, S.; Sharma, S.K.; Krishnan, M.Y.; Chaturvedi, V.; Lal, J.; Sinha, S.; Dasgupta, A.; Srivastava, R.; Saxena, A.K.; Saxena, A.K. Novel, potent, orally bioavailable and selective mycobacterial ATP synthase inhibitors that demonstrated activity against both replicating and non-replicating *M. tuberculosis*. *Bioorg. Med. Chem.*, **2015**, *23*(4), 742-752.

[198] Hirota, Y.; Ryter, A.; Jacob, F. Thermosensitive mutants of E. coli affected in the processes of DNA synthesis and cellular division. *Cold Spring Harb. Symp. Quant. Biol.*, **1968**, *33*, 677-693.

[199] Margalit, D.N.; Romberg, L.; Mets, R.B.; Hebert, A.M.; Mitchison, T.J.; Kirschner, M.W.; RayChaudhuri, D. Targeting cell division: small-molecule inhibitors of FtsZ GTPase perturb cytokinetic ring assembly and induce bacterial lethality. *Proc. Natl. Acad. Sci. USA*, **2004**, *101*(32), 11821-11826.

[200] Bi, E.F.; Lutkenhaus, J. FtsZ ring structure associated with division in *Escherichia coli*. *Nature*, **1991**, *354*(6349), 161-164.

[201] Mukherjee, A.; Lutkenhaus, J. Dynamic assembly of FtsZ regulated by GTP hydrolysis. *EMBO J.*, **1998**, *17*(2), 462-469.

[202] Scheffers, D.; Driessen, A.J. The polymerization mechanism of the bacterial cell division protein FtsZ. *FEBS Lett.*, **2001**, *506*(1), 6-10.

[203] Lu, C.; Reedy, M.; Erickson, H.P. Straight and curved conformations of FtsZ are regulated by GTP hydrolysis. *J. Bacteriol.*, **2000**, *182*(1), 164-170.

[204] Ben-Yehuda, S.; Losick, R. Asymmetric cell division in *B. subtilis* involves a spiral-like intermediate of the cytokinetic protein FtsZ. *Cell*, **2002**, *109*(2), 257-266.

[205] Thanedar, S.; Margolin, W. FtsZ exhibits rapid movement and oscillation waves in helix-like patterns in Escherichia coli. *Curr. Biol.*, **2004**, *14*(13), 1167-1173.

[206] Leung, A.K.; Lucile White, E.; Ross, L.J.; Reynolds, R.C.; DeVito, J.A.; Borhani, D.W. Structure of Mycobacterium tuberculosis FtsZ reveals unexpected, G protein-like conformational switches. *J. Mol. Biol.*, **2004**, *340*(3), 953-970.

[207] Romberg, L.; Simon, M.; Erickson, H.P. Polymerization of Ftsz, a bacterial homolog of tubulin. is assembly cooperative? *J. Biol. Chem.*, **2001**, *276*(15), 11743-11753.

[208] Ojima, I.; Kumar, K.; Awasthi, D.; Vineberg, J.G. Drug discovery targeting cell division proteins, microtubules and FtsZ. *Bioorg. Med. Chem.*, **2014**, *22*(18), 5060-5077.

[209] Huang, Q.; Tonge, P.J.; Slayden, R.A.; Kirikae, T.; Ojima, I.; Fts, Z. FtsZ: a novel target for tuberculosis drug discovery. *Curr. Top. Med. Chem.*, **2007**, *7*(5), 527-543.

[210] Goehring, N.W.; Beckwith, J. Diverse paths to midcell: assembly of the bacterial cell division machinery. *Curr. Biol.*, **2005**, *15*(13), R514-R526.

[211] de Pereda, J.M.; Leynadier, D.; Evangelio, J.A.; Chacón, P.; Andreu, J.M. Tubulin secondary structure analysis, limited proteolysis sites, and homology to FtsZ. *Biochemistry*, **1996**, *35*(45), 14203-14215.

[212] Nogales, E.; Downing, K.H.; Amos, L.A.; Löwe, J. Tubulin and FtsZ form a distinct family of GTPases. *Nat. Struct. Biol.*, **1998**, *5*(6), 451-458.

[213] Romberg, L.; Mitchison, T.J. Rate-limiting guanosine 5'-triphosphate hydrolysis during nucleotide turnover by FtsZ, a prokaryotic tubulin homologue involved in bacterial cell division. *Biochemistry*, **2004**, *43*(1), 282-288.

[214] Läppchen, T.; Hartog, A.F.; Pinas, V.A.; Koomen, G.J.; den Blaauwen, T. GTP analogue inhibits polymerization and GTPase activity of the bacterial protein FtsZ without affecting its eukaryotic homologue tubulin. *Biochemistry*, **2005**, *44*(21), 7879-7884.

[215] Leung, A.K.; White, E.L.; Ross, L.J.; Borhani, D.W. Crystallization of the *Mycobacterium tuberculosis* cell-division protein FtsZ. *Acta Crystallogr. D Biol. Crystallogr.*, **2000**, *56*(Pt 12), 1634-1637.

[216] White, E.L.; Suling, W.J.; Ross, L.J.; Seitz, L.E.; Reynolds, R.C. 2-Alkoxycarbonylaminopyridines: inhibitors of *Mycobacterium tuberculosis* FtsZ. *J. Antimicrob. Chemother.*, **2002**, *50*(1), 111-114.

[217] White, E.L.; Ross, L.J.; Reynolds, R.C.; Seitz, L.E.; Moore, G.D.; Borhani, D.W. Slow polymerization of *Mycobacterium tuberculosis* FtsZ. *J. Bacteriol.*, **2000**, *182*(14), 4028-4034.

[218] Margolin, W. Themes and variations in prokaryotic cell division. *FEMS Microbiol. Rev.*, **2000**, *24*(4), 531-548.

[219] Rothfield, L.; Justice, S.; Garcia-Lara, J. Bacterial cell division. *Annu. Rev. Genet.*, **1999**, *33*, 423-448.

[220] Huang, Q.; Kirikae, F.; Kirikae, T.; Pepe, A.; Amin, A.; Respicio, L.; Slayden, R.A.; Tonge, P.J.; Ojima, I. Targeting FtsZ for antituberculosis drug discovery: noncytotoxic taxanes as novel antituberculosis agents. *J. Med. Chem.*, **2006**, *49*(2), 463-466.

[221] Slayden, R.A.; Knudson, D.L.; Belisle, J.T. Identification of cell cycle regulators in Mycobacterium tuberculosis by inhibition of septum formation and global transcriptional analysis. *Microbiology*, **2006**, *152*(Pt 6), 1789-1797.

[222] Jaiswal, R.; Beuria, T.K.; Mohan, R.; Mahajan, S.K.; Panda, D. Totarol inhibits bacterial cytokinesis by perturbing the assembly dynamics of FtsZ. *Biochemistry*, **2007**, *46*(14), 4211-4220.

[223] Kumar, K.; Awasthi, D.; Berger, W.T.; Tonge, P.J.; Slayden, R.A.; Ojima, I. Discovery of anti-TB agents that target the cell-division protein FtsZ. *Future Med. Chem.*, **2010**, *2*(8), 1305-1323.

[224] Awasthi, D.; Kumar, K.; Knudson, S.E.; Slayden, R.A.; Ojima, I. SAR studies on trisubstituted benzimidazoles as inhibitors of Mtb FtsZ for the development of novel antitubercular agents. *J. Med. Chem.*, **2013**, *56*(23), 9756-9770.

[225] Barot, K.P.; Jain, S.V.; Gupta, N.; Kremer, L.; Singh, S.; Takale, V.B.; Joshi, K.; Ghate, M.D. Design, synthesis and docking studies of some novel (R)-2-(4'-chlorophenyl)-3-(4'-nitrophenyl)-1,2,3,5-tetrahydrobenzo[4,5] imidazo [1,2-c]pyrimidin-4-ol derivatives as antitubercular agents. *Eur. J. Med. Chem.*, **2014**, *83*, 245-255.

[226] Anderson, D.E.; Kim, M.B.; Moore, J.T.; O'Brien, T.E.; Sorto, N.A.; Grove, C.I.; Lackner, L.L.; Ames, J.B.; Shaw, J.T. Comparison of small molecule inhibitors of the bacterial cell division protein FtsZ and identification of a reliable cross-species inhibitor. *ACS Chem. Biol.*, **2012**, *7*(11), 1918-1928.

[227] Nepomuceno, G.M.; Chan, K.M.; Huynh, V.; Martin, K.S.; Moore, J.T.; O'Brien, T.E.; Pollo, L.A.; Sarabia, F.J.; Tadeus, C.; Yao, Z.; Anderson, D.E.; Ames, J.B.; Shaw, J.T. Synthesis and Evaluation of Quinazolines as Inhibitors of the Bacterial Cell Division Protein FtsZ. *ACS Med. Chem. Lett.*, **2015**, *6*(3), 308-312.

[228] Kumar, K.; Awasthi, D.; Lee, S.Y.; Zanardi, I.; Ruzsicska, B.; Knudson, S.; Tonge, P.J.; Slayden, R.A.; Ojima, I. Novel trisubstituted benzimidazoles, targeting Mtb FtsZ, as a new class of antitubercular agents. *J. Med. Chem.*, **2011**, *54*(1), 374-381.

[229] Haydon, D.J.; Stokes, N.R.; Ure, R.; Galbraith, G.; Bennett, J.M.; Brown, D.R.; Baker, P.J.; Barynin, V.V.; Rice, D.W.;

Sedelnikova, S.E.; Heal, J.R.; Sheridan, J.M.; Aiwale, S.T.; Chauhan, P.K.; Srivastava, A.; Taneja, A.; Collins, I.; Errington, J.; Czaplewski, L.G. An inhibitor of FtsZ with potent and selective anti-staphylococcal activity. *Science,* **2008**, *321*(5896), 1673-1675.

[230] Tan, C.M.; Therien, A.G.; Lu, J.; Lee, S.H.; Caron, A.; Gill, C.J.; Lebeau-Jacob, C.; Benton-Perdomo, L.; Monteiro, J.M.; Pereira, P.M.; Elsen, N.L.; Wu, J.; Deschamps, K.; Petcu, M.; Wong, S.; Daigneault, E.; Kramer, S.; Liang, L.; Maxwell, E.; Claveau, D.; Vaillancourt, J.; Skorey, K.; Tam, J.; Wang, H.; Meredith, T.C.; Sillaots, S.; Wang-Jarantow, L.; Ramtohul, Y.; Langlois, E.; Landry, F.; Reid, J.C.; Parthasarathy, G.; Sharma, S.; Baryshnikova, A.; Lumb, K.J.; Pinho, M.G.; Soisson, S.M.; Roemer, T. Restoring methicillin-resistant *Staphylococcus aureus* susceptibility to β-lactam antibiotics. *Sci. Transl. Med.,* **2012**, *4*(126), 126ra35.

[231] Warner, D.F.; Evans, J.C.; Mizrahi, V. Nucleotide Metabolism and DNA Replication. *Microbiol. Spectr.,* **2014**, *2*(5)

[232] Yoshida, T.; Nasu, H.; Namba, E.; Ubukata, O.; Yamashita, M. Discovery of a compound that acts as a bacterial PyrG (CTP synthase) inhibitor. *J. Med. Microbiol.,* **2012**, *61*(Pt 9), 1280-1285.

[233] Tamborini, L.; Pinto, A.; Smith, T.K.; Major, L.L.; Iannuzzi, M.C.; Cosconati, S.; Marinelli, L.; Novellino, E.; Lo Presti, L.; Wong, P.E.; Barrett, M.P.; De Micheli, C.; Conti, P. Synthesis and biological evaluation of CTP synthetase inhibitors as potential agents for the treatment of African trypanosomiasis. *ChemMedChem,* **2012**, *7*(9), 1623-1634.

[234] Conti, P.; Pinto, A.; Wong, P.E.; Major, L.L.; Tamborini, L.; Iannuzzi, M.C.; De Micheli, C.; Barrett, M.P.; Smith, T.K. Synthesis and in vitro/in vivo evaluation of the anti-trypanosomal activity of 3-bromoacivicin, a potent CTP synthetase inhibitor. *ChemMedChem,* **2011**, *6*(2), 329-333.

[235] Mori, G.; Chiarelli, L.R.; Esposito, M.; Makarov, V.; Bellinzoni, M.; Hartkoorn, R.C.; Degiacomi, G.; Boldrin, F.; Ekins, S.; de Jesus Lopes Ribeiro, A.L.; Marino, L.B.; Centárová, I.; Svetlíková, Z.; Blaško, J.; Kazakova, E.; Lepioshkin, A.; Barilone, N.; Zanoni, G.; Porta, A.; Fondi, M.; Fani, R.; Baulard, A.R.; Mikušová, K.; Alzari, P.M.; Manganelli, R.; de Carvalho, L.P.; Riccardi, G.; Cole, S.T.; Pasca, M.R. Thiophenecarboxamide Derivatives Activated by EthA Kill *Mycobacterium tuberculosis* by Inhibiting the CTP Synthetase PyrG. *Chem. Biol.,* **2015**, *22*(7), 917-927.

[236] Kent, C.; Carman, G.M. Interactions among pathways for phosphatidylcholine metabolism, CTP synthesis and secretion through the Golgi apparatus. *Trends Biochem. Sci.,* **1999**, *24*(4), 146-150.